UNIVERSIDADE FEDERAL DO PARANÁ
KARLSRUHE INSTITUTE OF TECHNOLOGY

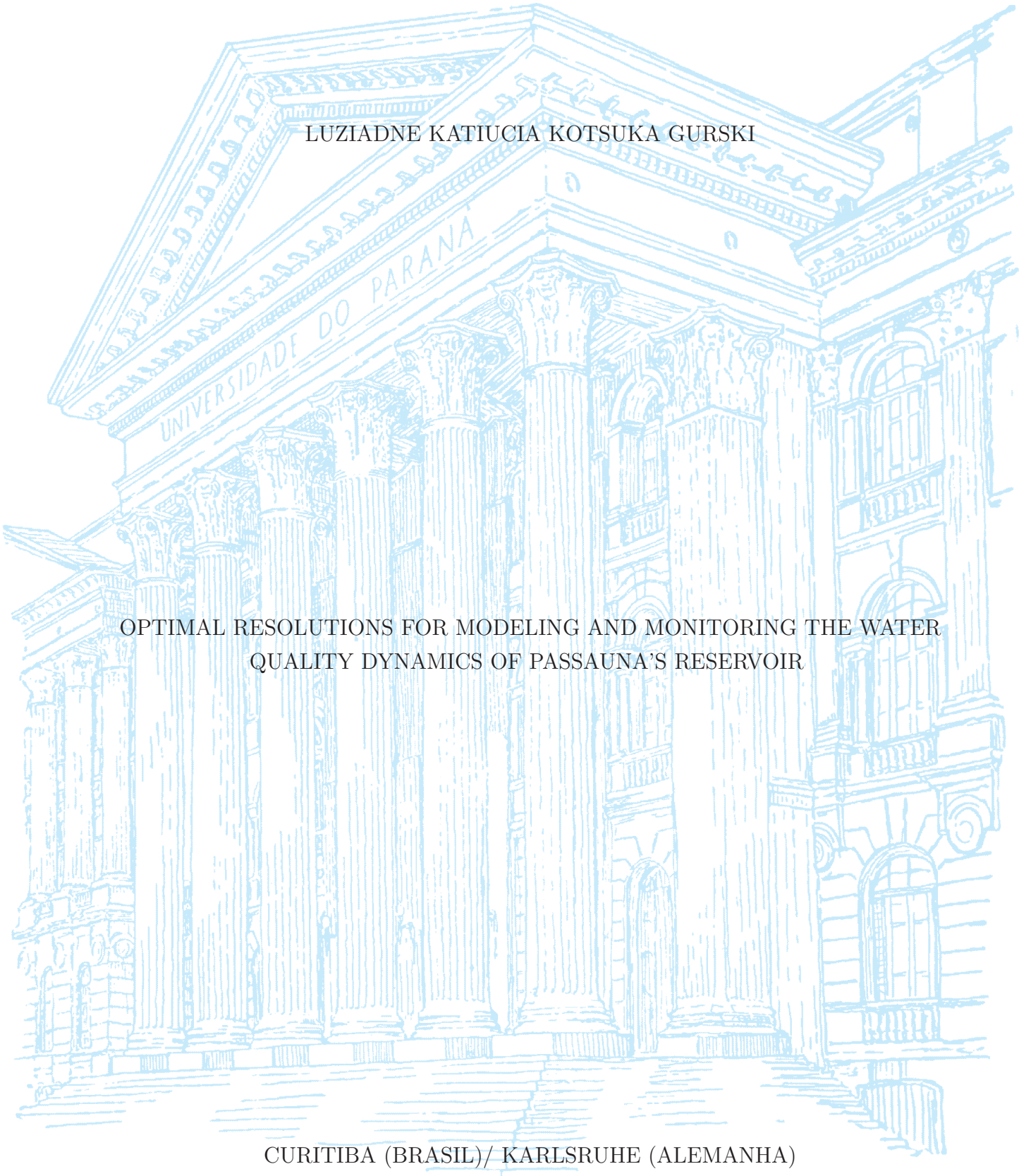

LUZIADNE KATIUCIA KOTSUKA GURSKI

OPTIMAL RESOLUTIONS FOR MODELING AND MONITORING THE WATER QUALITY DYNAMICS OF PASSAUNA'S RESERVOIR

CURITIBA (BRASIL)/ KARLSRUHE (ALEMANHA)

2022

LUZIADNE KATIUCIA KOTSUKA GURSKI

OPTIMAL RESOLUTIONS FOR MODELING AND MONITORING THE WATER QUALITY DYNAMICS OF PASSAUNA'S RESERVOIR

Tese apresentada como requisito à obtenção do título de Doutora, do Programa de Pós-Graduação em Engenharia de Recursos Hídricos e Ambiental, Setor de Tecnologia da Universidade Federal do Paraná em regime de cotutela entre a UFPR e o KIT (Instituto de Tecnologia de Karlsruhe), na Alemanha.

Orientador: Dr.-Ing. Tobias Bleninger (UFPR).

Coorientadores: Dr. Heloise Garcia Knapik (UFPR) e Dr.-Ing. Stephan Fuchs (KIT).

CURITIBA (BRASIL)/ KARLSRUHE (ALEMANHA)

2022

OPTIMAL RESOLUTIONS FOR MODELING AND MONITORING THE WATER QUALITY DYNAMICS OF PASSAÚNA'S RESERVOIR

Zur Erlangung des akademischen Grades einer

DOKTORIN DER INGENIEURWISSENSCHAFTEN (Dr.-Ing.)

von der KIT Fakultät für

Bauingenieur-, Geo- und Umweltwissenschaften

des Karlsruher Instituts für Technologie (KIT)
genehmigte DISSERTATION von

Luziadne Katiucia Kotsuka Gurski, M.Sc.

aus Laranjeiras do Sul, Brazil

Tag der mündlichen Prüfung: 20.12.2022

Referent: Prof. Dr-Ing. Stephan Fuchs (KIT)
Referent: Prof. Dr-Ing. Tobias Bleninger (UFPR)
Korreferent: Prof. Dr. Bruno Victor Veiga (UFPR)

Curitiba/Brazil and Karlsruhe/Germany (2022)

Catalogação na Fonte: Sistema de Bibliotecas, UFPR
Biblioteca de Ciência e Tecnologia

G981o Gurski, Luziadne Katiucia Kotsuka

Optimal resolutions for modeling and monitoring the water quality dynamics of passaunašs reservoir [recurso eletrônico] / Luziadne Katiucia Kotsuka Gurski – Curitiba, 2022.

Tese (Doutorado em Engenharia de Recursos Hídricos e Ambiental) apresentada ao Programa de Pós-graduação em Engenharia de Recursos Hídricos e Ambiental, Setor de Tecnologia da Universidade Federal do Paraná, em regime de cotutela entre a UFPR e o KIT (Instituto de Tecnologia de Karlsruhe), na Alemanha.
Orientador: Dr. Tobias Bernward Bleninger
Co-orientadores: Drª. Heloise Garcia Knapik; Dr. Stephan Fuchs

1. Reservatório – Rio Passaúna (PR). 2. Engenharia de Recursos Hídricos. 3. I. Bleninger, Tobias Bernward. II. Knapik, Heloise Garcia. III. Fuchs, Stephan. IV. Universidade Federal do Paraná. IV. Título.

CDD 627.042

Bibliotecária: Vilma Machado CRB-9/1563

MINISTÉRIO DA EDUCAÇÃO
SETOR DE TECNOLOGIA
UNIVERSIDADE FEDERAL DO PARANÁ
PRÓ-REITORIA DE PESQUISA E PÓS-GRADUAÇÃO
PROGRAMA DE PÓS-GRADUAÇÃO ENGENHARIA DE
RECURSOS HÍDRICOS E AMBIENTAL - 40001016021P0

APPROVAL MINUTE

The Examining Board is designated by the Faculty of the Graduate Program of the Federal University of Paraná in ENGENHARIA DE RECURSOS HÍDRICOS E AMBIENTAL where invited to argue the DISSERTATION of PHILOSOPHY DOCTOR by **LUZIADNE KATIUCIA KOTSUKA GURSKI** , entitled: **Optimal resolutions for modeling and monitoring the water quality dynamics of Passaúnas reservoir**, under the supervision of Dr. TOBIAS BERNWARD BLENINGER, which and after assessment of the candidate and the work, the Examining Board decided for the APPROVAL in the present rite.
The granting of the title of philosophy doctor is contingent upon the fulfillment of all the requirements indicated by the Examining Board and terms determined in the regulation of the Graduate Program.

CURITIBA, December 20th, 2022.

Eletronic Signature
02/01/2023 10:09:00.0
CRISTOVÃO VICENTE SCAPULATEMPO FERNANDES
President of the Examining Board

Eletronic Signature
22/12/2022 07:18:06.0
STEPHAN FUCHS
Co-Advisor

Eletronic Signature
02/01/2023 12:42:57.0
HANS-PETER BAHR
External Member (KARLSRUHE INSTITUTE OF TECHNOLOGY)

Eletronic Signature
21/12/2022 10:56:46.0
HELOISE GARCIA KNAPIK
Co-Advisor

Eletronic Signature
21/12/2022 16:08:32.0
TOBIAS BERNWARD BLENINGER
Internal Member(UNIVERSIDADE FEDERAL DO PARANÁ)

Eletronic Signature
21/12/2022 10:41:37.0
BRUNO VICTOR VEIGA
External Member (UNIVERSIDADE FEDERAL DO PARANÁ - DEP DE HIDRÁULICA)

Eletronic Signature
21/12/2022 11:56:30.0
MAURICIO BERGAMINI SCHEER
External Member (COMPANHIA DE SANEAMENTO DO PARANá)

Acknowledgements

I could not have undertaken this journey without the contributions, energy, and sacrifices of many others, for whom I am deeply indebted.

To my advisor Tobias Bleninger for believing and trusting in me and providing me with many fantastic opportunities over the past years. Thank you for all the enthusiastic support, problem-solving, motivation, assertiveness in decisions, and guidance whenever I needed it.

I'm very grateful to Professor Stephan Fuchs for providing many ideas, and insights, and raising important questions since the early stages of this thesis. Especially during my exchange period, for guiding me, providing important discussions, and showing a different angle of science.

I owe a debt of gratitude to my co-advisor Professor Heloise for her kindness and friendship. Your presence and guidance made all these years nicer and lighter. I feel very fortunate for had your companionship on this journey.

Thank you also to members of my defense committee Drs. Bruno Veiga and Maurício Scheer, for your helpful input and suggestions. In particular, I would like to knowledge Professor Cristovão for all the collaborative effort during data collection and for providing a different view for this thesis. Thank you very much for motivating me along my science path from the very beginning.

I have learned so much over the past years, and I feel very lucky to be a part of MuDaK's project. Thank you to all members of MuDaK's project, especially Klajdi Sotiri, Stephan Hilgert, Regina Kishi, and Ana Carolina. And for Luiza P. Dec, Luciane L. Prado, Carolina de Souza, Nanúbia Barreto, Jullyane da Silva de Oliveira, and Ellen C. O. Almeida for helping me through in lab analyses. I am also thankful to the members of TriOS company for receiving me at the head office during my Germany exchange period, particularly Harald Rohr and Neeske Lübben for being so welcoming and sharing lots of knowledge.

During this journey, I experienced partnership and friendship that I'll never forget. Thank you to all my friends from PPGERHA, mainly Felipe, Sabrina, Ana Paula, Patrícia, and Lais. Special thanks to some of the most incredible people I ever met: Lediane, Liège, Mayra, and Lucas. This dissertation would not have been possible without your support and efforts, and I am fortunate to have worked and learned with you.

This endeavor would not have been possible without the love, unconditional support, and encouragement of my parents, Alberto and Lucia. Thank you for

motivating me to always pursue my dreams, and guiding me to overcome obstacles with dedication and persistence. And, to my brother Alberto Junior and my sister-in-law Juliana, my deepest gratitude for always being there for me, believing in me, listening, and for offering good advice.

Words cannot express my gratitude to Eduardo, my partner, and husband, for his love and support throughout these intense academic years and very challenging times. Thank you for believing in me, having a lot of patience, being so understanding about my absence, listening to perhaps too much about water quality, and checking on a lot of graphics over the past few years.

"Look deep into nature,
and then you will understand
everything better."
Albert Einstein

ABSTRACT

The investigations of optimizing monitoring resolutions of Passaúna's reservoir revealed that monitoring Total Phosphorus (TP) at the main tributary (Passaúna's river) during mid-range and high flows provides more information regarding TP load input than the higher frequency at a large number of locations during base flow. Passaúna reservoir was monitored from February 2018 until April 2019, in 11 field campaigns, composed by monthly water sampling, in-situ measurements with sensors, and laboratory analyses. Additionally, high-temporal-resolution measurements were performed by optical sensors providing concentrations of nitrate, Dissolved Organic Carbon (DOC), and Chlorophyll-a (Chl-a). Data obtained were processed and used as the initial condition for the simulation period, to calibrate, and validate a zero-dimensional water quality model of Passaúna's reservoir. Passaúna reservoir was assumed as a completely mixed system, and a Continuously Stirred Tank Reactor (CSTR) model was applied and tested as steady and unsteady state solutions for TP concentrations. The steady-state solution resulted in good agreement with measured data an annual scale, and the unsteady-state solution presented a good agreement with monthly resolution measured data. Results from scenarios simulations based on decreasing the temporal resolution of input data to less frequent measurements, indicated quarterly temporal resolutions for monitoring TP at the reservoir to be a proper frequency. Additionally, from the monitoring processed data and application in a zero-dimensional water quality model, the optimal monitoring frequency in terms of management was also assessed with strategies proposed to optimize monitoring resolutions considering spatial-temporal integration. The integration of spatial-temporal water quality dynamics in the monitoring period was evaluated using comparative maps, using monitored data of TP, Chl-a, and Total Nitrogen (TN) classified according to the Water Quality Index of Reservoirs. The results indicated at least seasonally TN monitoring along Passaúna's reservoir. Moreover, an evaluation of effects in TP input loading due to storm events revealed that phosphorus monitoring programs should focus on storm events, to achieve more realistic phosphorus input calculations. Lastly, variability identified in 15 minutes and daily resolution' Chl-a data series indicated that the measurement date can be decisive in classifying the reservoir's WQIR status, results from the percentage of occurrence analysis show that a bimonthly frequency monitoring chlorophyll-a concentrations are more suitable for control and preventive management of water quality purposes.

Key words: Temporal and spatial variability. Optimal monitoring. Phosphorus Budget.

RESUMO

As investigações para otimizar as resoluções de monitoramento do reservatório de Passaúna revelaram que o monitoramento de Fósforo Total (FT) no afluente principal (Rio Passaúna) durante as vazões médias e altas fornece mais informações sobre a entrada de carga do FT do que o monitoramento em maior frequência durante vazões menores do rio. O reservatório Passaúna foi monitorado de fevereiro de 2018 até abril de 2019, em 11 campanhas de campo, compostas por amostragem de água, medições in situ com sensores e análises laboratoriais. Além disso, medições de alta resolução temporal foram realizadas por sensores ópticos fornecendo concentrações de nitrato, carbono orgânico dissolvido e clorofila-a. Os dados obtidos foram processados e utilizados como condição inicial para o período de simulação, para calibrar e validar um modelo zero dimensional de qualidade da água do reservatório de Passaúna. O reservatório de Passaúna foi assumido como um sistema completamente misto, e um modelo de reator completamente misturado foi aplicado e testado com soluções em estado permanente e não-permanente para a variável FT. A solução de estado permanente apresentou boa concordância com os dados medidos em escala anual, e a solução de estado não-permanente apresentou boa concordância com medidas em resolução mensal. Os resultados de simulações dos cenários reduzindo a resolução temporal dos dados de entrada para medições menos frequentes resultou em resoluções temporais trimestrais para monitoramento de dados FT no reservatório de Passaúna. Adicionalmente, a partir dos dados processados de monitoramento e aplicação em um modelo de qualidade de água com dimensão zero, a frequência ótima de monitoramento em termos de gestão também foi avaliada com estratégias propostas para otimizar as resoluções de monitoramento considerando a integração espaço-temporal. A integração da dinâmica espaço-temporal da qualidade da água no período de monitoramento foi avaliada por meio de mapas comparativos usando dados monitorados de FT, clorofila-a e Nitrogênio Total (TN) classificados de acordo com o Índice de Qualidade da Água de Reservatórios (IQAR). Os resultados indicaram que o monitoramento da variável TN deve ser realizada no mínimo com frequência sazonal no reservatório de Passaúna. Além disso, uma avaliação dos efeitos na carga de entrada de FT devido a eventos de precipitação revelou que a fim de obter cálculos de carga de fósforo mais realistas, os programas de monitoramento devem se concentrar em eventos de precipitação no que se refere ao FT. Por fim, a variabilidade identificada em série de dados de clorofila com resolução temporal de 15 minutos indicou que o dia da medição pode ser decisivo na classificação do status ecológico do reservatório. Destes dados, a análise de frequência de distribuição de ocorrência resultou em monitoramento bimestral das concentrações de clorofila-a para se obter controle e gestão preventiva mais adequada da qualidade da água do reservatório do Passaúna.

Palavras-chaves: Variações temporais e espaciais. Monitoramento otimizado. Balanço de massa de fósforo.

ZUSAMMENFASSUNG

Die Untersuchungen zur Optimierung der Überwachungsauflösungen des Passaúna-Stausees ergaben, dass die Überwachung des Gesamtphosphors (TP) am Hauptzufluss (Passaúnas-Fluss) während mittlerer und hoher Abflüsse mehr Informationen über den TP-Lasteintrag liefert als die höhere Frequenz an einer großen Anzahl von Standorten während Grundfluss. Das Passaúna-Reservoir wurde von Februar 2018 bis April 2019 in 11 Feldkampagnen überwacht, die sich aus monatlichen Wasserproben, In-situ-Messungen mit Sensoren und Laboranalysen zusammensetzten. Zusätzlich wurden Messungen mit hoher zeitlicher Auflösung durch optische Sensoren durchgeführt, die Konzentrationen von Nitrat, DOC und Chlorophyll-a (Chl-a) lieferten. Die erhaltenen Daten wurden verarbeitet und als Anfangsbedingung für den Simulationszeitraum verwendet, um ein nulldimensionales Wasserqualitätsmodell des Stausees von Passaúna zu kalibrieren und zu validieren. Das Passaúna-Reservoir wurde als vollständig gemischtes System angenommen, und ein Continuously Stirred Tank Reactor (CSTR)-Modell wurde angewendet und als stationäre und instationäre Lösungen getestet. Die stationäre Lösung ergab eine gute Übereinstimmung mit gemessenen Daten auf Jahresskala, und die instationäre Lösung zeigte eine gute Übereinstimmung mit gemessenen in monatlicher Auflösung. Ergebnisse von Szenariensimulationen auf der Grundlage der Verringerung der zeitlichen Auflösung von Eingabedaten auf weniger häufige Messungen zeigten, dass vierteljährliche zeitliche Auflösungen für die Überwachung von TP am Reservoir eine angemessene Frequenz sind. Darüber hinaus wurde anhand der verarbeiteten Überwachungsdaten und der Anwendung in einem nulldimensionalen Wasserqualitätsmodell die optimale Überwachungshäufigkeit in Bezug auf die Bewirtschaftung bewertet, wobei Strategien vorgeschlagen wurden, um die Überwachungsauflösungen unter Berücksichtigung der räumlich-zeitlichen Integration zu optimieren. Die Integration der räumlich-zeitlichen Dynamik der Wasserqualität im Überwachungszeitraum wurde anhand von Vergleichskarten von TP, Chl-a und Gesamtstickstoff (TIN) bewertet, die nach dem Wasserqualitätsindex der Stauseen klassifiziert wurden. Die Ergebnisse deuteten auf eine zumindest saisonale TN-Überwachung entlang des Stausees von Passaúna hin. Darüber hinaus ergab eine Bewertung der Auswirkungen auf die TP-Eintragsbelastung aufgrund von Sturmereignissen, dass sich Phosphor Überwachungs programme auf Sturmereignisse konzentrieren sollten, um realistischere Berechnungen des Phosphoreintrags zu erreichen. Schließlich deutete die Variabilität, die in den Chl-a-Datenreihen mit 15-minütiger und täglicher Auflösung identifiziert wurde, darauf hin, dass das Messdatum entscheidend für die Klassifizierung des WQIR-Status des Reservoirs sein kann. Ergebnisse aus der Analyse des Prozentsatzes des Auftretens zeigen, dass eine zweimonatliche Häufigkeitsüberwachung der Chl-a Konzentrationen höher ist geeignet für die Kontrolle und das vorbeugende Management der Wasserqualität.

Schlüsselworte: Zeitliche und räumliche Variabilität. Optimale Überwachung. Phosphor-Budget.

List of Figures

List of Tables

Contents

1 Introduction

A dam construction interrupts the natural river course, modifying its dynamics, affecting sediments transportation, temperature, biota, nutrients dynamics, and ecosystem of downstream flows (LEHNER et al., 2011). Substances carried by runoff or point sources, such as nutrients - fundamental for phytoplankton growth, are retained within the reservoir. This condition influences the physical and chemical characteristics of the water and sediment, and thus, the overall water quality dynamics in the reservoir (COQUEMALA, 2005; SAUNITTI; FERNANDES; BITTENCOURT, 2004)

In addition, the excess of organic matter and nutrients may compromise the use of water from the reservoir, especially for public supply, which may lead to taste and odor problems in the water, and also eutrophication process and oxygen consumption (ESTEVES, 1998). Besides the transport and external inputs, internal cycling varies seasonally depending on the hydrodynamics process, climate conditions, and other characteristics that may impact consumption and production pathways and rates in the reservoir (YANG et al., 2018; JIANG et al., 2017; ÇELIK, 2013; YAO et al., 2018; DALU; WASSERMAN, 2018).

Investigating dominant processes and reactions in a reservoir is essential to generate integrated management strategies considering water flows and contribution of organic matter, nutrients, and sediments. However, the limitations of quantification methods, such as difficulties in low concentrations detection and proper procedure, along with delay between sampling and laboratory analyses which determine the number of samples collected and stored, strongly influence the spatial resolution and temporal monitoring. On the other side, continuous automated water quality can contribute to better water resources management, and reservoir operation, thus ensuring the necessary quality for public supply (SADEGHIAN et al., 2018; SILVA et al., 2016; FRANZEN, 2009; OLIVEIRA et al., 2015).

Automated analyzers for in-situ measurements provide real-time temporal quantification with reliability, practicality, reducing time, and resources that need to be used with field campaigns (U.S. Geological Survey, 2018). Additionally, real-time probes enable faster response to events, especially in the case of contaminants that may need a rapid operation and management decision (STOREY; GAAG; BURNS, 2011). However, costs associated with the acquisition, implementation, and maintenance of site probes, usually lead to few or only one sensor installation for each study site. Thus, normally, continuous site stations do not provide information on spatial variability, but the problem of required temporal and spatial resolutions nevertheless remains, especially when analyzing reservoirs in terms of good ecological status for management purposes

or compliance. This leads to monitoring strategies often complemented with modeling (JIMENEZ et al., 2005; ARAUJO et al., 2008; KNOWLTON; JONES, 2006).

This thesis proposes to establish an optimal monitoring program for water quality in water supply reservoirs. The strategy relies on two interconnected objectives: in-situ monitoring and mathematical modeling.

The Passauna's Reservoir, located in Curitiba has been chosen as a case study for this thesis, as it is the second largest main source of drinking water in the region, has a diverse catchment, and has been studied intensively over the last years by several researchers, and more recently within the MuDak-WRM project (Multidisciplinary Data Acquisition as Key for a Globally Applicable Water Resources Management), in which this thesis is embedded, providing the dataset for the following analysis.

From water quality data, composed of high-temporal-resolution measurements, and analysis of several variables spatially distributed in monthly measurement campaigns, a 0-dimensional model was set up and calibrated. The modeling will allow a better understanding of the spatial and temporal variability of nutrients and other substances, and thus its consequences for the reservoir's water quality. Subsequently, the model will be tested until its minimal frequency and spatial variability complexities and resolutions can be reduced. And, from these results, the expectation is to determine an optimal monitoring program for water quality.

This study hypothesizes is that continuously monitoring water quality through probes providing high temporal resolution information combined with traditional monitoring could acknowledge the spatial and temporal features of reservoirs' complexity.

Further, applying the monitored data in a mass balance model could represent total phosphorus behavior in the reservoir. Additionally, modeling results and scenarios could be useful in defining an optimized water quality monitoring strategy for Passaúna's reservoir, providing relevant information for reservoir management.

1.1 Thesis Objectives

The main goal of this thesis is to define an optimal monitoring program for assessing water quality in a reservoir considering temporal and spatial variability.

In order to achieve this goal, conventional and high temporal resolution water quality monitoring techniques were explored, and the following complementary goals were pursued:

- Analyzing high-temporal resolution measured data from a fixed platform equipped with sensors using spectral technology to assess the temporal water quality dynamics

of Passauna's reservoir;

- Identifying the spatial variability of Passaúna reservoir's water quality by processing data from monthly measurements water sampling collection with subsequent physical and chemical analyses in the laboratory;
- Implementation of a zero-dimensional water quality model to test the monitored data frequency with scenarios, and possible monitoring resolutions reduction;
- Integrating and processing spatial-temporal water quality data and results from modeling to establish an optimal monitoring resolution program for assessing Passaúna's reservoir water quality.

1.2 Thesis Methodological Approach

The guiding aim of this thesis is to contribute in defining resolutions for monitoring and modeling the water quality dynamics of reservoirs, by acknowledging the spatial and temporal features of these ecosystems' complexity.

To address this topic, Passaúna's reservoir was investigated as the study site. The arisen research questions about the reservoir's water quality outlined the methodological approach of this thesis, into four interconnected branches (Figure 1): (i) field monitoring; (ii) mathematical modeling; and (iii) optimal monitoring; (iv) monitoring program strategy.

To answer 'Which are the drivers for water quality of Passaúna reservoir', field monitoring was planned and executed to identify and quantify the spatial properties of water quality, covering a wide range of variables measured at key sites distributed within the reservoir. Moreover, temporal variability was assessed with the use of optical sensors providing high temporal resolution monitoring, and its usage was verified to complement the frequency of traditional monitoring programs.

From the monitoring processed data and application in a zero-dimensional water quality model, the optimal monitoring frequency in terms of management was assessed with strategies proposed in this thesis to optimize monitoring resolutions considering spatial-temporal integration.

A graphic on map representing changes in monitored variables was applied to address "Which water quality variables should be monitored?" and "Where the monitoring sites should be placed?".

Nonetheless, the research question "When monitoring investigations should be performed?" was evaluated using the application of load duration curves with historical

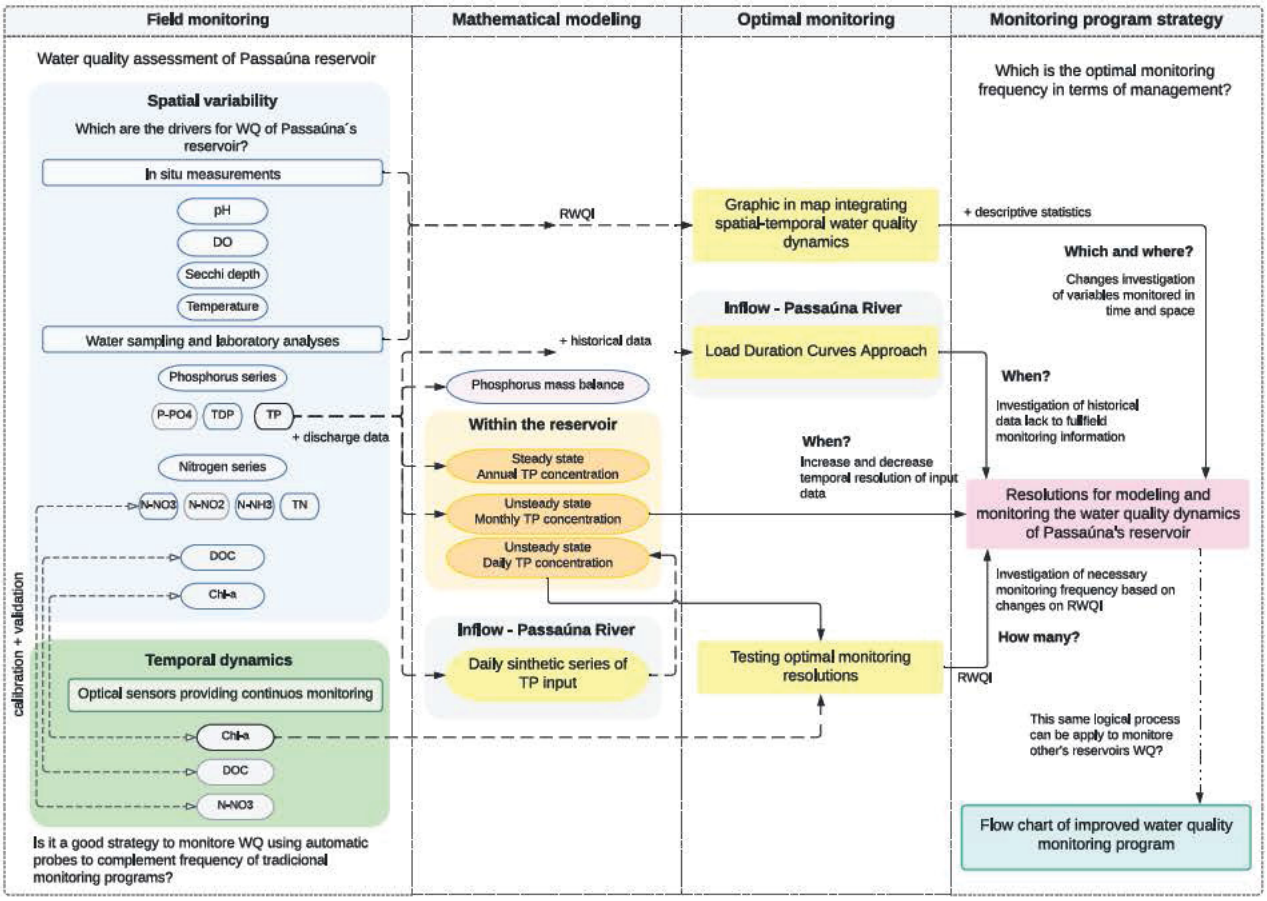

Figure 1 – Schematic representation of thesis methodological approach, where WQ is Water Quality, TP is Total Phosphorus and RWQI is Reservoir Water Quality Index.

and monitored total phosphorus data measured at Passaúna River and mathematical models testing several scenarios.

Additionally, the reservoir's ecological status variability was explored using percentage frequency of occurrence analysis for several data series with different temporal resolutions. This approach aimed to answer "How much data should be monitored?".

Lastly, a flow chart was developed based on the logical process obtained from Passaúna's reservoir monitoring experience and lessons learned, as suggestions to be applied in monitoring programs for reservoirs.

1.3 Thesis Outline

This document is structured in six major chapters. In the present Chapter, an introduction to the topic is given, the problems around water quality monitoring are outlined, and objectives are pointed out. The methodological approach was presented, and the following chapters are divided based on answering the research questions.

From there, Chapters 2 and 3 presented a brief literature overview of the theoretical basis for water quality monitoring and modeling. Scientific background of water quality of reservoirs was introduced, including variables usually monitored in traditional monitoring programs, along with spatial and temporal variations aspects. The main concepts of using spectral technology as a strategy for real-time in situ monitoring were highlighted, and monitoring requirements used for lakes and reservoirs worldwide were presented. The following Chapter 4 focuses on presenting and describing the research area of this study, Passaúna's reservoir.

In Chapter 5, a detailed description of procedures applied in monitoring and modeling the water quality of Passaúna's reservoir is presented, separated into four main sections: Monitoring Passaúna's reservoir water quality (Section 5.2), Modeling Passaúna's reservoir water quality (Section 5.3), Optimal monitoring strategies (Section 5.5), Data analyses and post-processing (Section 5.4). The first part focused on presenting the analytical methods for water quality characterization, including methodology applied in the field campaigns, procedures performed in the laboratory, and a description of optical sensors composing the floating platform system, which provided high temporal resolution water quality measurements. In the second part, the proposed zero-dimensional Total Phosphorus model, and the governing equations of mass balance analyses, are described with the application of Continuously Stirred Tank Reactor (CSTR) as steady and unsteady state solutions. The third part presents methods applied to optimize monitoring resolutions considering the integration of spatial-temporal water quality, modeling application, and historical data. The last part focused on an overall description of analyses and post-processing procedures of data collected during the monitoring period.

The results and discussions are presented in Chapter 6, following the same structure adopted for each methodology separately. The first part (Section 6.2) summarized the results obtained from the water quality monitoring program considering data collected in the monitoring performed over a year at nine sites along Passaúna's reservoir, considering spatial variability (water sampling, in-situ measurements with sensors, and laboratory analysis) and temporal dynamics (data from optical sensors providing high temporal resolution monitoring). In the second part (Section 6.3), all results regarding the assessment of mass balance application are presented, including the model simulations, results from calibration, and scenarios considered in this thesis development. The third and final part (Section 6.4) presented results from the analysis of overall strategies adopted to obtain optimal resolutions for monitoring Passaúna's reservoir water quality.

Chapter 7 summarizes the conclusion and this thesis's main findings. Complementarily, the outlook for further work and research is briefly discussed, followed

by a flow chart with recommendations for assessing optimal water quality monitoring programs of reservoirs.

2 Water quality monitoring in reservoirs

2.1 Overview

Freshwater availability is a key limiting factor for city development, but either an environmental challenge, since human activities impact water sustainability. Inland water resources are usually subject to anthropogenic influence, due to urban growth, agriculture expansion, and land management practices, and have reflected upon water quality and quantity, with high economic, social, and environmental costs (WMO, 2013; RIPL, 2003).

Water from rivers has been used for domestic use, agriculture, transportation, power generation, and industrial production (MULLIGAN; SOESBERGEN; SÁENZ, 2020). Reservoir construction is necessary to guarantee sufficient water supply and energy, flood control, and irrigation demands face the increasing water demands due to climate change and population growth (LEHNER et al., 2011; BOULANGE et al., 2021).

In response to this need, Lehner et al. (2011) estimated a total storage capacity worldwide of 6,197 km^3 address from 6,862 dams and their associated reservoirs in early 2011. Likewise, Zarfl et al. (2014) accounted for over 3,000 major hydropower dams were planned, while 700 dams were under construction in 2014.

Nevertheless, a dam construction interrupts the natural river course, modifying its dynamics, affecting sediments transportation, temperature, biota, nutrients dynamics, and ecosystem of downstream flows (LEHNER et al., 2011). The construction of human-managed reservoirs to expand hydropower, together with climate change, was classified by Reid et al. (2019), as one of the five emerging threats to freshwater ecosystems.

In reservoirs are retained substances introduced by runoff, erosion, and leaching of nutrients from degraded soils (SINGH et al., 2020). This environmental impact affects primary production and internal cycling of nutrients, organic matter, and biological conditions, changing as a consequence, the physical and chemical characteristics of the water (COQUEMALA, 2005; SINGH et al., 2020).

Many pathways of energy and nutrient flow connect biological and abiotic factors in aquatic ecosystems. The biological dynamics are possible due to atmospheric inputs, providing light together with heat energy, and nutrients. Photosynthesis requires light energy and afterward the energy and nutrients flow from phytoplankton and plant to zooplankton and larger animals (KALFF, 2001).

System attributes, morphometry (shape of the underwater basin), and regional properties play a determinant role in water composition. Between sediment and water

several important interrelations occur, affecting inorganic nutrients and organisms. As the catchment attributes influence the ecological water properties, they also act as a source of nutrients for the water body (KALFF, 2001).

Therefore, several parameters are necessary for water characterization. Figure 2 introduces a sort of factors and properties influencing the water body. The most important properties examine in this thesis are physical, chemical, biological, and ecological properties.

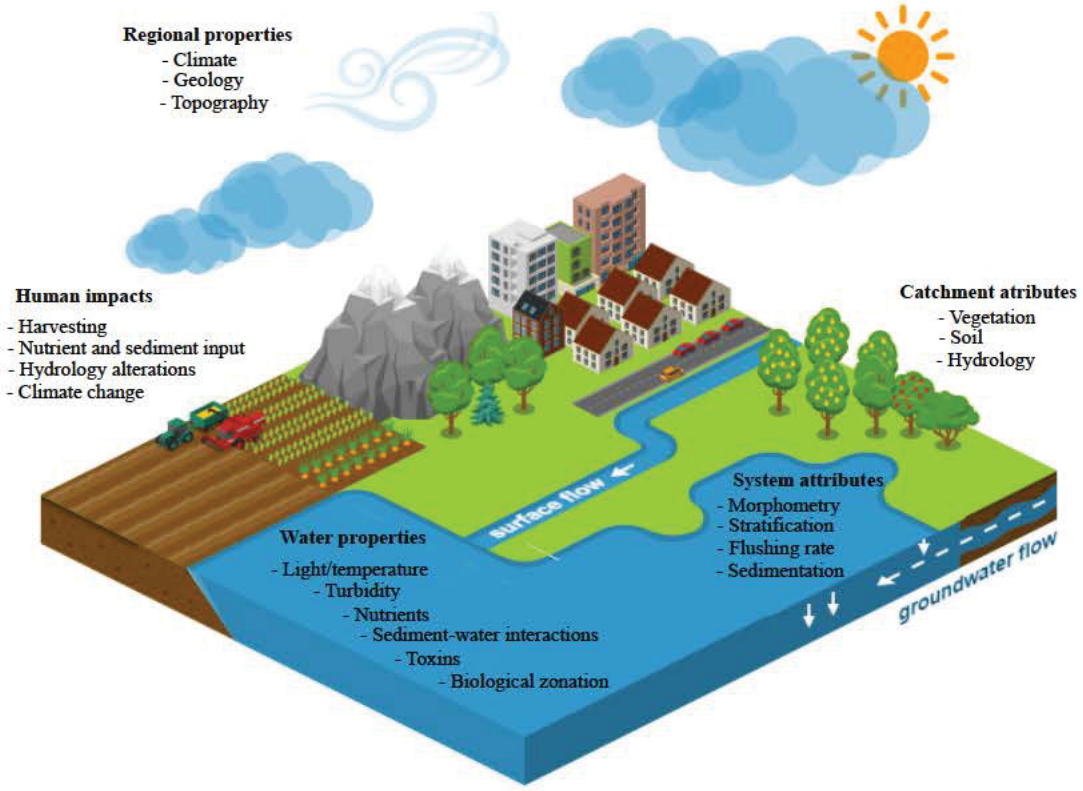

Figure 2 – A hierarchy of attributes and properties influencing aquatic ecosystem. Icons were adapted from Icograms.

Somehow all elements that influence the aquatic ecosystem characteristics are either connect or influenced by anthropogenic actions. In reservoirs, one of the most important anthropogenic impacts and freshwater quality issues is the eutrophication progression (CHAPMAN, 1996).

According to Chapra (1997), eutrophication is a natural process resulting in beneficial biomass productivity. However, when human-induced is called cultural eutrophication, which accelerates the eutrophication process and causes undesirable effects on water quality.

Eutrophication can result in algal blooms decreasing dissolved oxygen levels, changing pH balances, and increasing water turbidity. Human health and well-being are also affected and can result in higher costs for drinking-water treatment plants (ESTEVES, 1998; SPERLING, 2007).

In order to characterize the eutrophication stage, the trophic state is usually classified as oligotrophic, mesotrophic, and eutrophic. Oligotrophic reservoirs have high transparency waters and low concentrations of nutrients and as a consequence low productivity. The mesotrophic ones present intermediate productivity. Lastly, eutrophic reservoirs display high concentrations of nutrients and associated high biomass production, usually with a low transparency (ESTEVES, 1998; SPERLING, 2007).

The system and catchment attributes, along with regional characteristics define water properties, which are also affected by human impact (KALFF, 2001). The water quality criterion varies depending on variables such as use, time, and region. Usually, these criteria are established by national and international agencies in charge of water quality assessment and pollution control.

2.2 Features of water quality in reservoirs

Reservoirs are complex environments, where many variables interact spatially and temporally (TUNDISI; TUNDISI, 2011). As human-made enclosed water bodies, these ecosystem shares characteristics of flowing rivers and lakes (HAYES et al., 2017), relatively new to the current understanding of limnology (LOUCKS; BEEK, 2005). Whereas reservoirs usually present a larger catchment area and perimeter, lakes present higher water residence time and photic zone (HAYES et al., 2017).

Reservoirs exhibit generally longitudinal gradients regarding water quality, with spatial heterogeneity in response to inflow and outflow influence (U.S. Geological Survey, 2018; TUNDISI; TUNDISI, 2011). Often characterized by three zones: riverine, near tributaries entrance, transitional, in the middle of the reservoir, and lacustrine, close to the dam structure (HORNE; GOLDMAN, 1994; TUNDISI; TUNDISI, 2011). This longitudinal zonation, however, is dynamic in time and space depending on flow conditions and reservoir operation (U.S. Geological Survey, 2018), Figure 3.

Generally, the riverine zone has higher sediment and nutrient loading, leading to more eutrophic conditions than the lacustrine zone. And in the lacustrine zone with slower water velocities, there is often nutrient depletion and pronounced thermal stratification (HORNE; GOLDMAN, 1994; TUNDISI; TUNDISI, 2011; HAYES et al., 2017; U.S. Geological Survey, 2018).

Likewise, morphometric features such as size, water depth, and retention time influence reservoir limnological characteristics (STRASKRABA; TUNDISI; DUNCAN,

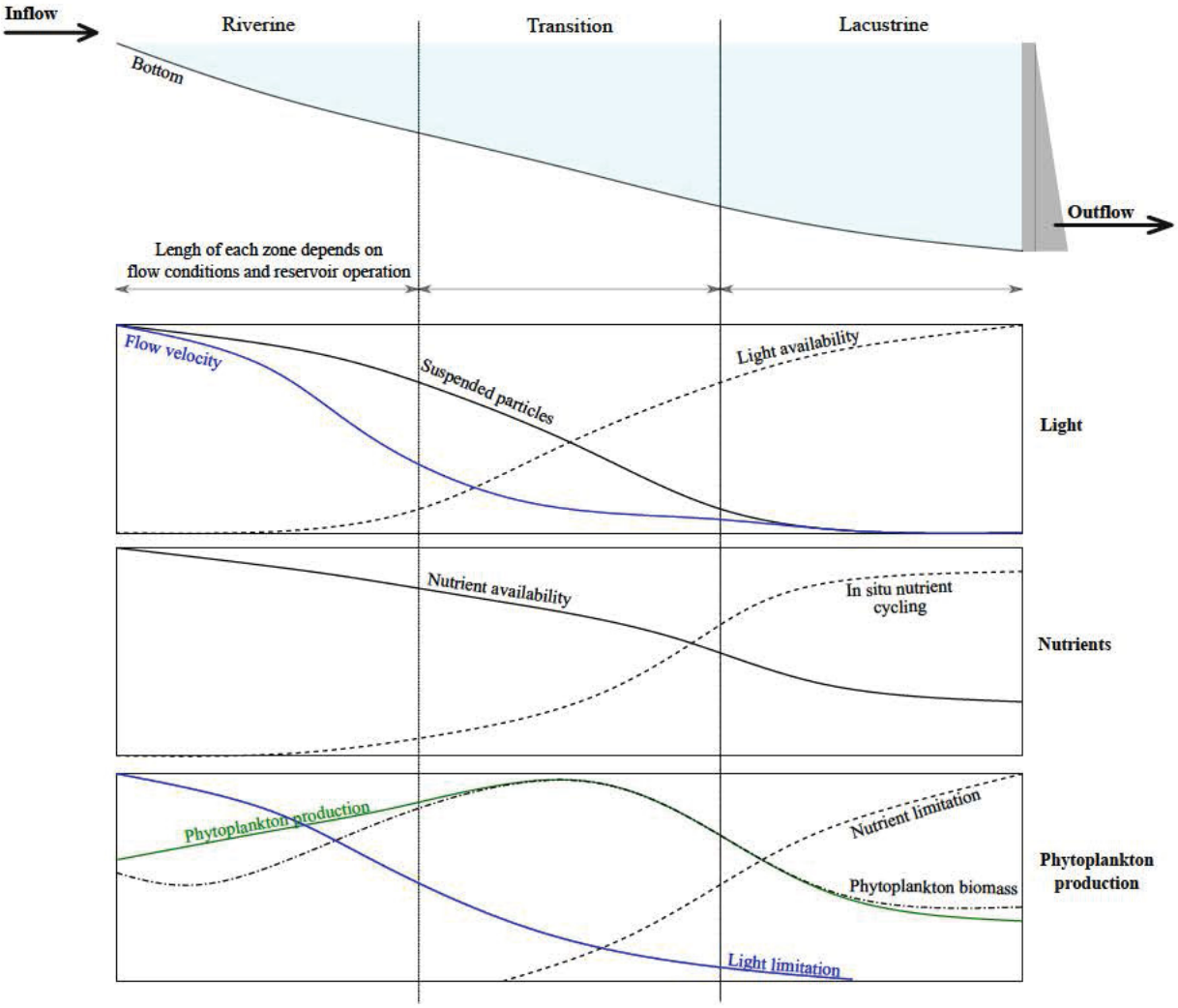

Figure 3 – Representation of cross-sectional view of gradients showing light, nutrients, and phytoplankton production along the longitudinal axis of an reservoir.

Source: Adapted from U.S. Geological Survey (2018)

1993).

The hydraulic retention time is the time required to refill an empty reservoir with its natural inflow and the retention time of a nutrient considers the time necessary for nutrients to enter and pass through the reservoir. These retention times are not usually the same, and the latter affects phytoplankton and zooplankton distribution and reproduction (TUNDISI; TUNDISI, 2011; HORNE; GOLDMAN, 1994).

The residence time of a nutrient is expressed as the relationship between the reservoir's volume (V - m^3) and the average inflow discharge (Q - m^3 / year or days), as indicated in equation 2.1.

$$RT = V/Q \tag{2.1}$$

According to Toné (2016) higher values of residence time indicate a greater

influence of wind action and density gradients influencing the reservoir's water quality. The author also states the importance of residence time on the concentration and distribution of chemical compounds and sediments and highlights that phosphorus retention in the reservoirs is considerably influenced by residence time.

Another important aspect concerning water characterization is the aging of reservoir waters, in which chemical and physical characteristics change during the filling phase of man-made ecosystems. According to Tundisi and Tundisi (2011), changes in thermodynamics and oxygen consumption are the result of primary production and organic matter decomposition. Interactions with drainage basins can impact biogeochemical cycles in the reservoir and downstream.

The aquatic environment quality description usually are achieved through quantitative measurements with physicochemical determinations, and biological tests, together with qualitative descriptions of biotic indices and visual aspects, among many others (CHAPMAN, 1996).

Physical, chemical, and biological characteristics are associated with processes occurring in the water body and the drainage basin. Physical factors vary by day and season, is determined by the distribution of light, heat, waves, and currents. The chemical structure includes the distribution of chemicals such as nutrients and dissolved oxygen. Additionally, the living organisms' distribution overlaps all these abiotic components (HORNE; GOLDMAN, 1994).

2.3 Physical characteristics

Solar energy available on the surface, and distributed over the water column, influences the entire dynamics of the freshwater ecosystem heating transference at the air-water interface. Almost all energy that drives and controls the metabolism of reservoirs is derived from solar radiation, which is converted biochemically via photosynthesis to potential chemical energy (WETZEL, 1983).

Only a portion of solar radiation reaches terrestrial and water surfaces. At the air/water interface, reflection and refraction depend on the angle of light incidence, in which the effects of refraction modify the underwater angular distribution. Moreover, the light on the water surface does not penetrate completely because of both scattering and absorption mechanisms (WETZEL, 1983; TUNDISI; TUNDISI, 2011).

In absorption, as the depth increases light is transformed into heat, resulting in a reduction of light energy, depending on particles suspended in water and dissolved organic compounds. Over half of solar radiation penetrating water is absorbed and dissipated as heat, and the distribution of this heat is influenced by wind energy. Thus, reservoir physics, especially the interaction of light, temperature, and wind mixing established a

great element of reservoir structure, Figure 4 (WETZEL, 1983; TUNDISI; TUNDISI, 2011).

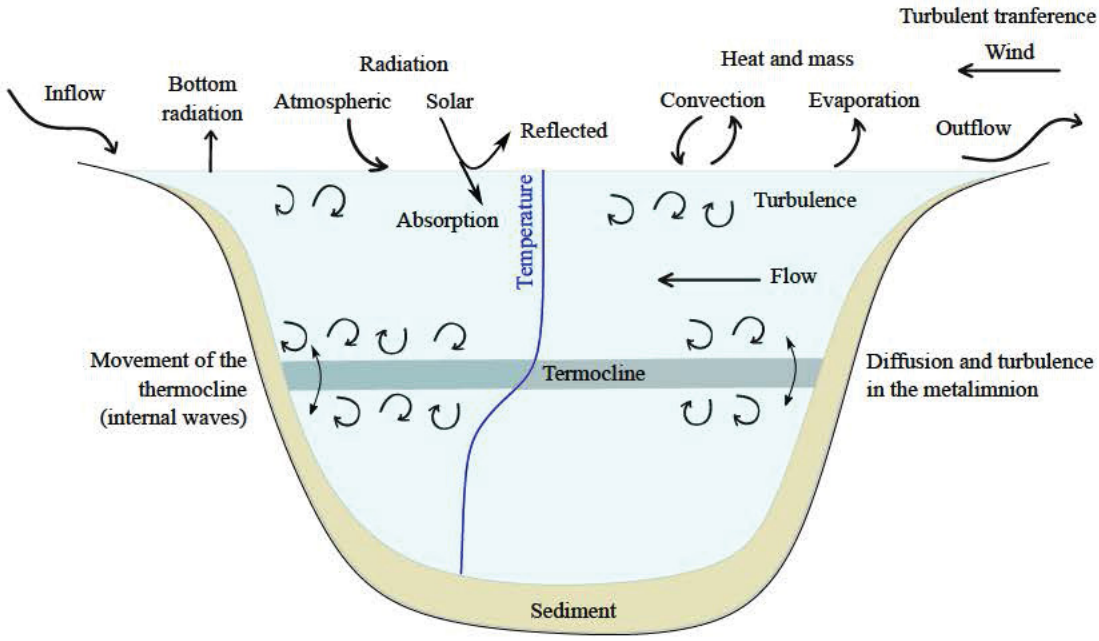

Figure 4 – The different mechanisms of inflow and outflow of mechanical energy, flows, movement of water masses and absorption of solar radiation in reservoirs.

Source: Adapted from Tundisi and Tundisi (2011)

Reservoir structures can be zoned based on the amount of sunlight as a function of depth. The absorption of solar energy and its dissipation as heat determinate thermal structure and circulation patterns of the reservoir (WETZEL, 1983). The photic zone is the sunlit upper water layer. The aphotic zone extends from below the photic zone to the reservoir bottom. As light does not reach these depths, there is no photosynthesis, only respiration consuming oxygen. The length of these depths depends on the water absorption, suspended particulate matter concentration, amount of dissolved organic substances, phytoplankton, and zooplankton (TUNDISI, 1988; HORNE; GOLDMAN, 1994).

Since solar radiation and light distribution in water play an important role in the vertical functioning of aquatic ecosystems, many regular reservoir sampling programs include transparency monitoring (TUNDISI; TUNDISI, 2011). Transparency is easily measured in the field with Secchi disk and indicates, among other features, biological activity level (CHAPMAN, 1996).

Likewise, temperature along the water column presents a vertical gradient, influenced by climatic and hydrological fluctuations (Figure 5). Density variation forms a physical barrier that hinders the mixing of adjacent layers. In the absence of wind action or currents to break density barriers, a three-layered system forming vertical stratification of temperature is exhibited along the water column (TUNDISI, 1988;

HORNE; GOLDMAN, 1994).

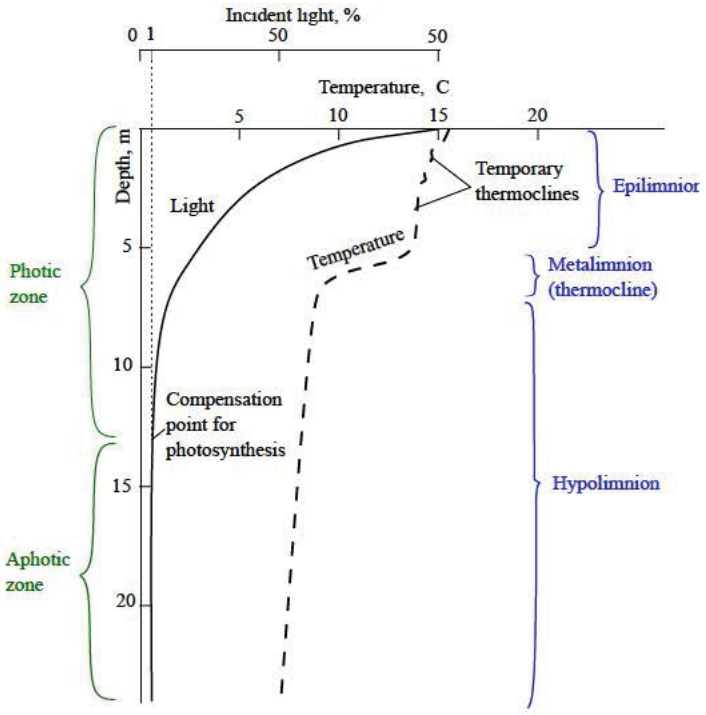

Figure 5 – Thermal structure of a reservoir with depth during period of summer thermal stratification.

Source: Adapted from Horne and Goldman (1994)

Epilimnion is the upper, hotter, and less dense layer of water. Generally, this layer presents a homogeneous pattern due to wind action and thermal heating during the day, proceeding with thermal cooling at night. The dense lower-water and bottommost layer is the hypolimnion. Both layers are separated by a narrow region exhibiting a temperature drop, called metalimnion (TUNDISI, 1988; LOPES; ARRUDA; PAGIORO, 2018; CHAPRA, 1997; HORNE; GOLDMAN, 1994).

Water temperature interferes with physicochemical parameters and biological distribution, and usually presents seasonal patterns due to meteorological and hydrological influence (CHAPRA, 1997). During the summer strong stratification is more likely to occur, while in winter a non-stratified period with intense vertical mixing is observed depending on Climate Zones.

Reservoirs are classified depending on the vertical thermal pattern and frequency of water temperature circulation. Monomictic reservoirs have a once-per-year long mixing period during the winter and autumn and have a stratified water column during the summer and spring. A reservoir presenting two annual periods of circulation, normally in autumn and spring, is called dimictic. A reservoir is polymictic when many periods of circulation occur annually. Lastly, amictic reservoirs, usually located in polar regions and at high altitudes, present year-round ice cover and the absence of the mixing process (ESTEVES, 1998; CHAPRA, 1997; CHAPMAN, 1996).

In tropical reservoirs, higher rainfall is expected in summer and consequently higher water levels. During this period, a water column stratified is often observed. While at winter the water column is usually mixed. Generally, Brazilian reservoirs are polymictic, as a consequence of combined wind action and morphometry (TUNDISI, 1981). Usually shallow, reservoir seasonality is dominated by rain patterns, influencing retention time and water level fluctuations (STRASKRABA; TUNDISI; DUNCAN, 1993).

As an effect of thermal variations, stratification pattern in reservoirs has consequences on several physical and chemical characteristics of the water quality. Including distribution of dissolved gases (such as O_2, CO_2, N_2, CH_4 and others), greenhouse gas emissions, accumulation, and transformations of chemical elements and substances.

The metabolic rate of aquatic organisms, their physiology, and their behavior are related to temperature. As the water temperature rises, the increased metabolic rate of reservoir organisms affects respiration rates leading to additional oxygen consumption and increased organic matter decomposition. Higher water temperatures also lead to increased bacteria and phytoplankton growth rates, resulting in water turbidity, macrophyte growth, and sometimes algal blooms (CHAPRA, 1997; HORNE; GOLDMAN, 1994).

Especially in water column stratification, the lower water column layer presents diminished oxygen rates, and the bottom sediments are submitted to anoxic conditions, where various compounds (ammonia, nitrate, phosphate, sulphide, silicate, iron, and manganese compounds) can diffuse into the lower water layer (BALLANCE; RICHARD; RICHARD, 1996).

Since temperature affects physical, chemical, and biological processes in water bodies, monitoring this variable is essential in the understanding biological and chemical processes in water bodies. Temperature can be measured in situ, using a mercurial thermometer or thermistor electrical thermometers (WETZEL; LINKENS, 2000). Particularly during periods of stratification, is recommended to perform measurements in vertical profiles (CHAPMAN, 1996).

Measurements of temperature associated with chemical analyses are considered key factors in determining the water quality status of a reservoir.

2.4 Chemical factors

Reservoir water's chemical factors are organic and inorganic substances composite. While organisms excrete ammonia (phosphate, and carbon dioxide), the inorganic nutrients are limiting factors for plants' growth (HORNE; GOLDMAN, 1994).

Small quantities of organic compounds usually occur in natural waters. However, human activity, as the agriculture intensification, industry, and urbanization, caused increased concentrations and fluxes of nutrients, organic matter, and toxins in streams. Those substances, when in excess, can compromise water quality, interfering with biological equilibrium. As a result, water quality deteriorates through enhanced eutrophication and reinforced algae growth (KRÖCKEL et al., 2011; BIGGS; DUNNE; MARTINELLI, 2004; JIANG et al., 2017).

Chemical concentrations are considered statics variables since chemical mass indicates the concentration of a certain compound per volume at a particular place and time within the water collection. Moreover, nutrient concentrations are highly dynamic because of their rapid storage, transformation, and excretion processes (WETZEL; LINKENS, 2000).

With this in mind, when collecting samples to further chemical quantification in the laboratory, some procedures must be taken in order to guarantee reliable results and avoid contamination interference. Low concentrations-environments, such as water supply reservoirs, require careful procedures in collecting water samples and further analyzing (APHA, 2006; WETZEL; LINKENS, 2000).

Water samples are usually collected through Van Dorn sampler, device that provides sampling at various depths. Further, samples are transported to the laboratory, where are processed, stored, and analyzed. When required by the chemical form quantification method, total concentrations are separated into fractions, by the filtration process (WETZEL; LINKENS, 2000).

2.4.1 Dissolved Oxygen (DO) and Carbon Dioxide (CO_2)

Dissolved oxygen (DO) and carbon dioxide (CO_2) are closely interrelated in photosynthesis and respiration processes (HORNE; GOLDMAN, 1994). Oxygen is produced by plant photosynthesis, when sufficient light and nutrients are available, and consumed by plants and algae, and animals in respiration. The primary production converts inorganic nutrients into more complex organic molecules storing chemical energy. In the reverse process of respiration and decomposition, when oxygen is consumed and carbon dioxide is liberated, the organic matter is used as an energy source for bacteria and animals.

Whereas DO concentrations reveal a balance between oxygen supply and the metabolic process consumption, depending on several factors: temperature, salinity, turbulence, photosynthesis activity of algae, and atmospheric pressure. Since DO is essential to aerobic aquatic organisms' metabolism involving biological and biochemical reactions, DO is one of the most frequent variables monitored in aquatic environment

investigations (KALFF, 2001; CHAPMAN, 1996).

Reservoir operating rules, advection currents, and phytoplankton bloom significantly affect DO concentrations in reservoir waters. Generally, DO solubility in natural conditions declines with increasing temperature and salinity. Thermal stratification processes usually drive chemical stratification occurrence, characterized by heterogeneous distribution of organic/inorganic compounds and DO gradients along the water column. Due to temperature and biological activity, DO concentrations present daily to seasonal patterns in reservoirs (IAP, 2017; CHAPMAN, 1996).

Diel changes (over 24 hours) depend on sunlight, which determines photosynthesis in the photic zones. At night, oxygen depletes in the overlying water, as a result of bacterial decomposition, and plants are added by invertebrates respiration (HORNE; GOLDMAN, 1994).

Regarding seasonal variations, in eutrophic freshwater reservoirs, winter and fall are usually periods of complete mixing, where oxygen and carbon dioxide levels reach equilibrium with the atmosphere and exhibit a nearly constant oxygen concentration in the entire water column. As thermal stratification occurs, during summer stagnation, DO concentrations increase in the epilimnion and decrease at hypolimnion, and sometimes become anoxic (KALFF, 2001; HORNE; GOLDMAN, 1994).

DO measurements are useful to indicate water pollution level since its consumption is the response to organic compounds degradation process (IAP, 2017). The introduction of untreated sewage in the water body, for instance, not only interferes with water turbidity, but also affects light penetration, and plant growth, and increases microbial activity (respiration) during the degradation of organic matter. (KALFF, 2001; HORNE; GOLDMAN, 1994; CHAPMAN, 1996).

In fresh unpolluted waters at sea level and water temperature of 25°C, DO concentrations range from 8mg/L to 10mg/L. DO concentration less than 5 mg/L affect the functioning and survival of biological communities, and DO concentration below 2 mg/L leads to most fish death. Reduced DO levels not only affect the distribution and growth of fish and invertebrates, but also change the reduction-oxidation state (redox potential), and as a consequence, the solubility of nutrients, metals, and inorganic nutrients (KALFF, 2001; HORNE; GOLDMAN, 1994; CHAPMAN, 1996).

Methods to measure DO concentration include the traditional Winkler method, and alternative methods applied with probes. The measurements provided by these probes are quick, provide measurements in situ, and sometimes continuous monitoring. However, the method requires frequent calibration (CHAPMAN, 1996; WETZEL, 1983).

2.4.2 Organic Carbon

Organic Matter in freshwaters has its origin in primary production, terrestrial organic matter, effluents, and the biota itself. Natural organic compounds control effects on hydrochemical and biochemical processes in water and usually are not toxic, however, could affect water taste and smell (ESTEVES, 1998).

Several factors and variables influence organic matter occurrence, assimilation, and degradation, such as hydrological regime, temperature, solar radiation, biological community, soil characteristic, use, and occupation, among others. Therefore, organic carbon determination and quantification could result in wide properties variations and analysis forms, depending on aquatic system type and source (LEITHOLD et al., 2017; KNAPIK, 2014).

Organic matter in aquatic systems exists as Dissolved Organic Carbon (DOC) and as Particulate Organic Matter (POM). Nutrient cycling, sediment composition, organic production, and decomposition are connected to the carbon cycle through photo-reductive and photo-oxidative processes. Organic matter submitted to photodegradation and biological assimilation (and respiration), can transform into nutrients and inorganic forms of carbon dioxide, Figure 6 (KNAPIK, 2014).

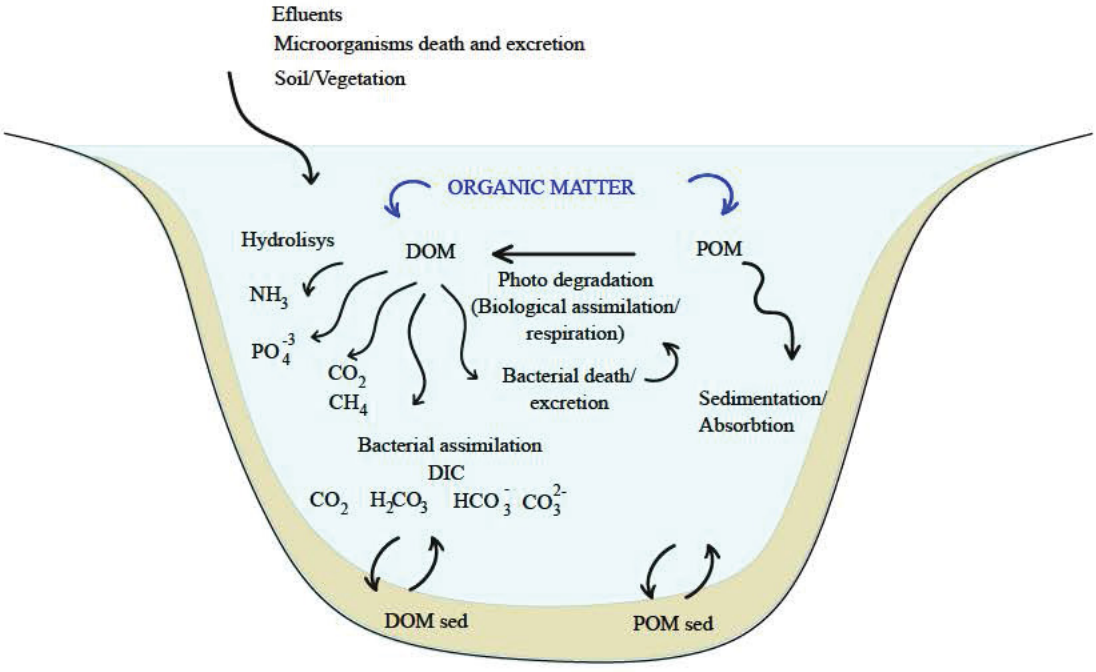

Figure 6 – Schematic representation of organic carbon sources and its pathways between air, water and sediment. DOM is dissolved organic matter and POM is particulate organic matter.

Source: Adapted from Knapik (2014)

Organic matter formed within the aquatic system by photosynthesis, decomposition, and plankton excretion is classified as autochthonous (or aquagenic organic matter). Organic matter from the external origin, carried in water due to runoff

action and atmospheric deposition, is classified as allochthonous, while organic matter from effluents is allochthonous synthetic of anthropogenic sources (LEITHOLD et al., 2017; KNAPIK, 2014).

Regarding composition, organic matter can be classified into two categories: humic and non-humic substances. Non-humic is those substances with easy degradation, formed by carbohydrates, amino acids, peptides, and protein compounds. Humic substance requires greater effort to break since is formed from microbial activity on plant and animal material. The humic substances are separated into three groups according to their acid-base-solubility (i)humin, insoluble at any pH; (ii) fulvic acids, soluble in all pH ranges; and (iii) humic acids, insoluble in acidic solutions - pH <2 (LEITHOLD et al., 2017; WETZEL, 1983; ESTEVES, 1998).

Organic matter in reservoirs is useful to indicate pollution degree, and its concentration can be quantified as dissolved and particulate organic carbon forms in the laboratory, DOC, and POC respectively (SUHETT et al., 2006; CHAPMAN, 1996). Methods for determining organic carbon are based on the principle of carbon oxidation to carbon dioxide (by combustion or chemical reaction) (SUHETT et al., 2006; CHAPMAN, 1996).

Complementary to DOC quantification in the laboratory, Thomas, Baurès and Pouet (2005) proposed the UV spectrophotometry method to investigate organic matter composition and origin, providing qualitative and quantitative information. Moreover, Knapik, Fernandes and Azevedo (2013) proposed the integrated application of UV-visible absorbance and fluorescence spectroscopy methods to characterize the organic matter of a river in an urban watershed. Both methodologies were successfully applied and provided information about the qualitative evaluation of organic matter by indicating its possible composition and, as consequence, its origin.

DOC is the most common form of organic matter in surface waters, and its depth-time distribution does not present strong vertical stratification or seasonal fluctuations (WETZEL, 1983). POC deposition at the water column bottom carries adsorbed substances to sediments, such as metals and organic contaminants, and when associated with organic carbon is transported to the water column (WETZEL, 1983; CHAPRA, 1997).

Brazilian regulation does not establish organic carbon concentration limits, related to organic matter quantification, the regulation establishes Biochemical Oxygen Demand (BOD) limits (CONAMA, 2005; APHA, 2006). BOD is an indirect parameter of matter quantification, represented by the oxygen amount used by the microbial biota to degrade available organic matter during the incubation time.

Monitoring qualitative and quantitative characteristics of organic matter is

important to determine the photo-oxidation rates at large spatial scales, providing characteristics of land use and occupation, pollution sources and water degradation (SUHETT et al., 2006; CHAPMAN, 1996; TUNDISI; TUNDISI, 2011).

2.4.3 Nitrogen

The vast majority of nitrogen on Earth is present as molecular N_2. However, nitrogen exists in several forms in water: nitrate NO_3^-, nitrite NO_2^-, ammonia NH_4^+, and organic nitrogen.

Nitrogen comes naturally from organic and inorganic materials. The main sources of nitrogen in water bodies are precipitation, fixation in water and sediments, and inputs from surface and groundwater drainage. On the other hand, nitrogen outputs include effluent from the basin, reduction by bacteria oxidative forms to N_2, which returns to the atmosphere, and inorganic/organic sedimentation to the sediments, Figure 7 (WETZEL, 1983).

Molecular N_2 gas is converted to reactive, biologically available forms of nitrogen through a process called fixation, which is controlled by ecological factors related to external inputs and water characteristics (APHA, 2006).

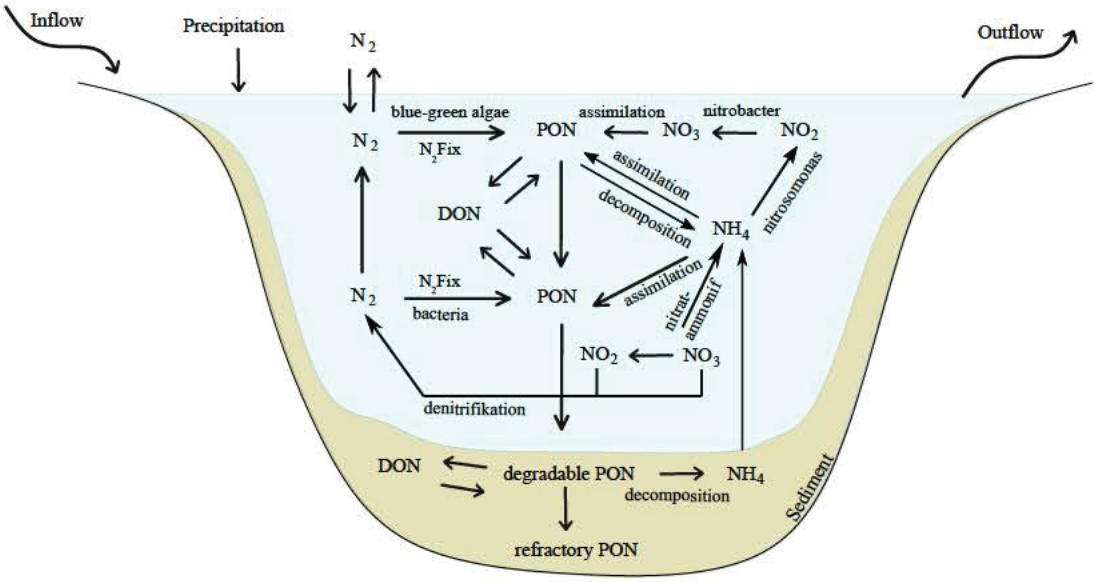

Figure 7 – Nitrogen cycle: a representation of major nutrients inputs, transformation pathways, and outputs to a general reservoir system. PON is particulate organic nitrogen and DON is dissolved organic nitrogen.

Source: Adapted from Wetzel (1983)

In recent decades, nitrogen concentrations have increased in aquatic systems caused by anthropogenic activity, such as fertilizer application, crop nitrogen fixation, and urban, and agricultural wastes (YAO et al., 2018; BURT et al., 2010; BURT et al., 2011).

Since ammonia and nitrate are essential nutrients for photosynthesis, nitrogen can be the nutrient element that most limits plants' growth, especially in eutrophic or oligotrophic environments. Nitrogen, when in excess stimulates plant growth, increase algal bloom episodes, and oxygen consumption in biochemical processes (CHAPRA, 1997).

Ammonia occurs naturally from organic matter from soil and water, as a product of organic matter decomposition, nitrogen gas reduction by micro-organisms, and from the gas exchange with the atmosphere (CHAPMAN, 1996). In many reservoirs, ammonia is the most significant source of nitrogen (WETZEL, 1983), and at high concentrations depending on the pH level is harmful to aquatic life (CHAPMAN, 1996).

In fresh waters, ammonia distribution varies depending on location, season, level of pollution from organic matter, and the reservoir productivity level (WETZEL, 1983). Death and decay of aquatic organisms, such as phytoplankton and bacteria, also cause ammonia natural seasonal fluctuation (CHAPMAN, 1996).

Usually, after periods of circulation in oligotrophic waters, ammonia is found in low concentrations. However, in stratified reservoirs, phytoplankton consumes ammonia in the epilimnion and at the vertical profile, bottom ammonia can accumulate and accelerate the process of anoxia. At conditions with nitrate reduction, the bacterial nitrification ceases, and NH_4^+ is not converted to NO_3^- and NO_2^- forms. At this condition, sediments could also release NH_4^+ (WETZEL, 1983).

Ammonia is a useful indicator of organic pollution, and higher concentrations may be related to recent domestic sewage, industrial waste, and fertilizer runoff. Unpolluted waters contain small amounts of ammonia, usually less than 0.1 mg/L, but may reach 2 to 3 mg/L (CHAPMAN, 1996). The Brazilian water resources regulation establishes the range limit related to pH level (CONAMA, 2005).

Regarding ammonia concentration quantified in the laboratory, since water samples can change quickly and commonly present low concentrations, ammonia detection should be analyzed within 24 hours from collection. For waters with little or no pollution, a suitable method for quantifying ammonia is a colorimetric method using the phenate method. In this method, ammonium reacts with phenol and hypochlorite under alkaline conditions to form indophenol blue, and the color developed is proportional to ammonium concentration (CHAPMAN, 1996; APHA, 2006; WETZEL; LINKENS, 2000).

In the nitrification process, organisms (such as bacteria, and fungi) convert inorganic nitrogen compounds from a reduced state (NH_4^+) to an oxidized state (NO_3^- and NO_2^-). Contrarily, in the denitrification process (or nitrate reduction), nitrate is assimilated by algae and reduced to ammonia. In eutrophic reservoirs, this process influences the vertical distribution of nitrate.

Nitrate is the nitrogen form most found in streams and reservoirs because it is related to land-use practices in the watershed, waste discharges from agricultural fertilizers, and waste discharges (JIANG et al., 2017). Seasonal fluctuations of nitrate depend on aquatic plant growth and decay (WETZEL; LINKENS, 2000), and in tropical reservoirs, nitrate concentration is related to water column oxygenation degree strongly influenced by nitrifying and denitrifying bacteria.

Natural concentrations rarely exceed 0.1 mg/L and above 5 mg/L usually indicates pollution by human/animal waste or fertilizer runoff (CHAPMAN, 1996). High nitrate concentrations contribute to jeopardizing the health of human beings. The health effects of nitrates are associated with inducing methemoglobinemia in infants and possibly stomach cancer. Thus a limit of 10 mg/L has been imposed on drinking water to prevent disorders in many countries and in Brazil established by the Brazilian water resources regulation, (APHA, 2006; JIANG et al., 2017; CONAMA, 2005).

Nitrite is an intermediate oxidation state of nitrogen and is usually present in very small quantities (WETZEL, 1983). Its production processes in aerobic waters include the oxidation of ammonia and assimilatory nitrate reduction by phytoplankton and heterotrophic bacteria. These oxidation and reduction processes may occur in wastewater treatment plants, water distribution systems, and natural waters (TEMINO-BOES et al., 2019; APHA, 2006).

In eutrophic reservoirs, during the periods of thermal stratification, nitrite concentration increases, as a consequence of denitrification processes during the hypolimnion anoxia period (ESTEVES, 1998).

Usually, in reservoirs nitrite concentration compared to the ammonia and nitrate concentration is low (in the range of 0.001 mg/L), only in polluted reservoirs nitrite concentration can assume significant values. High nitrate concentrations are associated with the unsatisfactory microbiological quality of water and are indicative of industrial effluents. In Brazil, the current regulation establish a limits of 1 mg/L for all freshwater classes (ESTEVES, 1998; CHAPMAN, 1996; CONAMA, 2005).

For nitrate and nitrite quantification, samples should be collected in glass or polyethylene bottles and filtered. Nitrate concentration is usually determined by reducing to nitrite in an alkaline-buffered solution through copperized cadmium metal fillings. However, nitrate can also be determined with optical sensors. Subsequently, both nitrite and the reduced nitrate are quantified using spectrophotometric methods (APHA, 2006; WETZEL; LINKENS, 2000).

Finally, organic nitrogen consists of particulate and dissolved organic detritus generally not available to photosynthetic organisms. Organic nitrogen is usually determined by using the Kjeldahl method (APHA, 2006; WETZEL; LINKENS, 2000;

CHAPMAN, 1996).

Nitrate, nitrite, and ammonia are compounds directly related to production and decomposition processes. Associated with carbon and oxygen concentrations, determining the predominant form of nitrogen can provide information on the pollution stage caused by upstream sewage release. While organic nitrogen or ammonia indicates recent pollution, nitrate indicates a lately one (SPERLING, 2007; ESTEVES, 1998).

Since nitrogen forms give a general indication of the nutrient status and level of organic pollution, these species are included in most basic water quality surveys and multipurpose monitoring programs (CHAPMAN, 1996).

Although monitoring nitrogen importance, nitrogen form determination in reservoir required extensive measurements due to the expected spatial and temporal variability (WETZEL, 1983). In eutrophic reservoirs, the ammonia concentration in summer at the epilimnion can fluctuate over periods of few days (HORNE; GOLDMAN, 1994).

2.4.4 Phosphorus

Phosphorus is essential to organisms' growth, and is usually the growth-limiting nutrient for primary productivity. In general, compared to other macronutrients, phosphorus concentration is low, due to the reduced solubility and phosphate tendency to bind with finely granulated particles. Phosphorus in water is found in solution, particles, detritus, or in aquatic organisms, and at the bottom sediment, as precipitated inorganic form and incorporated into organic compounds (CHAPMAN, 1996; WORSFOLD; MCKELVIE; MONBET, 2016).

According to Esteves (1998), phosphorus in water can be quantified as particulate phosphate (P - particulate), Dissolved Organic Phosphate (DOP), Dissolved Inorganic Phosphate or Orthophosphate or Reactive Phosphate (Ortho-P), Total Dissolved Phosphate (TDP), and total phosphate (PT).

Phosphorus dynamic in reservoirs involves organic and inorganic forms in both soluble and particulate phosphorus. Available inorganic phosphorus is the reactive soluble phosphorus, also called orthophosphate, being the form directly available to plants and algae. Particulate organic phosphorus consists of living organisms (plants, animals, algae, and bacteria). Particulate inorganic phosphorus comprises phosphate minerals, adsorbed orthophosphate, and phosphate complexed in solids. Nonparticulate unavailable organic phosphorus is composed of dissolved organic compounds that contain phosphorus, which is not available to aquatic organisms and is, thus, derived from the decomposition of particulate organic phosphorus (CHAPRA, 1997). Among all these phosphorus forms, phytoplankton can use only soluble phosphate (PO_4^{-3})

(HORNE; GOLDMAN, 1994; CHAPMAN, 1996).

Under natural conditions, the main sources of phosphorus are from the land by weathering of phosphorus-bearing rocks and organic matter decomposition, Figure 8. Catchment contributions are dominant and contribute to elevated phosphorus concentration levels, when influenced by human activities, such as domestic wastewaters, industrial effluents, and fertilizer runoff. Those conditions could lead the reservoir to eutrophication process (CHAPMAN, 1996; WORSFOLD; MCKELVIE; MONBET, 2016; XU et al., 2010; SPERLING, 2007).

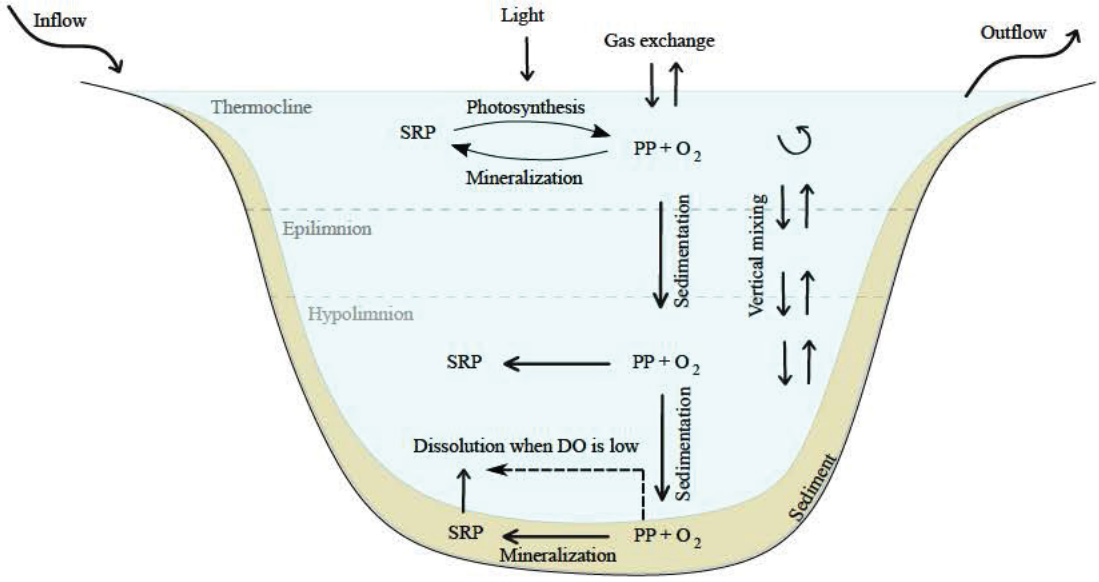

Figure 8 – Phosphorus cycle: a representation of major nutrients inputs, transformation pathways, and outputs to a general reservoir system. PP is the particulate phosphorus present in organic form as biomass. SRP is soluble and organic phosphorus.

Source: Adapted from Kalff (2001)

Phosphorus is mostly found in water in an organic form, from living or dead biomass (particulate phosphorus - PP). Soluble and organic phosphorus (SRP) are excreted by zooplankton, fish, and bacteria, and the decomposition of dead plants and animals releases organic phosphorus and phosphate, Figure 8 (HORNE; GOLDMAN, 1994; ESTEVES, 1998)

As phosphate tends to bind with granulated particles, sedimentation and excretion from planktonic organisms remove the phosphorus from the water column by transporting it to the bottom. Phosphate sedimentation is also associated with iron, aluminum, sulfide, organic compounds, and carbonates. Depending on the sediment-water interface conditions a phosphorus reservoir can be formed, in which phosphate could accumulate in the interstitial water and become chemically bound with sediment contains (SPERLING, 2007).

Under aerobic conditions, the sediment-water interface is oxygenated and has an oxidation layer acting as a barrier preventing phosphate releases into the water column.

Phosphate ions are precipitated at the sediment and do not pass freely to the water. However, when the water column is thermally stratified, and the sediment-water interface is anoxic (or with low oxygen concentrations), the hypolimnion becomes anaerobic and these layer becomes less thick and may even disappear. And, therefore, phosphate ions can pass across and resuspend to the water column, sometimes associated with organic and mineral constituents of sediments (HORNE; GOLDMAN, 1994; ESTEVES, 1998; CHAPMAN, 1996).

In Brazilian inland waters, phosphorus bound with iron ions is very common, due to acid and high iron concentration characteristics of most waters (ESTEVES, 1998).

Reservoirs with clinograde oxygen curves usually present variable vertical phosphorus distribution, marked with increased soluble and total phosphorus concentrations at the lower hypolimnion. On the other hand, oligotrophic reservoirs with orthograde oxygen curves show little variation in phosphorus content with depth (WETZEL, 1983).

Over the winter, phosphate is expected to accumulate, since remaining phosphorus compounds are consumed by algae and recycled back to phytoplankton via excretion from fish, zooplankton, and bacterial activity (HORNE; GOLDMAN, 1994).

Phosphate concentrations usually present values near analytical detection limits, making it difficult to precisely quantify (HORNE; GOLDMAN, 1994). In most natural surface waters, phosphorus ranges from 0.005 to 0.020 mg/L. In tropical reservoirs, the orthophosphate concentrations can be even lower, due to the effects of high temperature, in which the organism's metabolism increases and these compound is even more rapidly assimilated, and incorporated into biomass (ESTEVES, 1998).

For analytical purposes, according to APHA (2006) and Cade-Menun, Navaratnam and Walbridge (2006), total phosphorus as the dissolved form is determined by digestion and colorimetric techniques, and suspended fractions generally are determined by difference. The total phosphorus quantification covers all forms of phosphorus, and it was determined using unfiltered samples. If samples are filtered, total dissolved phosphorus and dissolved orthophosphate can be quantify (HORNE; GOLDMAN, 1994).

Since phosphorus could occur in combination with organic matter, a digestion method that releases phosphorus as orthophosphate is necessary to determine total phosphorus, by oxidizing organic matter effectively (APHA, 2006). To release phosphorus in combination with organic matter, it is necessary a digestion or wet oxidation technique. Orthophosphate reacts with ammonium molybdate to form molybdophosphoric acid, which in contact ascorbic acid is reduced to molybdenum blue - an intensely colored complex. Then, phosphorus fractions are quantified are using

spectrophotometric methods. In function of the digestion procedure, realized with strongly acidic reagents, before the residual disposal, pH correction must be performed (BALLANCE; RICHARD; RICHARD, 1996; WETZEL; LINKENS, 2000; HORNE; GOLDMAN, 1994).

Phosphorus quantification is often included in basic water quality surveys or background monitoring programs, despite difficulties and challenges in obtaining its concentrations. Particularly for water supply, phosphate levels need to be monitored, because could indicate rates and trends of algal growth (CHAPMAN, 1996).

2.5 Biological zonation

Physical and chemical variables provide water quality information. However, biomonitoring has been proven to complement biological data those traditional monitoring techniques, because they reflect long-term environmental changes (FERRARESI, 2015).

Since biological organism depends on chemical and physical variables, the characterization of these organism's communities indicate the current status of ecological and surface water degradation through its occurrence, absence, abundance, physiology, morphology, and diversity (FERRARESI, 2015).

There are several organisms in the water body, plankton is floating organisms that depend on waves and currents to move around, zooplankton are animals of this group, algae are termed phytoplankton, and benthic organisms are those located at the reservoir bottom (HORNE; GOLDMAN, 1994).

Algae is assessed to identify and quantify thought photosynthetic pigments presence of chlorophylls, carotenoids, and biliproteins. Among those pigments, Chlorophyll-a is the primary photosynthetic pigment of all oxygen-evolving photosynthetic organisms. Therefore, chlorophyll-a concentrations represent an indicator of phytoplankton biomass (WETZEL, 1983; ESTEVES, 1998).

Chlorophyll-a is traditionally tracked in water quality surveys and monitoring programs performed in reservoirs since chlorophyll-a concentrations are usually considered in water quality indices calculations as an indication of the trophic status of a water body (ESTEVES, 1998). When in excess, algae growth can give taste and odor to the water. Therefore, Chlorophyll-a measurements are especially important for the management of water abstracted for drinking water supply (CHAPMAN, 1996).

Chlorophyll-a concentrations fluctuate depending on the water depth, and from daily to seasonall basis, since primary production variability is influenced by temperature, nutrient cycles (nitrates and phosphates), hydrological cycles, rainfall, and

water level fluctuations (STRASKRABA; TUNDISI; DUNCAN, 1993). Changes in biological variables generally result from the abiotic environment or biological variables (FERRARESI, 2015).

Many studies have been performed by monitoring the association of physical and chemical variables with biological (CATHERINE et al., 2012; SILVA et al., 2016; XU et al., 2010; HENNEMANN; PETRUCIO, 2010). Indeed, biological data provide information for water body dynamics understanding (SADEGHIAN et al., 2018).

Moreover, many techniques have been developed and validated to facilitate biological factors monitoring (CATHERINE et al., 2012; CHEN et al., 2015), the more advanced ones can provide real-time measurements (SORENSEN et al., 2018).

All elements cited herein provide a way to describe many important reservoir features. However, the mentioned quantifications produce various types of data, which need post-processing and interpretative analyses to result in a water quality evaluation.

2.6 Water quality management indexes

Water quality can be assessed by monitoring physical, chemical, and biological parameters. In spite of that, in a reservoir, several ecological, economic, and social variables interact in space and time forming a complex environment. Hence, water quality indicators and indexes can be useful, whereas usually provide a single number defining an overall status of a water system, based on combined water quality variables (SENGUPTA; DALWANI, 2008; TYAGI et al., 2013)

The water quality index allows for the reduction of information bulk into a single value to express the data in a simplified and logical form, and transform the information into understandable and usable by the public and legislative decision-makers (TYAGI et al., 2013). Generally, data from multiple parameters are weighted according to the importance level of the overall water quality and further incorporate into a mathematical equation (SENGUPTA; DALWANI, 2008; UNEP, 2007).

Temporal variability and trends in water quality can be assessed using water quality indexes (TYAGI et al., 2013) to define monitoring strategies to detect changes in physicochemical parameter concentrations (POONAM; TANUSHREE; SUKALYAN, 2013).

Nevertheless, despite the benefits of indexes usage herein indicated, water quality indexes can disassemble varied conditions in the environment by converting complex phenomena to a single value or assessment. If properly employed, water quality indexes are a communicative tool, as long its intrinsic limitations are understood and an individualized evaluation of each index component is assessed to avoid subjectivity

(SPERLING, 2007).

A Water Quality Index (WQI) was initially proposed by Horton (1965), selecting the ten most commonly used water quality variables. Furthermore, Brown et al. (1970) also developed an index based on the weights of the individual parameters. Afterward, Steinhart;, Schierow; and Sonzogni (1982) applied a novel environmental quality index, to sum up, technical information on the status and trends in the Great Lakes ecosystem (POONAM; TANUSHREE; SUKALYAN, 2013; TYAGI et al., 2013; SENER; SENER; DAVRAZ, 2017).

Further Brown et al. (1970) developed an index, The National Sanitation Foundation Water Quality Index (NSFWQI), to provide a standardized method, considering nine main water quality parameters monitored: temperature, pH, dissolved oxygen, turbidity, fecal coliform, biochemical oxygen demand, total phosphates, nitrates, and total solids. NSFWQI was popularized and used as a base for several index adaptations (SENER; SENER; DAVRAZ, 2017).

Recently, many different methods for index calculations have been developed by several scientists and experts. Examples of different water quality indexes developed worldwide are Oregon Water Quality Index (OWQI), Bhargava method, Smith's index, British Columbia Water Quality Index (BCWQI), Canadian Council of Ministers of the Environment (CCME) Water Quality Index (WQI), Overall Index of Pollution (OIP), The River Ganga Index, Water quality index, Recreational water quality index (RWQI), Contamination index (CI) (TYAGI et al., 2013; POONAM; TANUSHREE; SUKALYAN, 2013).

Despite the many scientists' efforts to determine a universally acceptable general water quality index (SREBOTNJAK et al., 2012; RICKWOOD; CARR, 2009), the concept of water quality varies according to use and depends upon the prevailing conditions, time, and region.

Furthermore, the trophic classification is especially challenging in reservoirs, due to the potential spatial heterogeneity, usually presenting a tendency ranging from eutrophic conditions on the upper portion of the reservoir to oligotrophic conditions closer to the dam structure. A trophic classification of a reservoir can be misleading depending on the sampling station location, making it necessary to segment the reservoir into different regions for water quality distinction (CHAPMAN, 1996).

2.6.1 Trophic State Index (TSI)

The Trophic State indexes evaluate the water quality regarding the eutrophication process, by considering nutrient enrichment effects. The TSI index was developed by Carlson (1977) for temperate environments, and it is one of the most used

water quality indexes (MERCANTE; TUCCI-MOURA, 1999). The index relates transparency, chlorophyll-a, and total phosphorus concentrations to rank the aquatic system in trophy degree.

Since aquatic system metabolism in temperate regions differs from those found in tropical environments, the TSI index has undergone modifications to suit the limnological conditions of tropical reservoirs (LAMPARELLI, 2004).

Salas and Martino (1991) proposed a trophic state classification increasing upper limits for the oligotrophic, mesotrophic, and eutrophic status regarding TP and Chl-a concentrations. Later, Lamparelli (2004) analyzed water quality data of several rivers and reservoirs in Brazil from 1996 to 2001 and proposed TSI index equations through a modified Carlson's TSI equation for chlorophyll-a, transparency, and total phosphorus applied to river and reservoir environments, Table 1.

Table 1 – Trophic State Index (TSI) and concentration ranges of total phosphorus, chlorophyll-a, and transparency for each trophic status for both river and reservoirs environments

		Ultra-oligotrophic	Oligotrophic	Mesotrophic	Eutrophic	Super-eutrophic	Hyper-eutrophic
Riv.[1]	TP (mg/L)	≤ 0.013	0.013 - 0.035	0.035 - 0.137	0.137 - 0.296	0.296 - 0.640	>0.640
	Chl-a (ug/L)	≤ 0.74	0.74 - 1.31	1.31 - 2.96	2.96 - 4.70	4.70 - 7.46	>7.46
	S[3] (m)	≥2.4	2.4 - 1.7	1.7 - 1.1	1.1 - 0.8	0.8 - 0.6	<0.6
	TSI	≤ 47	47 - 52	52 - 59	59 - 63	63 - 67	≥ 67
Res.[2]	TP (mg/L)	≤ 0.008	0.008 - 0.019	0.019 - 0.052	0.052 - 0.120	0.120 - 0.233	>0.233
	Chl-a (µg/L)	≤ 1.17	1.17 - 3.24	3.24 - 11.03	11.03 - 30.55	30.55 - 69.05	>69.05
	S[3] (m)	≥ 2.4	2.4 - 1.7	1.7 - 1.1	1.1 - 0.8	0.8 - 0.6	<0.6
	TSI	≤ 47	47 - 52	52 - 59	59 - 63	63 - 67	≥ 67

Source: Adapted from Lamparelli (2004)
[1]Rivers
[2]Reservoirs
[3]Secchi Depth

Moreover, Lamparelli (2004) proposed a 'supereutrophic' category, which divides the eutrophic and hypereutrophic classes. These indexes present higher sensitivity, amplified the trophic classifications, and improved the agreement between chlorophyll-a and total phosphorus concentrations.

According to Sperling (2007), while the phosphorus index indicates eutrophication potential, the chlorophyll-a index refers to algae growth level. The average between both indexes incorporates the process' cause and effect.

2.6.2 Water Quality Index of Reservoirs (WQIR)

In the state of Paraná in Brazil, the Water and Earth Institute (IAT, https://www.iat.pr.gov.br/) periodically monitored 24 reservoirs to systematically evaluate the water quality of hydroelectric and water supply reservoirs from 1999 to 2013 (IAP, 2017). Unfortunately, since the monitoring program depends on public resources, it was canceled in 2020.

The monitored parameters by IAT were water temperature*, dissolved oxygen concentration*, transparency (Secchi depth)*, pH*, total alkalinity, electrical conductivity, Chemical Oxygen Demand (COD), Biochemical Oxygen Demand (BOD_5), nitrate*, nitrite*, ammonia nitrogen*, Kjeldahl nitrogen, total phosphorus*, turbidity*, chlorophyll-a*, phytoplankton* and zooplankton*. The variables analyzed in this study are the ones marked in the last sentence.

From the results of the above-mentioned monitoring, a water quality index (Water Quality Index of Reservoirs - WQIR) was developed based on pollution levels combined with physical, chemical and biological, morphometric, and hydrological variables (IAP, 2009). This index was formed by impairment classification matrix level, with nine variables (oxygen deficit, total phosphorus, total inorganic nitrogen, chlorophyll-a, transparency, COD, residence time, mean depth, and cyanobacteria). In calculating the index, a weighted average of all the variables is performed, and the importance level of each variable is considered based on different weights - Table 2.

Altogether, the reservoirs can be classified concerning the level of impairment into six distinct classes: Class I - Non-impacted to very little degraded, Class II - Little degraded, Class III - Moderately degraded, Class IV - Critically degraded to polluted, Class V - Very polluted and Class VI - Very polluted.

The WQIR class is determined by weight additive method thought the equation 2.2, taking into account the variable weight (w_i) and class (q_i) describe in Table 2.

$$RWQI = \frac{\sum(w_i.q_i)}{\sum w_i} \tag{2.2}$$

At Depth I, calculated as equation 2.3, lies the euphotic zone with 40% of the incident light layer, it is where primary phytoplankton production is expected.

$$DepthI = z_{sd}0.54 \tag{2.3}$$

The z_{sd} is the Secchi disk depth (m) and 0.54 is the factor to calculate 40% of incident light. At Depth II (equation 2.4), respiration and decomposition predominate over autotrophic production.

Table 2 – Water Quality Index of Reservoirs (WQIR) classes, concentration range and weight of its variables considered for the index calculation.

	Weight	CLASS I[6]	CLASS II[7]	CLASS III[8]	CLASS IV[9]	CLASS V[10]	CLASS VI[11]
		Not impacted to very poorly degraded	Poorly degraded	Moderately degraded	Critically degraded or polluted	Heavily polluted	Extremely polluted
Oxygen deficit (%)	17	≤ 5	6-20	21-35	36-50	51-70	>70
TP[1] (mg P/L)	12	≤ 0.010	0.011-0.025	0.026-0.040	0.041-0.085	0.086-0.210	>0.21
TIN[2] (mg N/L)	8	≤ 0.15	0.16-0.25	0.26-0.60	0.61-2.00	2.00-5.00	>5
Chl-a[3] (µg/L)	15	≤ 1.5	1.5-3.0	3.1-5.0	5.1-10.0	11.0-32.0	>32
Secchi Disk (m)	12	≥ 3	3-23	2.2-1.2	1.1-0.6	0.5-0.3	<0.3
COD[4] (mg/L)	12	≥ 3	3-5	6-8	9-14	15-30	>30
Residence Time (days)	10	≤ 10	11-40	41-120	121-365	366-550	>550
Average Depth (m)	6	≥ 35	34-15	14-07	6-3.1	3-1.1	<1
Cyanob.[5]	8	≤ 1000	1001-5000	5001-20000	20001-50000	50001-100000	>100000

Source: Adapted from IAP (2009)
[1]Total Phosphorus
[2]Total Inorganic Nitrogen
[3]Chlorophyll-a
[4]Chemical Oxygen Demand
[5]Cyanobacteria (cell number/mL)
[6]CLASS I: Reservoir with excellent or optimal quality - oxygen saturated water bodies, low concentration of nutrients, algae and organic matter, high transparency, short residence time and high average depth.
[7]CLASS II: Good quality - small input of organic and inorganic nutrients and organic matter, small DO depletion.
[8]CLASS III: Acceptable quality - considerable DO deficits and near-bottom anoxia at certain times. Medium intake of nutrients and organic matter and wide variety of algae with moderate tendency to eutrophication.
[9]CLASS IV: Critical quality - organic matter input can produce critical DO depletion, considerable nutrient input, and high tendency to eutrophication. Low water transparency associated with high biogenic turbidity. Also, fish death can occur.
[10]CLASS V: Very poor quality - At high nutrient concentrations, with supersaturation of dissolved oxygen in the surface layer and depletion in the bottom layer. Eutrophic water bodies with algae blooms.
[11]CLASS VI: Poor quality - Severe pollution from organic matter or other DO consuming substances. Anoxia may occur throughout the water column. Intense algae blooms and possible presence of toxic substances.

$$DepthII = \frac{z_{max} + z_{eu}}{2} \tag{2.4}$$

Where z_{max} is total depth and z_{eu} is considered as euphotic zone, corresponding to 3 times the Secchi depth (approximately 1% of the water surface incident light). Finally, Depth III occurs only when there is water column anoxia and is given by the mean between the beginning and ending depths of the anoxic zone.

The average of the entire water column measurements are taken into account for DO deficit. For total phosphorus, total inorganic nitrogen, and DOC, should be used as the mean of Depth I and II. At last, for chlorophyll and cyanobacteria only concentration at Depth I is required.

Despite the reductionist aspect, the use of the water quality index provides standards for the assessment of water quality and relevant information to support and define monitoring strategies for decision-making for environmental conservation by public authorities.

2.7 Water Quality Monitoring

Water quality monitoring is the basis for management and assessment, because provides data for the identification of variability, understanding, protection, and improvement of the environmental system (BALLANCE; RICHARD; RICHARD, 1996; JIANG et al., 2020). By investigating dominant processes and reactions in-water, integrated management strategies can be generated to ensure the necessary quality for public supply (CHAPMAN, 1996).

Water quality monitoring data not only provide information to governments but also to the scientific community and the public (CHAPMAN, 1996). Since, water quality monitoring provides information on spatial-temporal changes, due to differences in background concentrations, pollution sources, or hydrological conditions (CHEN et al., 2012).

Assessment of water quality conditions through several monitoring stations at selected sites operating in coordination constitutes a water quality monitoring network (HARMANCIOGLU; OZKUL; ALPASLAN, 1999). One of the main objectives of a water quality monitoring network is to capture and understand variables patterns and temporal evolution in terms of the presence, variability, or occurrence of different parameters (MARCÉ et al., 2016).

Therefore, the sampling frequency of a monitoring program must be capable of registering environmental change with a high degree of sensitivity, and even providing information on unforeseen change (KLEEMOLA, 1998). An inadequate sampling rate

could result in loss of environmental information and sometimes distorting the data obtained (MARCÉ et al., 2016).

However, water quality processes usually present different time scales, increasing the complexity involved in defining the temporal variation of water quality variables (Figure 9). Water column circulation could present daily variability linked to meteorological conditions and aquatic body size. A daily dynamic is also observed in biological cycles limited and connected to light-dark cycles, while pollution sources together with climate factors usually present day-to-month variability, reflecting seasonal fluctuations (CHAPMAN, 1996).

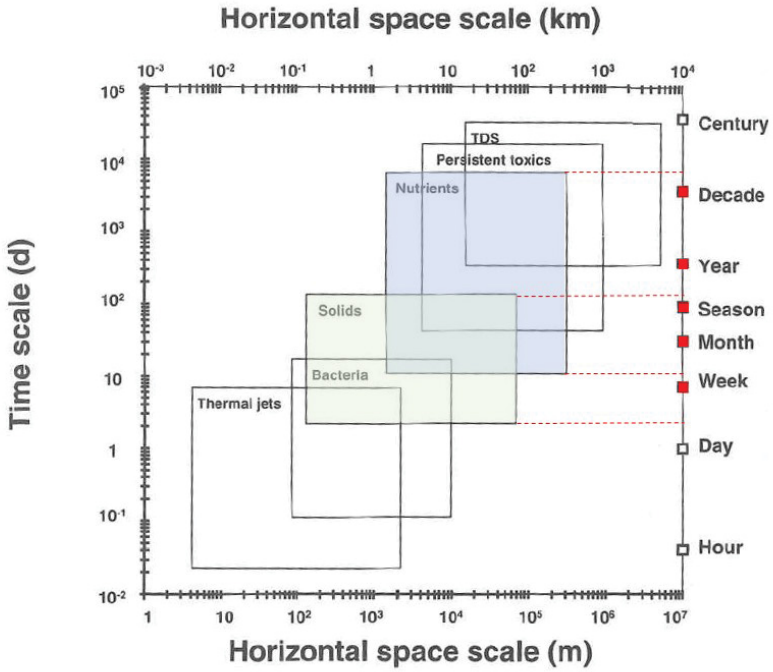

Figure 9 – Time and spatial scales of water quality variables.

Source: Adapted from Chapra (1997)

Additionally, a monitoring program requires resources, trained manpower, a well-equipped laboratory, equipment and material for fieldwork, and transportation to the study site. Thus, an optimal program definition could improve monitoring performance and minimize costs, since could reduce field effort in sampling, processing, and analyzing samples by defining assertive locations and frequency (TALEBBEYDOKHTI et al., 2017).

Nevertheless, spatial variation in water quality depends on the main features and hydrodynamic characteristics of the aquatic body (Figure 10). Surface water hydrodynamic characteristics, such as flow direction, discharge, and time, determine spatial dynamics in the water quality. In reservoirs, water quality varies in three dimensions influenced by changes in inflow discharge, water column stratification, and time (CHAPMAN, 1996).

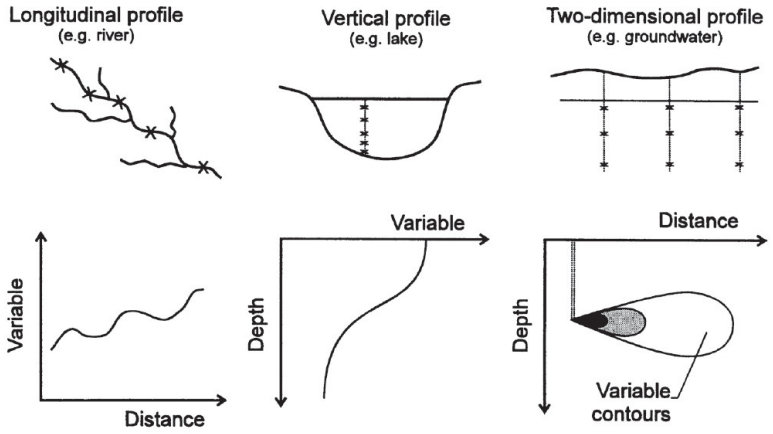

Figure 10 – Description of spatial variations in water quality variables in both horizontal and time scale.

Source: Chapman (1996)

According to HEM (1985), although associated changes in water composition due to the stratification process in reservoirs are frequently observed, most samples from water supply reservoirs are located close to the outlet, due to practical and economical reasons.

Therefore, the purpose, scale, and constraints delimitate the monitoring resolutions. Among the constraint in designing a monitoring network, there are costs (financial resources), available technologies, location accessibility, data availability of monitoring data, hydrological model, and natural, and social conditions (JIANG et al., 2020). Additionally, the environmental pollution degree could also lead to different sampling frequencies (TORRES et al., 2022).

2.7.1 Water Quality Monitoring Networks

The key questions when structuring a water quality monitoring network are related to location (where), frequency (when), and indicators or variables (what) (JIANG et al., 2020). However, the main question guiding the water quality monitoring network is the objective.

According to Canadian Council of Ministers of the Environment (CCME) (2015), defining the monitoring goal and selecting monitoring variables, along with space and temporal frequencies are related to the planning step, followed by data collection and analyses activities, data analysis and interpretation, and lastly informing through reporting and follow-up (Figure 11).

Water quality monitoring programs can be built into several different assessment protocols, depending on the purpose, duration, and end user of the provided information. Table 3 specified major types of water quality monitoring program based on objectives defined by the EU Water Framework Directive (European Communities, 2003), the USGS (U.S. Geological Survey, 1995), and the CCME (Canadian Council of

Figure 11 – Summary of different activities, and key processes involved in designing water quality monitoring program

Source: Adapted from Canadian Council of Ministers of the Environment (CCME) (2015)

Ministers of the Environment, 2006). The first and second ones sort monitoring programs based on management objectives, while the last one considers both the purpose and duration.

Table 3 – Objectives of monitoring programs defined by European, United States, and Canada's frameworks.

EU Water Framework Directive (WFD)	**United States Geological Survey (USGS)**	**CCME Canada-wide Framework for Water Quality Monitoring**
- Surveillance (long-term); - Operational (short-term); - Investigative (short-term).	- Reconnaissance Studies; - Diagnostic; - Interpretative.	- Longer-term status and trends monitoring; - Shorter-term survey (investigation) or compliance monitoring.

Defining the monitoring objectives determines not only the protocols themselves, but also costs, approaches to be implemented, variables measured, spatial extent, frequency of the measurements, and the data usefulness (STROBL; ROBILLARD, 2008; LOVETT et al., 2007). Nevertheless, clear objectives and information expectations are complex to be identified, because depend on several other factors, such as financial constraints, spatial and temporal boundaries, and changing government priorities (Canadian Council of Ministers of the Environment (CCME), 2015).

According to U.S. Geological Survey (2018), this initial monitoring program is a reconnaissance study, which allows managers to target immediate questions and address the purpose of the water quality investigation, and possible concerns to provide a

foundation to define the monitoring program scope. On the other hand, diagnostic surveys are indicated for providing information to water resources managers or evaluating of strategies for vulnerable or impaired reservoirs. And interpretive studies are those to complement existing monitoring data, where usually statistical and mathematical simulations are performed.

Samwise Chapman (1996) divided monitoring programs into monitoring, survey, and surveillance. Monitoring refers to long-term observations defining status and trends, surveys for a finite duration to measure and observe water quality for a specific purpose, and surveillance to continuously management and operational activities. Table 4 presents a few categories and characteristics of assessment operations suggested by Chapman (1996).

Table 4 – Categories and principal characteristics of water quality assessment operations.

Type of operation	**Station density and location**	**Sampling or observation frequencies**	**Number of variables considered**	**Duration**
Multi-purpose monitoring	medium	medium (12 per year)	medium	medium (>5 years)
Other common water quality operations				
Trend monitoring	low: major uses and international stations	very high	low for single objective; high for multiple objective	>10 years
Basic survey	high	depending on media considered	medium to high	once per year to once every 4 years
Operational surveillance	low: at specific uses	medium	specific	variable
Specific water quality operations				
Background monitoring	low	low	low to high	variable
Preliminary surveys	high	usually low	low to medium (depending on objectives)	short <1 year
Emergency surveys	medium to high	high	pollutant inventory	very short (days-weeks)
Modelling surveys	specific (e.g. profiles)	specific (e.g. diel cycles)	specific (e.g. O2, BOD)	short to, medium two periods: calibration and validation

Source: Adapted from Chapman (1996)

Trend monitoring requires a very high sampling frequency to identify fluctuations' tendencies. And, background monitoring does not require high station density and sampling frequency. The level of deterioration also could define the monitoring need, and for modeling applications, the sampling frequency and variables measured are related to the modeling purpose (CHAPMAN, 1996).

After defining the monitoring objective, the planning phase begins, in which the monitoring program is designed, defining monitored variables, temporal frequency, and

spatialization of points.

Table 5 presents typically physical, chemical, and biological variables monitored in water quality monitoring protocols. For reservoirs with little or no relevant data, or either lack of resources and time, variables are ranked according to priority to establish the scope of monitoring or defining the background water quality.

The observation of major water quality concerns and the possible contributing factors or causes can be assessed in defining water quality variables to be monitored (U.S. Geological Survey, 2018; GILLIOM; ALLEY; GURTZ, 1995). In such a case, the selection of variables is impacted oriented (HARMANCIOGLU; OZKUL; ALPASLAN, 1999). According to Thomann and Mueller (1987), the manifestation of problem interference with water use indicates the major problem, that can be associated with water quality variables. For example, an unbalanced ecosystem with the manifestation of tastes and odors indicates the eutrophication process, and excessive plant growth is associated with nutrients (nitrogen and phosphorus), and phytoplankton.

Otherwise, the selection of base variables can also be defined using oriented, where depends on the priority of water use (Canadian Council of Ministers of the Environment, 2006; CHAPMAN, 1996; HARMANCIOGLU; OZKUL; ALPASLAN, 1999).

Whether impacted or use-oriented, determining variables be monitored in a network require resources, specialized sampling, preservation, and analytical laboratory techniques. To target variables and minimize both cost and efforts, should be taken into account the correlations between variables.

Usually, variables such as temperature, dissolved oxygen, pH, sulfides, hydrogen sulfide, iron, and manganese are indicators of stratification. Nutrients, transparency, chlorophyll-a, and composition of phytoplankton, zooplankton, and fish stock are associated with the eutrophication process. Organic matter content can be assessed through analyses of COD, BOD, and color. Moreover, the possible mineral budget can be investigated with analyses of conductivity, alkalinity, sulfates, and chlorides (STRASKRABA; TUNDISI, 1999). More recently, monitoring programs have included micropollutants and indicators of microbial contamination (STROBL; ROBILLARD, 2008).

Besides the interrelation among water quality variables, the limitations of quantification methods and the delay between sampling and laboratory analyses determine the number of samples collected, stored, and analyzed. To face this limitation, technological advances have been providing the use of in-situ and high-frequency measurements, reducing sampling and laboratory analysis efforts, see Section 2.7.4 (CORAGGIO et al., 2022).

As for the definition of variables, determining sampling frequency depends on the

Table 5 – List of typical physical, chemical, and biological components often measured in water quality monitoring programs. Numbers represent priority in a reconnaissance study, in which 1 represents variables with maximum utility, 2 with moderate utility, and 3 variables with some utility.

	Priority	**Supplementary variables or analytical constituent**
Physical		
Water depth	1	Supplementary variables usually monitored: Alkalinity, Color, and Suspended sediment (suspended solids).
Water temperature profile	1	
Secchi disk transparency	1	
pH profile	2	
Specific conductance profile	2	
Turbidity profile	3	
Chemical		
Dissolved oxygen profile	1	
Nutrients (phosphorus and nitrogen species)	1	Orthophosphate, Total phosphorus, Nitrite plus nitrate nitrogen, Ammonia nitrogen, Ammonia plus organic nitrogen, and Total nitrogen.
Total and dissolved organic carbon	2	
Major ions	3	Calcium, Chloride, Dissolved solids, Fluoride, Iron, Magnesium, Manganese, Potassium, Silica, Sodium, and Sulfate.
Trace elements	3	Antimony, Arsenic, Barium, Beryllium Cadmium, Chromium, Cobalt, Copper, Lead, Manganese, Molybdenum, Nickel, Silver, Uranium, and natural Zinc.
Biological		
Chlorophyll	1	
Pathogenic indicators (Escherichia coli, fecal coliform)	2	
Phytoplankton: diversity, abundance, and biovolume	3	
Macrophytes	3	
Zooplankton	3	
Littoral macroinvertebrate fauna	3	
Profundal macroinvertebrate fauna	3	
Fish diversity and abundance	3	

Source: Adapted from U.S. Geological Survey (2018)

water quality monitoring objective. However, the expected spatial distribution for horizontal and vertical characterization of data should also be considered in defining monitoring stations (STROBL; ROBILLARD, 2008). The vertical characterization

represents a relevant aspect in reservoir monitoring programs, due to stratification (CHAPMAN, 1996). However, must be also considered temporal variations due to inflow, water levels, and seasons (STRASKRABA; TUNDISI, 1999).

Among several different complex aspects of locating sample stations, the monitoring program can oversample at the beginning of a study (U.S. Geological Survey, 2018). In such a case, the provided data allows distinguishing statistical similarities and differences between the sampling sites (CHAPMAN, 1996).

Although there is no single quantitative method for sampling-site selection, the riverine, transition, and lacustrine zones should be considered in selecting locations (U.S. Geological Survey, 2018). Pollution sources, tributaries numbers, and relevance to the total input discharge also play important roles in the reservoir water quality variability (STROBL; ROBILLARD, 2008).

Samwise, monitoring frequency determination are usually related to random changes due to storms, and seasonal temperature change, mostly to detect standard violations (HARMANCIOGLU; OZKUL; ALPASLAN, 1999).

According to Ballance, Richard and Richard (1996), to characterize the reservoir water quality it is acceptable one minimum field campaign per year at turnover or a maximum of two field campaigns per year (one at turnover and the other during thermal stratification). For eutrophic reservoirs, the authors suggest sampling frequency in monthly intervals, although during summer it can be amplified to twice.

Monitoring purpose also plays an important role, a study performed by Torres et al. (2022) evaluated the sampling frequency impact on determining water quality status depending on different water quality monitoring objectives of Maumee River and Raisin River, located in the Western Lake Erie Basin, USA. The results found revealed that sediments and nutrients required require more than 50 samples/year to provide an error of less than 10%. In defining water quality status, monthly and seasonal sampling are sufficient, and to capture long-term trends bi-weekly sampling is necessary. The author also highlighted the inclusion of storm events to improve sampling frequencies.

For existing networks, few statistical and programming methods can be assessed concerning sampling sites and temporal frequencies to redesign the process to assure an optimal network, on which the monitoring objectives can be met with minimum costs (HARMANCIOGLU; OZKUL; ALPASLAN, 1999; Canadian Council of Ministers of the Environment (CCME), 2015; KHALIL; OUARDA, 2009).

2.7.2 Optimal reservoir's water quality monitoring network

Ideally, water quality monitoring networks should be determined by the variability of target indicators. However, usually, the many constraints, such as financial

resources, available technologies, and data availability, determine the monitoring network (SOKOLOV et al., 2020). In this context, some institutions' efforts have already definitions of optimal and minimum programs, such as the World Meteorological Organization (WMO, 2013; KLEEMOLA, 1998).

(WMO, 2013) in the technical report "Planning of Water Quality Monitoring Systems", the recommended annual sampling frequencies are divided into baseline and trend station types. Baseline approach content a minimum of one sampling collection at turnover, and for an optimum basis an additional vertical profile at end of the stratification period. For detecting trends if the issue to be studied is related to eutrophication, a minimum of 12 samples per year are required, including twice monthly during summer.

The International Co-operative Program on Integrated Monitoring of Air Pollution Effects on Ecosystems (KLEEMOLA, 1998) on the other side, recommended as a minimum and optimum sampling protocol as shown in Table 6.

Table 6 – Minimum and optimum sampling protocol and sequence for physical-chemical measurements, plankton and sedimentation. Vertical extent: E = samples from epilimnion only, EH = samples from epilimnion and hypolimnium, D = samples from discrete depths, C = column samples.

	Monthly frequency				
Variables	Minimum	Optimum	Sampling sites	Vertical extent	Samples
Physical and chemical samples	1	4	1	EH	D
Primary production	1	4	1	E	D
Dark fixation	1	4	1	E	D
Respiration	1	4	1	EH	D
Chlorophyll concentration	1	4	2	EH	C
Phytoplankton flora and biomass	-	4	2	EH	C
Bacterioplankton	-	4	2	EH	C
Protozoan plankton	-	4	2	EH	C
Zooplankton (excl. Protozoa)	-	2	2	EH	C
Sedimentation	-	2	1		

Source: Kleemola (1998)

According to Kleemola (1998), the physical and chemical characteristics of the water (temperature, alkalinity, color, conductivity, oxygen, inorganic nitrogen, total nitrogen, inorganic phosphorus, and total phosphorus) should be determined together

with the biological parameters. Additionally, meteorological conditions must also be considered in interpreting the results.

The Canadian Council of Ministers of the Environment Canadian Council of Ministers of the Environment (CCME) (2015) also produced a guidance manual for optimizing water quality monitoring program design, based on Canadian conditions, various monitoring requirements, and case studies. Canadian surface water bodies include rivers, lakes, estuarine, and coastal waters in temperate, sub-Arctic, and Arctic climates. The document guides each type of water body, depending on different responses to stressors, depending on the process, and physical and chemical features.

These official guidelines are designed for the organization of monitoring activities and were produced based on data from temperate regions, which differs from those found in tropical environments. Additionally, although the extensive literature about monitoring networks optimization of rivers, and groundwater systems, defining monitoring strategies for reservoirs is challenging, because of the three-dimensional flow characteristics, and the complex dynamics of several specific-located aspects, such as physical conditions, hydrodynamics, thermal stratification, and wind mixing processes. Therefore, previous studies on the reservoir optimization of monitoring networks have been very limited (MAYMANDI; KERACHIAN; NIKOO, 2018).

Jiang et al. (2020) performed a comprehensive review providing a systematic overview of water quality monitoring design approaches from ninety articles published in the last 20 years, from the overall researched articles, only 13 focused on the lake or reservoir monitoring. The author's results also revealed that the majority of reviewed papers focus on optimization of monitoring location, followed by the sampling frequency, and water quality variables.

The optimization of monitoring programs usually used statistical tools for this purpose, based on the variability of data, concentrations measured, and changes detection (TRAUTMANN; MCCULLOCH; OGLESBY, 1982; JIMENEZ et al., 2005). However, those approaches require a large amount of already monitored data.

Lee, Paik and Lee (2014) applied objective function using the concept of multi-variate weighted total information for optimal selection of sampling stations at Lake Yongdam, South Korea. The results revealed that nine sampling locations could be reduced to six optimal locations, without losing representative water quality information and decreasing redundant sampling locations.

Samwise, Yenilmez, Düzgün and Aksoy (2015), based on dissolved oxygen measurements and spatial correlation structure, suggested a systematic approach in designing the network sampling location to minimize monitoring stations in the Porsuk Dam Reservoir, Turkey.

While, Jimenez et al. (2005) divided Porce II reservoir, Colombia, into five subdomains using surface temperature distributions and stated that more monitoring stations are necessary for reservoir entrance areas, where the maximum surface temperature is more complex than at dam and transition regions.

Moreover, the optimization program performed in the IJsselmeer area, Netherlands, revealed that a higher sampling frequency (12 times a year) at fewer locations (50% less) provides more information than a lower frequency at a large number of locations, and reduces the cost by 35-50% (OLC, 2014).

Modeling can also be used in determining optimal monitoring resolutions, as performed by Nikoo et al. (2016) investigations of water quality variations in simulations using CE-QUAL-W2 model, set up with a long-term set of Karkheh's reservoir (Iran) historic data. The results, using data at different depths and seasons, showed that 3 out of 22 potential stations are sufficient as optimized monitoring locations across all seasons. However, optimal location and depths varied depending on the season.

According to Strobl and Robillard (2008), an optimal monitoring network design configuration should also be flexible, since each new measured data may guide revisions in the network design. The authors emphasize that although networks are not usually redesigned during the monitoring process, such a procedure could reduce costs and efforts in measuring unnecessary data.

Budgetary resources and costs also play an important role in defining monitoring strategies, since economic constraints could limit the data collection in time and space (STROBL; ROBILLARD, 2008). According to Jiang et al. (2020), the forefront in relevant studies of optimal water quality monitoring belongs to northern hemisphere countries. Nevertheless, regions with more challenging environmental problems usually are formed by developing countries, where financial resources are usually scarce and often do not have well-defined and organized monitoring programs, and lack monitored data.

An efficient technical guideline for planning optimal monitoring networks is especially necessary for such countries, to reduce monitoring costs and provide sufficient data to guide water resources management programs (ALMEIDA et al., 2022; CAMARA et al., 2020).

Computational methods and numerous techniques have been applied for the optimization of monitoring networks, in particular, the use of Value of Information (VOI) (POURSHAHABI et al., 2018; MAYMANDI; KERACHIAN; NIKOO, 2018), dynamic programming (ASADOLLAHFARDI et al., 2021), smart city and Internet of Things technology (IOT) (CHEN; HAN, 2018), statistics (KHALIL; OUARDA, 2009), and geostatistical (BEVERIDGE et al., 2012), however, the majority of these studies requires spatially distributed medium to long-term data.

2.7.3 Current Status of Water Quality Monitoring Systems Worldwide

Despite water quality network designs having been studied since late 1960, defining an optimal monitoring program is still a challenge for either developed or developing countries (ALMEIDA et al., 2022). Since water quality assessment responsibility usually is fragmented between the general existence of national water quality authority in different government departments (WMO, 2013).

Sampling frequencies adopted by monitoring programs worldwide was presented in the report on surface water quality monitoring developed by the European Topic Centre on Inland Waters (KRISTENSEN; BOGESTRAND, 1996). This report presents an overview of national monitoring activities in the countries forming the European Environment Agency area, including European Union Member States, Iceland, and Norway (Table 7).

Some countries have a long tradition of monitoring reservoir water quality, such as Austria (since 1953) and The Netherlands (since 1955). Indeed, among all monitoring programs, the ones covering a great number of reservoirs are usually sampled at longer intervals (KRISTENSEN; BOGESTRAND, 1996).

Besides the herein monitoring programs, some countries as Germany, undertake local monitoring reservoirs in their respective areas. The local reservoir monitoring activities are generally not standardized at a national level, and the variables and sampling frequency vary across the country (KRISTENSEN; BOGESTRAND, 1996).

In Brazil, monitoring water quality for control in rivers and reservoirs is provided by CONAMA resolution nº396/2008, where a frequency of six months is indicated as a minimum recommendation, depending on hydrogeological and hydrogeochemical characteristics, pollution sources, and water use. Each environmental state agency is responsible for establishing the monitoring program frequency and variables, which varied from 3 to 50.

The large extension of the territorial area of Brazil, and the diverse cultural, social, climatic, and economic variability, lead to the need for different water quality monitoring programs, which must be adapted depending on the water use, monitoring objectives, climate, soil, main sources of pollution (agriculture, livestock, industrial, domestic sewage), water quality trophic state, among other characteristics.

According to ANA (2005), currently, 1,671 monitoring sites are registered in the water quality monitoring of the National Hydrometeorological Network (`http://pnqa.ana.gov.br`), operated by the Brazilian Nacional Water Agency (ANA), federal entities Brazilian states agencies. However, in the current scenario, measurement frequency presents no regularity in frequency and variables monitored, Table 8.

Water quality monitoring in Santa Catarina and Rio Grande do Sul states are perform quarterly, carried out by the respective environmental agencies, SEMA

Table 7 – Overview of usual sampling frequency for monitoring water quality in reservoirs worldwide

	Variables	**Sampling frequency (per year)**	**Since**
Austria	physical, chemical, bacteriological, and biological	5	1953
Brazil - general terms	pH, turbidity, conductivity, temperature, and dissolved oxygen	2	1999
Canada[1]	Physical and Chemical Parameters, major ions, nutrients, and trace elements, and metals	6 - 12	1986
Denmark	Chemical and physical, Phyto and zooplankton, fish and macrophytes, and sediment composition in reservoir water	Reservoir water: 19 Tributaries: 12-26 Plankton: 19 Fish, macrophytes and sediment: 1/5 yr	1989
Finland[2]	28 physical and chemical	3	1962
Greece	organic and inorganic, chemical and physical	monthly and seasonally	1980
Ireland[3]	Chemical and physical	several times per year	1960
Luxembourg	22 chemical, physical and microbiological	8	
The Netherlands[4]	120 chemical, physical and biological	Chemical and physical: 6-52, biological variables: 1-13	1955
Norway[5]	physical, chemical and biological	2/month	1971
Spain[6]	Physical, chemical and biological	4	1972
Sweden[7]	physical, chemical and biological variables, sediment, palaeoreconstruction	4-12, depends on parameter	1960
United Kingdom[8]	Microbiological indicators and blue-green algae	5	1992
USA[9]	Physical properties, major ions, suspended-sediment, pesticide concentration, and selected trace elements	12 - 24	1962

[1]Additional biological monitoring, and automated temperature, conductivity, and pH monitoring
[2]Additional acidification, heavy metals, organic compounds, and pesticides monitoring of surface waters
[3]Additional remote sensing surveys from 1989 to 1990
[4]There is also an monitoring program called Aqualarm Early warning network, in which chemical and physical variables are analyzed at 7 online stations along the rivers Rhine and Meuse since 1974
[5]Additional acidification, and heavy metals, heavy metals monitoring in reservoirs sediments and mercury in fishes
[6]Additional survey of eutrophication through remote sensing
[7]Additional intensive timeseries of sediment, paleoreconstruction, and contaminants in fish in reservoirs and streams
[8]Additional Blue-green algae annual sampling program
[9]Monitoring sites are paired with streamgages providing hourly to daily information on streamflow conditions. Additional hourly measurements of water temperature, pH, specific conductance, turbidity, and dissolved nitrate concentration on selected sites.

Table 8 – Outlook of Water quality sampling frequency of monitoring networks in the Brazilian States

Brazilian state	Number of variables monitored	Sampling per year
São Paulo	50	6
Minas Gerais	50	4
Bahia	43	1-3
Rio Grande do Sul	32	3
Rio de Janeiro	21	6
Mato Grosso do Sul	20	3
Mato Grosso	19	4
Paraíba	16	2
Amapá	16	2
Distrito Federal	15	12
Espírito Santo	15	3
Paraná	14	1-4
Pernanbuco	10	6
Goiáis	10	4
Ceará	3	4
Santa Catarina	-	3

Source: Adapted from ANA (2005)

(Secretaria Executiva do Meio Ambiente) and FEPAM (Fundação Estadual de Proteção Ambiental Henrique Luis Roessler). Variables monitored include dissolved oxygen, biochemical oxygen demand, total phosphorus, *Escherichia Coli*, and ammonia (FEPAM, 2020; SEMA, 2020)

On the other hand, the water quality monitoring program carried out by CETESB (Companhia Ambiental do Estado de São Paulo), in São Paulo state, presents a bimonthly frequency. Several variables are monitored, including total and dissolved solids, chlorophyll-a, heavy metals, total organic carbon, chloride total, biochemical oxygen demand, hardness, total phosphorus, phosphorus-orthophosphate, ammonia, Kjeldahl nitrogen, nitrate-nitrogen, nitrite-nitrogen, dissolved oxygen and pH (CETESB, 2020).

In the state of Paraná, monitoring is performed on at semiannual basis, less frequently than in the aforementioned states. Variables monitored are dissolved oxygen, ammoniacal nitrogen, nitrate, total phosphorus nitrite, chemical oxygen demand, biochemical oxygen demand, total solids, chlorophyll-a, phytoplankton, and zooplankton (IAP, 2017).

The limitations of quantification methods and the delay between sampling and laboratory analyses determine the number of samples collected, stored, and analyzed.

And, as a consequence, the spatial and temporal monitoring frequency. To investigate water quality variability, high-frequency accurate and precise measurements are necessary.

Responding to this challenge, new generations of online monitoring tools based on sensor technology have emerged in recent years (POLONSCHII; GHEORGHIU, 2017). The application of these methods to several parameters can represent a significant advance for water control strategies and promote an improvement in water quality control techniques to streamline decision-making processes and generate savings in water treatment. The use of such a technology could provide data with a high temporal resolution, and sometimes a monitoring network with the least number of sampling points. According to Jiang et al. (2020), the usage of such technology also reduces the importance of the design of optimal monitoring frequency and variables.

2.7.4 Future perspectives in water quality monitoring

As water quality in reservoirs and lakes can change in different time scales (CHAPMAN, 1996), measurements performed regularly to characterize the temporal variations in quality are required (U.S. Geological Survey, 2018).

Automated analyzers for in situ measurements provide real-time temporal quantification with reliability, only requiring small sample volumes, no reagents, and low energy consumption. Sensors also can be cost-effective, because minimize costly field visits (WMO, 2013). Nevertheless, real-time monitoring ensures an appropriate time response in case of contaminations, therefore improvement in the water supply system, because enables faster response to events (STOREY; GAAG; BURNS, 2011).

Nearly continuous water quality monitoring records generally are provided by a platform with multiparameter sondes. Usually, these systems can be mounted or moored on fixed structures (such as piers and dam walls), mounted on an anchored barge, or suspended from an anchored buoy - See Figure 12. Its operation, depending on the environment condition, may include a single sensor at a fixed depth, multiparameter sondes with multiple sets of sensors at fixed depths, or sondes can be raised or lowered using a mechanical wench or ballast system (U.S. Geological Survey, 2018).

Not only traditional variables can be monitored through in situ instrumentation, such as temperature and dissolved oxygen, but also pH, turbidity, pigment fluorescence, ammonia, nitrate, chlorine, and discharge can be monitored (U.S. Geological Survey, 2018).

Currently, available instruments for field-measured variables are thermometers or thermistors, portable pH and conductivity-meters, DO meters, optical turbidity meters, fluorometers, among others (WMO, 2013). Table 9 presents a list of variables usually measured with probes using electronic and optical technology.

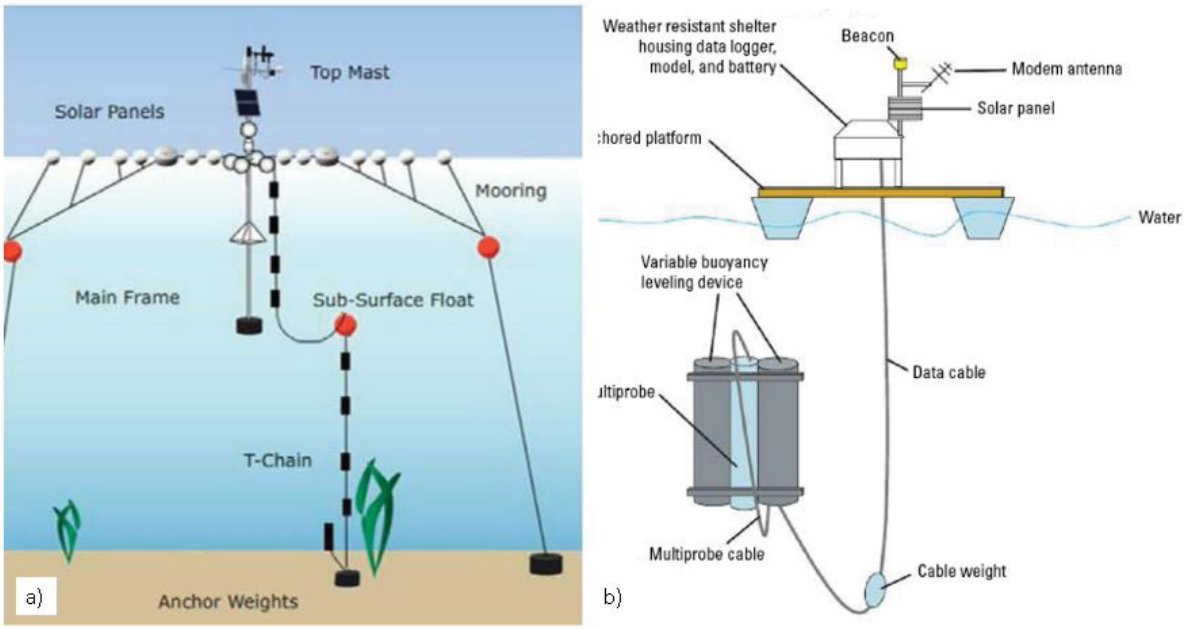

Figure 12 – Diagram of a continuous water-quality monitoring system with multiple sensors (a) and with a single set of sensors (b). In (a) the submerged buoys above each anchor allow the buoyed station to rise and fall with the changing pool elevations. In (b) the sensors can move to various depths by use of a variable-buoyancy system.

Source: (a) U.S. Geological Survey (2018), (b) U.S. Geological Survey (2018) citing Rowland and others, 2006

The measurement frequency depends on the sensor and equipment settings, for instance, hourly data may be adequate to capture the temporal variation of stables waters. Yet for polimitics reservoirs more frequent data collection may be needed (U.S. Geological Survey, 2018).

For example, in Lake Maumelle (Arkansas), a shallow drinking-water reservoir, a continuous water-quality monitoring platform was installed equipped with 12 sensors positioned in depths every 1 meter from 0.5 meters below the surface to 1 meter above the bottom. Dissolved-oxygen concentrations were measured every 5 minutes, and the resulting concentrations indicated wind-induced upwellings of hypolimnetic water and downwellings of epilimnetic surface water. From the monitoring results, the drinking-water treatment facility performs adjustments to the treatment process to reduce taste, odor problems, and clog filters (U.S. Geological Survey, 2018).

A method widely used nowadays in in-situ sensors to monitor quantitative and qualitative changes, and identify specific compounds, is fluorescence (SHIN; Teresa Gutierrez-Wing; CHOI, 2021).

Fluorescence is a technique in which emitted infrared waves, at a certain wavelength, cause excitation in molecules. Its operation is based on the emission and adsorption of a light beam, where the light passes through the optical path and is partially absorbed by it. An analysis is made of the complete UV spectrum and indicates

Table 9 – Selected environmental variables that can be monitored automatically using either electronic or optical technology.

Automatic measurements	**Electronic**	**Optical**
Temperature	x	
Conductivity/salinity	x	
Chlorophyll a		x
Cyanobacterial		x
pH	x	
DO	x	x
Turbidity		x
Suspended solids		x
DOC		x
TOC		x
Nitrate	x	x
Nitrite	x	x
COD		x
Water level	x	
Water speed/direction	x	

Source: WMO (2013)

the concentration of the water quality parameter. The remaining light is detected by the spectrometer and concentration is calculated through the spectrally resolved light intensity at different wavelengths. When the radiative decay rate is comparable to the non-radiative decay rate, fluorescence occurs (STEDMON et al., 2011).

Fluorescence occurs when an electron temporarily is lifted to an energy state greater than its natural state (became excited), and the photons are absorbed. Electrons do not stay in the excited state for very long, so they fall back to their original energy state emitting instantaneously and spontaneously a photon with the same energy as the one that was absorbed. Also, call as fluorescent light, it corresponds to the wavelengths 682, 655, and 460, for Chlorophyll-a, cyanobacteria, and CDOM, respectively.

Some advantages of using this technology are that these sensors do not consume chemical elements during the measurement process, easily could be adapted for online measurement, and are insensitive to flow rates or water body velocity (CHOI; XIAO, 1999). Moreover, fluorescence-based portable sensors usually are low power consumption and compact size and can perform measurements at a fast speed (SHIN; Teresa Gutierrez-Wing; CHOI, 2021).

However, the drawback of sensor utilization is the presence of noise in measurements, the requirement of specialized services to manipulate and calibrate equipment, and the need for local calibrate measurements through conventional laboratory analysis (ZAMYADI et al., 2016). Table 10 presents a summary of the

Table 10 – Biological, chemical and in situ water quality monitoring: advantages and shortcomings

Biological monitoring	**Sampling for chemical laboratory analysis**	**In situ sensors**
Advantages		
Good spatial and temporal integration	Possibility of very fine temporal variations	Relatively low cost
Good response to chronic, minor pollution events	Possibility of precise pollutant determination	Possibilities for continuous surveillance
Signal amplification (bioaccumulation, biomagnification)	Determination of pollutant fluxes	Real-time studies
Real-time studies (in-line bioassays) Measures the physical degradation of the aquatic habitat	Valid for all water bodies Standardization possible	Valid for all water bodies, Possibility of very fine temporal variations and good spatial coverage
Shortcomings		
General lack of temporal sensitivity	High detection limits for many routine analyses (micropollutants)	No precise pollutant or trace element determination
Many semi-quantitative or quantitative responses possible	No time-integration for water grab samples	General precision lower
Standardization difficult	Possible sample contamination for some micropollutants (e.g. metals)	Advanced technology needed
Not valid for pollutant flux studies	High costs involved in surveys	

Source: WMO (2013)

advantages and shortcomings of using biological monitoring, sampling for chemical analyses, or in situ sensors.

In additionally to fluorescence, optical analysis of biological and physicochemical investigations also is applied in in-situ probes. The operation of such sensors is based on the capability of substances to absorb radiant energy. Since the absorption of ultraviolet, visible, and infrared radiation depends on the molecule's structure, when light passes through a substance the energy absorbed and remained is quantified and further converted in concentration (TRIOS, 2017a).

The spectrophotometer allows comparing the radiation absorbed or transmitted by a solution containing an unknown quantity of solute, and a known amount of the same substance. To obtain UV and visible at a certain wavelength the sample is inserted into the optical path of the spectrophotometer, which measures how much light has been absorbed by the sample (TRIOS, 2017a). The calculation of transmission (T) for individual wavelengths is performed by the ratio through the Equation 2.5.

$$T = \frac{I}{I0} \tag{2.5}$$

Transmission (T) is calculated by comparing the current light intensity passing through the measurement medium and by passing through ultra-pure water, so-called basic intensity (I0). Using Equation 2.6, the absorbance (A) in AUs (AU = absorbance unit) are also calculated.

$$A = -\log_{10} T \tag{2.6}$$

Blaen et al. (2016) corroborates those in-situ optical measurements through long-term, field-deployable fluorometers, and spectrophotometers that provide high-frequency sampling with an enormous potential for the use of these in freshwater environments. However, as placement of instrumentation in a lake or reservoir is based on the data objectives of the project (U.S. Geological Survey, 2018), costs imply in acquisition and implantation of monitoring probes, and additional regular maintenance usually results in few or only one sensor installation for each study site.

Additionally, some challenges in continuous monitoring include corrosion of electronic components due to high humidity areas, for highly productive environments rapid biofouling, require for field observation (U.S. Geological Survey, 2018), the possibility of weathered or damaged equipment, and depending on the region where the sensor is installed are susceptible to vandalism (U.S. Geological Survey, 2006). And the need for recalibration between deployments, which may vary according to the manufacturer (CARSTEA et al., 2020).

As consequence, normally, continuous monitoring with one-site fixed stations does not provide information on spatial variability. This obstacle can be overcome with the use of portable sensors, which allow in situ monitoring, but still require dislocation efforts to the study site, and do not allow measurements with high temporal resolution. Since sampling locations must be enough to allow sufficient data on spatial correlation structure, monitoring strategies are often complemented with modeling (JIMENEZ et al., 2005; ARAUJO et al., 2008; KNOWLTON; JONES, 2006).

Some variables require additional processes and appropriate sample collection methods to be quantified. The determination of total phosphorus is only possible after the sample digestion converting phosphorus forms to be detectable. Moreover, total dissolved phosphorus quantification requires also a filtration process. Such procedures are not easily automatically operate with reliable concentrations (WORSFOLD; MCKELVIE; MONBET, 2016).

Sample contamination and the low range detection limits of the usual spectrophotometric methods employed in the quantification of phosphorus

concentrations also determine difficulties of situ water quality monitoring developments of this variable (WORSFOLD; MCKELVIE; MONBET, 2016). Hence, modeling could represent a useful approach to obtaining phosphorus data in higher temporal resolution.

2.8 Summary

Monitoring practices can be used to improve the understanding of catchment processes, identify heterogeneous and spatial water characteristics affecting the water quality, and provide data for management decisions. In order to achieve water quality assessment, several parameters are necessary for aquatic characterization, such as the above-mentioned physical, chemical, biological, and ecological properties. These elements vary according to the aquatic ecosystem characteristics but are either connect or influenced by anthropogenic actions along with regional characteristics defining water properties.

The key questions when structuring a water quality monitoring network related to location (where), frequency (when), and indicators or variables (what) vary depending on climate, degree of pollution, soil use, and the watershed, among others. Therefore, an optimal water quality monitoring network is designed to reduce monitoring costs, identify representative sampling locations, and provide sufficient data to guide water resources management programs.

However, developing countries usually do not have well-defined and organized monitoring programs and present a lack of monitored data. An efficient technical guideline for planning optimal monitoring networks is necessary for such countries, reducing monitoring costs and providing sufficient data to guide water resources management programs. Additionally, the limitations of quantification methods and the delay between sampling and laboratory analyses determine the number of samples collected, stored, and analyzed. As a result, the spatial and temporal monitoring frequency.

In this context, the application of online monitoring tools based on sensor technology represents a significant advance for water control strategies and promoted an improvement in water quality control techniques. This generates savings in water treatment and monitoring since sensors provide high-frequency and accurate measurements.

Automated analyzers for in situ measurements provide real-time temporal quantification with reliability, only requiring small sample volumes, no reagents, and low energy consumption. However, some limitations of the use of sensors are associated with the acquisition, implementation, and maintenance of site probes.

Thus, monitoring strategies can be integrated with modeling providing better

information for water quality assessment, could help to predict water quality changes when no measurement data is available, also to identify situations in which the critical load could be exceeded in the water body, and even, to test impacts of water resources management actions, or changes of climate conditions. By testing scenarios in models is possible to evaluate several different conditions and their consequences on the reservoir's water quality.

3 Water quality modeling in reservoirs

3.1 Overview

According to Chapra (1997), mathematical models are developed as instruments for solving problems, allowing the understanding of complex ecosystems, and depicting the environment and possible scenarios, by the association of physical, chemical, and biological processes.

In natural water bodies, the hydrodynamics and biological and chemical processes are interrelated. As the water quality variations exhibit multidimensional character, integrated tolls are fundamental for the application of water resources management. The computational modeling allows simulation and provides a dynamic view of complex phenomena and processes (VIRTANEN et al., 1986).

In the water column, as stated by Virtanen et al. (1986), water quality is a result of overall hydrophysical and biogeochemical interactions. Besides the water movement and mixing processes related to other mechanisms determining water quality, the temperature of water in a reservoir affects directly air and water through interactions of material energy exchange. Hence Yang et al. (2018) argues that water temperature is the most important indicator of a reservoir's ecological environment. Thus, this parameter may reveal changes between various factors of reservoir water quality.

Morphometry characteristics determine circulation and movement of water, along with freshwater inputs, stratification due to temperature, wind, wind-influenced, and thermal cooling de-stratification. The pollutant transport is controlled by surface water flow and mixing processes (PEREIRA, 2003).

Since the mathematical models represent alternatives with low operational cost, flexibility, and a good level of results presented, the application of mathematical modeling to the planning and integrated plans of actions can enable the quantitative and qualitative conservation of water.

Hydrodynamic models use complete continuity and momentum equations, requiring a large amount of data for simulations. And, water quality models demand much more state variables than hydrodynamic models, which means that the model has to be run many times until the calibration is complete (WENDT, 2009; PEREIRA, 2003).

As stated by Veiga and Dziedzic (2010), predictive water quality modeling is a useful tool for watershed management, and can help in decision-maker thought simulating scenarios to support planning and management of water resources. The quality of modeling

results depends directly on the input data (VEIGA; DZIEDZIC, 2010). Besides, rate coefficients are required in calibration to suit site-specific conditions. And, the scarcity of input and processing data are the main factors that make it difficult to apply modeling tools for management in several basins around the world.

Modeling can be performed considering the dimensions of spatial representation (1D, 2D, or 3D). Ayres (2015) recommends 1d models in river studies where the flow is not stratified and cross channel currents are not a major concern when it was assuming a gradient in only one direction. For water quality aim, one-dimensional models can be performed for applications where the primary concern is variations along the axes, and lateral variations are small, such as long, deep, and relatively narrow systems (PEREIRA, 2003).

Two dimensions (2D) models are indicated for studies of horizontal and lateral gradients in estuarine and river systems. Finally, there are models capable of representing the gradients in three dimensions (3D). These models can represent bathymetry and the coastline providing a very large resolution. The use of 3D models for water quality analyses may be determinant for some case studies, as a comment by Virtanen et al. (1986) for water currents and the location of point sources.

There are water quality models available for water resources management. Each one presents characteristics of spatial representation, a numerical method for solving differential equations, processes to describe state variables, and model parameters, among other attributes.

In terms of spatial representation, some models such as HEC, QUAL2K, DYRESM-WQ, MIKE11, and GLM are limited to one-dimensional simulations. CE-QUAL-W2 is restricted to two dimensions, while DELFT3D, CAEDYM, and RMA-11 can simulate from one to three dimensions. About the state variables, the majority of variables listed can be used for water quality simulation.

Among so many modeling alternatives with sophisticated computer models to understanding complex interactions of aquatic systems requiring several input data, often a simple approach to assessing study site water quality can be quick and useful in defining water quality status, in which few basic physical principles can be used to explain a wide variety of natural phenomena. Moreover, the complexity and data reduction enable the simple model to act as an applicable tool, easily adapted for wide applications in different environments, even when there is a lack of monitoring data.

According to Canale and Seo (1996) the increase of the model's complexity decreases reliability due to propagated error resulting from the uncertainty of coefficients employed because is impossible to simulate abstractions of complexes environmental problems without error.

Most efforts in developing analyses over the past years focused on eutrophication processes, where the simple mass balance models produce useful results for water quality control and estimations. In such applications, reservoirs are assumed as completely mixed systems, both horizontally and vertically. Such a simplification allows useful estimates of the reservoir's inputs behavior, resulting in concentrations with significant value in estimating the effects of anthropogenic activities (THOMANN; MUELLER, 1987).

3.2 Mass Balance Analyses

Mass balance equations are applied for several water quality assessments, in which the most common application is to phosphorus balance. Phosphorus is essential to an organism's growth, and its quantification is often included in basic water quality surveys or background monitoring programs. Particularly for water supply reservoirs, phosphorus concentrations are frequently monitored and modeled, since could indicate rates and trends of algal growth.

Usually, phosphorus concentrations are associated with eutrophic conditions, since the element is a key factor in the biological cycle in water bodies and an indicator of trophic state. Recently Wu et al. (2022) evaluated the ratio between P and N in inflows and outflows of more than 5,000 lakes globally distributed using a multi-faceted approach to identify lake nutrient retention. The study resulted in almost 90% of the lakes presenting preferential retention of phosphorus instead of nitrogen, causing negative effects within aquatic bodies and downstream regions.

First proposed by Vollenweider (1968), the phosphorus loading concept originally presented phosphorus loads related to morphometry and hydrology assuming a constant settling velocity. From this model, a variety of models has been proposed as a steady-state solution to the input-output or mass balance approach (DILLON; RIGLER, 1974; VOLLENWEIDER, 1975; VOLLENWEIDER, 1976; CHAPRA; TARAPCHAK, 1976; CHAPRA; RECKHOW, 1979).

Total phosphorus mass balance applications have been used to display long-term trends in phosphorus loading to follow the effects of management programs controlling phosphorus emissions (HAVENS; JAMES, 2005), to estimate loading of total phosphorus (VIDAL; NETO, 2014), to determine carrying capacity (MHLANGA; MHLANGA; MWERA, 2013), to determinate mean annual concentrations within the reservoir (WALKER; HAVENS, 2003), and compute the concentration of Chl-a to further define trophic state and eutrophication (DODDS; WHILES, 2019; CHAPRA, 1997).

Models using the phosphorus loading concept usually represent easier applications than nitrogen, due to nitrification-denitrification balance, nitrogen mass balance is usually

more susceptible to errors (VIDAL; NETO, 2014).

The application of mass balance is a simple technique useful for understanding nutrient behavior, tracking changes, and assessing the effects of water resources management, through the estimation of nutrient budgets (WATERS; WEBSTER-BROWN, 2016; ETHERIDGE, 2013).

A fundamental law of physics state that mass is conserved, and can neither be produced nor destroyed. The conservation of mass is the basis of mechanistic water-quality models, in which this principle is applied to a volume of water (CHAPRA, 1997).

The following sections present equations required for the implementation of mass balance for water quality variables.

3.2.1 Mass balance equations

According to the principle of conservation of mass (equation 3.1), as the mass can be neither produced nor destroyed, the mass in a system (M_{sys} - kg) must remain constant over time disregarding the nuclear reactions. In which a system is an amount of matter of fixed identity.

$$(\frac{dM}{dt})_{sys} = 0 \tag{3.1}$$

The total mass of the system is a integral equation about the volume (V_{sys} - m^3) of the system related to the density (ρ - kg/m^3).

$$M = \int_{V_{sys}} \rho dV \tag{3.2}$$

The mass can be computed in a limit, involving a system and a control volume that coincide at a certain moment. Reynolds transport theorem establishes a relation between system rates of change and control volume surface and volume integrals. From deriving a control volume description for a system description of a fluid flow, the mass balance can be written as equation 3.3. The mass system variation over time is defined by the sum of the control volume mass plus the mass rate of flow out ($\dot{m_{out}}$ - kg/s) of the control volume minus the mass rate of flow into ($\dot{m_{in}}$ - kg/s) the control volume. The control volume mass is a partial derivative because represents only a system mass part of the system.

$$(\frac{dM}{dt})_{sys} = (\frac{\partial M}{\partial t})_{CV} + \dot{m_{out}} - \dot{m_{in}} \tag{3.3}$$

The mass rate passing through a surface defined the flow. Therefore, the integral of the volume over time is the total volume rate of flow (Q - m^3/s) through the surface

(C_S - m²). Where '$\vec{V}$' represents the flow velocity vector and '$\vec{n}$' is the unit vector normal to dS.

$$Q = \int_{CS} (\vec{V}.\vec{n}) dS \tag{3.4}$$

The mass rate of flow ($\dot{m}$) is obtain by multiplying the volume flow by density.

$$\dot{m} = \int_{CS} \rho(\vec{V}.\vec{n}) dS \tag{3.5}$$

Then applying the equation 3.5 on equation 3.3, the system and control volume are related in equation 3.6, which is the mathematical expression of the Reynolds Transport Theorem.

$$(\frac{dM}{dt})_{sys} = \frac{\partial}{\partial t} \int_{CV} \rho dV + \int_{CS} \rho(\vec{V}.\vec{n}) dS \tag{3.6}$$

Applying the mass conservation principle (equation 3.1) in the mass balance equation of a system (equation 3.6) results in the integral mass balance equation (3.7). In which in given moment if there is a temporal variation of mass within a control volume (V_c - m³), this must be balanced by the mass flow through the surface (S_C - m²)

$$0 = \frac{\partial}{\partial t} \int_{CV} \rho dV + \int_{CS} \rho(\vec{V}.\vec{n}) dS \tag{3.7}$$

3.2.2 Water balance

The concepts presented before can be applied to water balance calculations, in which the mass variation rate in the control volume over time corresponds to the net mass flow rate through the control surface (C_S) - also called discharge. This application results in equation 3.8. Sources are represented by the term 'Q_{in}'(m³/s) and sinks are represented by the term 'Q_{out}'(m³/s). Possible sources of water balance are precipitation over the surface, stream flow, and direct runoff, among others, and sinks are evaporation or infiltration, among others. Water balance calculation is directly connected with the solutes mass balance calculations, which will be approached later on in this thesis.

$$\frac{dV}{dt} = Q_{in} - Q_{out} \tag{3.8}$$

The water balance is paramount to achieving accurate mass balance for the variable of interest since water is considered a conservative substance with inputs and outputs from the aquatic system (SCHNOOR, 1996).

3.2.3 Solute mass balance

For water-quality context, by applying the mass balance concepts and equations for a solute, it is possible to determine the mass balance of nutrients and other substances. The total mass of a solute in a system is an integral equation about the volume (V_{sys} - m^3) of the system related to the solute concentration (c_A - mg/L).

$$m_A = \int_{V_{sys}} c_A dV \tag{3.9}$$

The mass conservation law of a solute establishes that the variation in a solute mass must be equal to the diffuse mass flow of the solute ($\vec{j}$) across the system's boundaries. Because when there is a concentration gradient of a component (in this case component 'A'), as a result, there is a mass flow through the molecular diffusion of this component, superimposing on convective mass transport due to the flow velocity field.

$$\vec{j} = (\frac{dM_A}{dt})_{sys} \tag{3.10}$$

In the mass balance of a solute, added to the variables already considered in the integral mass balance equation 3.7, the mass gained or lost by transformations or reactions of the substances within volume should also be accounted for, named as variable 'Reactions' in equation 3.11. This variable removes or adds mass depending if the substance in question is transforming into another constituent or changing another constituent to the substance being modeled.

$$(\frac{dM_A}{dt})_{sys} = \vec{j} = \frac{\partial}{\partial t}\int_{CV} c_A dV + \int_{CS} c_A(\vec{V}.\vec{n})dS \pm Reactions \tag{3.11}$$

3.2.4 Phosphorus mass balance

For phosphorus mass balance there are several process and pathways which plays a role in the dynamics and fractions exchange of boundary conditions. The most common process observed in the literature is presented in Figure 13 below.

The usual sources of phosphorus mass flux into the reservoir are direct runoff, stream flow, air deposition, rainfall at the reservoir surface, and internal loading. The usual sinks of phosphorus mass flux are a bottom outlet, dam percolation, Spillway, and water withdrawal. Groundwater can both act as a sink or source.

$$\begin{aligned}\frac{dc_A V}{dt} = Q_{rivers}c_{rivers} + Q_{rain}c_{rain} + Q_{dp}c_{dp} + D_S\phi\frac{\partial c_A}{\partial z} - Q_{intake}c_{intake} \\ -Q_{spill+bott}c_{spill+bott} - Q_{perc}c_{perc} - kVc_A - vA_sc_A\end{aligned} \tag{3.12}$$

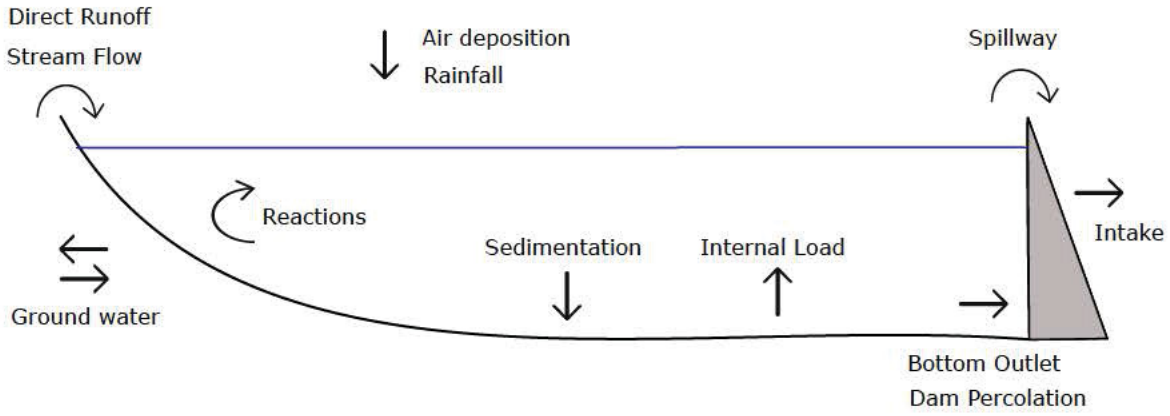

Figure 13 – Process usually considered in phosphorus mass balance studies in reservoirs

$$\frac{dc_pV}{dt} = Q_{tributc}c_{tribut} + InternalLoading - Q_{intakec}c_{intake} - Q_{spill+bottc}c_{spill+bott} \quad (3.13)$$

In which, sources of phosphorus in the reservoir included all tributaries of the river basin ($Q_{riversc}c_{rivers}$), rainfall over the reservoir ($Q_{rainc}c_{rain}$), atmospheric deposition ($Q_{dpc}c_{dp}$) and internal loading ($\frac{\partial c_A}{\partial z}$). Sinks of phosphorus considered are the water withdrawal ($Q_{intakec}c_{intake}$) since it is a water supply reservoir, spillway ($Q_{spill+bottc}c_{spill+bott}$), dam percolation ($Q_{percc}c_{perc}$), reactions ($kVc_A$), and sedimentation ($vA_sc_A$).

$$\frac{\mathrm{d}C.V}{\mathrm{d}t} = Q_e.C_e - Q_S.C - k.V.C - \nu.A_S.C \quad (3.14)$$

Phosphorus mass balance calculations can also be applied in steady approaches. In this condition, it is assumed there are no changes within the time and this condition usually represents the seasonal and annual averages.

$$c = \frac{W}{Q + k_SV} \quad (3.15)$$

In which, phosphorus concentration in the reservoir (c) is the result from external sources of phosphorus (W) divided by discharge (Q) summed up with net settling velocity (k_S) and volume (V).

3.3 Summary

The application of mathematical models in water quality assessments can provide a better understanding of the transport and fate of chemicals and predict future conditions

through scenarios. Besides, models represent alternatives with low operational costs and flexibility.

The modeling approach is a useful alternative to complement and fulfill data gaps on monitoring water quality variables while reducing monitoring efforts. This application also allows water quality data in high temporal resolution, which could not be obtained through equipment, either by limiting detection limits or by the need for specific laboratory processes that provide reliable results.

The integration of reservoir water quality monitoring and modeling techniques provides an improvement in water quality assessments, in which few basic physical principles can be used to explain a wide variety of natural phenomena. A simple approach can be used in defining the status of an aquatic body, where the mass balance models produce useful results for water quality control and estimations.

Mass balance equations are useful tools for understanding nutrient behavior, tracking changes, and assessing the effects of water resources management, through the estimation of nutrient budgets, such as phosphorus.

4 Understanding the water quality change of Passaúna's Reservoir and the background

4.1 Overview

Passauna is a water supply reservoir built in 1989, located in a southern region of Brazil (25.53°S and 49.39°W). Together with the Iraí, Piraquara I, and II reservoirs, Passaúna' reservoir is part of an integrated public supply system in the metropolitan region of Curitiba (RMC) managed by the Water and Sanitation Company of Paraná state (Sanepar).

Passauna's reservoir represents the second largest main source of drinking water for RMC population, responsible for supplying 22% with a flow rate of 2,000 L/s, providing drinking water for more than 800,000 inhabitants of the region (IAP, 2017).

The basin has about 214 km^2 of drainage area, covering the municipalities of Almirante Tamandaré, Campo Magro, Campo Largo, Curitiba, and Araucária. The reservoir has a surface area of 8.5 km^2, a maximum depth of 17.5 m, and an average depth of 8.5 m (unpublished data from MuDak project).

The main inflow to the reservoir is Passaúna and Ferraria rivers. Passaúna river contributes with a mean flow rate of 1 m^{3}s^{-1} entering the reservoir system at an upstream portion called Buffer area. The second main inflow contribution is from Ferraria river (reservoir's left side arm) with a mean flow rate of 0.2 m^{3}s^{-1} (XAVIER, 2005). There are several other inflows to the reservoir, but with a minor contribution in terms of water flow rate.

According to the Koeppen-Geiger classification system, the climate in Passaúna's reservoir region is characterized as Cfb, humid subtropical with temperate summer (ALVARES et al., 2013). This climate is characterized by average annual temperatures of 17 °C, reaching maximum rainfall during the summer mainly between January and February. July and August usually are marked with minimum rainfall.

Concerning meteorological data, there are two weather stations close to the reservoir (Sanepar and Tecpar stations) - See Figure 14. Sanepar station registers at 15 min time intervals and it is located near the reservoir dam. While TecPar-Smart Energy station is located 4 km away from the water intake and measures at 1 min time intervals.

Measurements of radiation (W/m^2), wind direction (degrees) and speed (m/s), precipitation (mm), air temperature (ºC), and air humidity (%UR) are performed by Sanepar weather station. And, in Tecpar station are measure radiation (W/m^2 - diffuse,

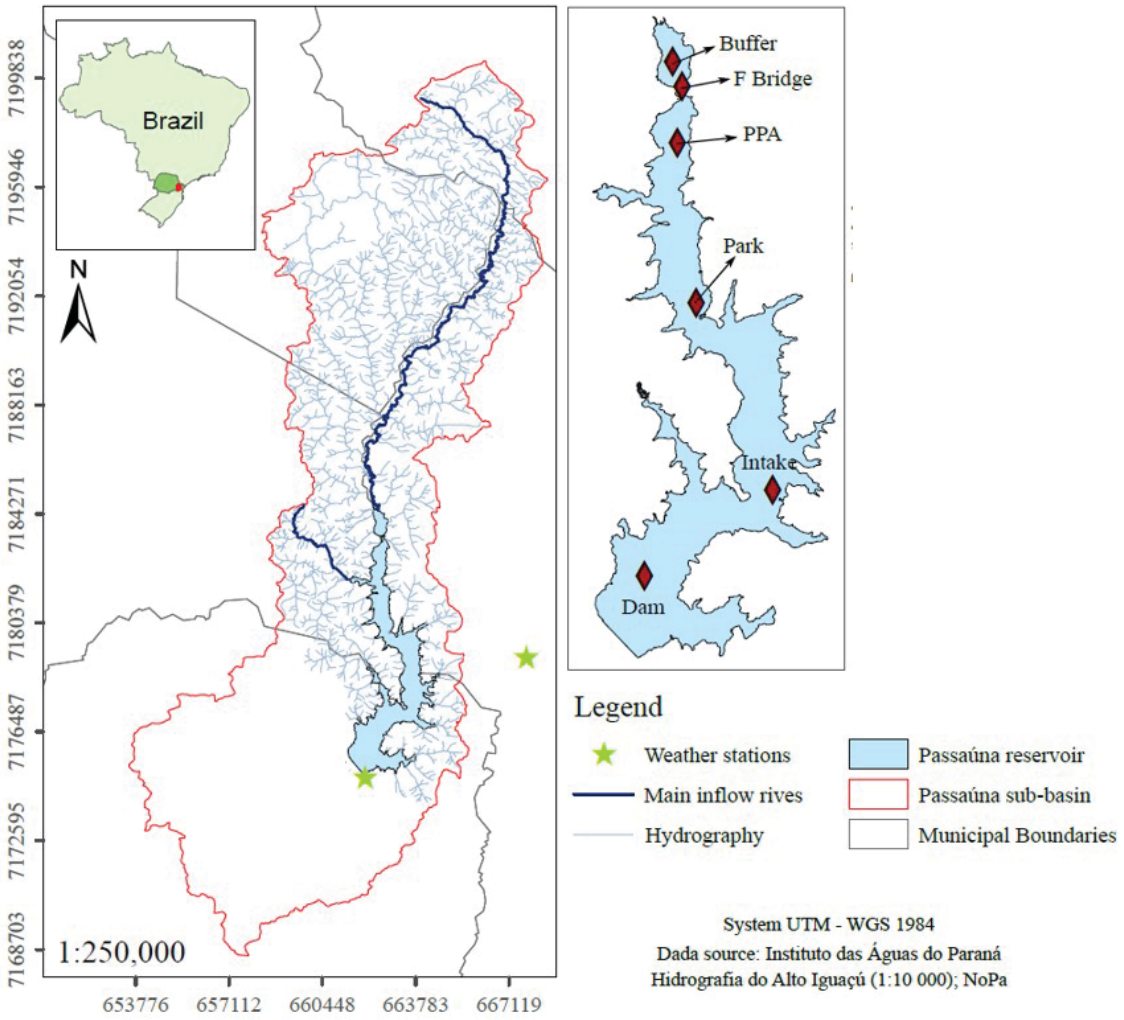

Figure 14 – Passaúna sub-basin map with the hydrography that contributes as runoff to Passaúna reservoir. The diamond symbols represent the locations of monitoring sites in the present study: Buffer, Ferraria Bridge, PPA, Park, Intake, and Dam

global, direct), air temperature (ºC), air humidity (%UR), atmospheric pressure (mbar), wind direction (degrees) and speed (m/s), and longwave radiation.

Additionally, there is a rain station located about 5 km from the upstream reservoir - Colônia Dom Pedro, providing measurements of precipitation (mm) within 12 hours of the time interval. At the Passaúna reservoir inlet, there is a gauging station 'BR 277 Campo Largo' - code 65021800, operated by the official data water agency, Water and Earth Institute (IAT). The station is located approximately 1 km upstream the river and reservoir confluence (coordinates 25º25'37" south, 49º23'17" west). Discharge and water quality data measurements are available at Hydrological Information System (SIH) repository.

Passaúna's reservoir and the Passaúna River portion upstream of the reservoir are classified as Class 2 (COALIAR, 2013), according to the Brazilian water resources planning and management resolutions. In Passaúna's watershed, the land use and

occupation is predominantly rural. There are industrial and agricultural activities, such as potato cultivation, and consequent intensive use of fertilizers and pesticides (IAP, 2009).

Even though, Passaúna's watershed presents a low rate of urban occupation, in the last few years the water quality of Passaúna reservoir is being affected by the anthropic occupation. In a survey conducted by Drummond et al. (2019), land use of the Passauna river basin was evaluated using Landsat images from 1990 to 2017. The supervised classification process showed over the examined years reduction of vegetation area (from 43.5% to 32.4%) and an increase in urban occupation and exposed soil (from 3% to 12%), Figure 15.

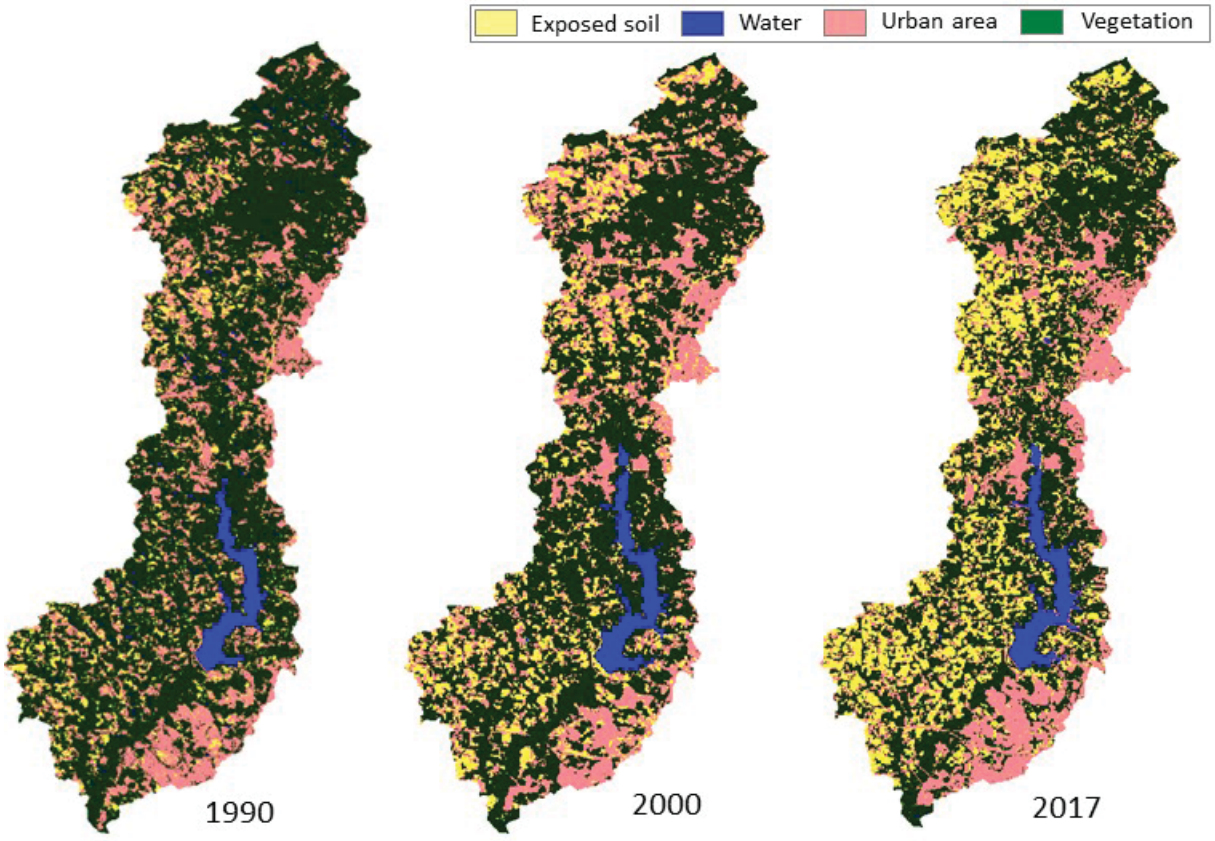

Figure 15 – Landsat images classification as exposed soil, urban, and vegetation areas for the years 1990, 2000, and 2017.

Source: Adapted from Drummond et al. (2019)

Moreover, Filho (2010) pointed out problems of irregular occupation on the banks of Passaúna River, and the presence of industries since the 1980s. Veiga and Dziedzic (2010) also reported the influence of urban occupation in the upstream portion of the reservoir, from the estimation of phosphorus loads for Passaúna's reservoir.

According to Saunitti, Fernandes and Bittencourt (2004), Coquemala (2005) and Conceição (2014) demographic growth and the consequent advance of the urban network by the expansion of municipalities around the reservoir generates the contribution of

domestic and industrial effluents. Deforestation and the growing area with agriculture in the catchment area are leading to nutrients leaching from degraded soils. The result is increase of diffuse loads, and clandestine sewage, in addition to a high rate of sediment production transported to the reservoir (FILHO, 2010).

In addition to this qualitative aspect, problems are also faced in quantitative sphere. Over the last three years (2020-2022), Paraná state faced a severe dry season that led to the worst drought in 30 years. For several months, water supply in Curitiba and region was provided in turns of 36 hours (36 hours of supply resumption and 36 hours of suspension), because the reservoir's levels of Integrated Supply System of Curitiba and Metropolitan Region were all below necessary.

This water crisis exposed the importance of regularly monitoring Passaúna's reservoir water quality of reservoirs, especially in the face of potential climate change.

4.2 Water Quality Studies Outlook

The water quality of the Passaúna reservoir has been investigated since the reservoir was still in the stabilization phase. Dias (1997) carried out monthly campaigns from July 1993 to June 1994, at several monitoring sites, and identified that water from the reservoir was compromised due to the presence of load from the flooded vegetation.

Ever since, a wide history of surveys has been placed in the Passaúna reservoir involving several researchers concerning phytoplankton annual variation (COQUEMALA, 2005), potential risks due to urban occupation in the reservoir surroundings (BUSCH, 2009), suspended particulate material and ionic macroconstituents (MEGER, 2007), heavy metals assessment on sediments from the Passaúna River (BOCALON, 2007; PITRAT, 2010), macroinvertebrates as indicators of water quality (FERRARESI, 2015), among many others.

Concerning sediments, Saunitti, Fernandes and Bittencourt (2004) investigated the erosion process at the basin and Rauen, Castro and Silva (2017) assessed the hydrossedimentological characterization of Passauna River.

Modeling strategies have also been evaluated by Veiga (2001), the authors developed numerical modeling for attempting the eutrophication process and nutrients (phosphorus and nitrogen) mass balance of Passaúna reservoir using FLUX, PROFILE, and BATHTUB computational models. Likewise, Smaha and Gobbi (2003) implement a model programmed in Matlab language to simulate the Passaúna Reservoir's eutrophication process.

More recently, Carneiro, Kelderman and Irvine (2016) evaluated phosphorus sediment water exchange through water and mass budget in the reservoir, and both

Grudzien (2019) and Drummond (2020) explored the use of automatic sampler to identify pollutants in Passaúna River.

Despite the above-mentioned studies, in the past recent years, Passaúna's reservoir became extensively studied by several researchers involved in research projects with Brazil-Germany cooperation, such as NoPa call (Novas Parcerias, funded by CAPES and DAAD, 2015 - 2018) and the MuDaK project (Multidisciplinary Data Acquisition as Key for a Globally Applicable Water Resources Management, 2017 - 2021). In those project's contexts, there are several scientific investigations focused on internal phosphorus loading (ZAREBSKA, 2016), water quality dynamics and organic matter analyses (GODOY, 2017), ebullition processes (MARCON, 2018), use of optical sensors for measuring water quality variables (UNGARATTI, 2019; BERNARDINI, 2019), calculation of trophy degree and variation of phytoplankton (BARRETO, 2020), the study of organic matter photodegradation (SOUZA, 2020), technologies for suspended solid dynamics assessment (WOSIACKI, 2020) and flux assessment (WAGNER, 2019), use of sediment traps to estimate sedimentation rate (ONO, 2020), multi-frequency echo-sounding for sedimentation analysis (SOTIRI, 2016), and phosphorus input from urban areas (SOTIRI et al., 2022).

Moreover, Sales (2020) implemented the General Lake Model - GLM, a one-dimensional hydrodynamic open source model complemented with a water quality library (AED), to simulate variables such as dissolved oxygen, phosphorus, and nitrogen in vertical profiles. Ishikawa et al. (2022b) combined numerical simulations using a three-dimensional hydrodynamic model, high-frequency measurements from satellite remote sensing, and in-situ sensors to assess the influence of density currents on Chl-a concentrations.

More recently, Ishikawa et al. (2022b) explored the hydrodynamic drivers of nutrient and phytoplankton dynamics of Passaúna's reservoir, combining in-situ Chl-a measurements from sensors and satellite remote sensing, with samples analyzed in the laboratory.

Some of the most recent and current works in the Passaúna reservoir are the evaluation of remote sensing use and drone's images monitoring water quality parameters, and modeling hydrodynamics and water quality during the drought period.

4.3 Water Quality Indexes Outline

Passaúna reservoir water quality has been evaluated by several indexes over the past few years. A summary of some studies and reports developed is presented in Table 11.

According to the Water Quality Report IAP (2017) Passaúna's reservoir is

Table 11 – Water quality indexes calculated for Passaúna's reservoir over the past few years, from 1999 to 2019, with different frequencies of monitoring data, considering the indicated variables analyzed

Conducted by	Water Quality Index	Period Frequency	Variables analyzed
IAP (2017)	WQIR	1999 - 2013 Twice per year	Water temperature, dissolved oxygen, transparency (Secchi depth), pH, total alkalinity, electrical conductivity, Chemical Oxygen Demand, Biochemical Oxygen Demand, nitrate, nitrite, ammonia nitrogen, Kjeldahl nitrogen, total phosphorus, turbidity, chlorophyll-a, phytoplankton, and zooplankton
	TSI adapted by Lamparelli (2004)	1999 - 2013 Twice per year	Total phosphorus and chlorophyll-a
Moreira et al. (2017)	WQIR adapted by Sanepar	2015 - 2016 Monthly and every 3 months	Dissolved oxygen, transparency (Secchi depth), Chemical Oxygen Demand, total nitrogen, total phosphorus, residence time, and average depth, and cyanobacteria
Rauen et al. (2018)	WQI and TSI adapted by Lamparelli (2004)	1991 – 2014 Diverse	Biochemical Oxygen Demand, thermotolerant coliform or E. coli, total phosphorous or total phosphate, total nitrogen, temperature, and turbidity
Barreto (2020)	TSI adapted by Lamparelli (2004)	2018 - 2019 Monthly	Total phosphorus, transparency (Secchi depth), and chlorophyll-a

moderately degraded and is considered acceptable to be used as a source of drinking water reservoir for public supply. This result was obtained by calculating the Water Quality Index of Reservoirs (WQIR) for sampling campaigns carried out in the period from 1999 to 2013 collected twice a year at summer and winter.

The parameters monitored to classify the reservoirs according to degradation level are water temperature, dissolved oxygen concentration, transparency (Secchi depth), pH, total alkalinity, electrical conductivity, Chemical Oxygen Demand (COD), Biochemical Oxygen Demand (BOD5), nitrate, nitrite, ammonia nitrogen, Kjeldahl nitrogen, total phosphorus, turbidity, chlorophyll-a, phytoplankton, and zooplankton (Figure 16).

In the same report, Passaúna's reservoir was classified as mesotrophic toward

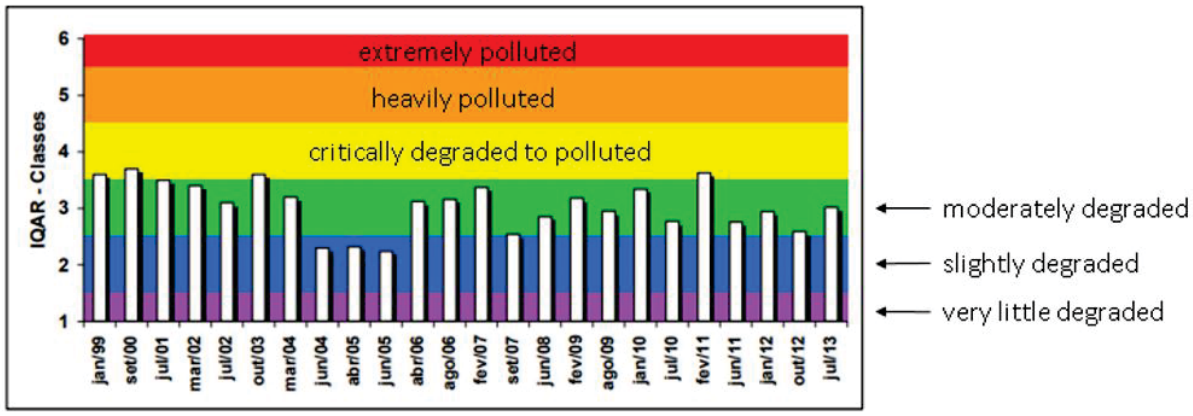

Figure 16 – Water Quality Index of Reservoirs (WQIR) calculated by the Environmental Protection Agency of the State of Paraná (IAP) at Passaúna reservoir from sampling campaigns carried out from 1999 to 2013.

Source: Adapted from IAP (2017)

Trophic State Index (TSI) adapted by Lamparelli (2004), Figure 17. This classification depends on concentrations of total phosphorus and chlorophyll-a.

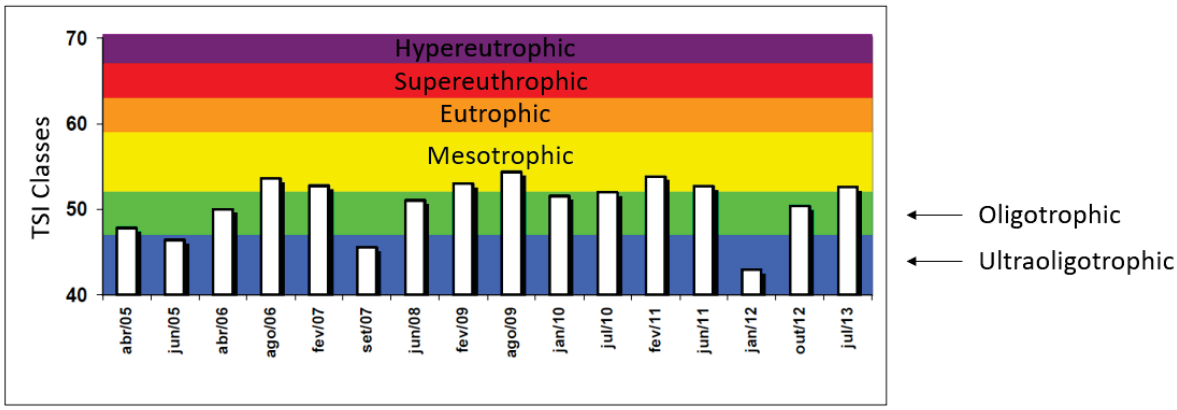

Figure 17 – Trophic State Index (TSI) calculated by the Environmental Protection Agency of the State of Paraná (IAP) at Passaúna reservoir from sampling campaigns carried out from 1999 to 2013.

Source: Adapted from IAP (2017)

A more recent survey published by Moreira et al. (2017) presented an evaluation of the water quality of all four reservoirs of the integrated public supply system in the metropolitan region of Curitiba using WQIR calculations with some Sanepar's adaptations - for more details see Moreira et al. (2017). The classification system rates water bodies as great, good, regular, or bad. For all study sites, water samples were collected, in the years 2015 and 2016, on a monthly (March to September 2015), and after on quarterly (September 2015 to October 2016) basis in several monitoring sites (main tributaries, water outlets after spillways, in the abstractions and inlets of water treatment plants). At the Passaúna reservoir, next to the intake facility water samples were taken at three different depths: surface, 7 meters, and 14 meters.

The resulting WQIR average classified water from Passaúna as good for most of the monitoring period. However, the above-cited samples collected in-depth presented good, regular, and bad WQIR. According to the authors, regular and bad classifications are mainly due to the high concentrations of total phosphorus and Chemical Oxygen Demand (COD), and low DO.

Passaúna River was also evaluated on this survey, and it was classified through WQIR as good for almost all monitoring periods, except for July 2017. When an occurrence of high turbidity, high TP concentration, thermotolerant coliforms, and COD resulted as "good" in the WQIR classification.

Despite water from the Passaúna reservoir mostly being classified as good by the study, among the three other reservoirs, Passaúna was ranked with the worst WQIR average together with the Piraquara II reservoir. However, it is important to mention, as pointed out by Moreira et al. (2017), that, unlike the other reservoirs, Passaúna receives water only from its catchment. In that way, improvements or worsening in this basin's water resources management could lead to a significant impact and reflect directly on Passaúna's water quality.

Samwise, Rauen et al. (2018) analyses of Passaúna reservoir waters resulted mostly classified as good, oscillating between mesotrophic and oligotrophic as TSI index. The authors suggested further watershed and soil use controlled to reduce anthropogenic impacts, because of a water quality decrease to moderate classification between 2004 and 2014.

Ultimately, Barreto (2020), also embedded in Mudak's project, evaluated Passaúna's reservoir water quality index by applying the Trophic State Index (TSI) adapted by Lamparelli (2004) with data of TP, transparency, and Chl-a, from water sampling and laboratory analysis described in Section 5.2.1. Using an innovative approach, the author calculated TSI for several monitoring sites along the reservoir, and at the inflow and outflow, Figure 18.

Over the monitoring period (2018 and 2019), most of the monitoring sites, and especially the site located next to the water supply water withdrawal (intake site), were classified as mesotrophic. This fits with IAP (2017) classification above mentioned. Monitored sites close to the entrance (Buffer and Ferraria Bridge) were classified as eutrophic or mesotrophic, presenting fluctuations at the classification throughout the year. These results support Barreto (2020) argument that single monitoring could be not able to represent the entire environment's trophic state.

This leads to the importance of determining optimal monitoring requirements not only regarding time scales but also determining the spatial distribution of sites to be monitored along the reservoir. Further, water quality indexes will be calculated to evaluate

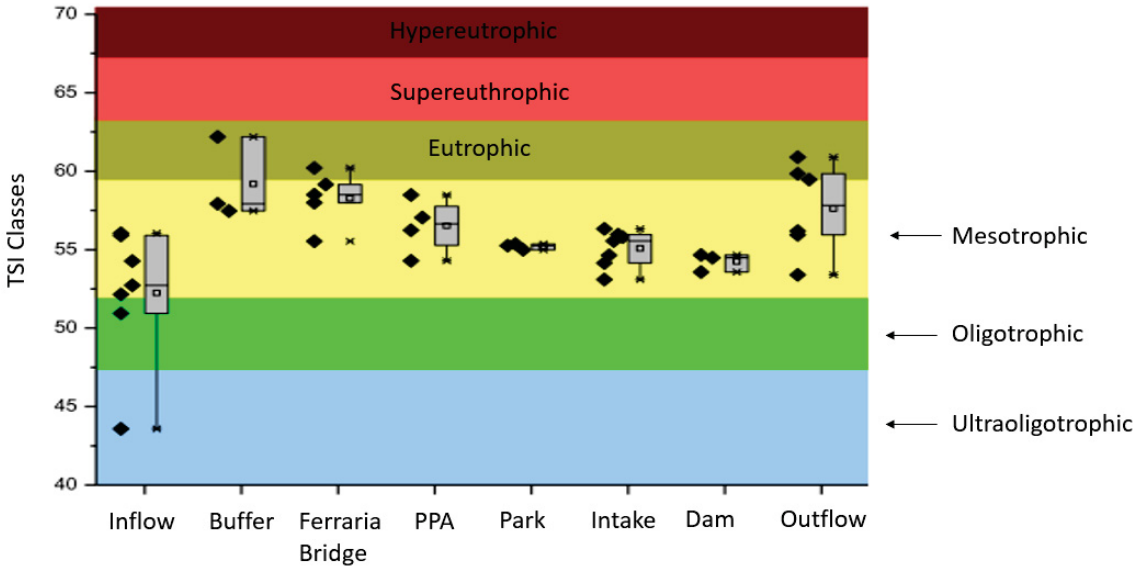

Figure 18 – Trophic State Index (TSI) calculated at Passaúna reservoir from sampling campaigns carried out from 2018 to 2019 at eight monitoring sites distributed along the reservoir, at inflow, and outflow.

Source: Adapted from Barreto (2020)

results from modeling scenarios and to identify spatial and temporal variations.

Monitoring the water quality of Passaúna reservoir is not only important to understanding the ecosystem dynamics in spatial and temporal scale, but also to guarantee public supply and conservation of water quality. It is also an instrument which provides the necessary information to support decisions making on managing water resources in the basin.

5 Water quality monitoring and modeling for Passaúna's reservoir: strategies to defining an optimal program

5.1 Overview

This chapter presents descriptions of the methodology approach and tools applied to resolve an optimal monitoring program for the water quality of Passaúna's reservoir. The first part of this chapter summarizes the water quality monitoring strategy for the reservoir, considering spatial variability (water sampling, in-situ measurements with sensors, and laboratory analyses) and temporal dynamics (data from optical sensors providing high temporal resolution monitoring).

Data obtained in the field campaigns was processed and used as the initial condition for the simulation period, to calibrate, and validate a zero-dimensional water quality model of Passaúna's reservoir. Detailed assumptions and equations used to assess total phosphorus concentrations are presented in the second part of this chapter. Passaúna reservoir was assumed as a completely mixed system. Thus, the Continuously Stirred Tank Reactor (CSTR) model was applied and tested as steady and unsteady state solutions, because it represents a screening and rapid assessment tool, with a focus on mass balance application, and not the internal processes.

In this thesis, the usage of mathematical models aims to evaluate the frequency and spatial variability of total phosphorus monitored data, testing several scenarios until their resolutions can be reduced.

The third and last part of this chapter presented methods applied in this thesis as strategies to optimize monitoring resolutions considering integration of spatial-temporal water quality dynamics and load duration curves application for Passaúna River historical data. Additionally, a description of modeling applications with improvements in temporal TP resolution data creating a daily synthetic series is presented.

This thesis study has been embedded in the MuDak-WRM project (Multidisciplinary Data Acquisition as Key for a Globally Applicable Water Resources Management, https://www.mudak-wrm.kit.edu/). This project involves universities and companies from different areas studying aspects of water quality, sedimentation, land use, production, and emission of greenhouse gases in public supply reservoirs. The focus lies on monitoring and developing models for medium and long-term water quality predictions for reservoirs and, contemplates different activities of monitoring and management of reservoirs, having as a Brazilian case the Passaúna reservoir.

5.2 Monitoring Passaúna's reservoir water quality

To establish an ideal monitoring program for water quality in Passaúna's reservoir the strategy relies on processing two interconnected sources of data: analysis of several variables spatially distributed in monthly measurement campaigns and high-temporal-resolution measurements in a single monitoring site (Figure 19).

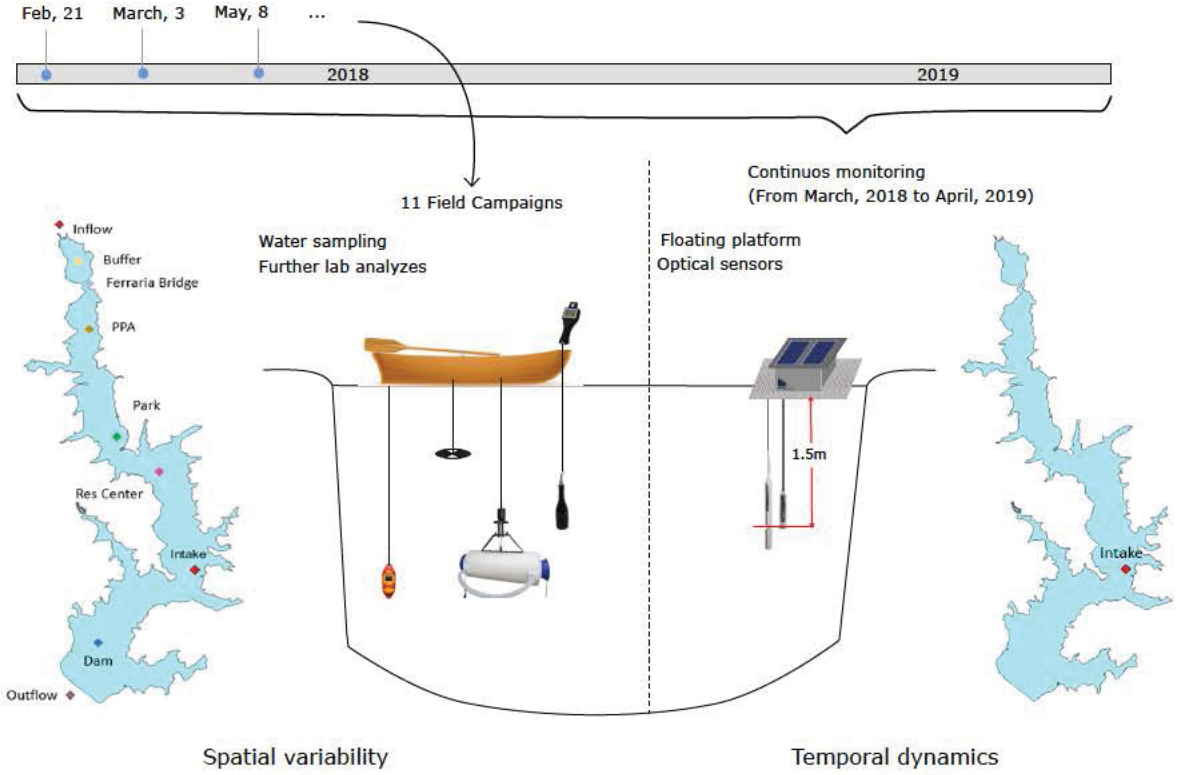

Figure 19 – Overview of approach to monitoring Passaúna reservoir over the monitoring period, from February 2018 to April 2019. On the left side is represented the spatial variability evaluated in water sampling and laboratory analysis performed at 9 monitoring sites in 11 field campaigns. On the right side is represented the temporal dynamics with data collected from measurements of optical probes, installed next to the water supply intake facility, set to perform measurements with a temporal resolution of 15 minutes.

The sampling schedule and sites monitored during field campaigns are described in the following items. Additionally, a more detailed explanation of the water sampling procedures, a description of sensors employed at in-situ measurements, and analytical methods considered in laboratory analysis are presented in Section 5.2.1.

Furthermore, optical sensor features, which compose the platform and provide continuous monitoring of several water quality variables with a high temporal resolution are presented in Section 5.2.2.

5.2.1 Spatial variability: Water sampling, in-situ measurements with sensors, and laboratory analysis

Passaúna Reservoir was monitored for over one year, from February 2018 until April 2019 (i.e., 11 sampling/measurements). Monthly water sampling, in-situ measurements with sensors, and laboratory analyses were carried out to monitor changes caused by the seasonal hydrological and meteorological cycle.

The monitoring program was designed to cover a wide range of variables measured at key sites to identify the spatial variability of the water quality within the reservoir ecosystem and account for the main tributary input that can have important impacts on downstream water quality.

Samples and in-situ measurements were taken considering horizontal distribution from upper, mid, and downstream sites. Sampling sites were located at the main water inflow, and outflow, at nine monitored sites distributed inside the reservoir from the upstream region so-called 'buffer' at the reservoir's entrance to the reservoir's deepest regions, close to the dam. The sampling site's location, water depths, and the Secchi disk depth measured at each location are provided in Figure 20.

The buffer region is considered a pre-dam due to a narrowing created by the Ferraria Bridge. Shallower locations upstream PPA site are close to, and therefore more influenced by the main river entrance. The so-called ´intake´ site is located in the lacustrine zone, close to water withdrawal. Downstream the dam is named the 'outflow' site, where the discharge is composed of the dam's bottom outlet and spillway, depending on the reservoir operation.

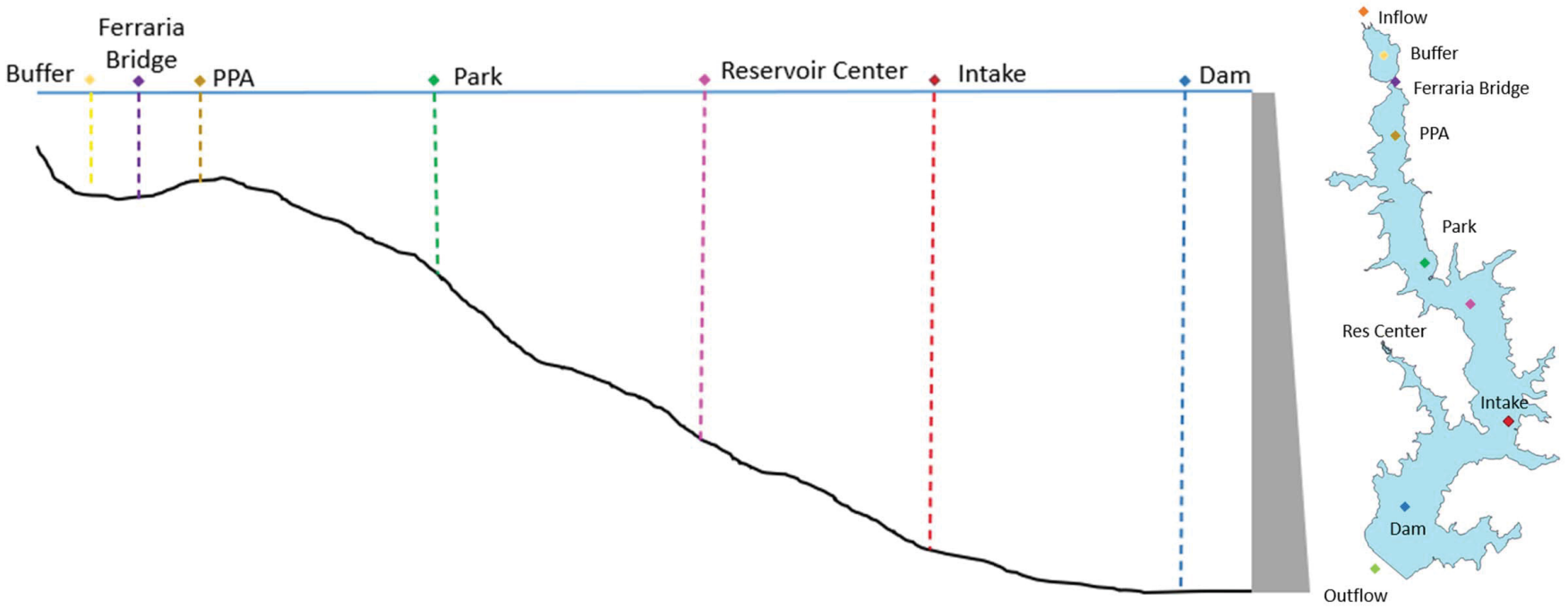

	Inflow	Buffer	Ferraria Bridge	PPA	Park	Reservoir Center	Intake	Dam	Outflow
	River	Reservoir							River
Distance from the inflow (km)		0.5	1.5	2.5	4	6	8	11	
Coordinates	-25.4221 -49.3854	-25.4534 -49.3837	-25.4567 -49.3825	-25.4587 -49.3823	-25.4848 -49.3809	-25.4922 -49.3754	-25.5112 -49.3703	-25.5277 -49.3885	-25,5327 -49.3934
Depth (m)	1.27 (1.20 – 1.35)	1.27 (0.45 - 2.10)	3.21 (2.50 - 4.40)	2.33 (1.80 – 3.00)	7.20 (6.60 – 7.60)	9.43 (9.00 – 10.00)	12.10 (10.50 - 12.80)	14.70 (14.20 – 15.50)	0.75 (0.50 – 1.40)
Transparency (m)	-	0.70 (0.20 - 1.25)	1.48 (0.10 - 3.00)	1.27 (0.40 - 1.80)	1.83 (1.30 – 2.40)	2.25 (1.70 – 2.80)	2.62 (1.95 – 3.05)	2.80 (2.40 – 3.20)	-

Figure 20 – Location of sampling/measurement sites and descriptive statistics (mean, minimum and maximum) of depth and transparency (Secchi disk depth) monitored in Passauna reservoir within the monitoring period from February 2018 to April 2019

The monitoring program, regarding sample collection sites and depths, was adapted over time according to strategic analysis of variables measured, and the need to explore additional sites for relevant spatial variability investigations of quantified parameters. In total, seven smaller and three extensive campaigns were performed. The latter covered more sampling locations along the reservoir and were taken in February 2018, August 2018, and February 2019 (Table 12).

Table 12 – Sampling schedule and sites monitored in each field campaign along Passaúna's reservoir within the monitoring period from February 2018 to April 2019. Extensive campaigns are marked as blue lines and months with no field campaigns as grey lines.

Campaigns		Inflow	Buffer	Ferraria Bridge	PPA	Park	Reservoir center	Intake	Dam	Outflow
2018	February	•	•	•	•	•	•	•	•	•
	March									
	April (03)	•						•		•
	April (24)							•		
	May	•						•		•
	June	•		•				•		•
	July									
	August	•	•	•	•	•	•	•	•	•
	September									
	October	•	•	•	•			•		•
	November	•	•	•	•			•		•
	December	•	•	•	•			•		•
2019	January									
	February	•	•	•	•	•	•	•	•	•
	March									
	April	•		•	•			•		•

To assess vertical characterization, water samples were collected at several depths using a horizontal Van Dorn water sampler. The sampled depths included the water surface (0.2 m depth), the near-bottom layer (approximately 0.5 m above the bottom), and up to three additional depths according to the temperature stratification measured with a CTD - Conductive-Temperature-Depth sensor (Castway, Sontek, Figure 5.2.1). The sampling depths were defined after the assessment of the temperature profile to sufficiently resolve the vertical gradients. An overview of sampling and in-situ measurement depths is presented in Table 13.

Laboratory analyses of water samples were performed for quantification of total nitrogen (TN), organic nitrogen (Organic N), ammonium (N-NH_3), nitrate (N-NO_3), nitrite (N-NO_2), total phosphorus (TP), total dissolved phosphorus (TDP), particulate

Table 13 – Overview of sampling depths and locations of water sampling collection in each field campaign along Passaúna's reservoir within the monitoring period from February 2018 to April 2019. Months with no field campaigns are marked as grey lines.

Campaigns		Inflow	Buffer	Ferraria Bridge	PPA	Park	Reservoir Center	Intake	Dam	Outflow
2018	February 21	Surface	Surface 1.0 2.0	1.0 2.0 3.0	Surface	Surface 3.0 5.0 6.0	Surface 7.0 9.0	Surface 6.0 9.0 11.0	Surface 2.0 5.0 10.0 14.0	Surface
	March									
	April 3	Surface						Surface 1.5 4.0 10.0		Surface
	April 24							Surface 0.7 2.0 4.0 7.0 10.0 12.0		
	May 8	Surface						Surface 1.5 6.0 10.0 12.0		Surface
	June 12	Surface						Surface 1.5 6.0 12.0		Surface
	July									
	August 13	Surface	Surface 1.0	Surface 1.0 2.0	Surface 1.0 2.0	Surface 3.0 6.0	Surface 4.0 8.0	Surface 4.0 8.0 10.0	Surface 4.0 8.0 13.0	Surface
	September									
	October 25	Surface	Surface	Surface 2.5	Surface 2.5			Surface 1.5 10.0		Surface
	November 20	Surface	Surface	Surface 2.5	Surface 2.0			Surface 1.5 10.0		Surface
	December 11	Surface	Surface	Surface 2.5	Surface 1.5			Surface 1.5 10.0		Surface
2019	January									
	February 4	Surface	Surface	Surface 2.0	Surface 1.5	Surface 3.0 7.0	Surface 3.0 9.0	Surface 2.5 7.0 10.0	Surface 6.0 10.0 14.0	Surface
	March									
	April 2	Surface		Surface 3.5	Surface 2.5			Surface 1.5 11.0		Surface

phosphorus (particulate P), orthophosphate (P-PO_4), total suspended solids (TSS), total dissolved solids (TDS), dissolved organic carbon (DOC), and Chl-a (Table 14).

Table 14 – Summary of variables analyzed in laboratory over the monitoring period. Extensive campaigns are marked as blue columns and months with no field campaigns as grey columns.

Analyses	2018									2019	
	Feb	Apr-03	Apr-24	May	Jun	Aug	Oct	Nov	Dec	Feb	Apr
Chlorophyll-a	•	•	•	•	•	•				•	•
DOC	•	•		•	•	•	•	•	•	•	•
Phosphorus forms	•	•		•	•	•	•	•	•	•	•
Nitrogen forms	•	•		•	•	•	•	•	•	•	•
Solid forms	•	•		•	•	•	•	•		•	•

Sampling, transportation, preservation, and analytical protocols were conducted following Standard Methods for Surface Waters (APHA, 2006). Polyethylene bottles were used for sample collection of solids and Chl-a analyses, and glass bottles for nutrient and DOC analysis. Water sample bottles were first cleaned and then decontaminated with a hot acid wash in 5% HCl solution. Bottles for analyses of solids and DOC were calcined to eliminate organic matter traces. Chl-a samples were stored in darkness until analysis in the laboratory.

The laboratory analyzes were performed at Francisco Borsari Netto Environmental Engineering Laboratory - LABEAM. Within 24 hours from sample collection, samples were filtered using a 0.45-μ membrane filter, and measurements of N-NO_3, P-PO_4, and N-NH_3 were conducted. Only samples for TN and TP determination were kept unfiltered. Samples for DOC quantification require preservation and were acidified with sulfuric acid. Samples were stored at 4ºC with minimum exposure to light and air until analyzed within 10 days after sampling. Before analysis, water samples were equilibrated to ambient temperature.

Table 15 presents the analytical methods employed in chemical analysis for the determination of variables in the laboratory. TN concentration was determined with the persulfate method, by oxidation of all nitrogenous compounds to nitrate. N-NH_3 concentrations were measured by the phenate method, and N-NO_3 and N-NO_2 concentrations were analyzed by the cadmium reduction method (APHA, 2006). Organic N concentration was obtained as the difference between TN and inorganic nitrogen forms (N-NH_3, N-NO_3, and N-NO_2).

TP and TDP concentrations were determined with acid digestion, followed by the ascorbic acid method. P-PO_4 concentrations were quantified using the ascorbic acid method. While particulate phosphorus was determined as the difference between TP and TDP. Due to very low concentrations, total and dissolved phosphorus samples were

Table 15 – Analytical methods employed in the laboratory analyses for quantification of Nitrogen, Phosphorus, and Solids forms, Dissolved Oxygen Carbon (DOC) and Chlorophyll-a.

Parameter analyzed		**Analytical Method**	**Reference**
Dissolved Organic Carbon (DOC)		Non-dispersive infrared detection high-temperature combustion	TOC-VCPH Shimadzu Corporation (2003)
Nitrogen forms	Total Ammoniacal Nitrogen ([N-NH3)	Phenate method	Adaptation of 4500-NH3 F Standard methods (APHA, 1998)
	Nitrite (N-N02-)	Cadmium reduction and colorimetric method	4500-NO2 B, Standard methods (APHA, 1998)
	Nitrate (N-N03-)	Cadmium reduction and colorimetric method	4500-NO3 E, Standard methods (APHA, 1998)
	Total Organic Nitrogen (Norgt)	Norgt = NT - N_{INORG} - where N_{INORG}: Inorganic Nitrogen N_{INORG} = [N-NH_3] + [N-NO_2-] + [N-NO_3-]	
	Total Nitrogen (NT)	Persulfate method - Alkaline digestion method using potassium persulfate ($K_2O_2O_8$) and sodium hydroxide (NaOH)	4500-N C, Standard methods (APHA, 1998)
Phosphorus forms	Orthophosphate (P-PO_4)-	Ascorbic acid method	4500-P E, Standard methods (APHA, 1998)
	Dissolved Phosphorus (PTD)	Acid digestion and ascorbic acid method	4500-P E, Standard methods (APHA, 1998) and Prado (2015)
	Total Phosphorus (PT)	Acid digestion and ascorbic acid method	4500-P E, Standard methods APHA (1998) and Prado (2015)
	Particulate Phosphorus (P_{PART})	P_{PART} = [PT] - [PTD]	
Solid forms	Total, fixed and volatile (total fractions, dissolved and suspended)	Gravimetric method	Adaptation of 2540 F, B, E, Standard methods (APHA, 1998)
Chlorophyll-a		Acetone 90% extraction and spectrophotometric analysis	CETESB Technical Standard L5.306 (2014)

concentrated 10 times and acidified with ascorbic acid, according to quantification method suggested by PRADO (2018).

Chl-a concentration was determined according to CETESB (2014). The water

sample was vacuum filtered onto a glass fiber filter. The filter was macerated and steeped in 90% acetone to extract chlorophyll from the algal cells, followed by sample clarification through centrifugation. The absorbance of the clarified extract was then measured in a UV-visible spectrophotometer (Kazuaki IL-0082-BI) before and after HCl acidification.

All analysis results were quality checked by careful standardization, procedural blank measurements, and triplicated analyses, in which samples were measured three times and averaged.

In-situ measurements of water quality parameters were performed with a multi-parameter water quality probe (U-53G Horiba or AP-800 Aquaread, Figure 21). The measured parameters include field dissolved oxygen (DO), pH, turbidity, temperature, depth, conductivity, salinity, total dissolved solids (TDS), and oxidation-reduction potential (ORP). Before each field campaign, sensor set up were regularly calibrated in the laboratory through auto calibration with a standard solution.

Probe/sensor	Multiparameter		Multiparameter		Conductive-Temperature-Depth	
Equipment	U-53		AP-800		CTD Castway	
Manufacturer	HORIBA		AQUAREAD		SonTek	
Parameter	Unit	Measurement range (Accuracy)	Unit	Measurement range Detection limit)	Unit	Measurement range (Accuracy)
DO	mg/L	0 – 50 (± 0.20)	mg/L	0 – 50 (± 1%)	-	-
pH	-	0 – 14 (± 0.10)	-	0 – 14 (± 0.10)	-	-
Turbidity	mg/L	0 – 1000 (±0.10)	mg/L	0 – 3000 (±0.20)	-	-
Temperature	C	0 – 1000 (±0.10)	C	-5 – 50 (± 0.50)	C	0 – 200 (0.05)
Conductivity	FS	0 – 100 (± 5%)	FS	0 – 200 (± 1%)	µS/cm	0 – 200 (5)
Salinity	ppt	0 – 70 (± 3)	ppt	0 – 70 (± 1%)	-	-
TDS	g/L	0 – 100 (± 5)	g/L	0 – 100 (± 1%)	-	-
Depth	m	0 – 30 (± 0.30	-	-	m	0 – 200 (0.25%)

Figure 21 – Technical information of Conductive-Temperature-Depth (CTD) sensor, and multiparameter probes U53 (Horiba) and AP-800 (Aquaread) - used to perform in-situ measurements of water quality in field campaigns profiles

Source: Adapted from HORIBA (2009), AQUAREAD (2017), and SONTEK (2012)

Quality standards established for Passaúna reservoir water quality evaluation were based on threshold values as Class II to surface water and quantitative recommendations

for a good ecological status of water bodies given in the "CONAMA Resolution 357/2005" by the Environment National Council (Brasil, 2005), responsible for establishing water bodies classification - See Table 16 at section 2.

With the aim of enhancing water quality analyses, in addition to the already mentioned parameter quantification, biological zonation was also performed within Mudak's Project. Surveys of two storm events were performed on October 2018 by MuDaK partners in Passaúna River. Additionally, Barreto (2020) prospected the presence of phytoplankton in samples collected at monitored sites Buffer, Ferraria Bridge, PPA, and Intake, in field campaigns in November 2018, February, and April 2019. Using microscopy examination identifying organisms and analyzing the genera variability, 34 phytoplankton genera were identified in the Passaúna reservoir. More information about the collection, conservation, and treatment of the samples, as well the methodology adopted in the analyzes, and results can be found at Barreto (2020).

5.2.2 Temporal dynamics: Data from platform equipped with optical sensors providing continuous monitoring

In addition to spatial variability monitoring strategies, to assess the temporal water quality dynamics, a floating platform system equipped with sensors providing real-time water quality measurements were installed next to the water intake facility (coordinates: -25.5112, -49.3700, Figure 22).

Figure 22 – Floating platform system located in Passauna reservoir next to the water intake

With the exception of the metallic support structure and floats (made of blue

gallons that kept the system floating), the platform unit used in this research was developed and provided by the German company TriOS Optical Sensors (https://www.trios.de/) within the Mudak Project.

The platform unit, installed on March 01st 2018, was composed of a data logger controller (TriBox3 - Figure 24), a photometer sensor (OPUS), and a fluorometer sensor (nanoFlu), Figure 26. The sensors stayed entirely submerged in the water attached to the floating system at 1.5 m from the surface with stainless steel bars, to provide measurements with no solar radiation influence and ensure the device's safety.

To assure a sufficient power supply for measurement operation over the monitoring period, both the data logger and sensors were powered with a self-sufficient photovoltaic system. The procedure of using solar energy only was a TriOS prototype, tested in MuDaK's research project.

Both data logger controller and solar energy operation devices were placed in a robust aluminum housing, roof by a solar cell panel. A series system of three batteries secured the system's energy in the lack of enough solar radiation. To avoid overheating was installed a cooler inside the aluminum housing, Figure 23.

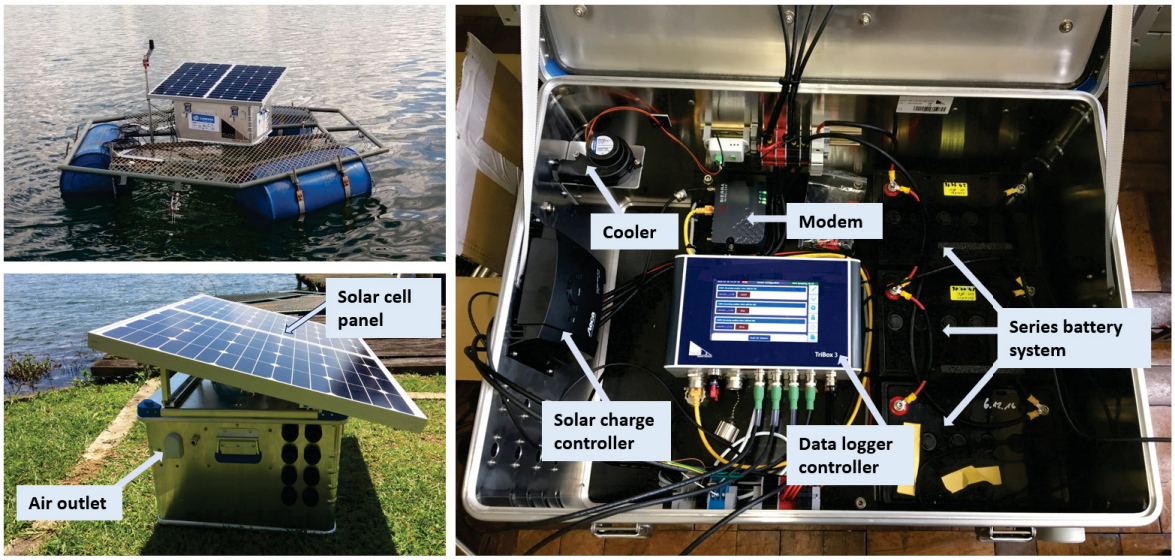

Figure 23 – An inside view of the platform system housing

Another necessary adaptation was related to the system for clean probes windows. Usually, this system works with a compressed-air unit, but in Passaúna reservoir this system would consume more energy than the solar structure could provide. Therefore, wipers were attached to the probes promoting window probe cleaning and preventing measurement interference. As the measurement technology is optical for such probes, this is a crucial site to assure reliable measurements.

The digital measurement and control unit (Tribox3, Figure 24) was set to collect data from probes with high temporal resolution. Both the photometer and fluorometer

performed measurements every 15 minutes. The data collected was transmitted to the cloud via telemetry in real-time, through a modem and a SIM Card (Subscriber Identity Module).

Figure 24 – Digital measurement and control unit - Tribox3

Source:TriOS (2017b)

The raw data measured by the probes, as 'csv' file (comma separated values), were accessed either in the cloud through an exclusive online platform (Figure 25) or downloaded with a flash-driver directly from the data logger. Usually, the procedure was to download the sensors' measurements directly on field campaigns once per month, in which was also performed the platform maintenance. At service, sensors lenses were checked for bio-film growth and wiper's repair.

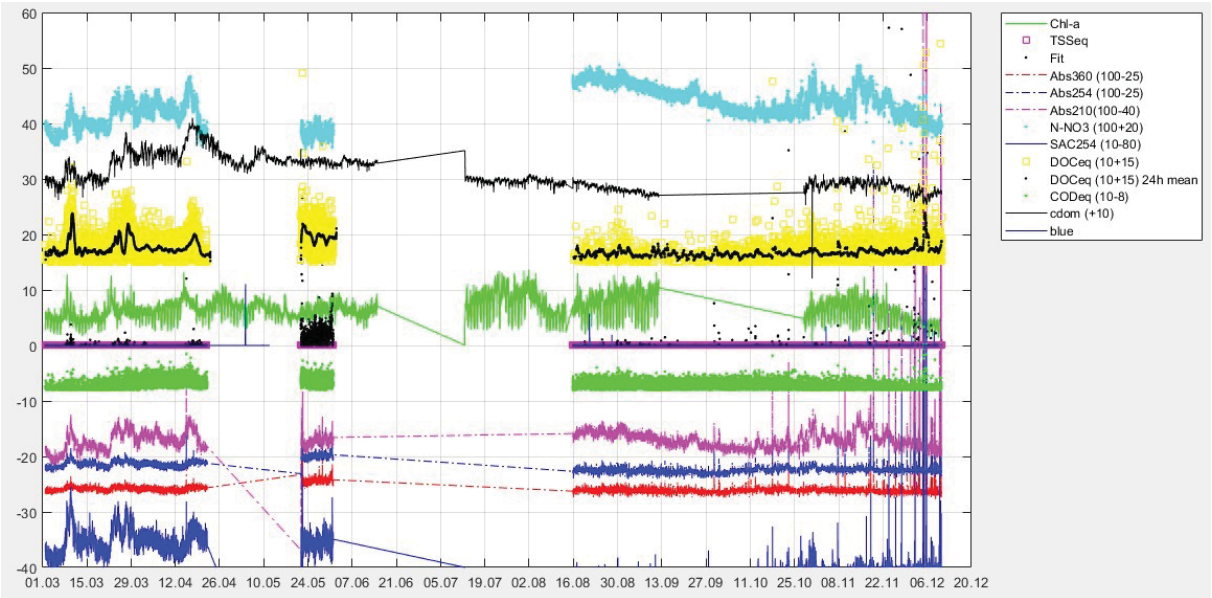

Figure 25 – Visualization of the exclusive online platform showing real-time measurements performed by platform probes.

The substances measured by both photometer and fluorometer are described in

Figure 26, along with the measurement range and detection limit of each variable. Measurements principles are absorption for the photometer and fluorescence for the fluorometer. OPUS performed measurements of nitrate ($N - NO_3$), nitrite ($N - NO_2$), potassium hydrogen phthalate (KHP), and spectral absorption coefficient at 254 nm (SAC254), and as equivalent, measurements of chemical oxygen demand (COD), biological oxygen demand (BOD), dissolved organic carbon (DOC), total organic carbon (TOC), and total suspended solids (TSS). NanoFlu measures colored dissolved organic matter (CDOM), chlorophyll-a, cyanobacteria, rhodamine, and fluorescein. A more detailed description of the probes system and technical information can be found in TriOS (2017b) and TriOS (2017a).

TriOS Optical Sensors OPUS (Photometer)			TriOS Optical Sensors nanoFlu (Fluorometer)		
Absorption			Fluorescence		
Parameter	Unit	Measurement range (Detection limit)	Parameter	Unit	Measurement range (Detection limit)
Nitrate NO_3 – N	mg/L	0 – 10 (0.03)	CDOM	µg/L	0 – 200 (0.3)
Nitrite NO_2 – N	mg/L	0 – 15 (0.05)	Chlorophyll-a	µg/L	0 – 200 (0.2)
CODeq	mg/L	0 – 220 (3)	Cyanobacteria	µg/L	0 – 200 (0.3)
BODeq	mg/L	0 – 220 (3)	Rhodamine		
DOCeq	mg/L	0 – 100 (0.5)	Fluorescein		
TOCeq	mg/L	0 – 100 (0.5)			
TSSeq	mg/L	0 – 150 (6)			
KHP	mg/L	0 – 400 (0.5)			
SAC_{254}[1]	1/m	0 -220 (1.5)			

1- measurement principle: single wavelength

Figure 26 – Technical information of OPUS (with 10 mm optical path) and nanoFlu, sensors attached to the platform system setup to perform measurements with a time resolution of 15 minutes.

Source: TriOS (2017b)

As an optical sensor, the operation mechanism of the fluorometer (nanoFLu) is fluorescence emission, in which a LED lamp acts as a source, emitting light in a defined wavelength to each one of the variables to be measured. For Chlorophyll-a, cyanobacteria, and CDOM, the emission wavelength are 460, 620, and 360, respectively.

Each fluorescent substance has its fluorescence behavior, meaning that it will absorb a certain wavelength and emit at a different one, depending on the concentration, chemical composition, and structure of the substance. In this probe, reflected fluorescent light is collected by a lens system, and a photodiode detector measures fluorescence intensity (Figure 27).

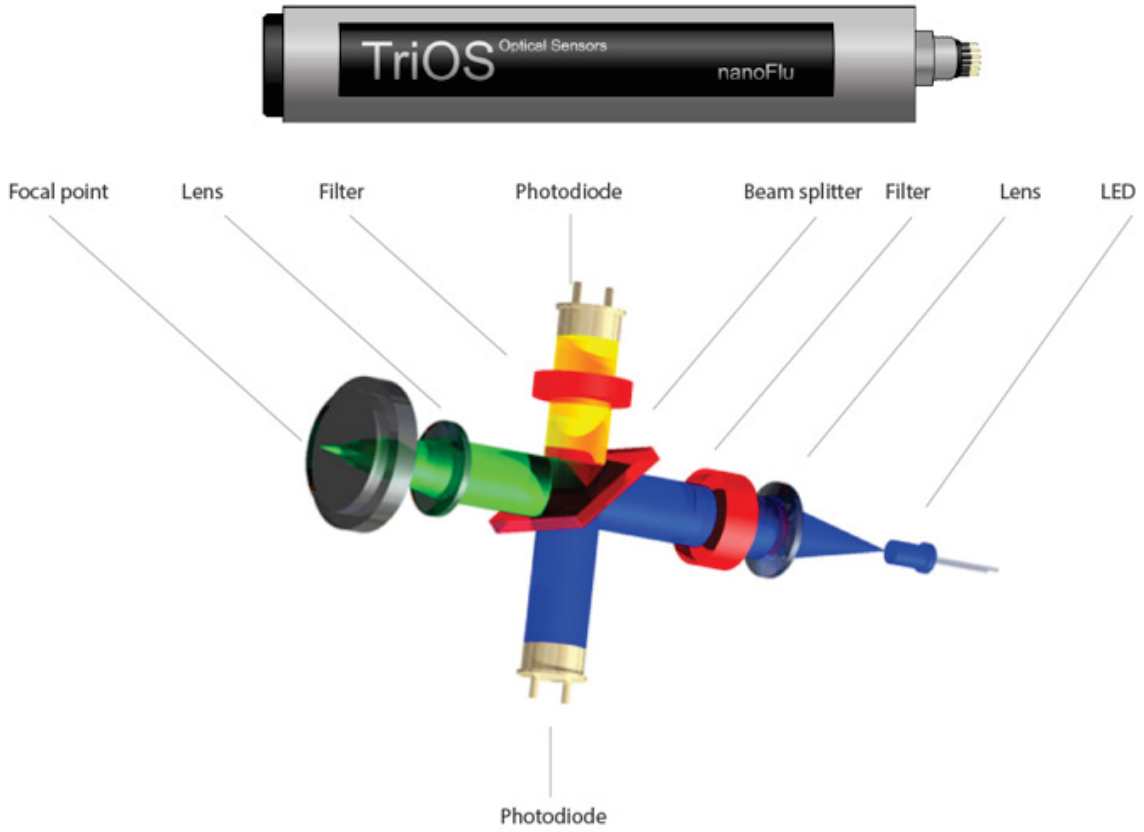

Figure 27 – Optical arrangement of nanoFlu probe, consisted of light source, lens system, optical path and fluorescence detector with a filter, which acts to ambient light suppression

Source: TriOS (2017b)

Fluctuations in the light source could interfere with the measurements, so nanoFlu has a reference diode to compensate for possible fluctuations. In addition, an electronic circuit eliminates the ambient light. In any case, to avoid interference it is advisable to perform measurements only under sunlight.

Also an optical sensor, the Photometer (OPUS, Figure 28) has as measurement principle of absorption and spectral analysis. A xenon flash lamp acts as a source of broadband light, which passes through an optical path until reaches the spectrometer. Some of the light emitted is absorbed in the pathway, and the remaining intensity is detected by the spectrometer, as spectral analysis over the wavelength range from 200 to 360 nm.

Thus, an important aspect of the photometer analysis is the optical path length. It must be determined based on the expected concentrations of the waters. Small

concentrations require longer optical path lengths when using photometric method. The available optical path length comprises in TriOS catalog are 0.3, 1, 2, 5, 10, 20, and 50 mm. For Passaúna's reservoir, an optical path of 10 mm was used.

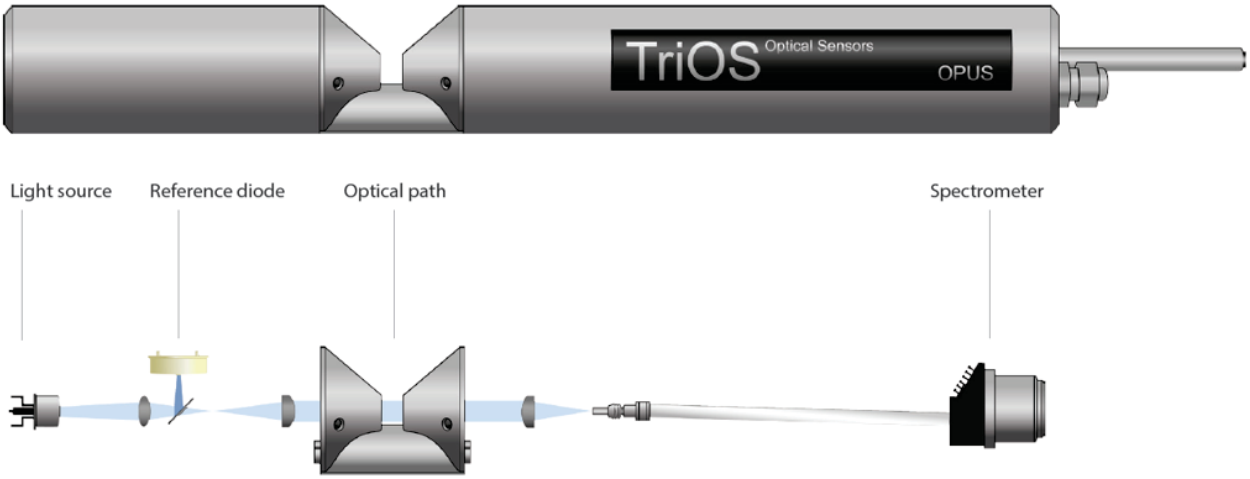

Figure 28 – Optical arrangement of OPUS probe, consisting of a light source, reference diode, optical path and spectrometer

Source: TriOS (2017b)

Nitrate and nitrite are substances that present a specific absorption spectrum. Yet, organic substances (COD, BOD, DOC, TOC) present theoretical absorption spectra identified by the sensor's company producer, Figure 29. In the sensor programming, a set of absorption spectra for each one of the foreseen substances are saved for calibration. When surveying with the probe, the measured absorption spectrum of the water is compared with stored absorption spectra, calculating concentrations using Equations 2.5 and 2.6 presented in Section 2.7.4. Measurements in ultra-pure water (factory-proven calibration) are necessary to be used as a reference.

A residual error, the so-called fit error, results from the calculations by spectral deviation of the absorbed and reconstructed spectrum. When this value is significant, the measurement isn't reliable whether by interference in measurements caused by the probe failure, or even by wiper bad-functioning.

Therefore, for both sensors, data processing required specialized services to be manipulated. The raw data, collected in high temporal resolution measuring several parameters, was checked to be among wavelength measurable range, for high fit error, and by simple visual correlation.

Subsequently, data measured between 8 am and 8 pm were eliminated as recommended by Rousso et al. (2021), since during the daytime there is a decline in the fluorescence emitted by phytoplankton, can result in an underestimation of more than 79% in Chl-a concentrations.

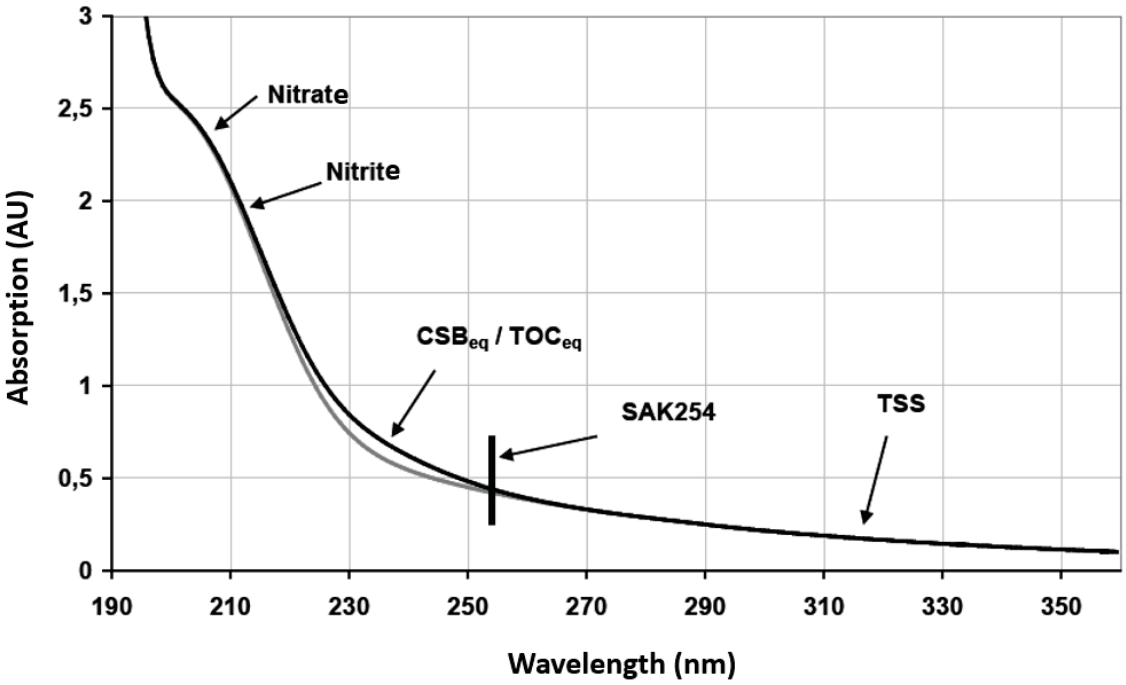

Figure 29 – Absorption spectrum and correspondent wavelength relation used by OPUS probe to quantify water quality variables concentrations

Source: TriOS (2017b)

As mentioned in last section 5.2.1, an Opus photometer was adapted to be used as a profiler in field campaigns. Its operation is basically the same of continuous monitoring sensor, with exception of the procedure for data downloading and the trigger for measurements. Instead of measuring every 15 minutes, as a profiler, Opus performed measurements through a signal sent by an interface operated by a user at measurement time. The raw data are further downloaded using a device (G2 interface box), which translates the sensor plug to the conventional power supply connections and to the network access (Figure 30).

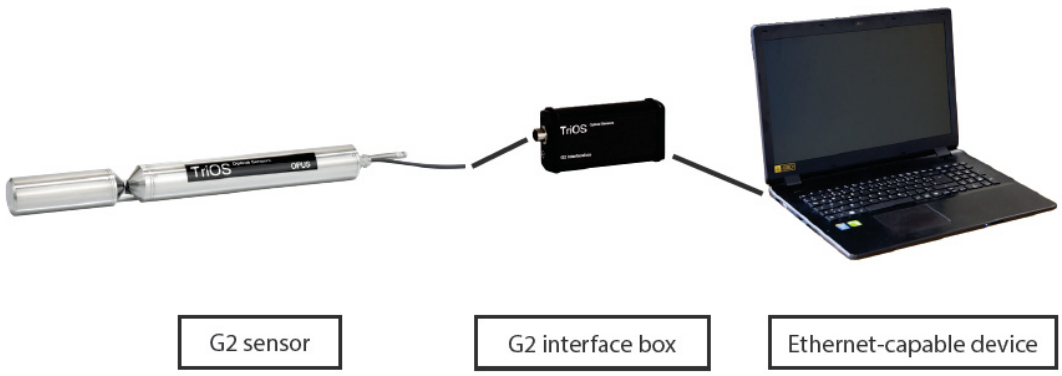

Figure 30 – The G2 interface box translates the sensor plug to the conventional power supply connections and to the network access to download the data directly from the probe profiler.

Source: TriOS (2017b)

As substances in natural waters are variable according to local conditions, measurements performed by the optical probes need calibration, based on laboratory results, to validate the measurements. If sensor measurements don't fit with laboratory analysis, a scale factor can be applied to the probe's configuration of nanoFlu and OPUS.

5.3 Modeling Passaúna's reservoir water quality

In addition to the monitoring strategies, modeling techniques were also applied to assess an optimal monitoring program for water quality for Passaúna's reservoir. Modeling approaches allow a better understanding of the spatial and temporal variability of nutrients and other substances, could help to predict water quality changes when no measurement data is available, also to identify situations in which the critical load could be exceeded in the water body, and even, to test impacts of water resources management actions, or changes of climate conditions. By testing scenarios in models is possible to evaluate several different conditions and their consequences on the reservoir's water quality.

From one to three dimensions, numerical modeling has been applied to represent Passaúna reservoir hydrodynamics and water quality dynamics using data acquired during the monitoring period. Sales (2020) implemented the General Lake Model - GLM, a one-dimensional hydrodynamic open source model complemented with a water quality library (AED), to simulate variables such as dissolved oxygen, phosphorus, and nitrogen in vertical profiles. Furthermore, Golyjeswski (2020) employed CE-QUAL-W2 in a laterally averaged model (2DV model) to represent the reservoir's hydrodynamics. Moreover, Ishikawa, Bleninger and Lorke (2021) employed Delft3D in a 3-dimensional hydrodynamic model.

All three applications were calibrated with data described in Section 5.2, and have the same setup regarding modeling period (from 01 August 2017 to 28 February 2019), temporal resolution, boundary, and initial conditions. It is not the aim of this study to explore the limitations and potentialities of the models used, nor to evaluate and compare the results of water quality assessment.

Comparison of differences between the three models with different dimensionalities regarding thermal stratification, flow velocity, and substance transport by density currents were assessed by Ishikawa et al. (2022a).

In the present study, a zero-dimensional water quality model of Passaúna's reservoir was set up from water quality data, obtained in the field campaigns.

5.3.1 Phosphorus mass balance of Passaúna Reservoir

A zero-dimensional phosphorus mass-balance model for Passaúna's reservoir was set up based on total phosphorus (TP) budget data of inputs, outputs, and concentrations measured in field campaigns, as presented in Section 5.2. The period assumed for simulation was from February 2018 to January 2019, because of the measured field data availability in this period to evaluate the simulations results. TP data was processed and set as the initial condition for the simulation period, to calibrate, and validate the modeling results.

Usually, phosphorus concentrations are associated with eutrophic conditions, since the element is a key factor in the biological cycle in water bodies. Additionally, phosphorus was pointed out as the limiting nutrient of Passaúna's reservoir by Coquemala (2005), Smaha and Gobbi (2003), and more recently by Barreto (2020) using the same data from the monitoring period of this study. Barreto (2020) claimed that phosphorus low concentrations within the reservoir limits phytoplankton growth and influences bloom episodes.

Moreover, recently Wu et al. (2022) evaluated the ratio between P and N in inflows and outflows of more than 5,000 lakes globally distributed using a multi-faceted approach to identify lake nutrient retention. The study resulted in almost 90% of the lakes presenting preferential retention of P, causing negative effects within aquatic bodies and downstream regions.

TP mass balance applications have been widely used in defining trophic states and eutrophication (DODDS; WHILES, 2019; CHAPRA, 1997). Although total nitrogen can also be estimated using the mass balance approach, due to nitrification-denitrification balance, is usually more susceptible to errors (VIDAL; NETO, 2014).

A Continuously Stirred Tank Reactor model (CSTR) application was adopted to assess Passaúna's reservoir phosphorus mass balance, since represents one of the simplest cases and aims to identify the nutrient reservoir dynamics by quantifying TP accumulation, Figure 31.

The general assumptions of such an application is the steady-state of phosphorus concentration, complete mixing, constant sedimentation, and limited phosphorus input from sediments.

Since the sources and sinks of phosphorus are directly connected with the amount of water coming into and leaving the reservoir, a first step in quantifying mass flux is to set up the reservoir's water budget. A water budget with good accuracy is crucial to develop a mass balance with reliable results.

From the general water budget equation (Equation 3.13), possible sources and sinks described in Section 3.2.4, and available data, the total balance is expressed with

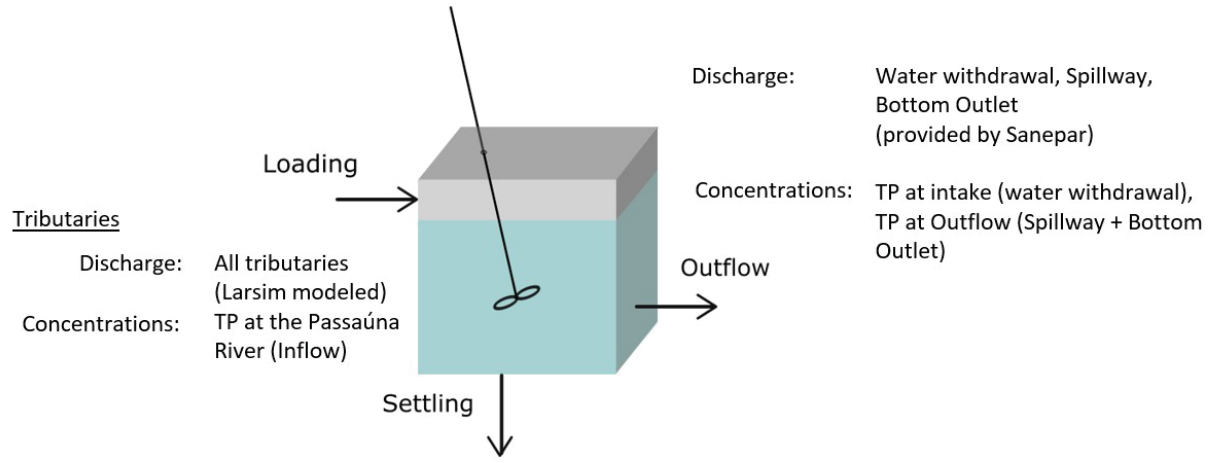

Figure 31 – Graphical summary of sources and sinks adopted in CSTR application for Passaúna reservoir

an equation combining terms representing loading, outflow, and settling, Equation 5.1. Phosphorus retained within the reservoir is represented by the difference between inputs and outputs.

The river basin tributaries were considered as sources of TP, while the water withdrawal, spillway summed up with bottom outlet, and settling losses were considered as sinks of TP.

$$\frac{dc_A V}{dt} = Q_{rivers}c_{rivers} - Q_{int}c_{int} - Q_{spill+bott}c_{spill+bott} - \nu.A_s \tag{5.1}$$

Where Q_{rivers}, $Q_{int}c$,$Q_{spill+bott}$ represents respectively river, water withdrawal, and spillway summed up with bottom outlet discharges (m^3/s), c_{rivers}, c_{int}, $c_{spill+bott}$ represents TP concentrations (mg/L), and $\nu.A_s$ represents settling losses obtained from apparent settling velocity (ν, m/s) multiplied with surface area of the sediments (A_s, m^2).

Measuring and monitoring phosphorus sources and sinks in reservoirs could be very challenging, therefore some simplifications can take place when calculating mass budgets. In this study were not considered possible contributions of total phosphorus from air deposition, internal loading process, and rainfall input over the reservoir.

The inflow discharge data series applied in the mass-balance model was provided by Hydron in daily resolution. Hydron is a German company, which modeled continuous runoff processes in Passaúna's watershed and its rivers tributaries, using the rainfall-runoff model Large Area Runoff Simulation Model (LARSIM). The model's results are a function of several local conditions such as river network, topology, soil hydraulic properties, land use, and meteorological data.

Passaúna watershed was divided into 64 elements of river tributaries contributing to Passaúna's reservoir. The model's calibration and validation were performed with measured discharge from BR-277 Campo Largo gauge station (see Figure 14). Resulting

in a simulated data series of hydrological data, composed of discharges and temperatures inflow into the reservoir.

Figure 32 presents an extract from January 2018 to February 2019 of Passaúna's reservoir inputs data series. The main discharge input into the reservoir is from Passaúna's River, followed by Ferraria's River. The sum up of the remaining 62 tributaries represents only a small fraction of the total input discharge.

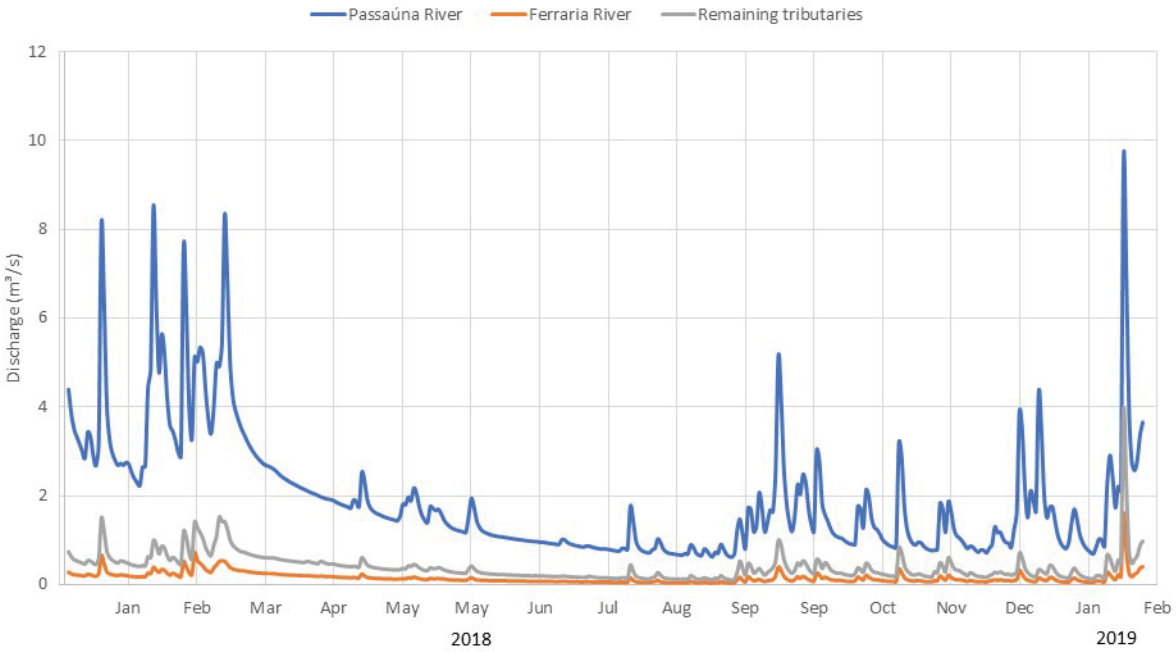

Figure 32 – Discharge data series (m^3/s) of Passaúna's reservoir tributaries from January 2018 to February 2019, provided by Hydron in daily resolutions. The blue line represents Passaúna's River discharge input into the reservoir, the gray line is Ferraria's River, and the orange line is the sum-up of the remaining 62 tributaries.

Source: Data provided by Hydron, MuDak's research project partner.

The monthly TP load into the reservoir was calculated by multiplying the discharge inflow (including all tributaries - m^3/s) with total phosphorus concentration (mg/L) measured at the inflow monitoring site. Linear interpolation of concentrations missing data was performed for March, July, September 2018, and January 2019.

The outflow data was provided by Sanepar (Water and Sanitation Company of Parana State), composed of drinking water abstraction (hourly data, L/s), discharge via flood spillway (daily values, L/s), and discharge via bottom outlet (daily values, L/s).

Initially, the evaluation of input and output data showed a considerable water deficit in the reservoir. This was deeply analyzed, and after an integrated evaluation made by MuDak project partners, the bottom outlet discharge data and the spillway data series were corrected and actualized for multiple purposes, such as this application.

Phosphorus load out of reservoir was calculated as the sum up of drinking water

abstraction discharge (m^3/s) multiplied by total phosphorus concentration (mg/L) of samples collected at intake monitoring site on the surface, plus the sum of discharge via flood spillway and discharge via bottom outlet (m^3/s) multiplied by total phosphorus concentration (mg/L) of samples collected at the outflow monitoring site.

Reservoir's volume was calculated in daily resolution by applying data from the reservoir's level provided by Sanepar (in daily resolutions) in a hypsography curve provided by MuDak-WRM project partners computed with multibeam sonar measurements (Figure 33).

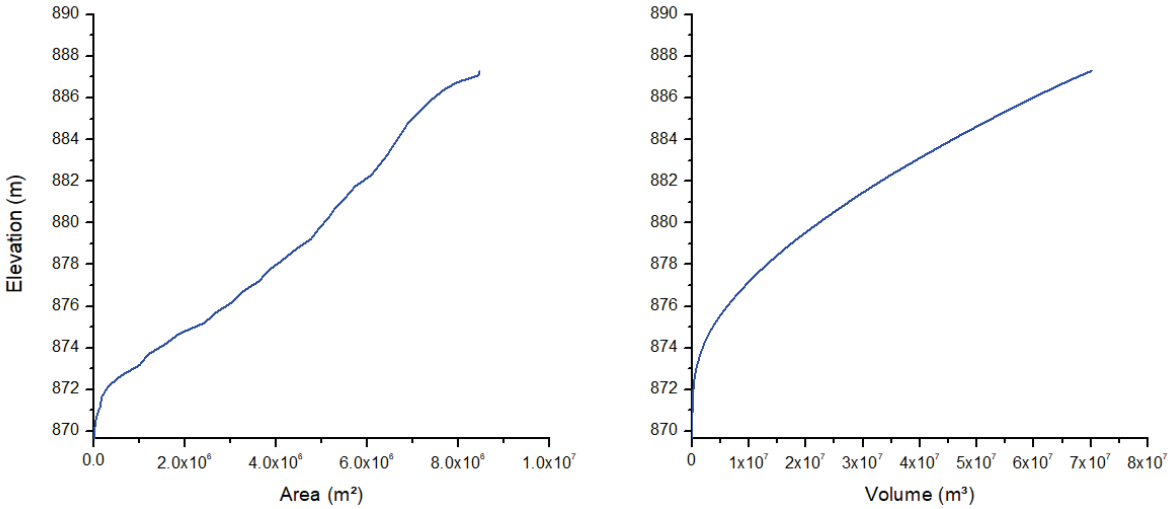

Figure 33 – Hypsographic curve of Passaúna reservoir provided by MuDak's project partners.

Mass balance application was assessed using two different solutions: steady state and unsteady state.

From mass-balance models for well-mixed systems, phosphorus concentration can be solved with steady-state solution.

Firstly, a mass balance of phosphorus was set up, and both sources and sinks of phosphorus are connected with discharge coming into and leaving the reservoir. Secondly, a Continuously Stirred Tank Reactor (CSTR) model application was adopted, where the Passaúna reservoir was assumed as a completely mixed system.

5.3.2 Steady-state solution for Passaúna's Reservoir

Firstly, to obtain annual TP concentrations within the reservoir, data were submitted to the steady-state, where discharge and concentration don't change over time. The steady-state solution provides the concentration of a solute considering the system in dynamic equilibrium (CHAPRA, 1997).

The steady-state concentration was solved by the equation 5.2, in which TP concentration (c, mg/m^3) within the reservoir was obtained from TP loading (W,

mg/year), outflow discharge (Q, m^3/year), volume (V, m^3), and a first-order settling loss rate (K_s, /year).

$$c = \frac{W}{Q + k_S V} \tag{5.2}$$

Phosphorus loading (W, kg/year) was calculated using TP concentrations of monthly measurements at the main inflow during the monitored period - February 2018 to February 2019. Moreover, the first-order settling loss rate (k_s) was obtained as function of residence time (RT, year), as proposed by Toné (2016) in Equation 5.3, calibrated using data collected from 33 reservoirs located in the Brazilian semi-arid region.

$$k_s = \frac{4}{\sqrt{RT}} \tag{5.3}$$

Subsequently, monthly TP concentrations within the reservoir were calculated through the unsteady-state solution.

5.3.3 Unsteady-state solution for Passaúna's Reservoir

The unsteady-state TP concentrations were calculated using Equation 5.4, with both discharge and TP concentration changing over time. This equation was obtained in a study conducted by Becker (2021) based on the numerical method of finite difference to approximate the derivative as differences of Equation 5.1. Becker (2021) applied the same approach of this study to three Brazilian reservoirs in Paranapanema watershed, integrating river-reservoir and dividing the reservoir into several sectors.

$$C_{i+1} = \frac{C_i + \frac{\Delta t}{V_{i+1}}(Q_{in}.C_{in})}{1 + \frac{\Delta t}{V_{i+1}}(Q_{out} + \nu.A_s + \frac{\Delta V}{\Delta t})} \tag{5.4}$$

TP concentration within the reservoir (C_{i+1}, mg/L) changing in the time step length (*Deltat*, s) is calculated based on the initial TP concentration (C_i, mg/L), volume (V, m^3), difference of the volume (Delta V, m^3), outflow discharge (Q_{out}, m^3/s), and inflow discharge (Q_{in}, m^3/s) and concentration (C_{in}, mg/L).

Since the loss of phosphorus goes through the water-sediment interface, settling losses are represented as apparent settling velocity (ν, m/s) multiplied by the surface area of the sediments (A_s, m^2), as suggested by Chapra (1997). The apparent settling velocity (ν) was used as a calibration coefficient, and a sensibility test was performed for defined its value.

To assess optimal monitoring resolutions for modeling, the unsteady-state input data was tested through several scenarios. All scenarios were created decreasing the

temporal resolution of input data to less frequent measurements, gradually from monthly to bimonthly, seasonally, and lastly as twice per year. Results calibration and validation were performed by comparing calculated unsteady-state TP concentration with concentrations measured in field campaigns, as presented in Section 5.2.

Model performance was assessed by Mean Absolute Error (MAE, Equation 5.5) and Root Mean Square Error (RMSE, Equation 5.6). N is the number of observations, $-O_i$ is the observed data, while P_i is model predicted data.

$$MAE = \frac{1}{N}\sum_{i=1}^{N}|P_i - O_i| \tag{5.5}$$

$$RMSE = \sqrt{\frac{1}{N}\sum_{i=1}^{N}(P_i - O_i)^2} \tag{5.6}$$

5.4 Data analysis and post processing: Water Quality Index of Reservoirs (WQIR) and Brazilian resolution

In Brazil, water bodies have quality criteria established by current environmental legislation (Federal Law number 9433 / 97), which defined the National Water Resources Policy for Brazil and created the National Water Resources Management System. The water quality is divided into classes, according to multiple uses, aiming to assure quality compatible with demanding uses and to reduce pollution controls cost.

The Environment National Council resolution 357/05 establishes the classification of water, providing environmental guidelines. Waters were classified as freshwater (special, 1, 2, 3, and 4 classes), brackish waters (classes 7 and 8), and saline waters (classes 5 and 6). For fresh waters, classes (1 to 4) are defined according to their usage, ranging from drinking to lower uses, such as navigation and landscaping. For each water usage class, the CONAMA Resolution sets thresholds and conditions for a broad set of water quality variables (Table 16).

The measured and simulated data were compared with quality standards established by CONAMA Resolution 357/05 (CONAMA, 2005) as Class 2 was, the same as Passaúna's River and Reservoir are classified.

Water quality management index calculations not only define the status of water quality, but their usage also allows the variations to display over several circumstances, such as over time and spatially distributed. In this study, the Water Quality Index of Reservoirs (WQIR) was explored in several aspects, from testing minimal resolutions for monitoring, and to verifying modeling results, and identifying variations in monitoring campaigns.

Table 16 – The classification system of freshwater bodies quality standards according to Brazilian Resolution CONAMA 357/2005 for Dissolved Oxygen, Chlorophyll-a, Nitrogen forms, and Phosphorus.

Parameter	Class			
	1	2	3	4
Dissolved Oxygen (mg DO/L)	≥ 6	≥ 5	≥ 4	>2
Chlorophyll-a (µg Chl-a/L)	10	30	60	
Total Phosphorus (mg TP/L)				
Lentic environment	0.020	0.030	0.050	
Intermediate environment[1]	0.025	0.050	0.075	
Lotic environment	0.10	0.10	0.15	
Nitrate (mg N-N03-/L)	10	10	10	
Nitrite (mg N-N02-/L)	1	1	1	
Total Ammoniacal Nitrogen (mg N-NH3/L)				
pH $\leq$ 7.5	3.7	3.7	13.3	
7.5 <pH $\leq$ 8	2.0	2.0	5.6	
8.0 <pH $\leq$ 8.5	1.0	1.0	2.2	
pH >8.5	0.5	0.5	1.0	

[1]Residence time between 2 and 40 days
Class 1: Waters for human consumption after simplified treatment, primary contact recreation, and vegetable irrigation.
Class 2: Supply for human consumption after conventional treatment, primary contact recreation, vegetable irrigation, aquaculture, and fishing.
Class 3: Waters for human consumption after conventional or advanced treatment, crop irrigation, secondary contact recreation, and animal desedentation.
Class 4: navigation and landscape harmony.
Source: CONAMA (2005)

The WQIR is periodically assessed by the Environmental Protection Agency of the State of Paraná for evaluation of spatial and temporal changes in the water quality of 24 reservoirs located in Paraná State (IAP, 2009). Likewise, it was applied for the evaluation of Passaúna's reservoir water quality by Moreira et al. (2017) and Rauen et al. (2018).

In order to assess the WQIR's classification, concentration ranges presented in Table 2, Section 2.6.2 was used, given the incomplete samples to correctly weigh all nine parameters required for the index calculation.

5.5 Optimal monitoring strategies

In this study, a few strategies to optimize monitoring resolutions are proposed based on temporal and spatial dynamics observed during field monitoring, and further evaluation of results from modeling applications. Figure 34 presents each strategy and its relative interconnected branches of the methodological approach according to the presented in section 1.2.

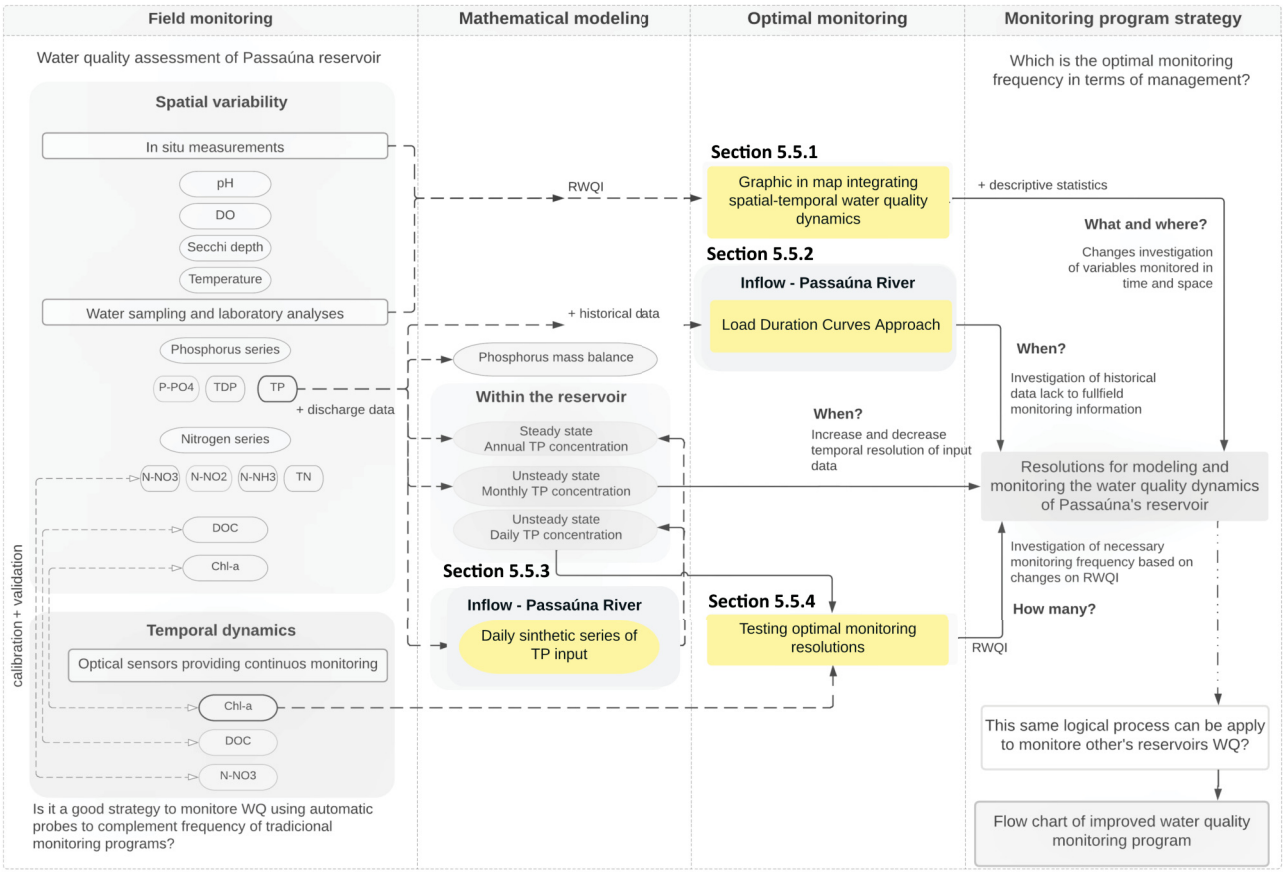

Figure 34 – Schematic representation of thesis methodological approach, with a highlighted indication of optimal monitoring strategies propose in this study.

Firstly, spatial-temporal integration of water quality dynamics in the monitoring period was evaluated using comparative maps, in which water quality data (TP, TIN, and Chl-a) throughout the seasons was compiled in corresponding ecological status assessed with WQIR classification, Section 5.5.1. The graphic map approach is intended to answer questions related to "Which" and "Where", since displays changes in time and space of the variables monitored.

Secondly, load duration curves analysis was performed using historical and monitored total phosphorus data measured at Passaúna River, Section 5.5.2. With this approach is possible to assess the lack of monitoring data and identify potential effects

of storm events on water quality conditions, and answer questions related to "When" monitoring should take place.

In sequence, an evaluation of effects in TP input loading due to storm events was performed, by improving the temporal resolution of TP data series for Passaúna River associated with discharge data in daily resolution. Further, the created synthetic series was applied as input data in the zero-dimensional model, as steady and unsteady state conditions.

Lastly, additional investigations of changes in the ecological status of Chl-a (from optical sensor's measurements) and TP (from unsteady state application in daily resolution) were evaluated using percentage frequency of occurrence analysis for several data series with different temporal resolutions, Section 5.5.3. Based on monitored and modeled results, this investigation intends to answer "How many" data should be monitored through quantification of ecological status variability.

5.5.1 Comparative maps integrating spatial-temporal water quality dynamics through Water Quality Index of Reservoirs (WQIR)

Comparative maps were compiled to integrate spatial-temporal water quality dynamics in the monitoring period. Variation throughout the seasons was assessed by grouping measured data of TP, TIN, and Chl-a of each monitoring site.

Since, Total Inorganic Nitrogen (TIN, mg/L) concentrations were not quantified in the laboratory (see Section 5.2.1), TIN values were obtained from the sum up of inorganic Nitrogen forms (N-NH3, N-NO3, and N-NO2).

The mean of all measurements for each monitoring point (including all depths) was performed, and from the WQIR classification matrix (Table 2, Section 2.6.2), ranges of concentration values were used to assess the ecological status.

5.5.2 Load Duration Curves Approach to improve Water Quality Monitoring Program: a phosphorus load investigation

Duration Curve applications are widely used to integrate qualitative and quantitative aspects of hydrological studies, when associated with water quality variables allow for evaluation of compliance with regulation standards of biochemical oxygen demand (BIANEK; MANNICHI, 2021; FORMIGONI et al., 2011), total phosphorus (CUNHA; CALIJURI; MENDIONDO, 2012), Escherichia coli (SERRANO et al., 2020), and dissolved oxygen (FORMIGONI et al., 2011).

However, load duration curves can also be useful to indicate the lack of monitoring data and to identify potential effects of storm events on water quality conditions, since

their graphics display historical data patterns that help to interpret the water quality in the context of regionalization studies with environmental standards.

Load duration curves for Passaúna River were assessed based on discharge and phosphorus concentration historical data, available at Hydrological Information System (SIH) repository, monitoring station 'BR 277 Campo Largo' - code 65021800 (25.42°S, 49.38°W - ca. 1 km northeast of the Passaúna reservoir pre-dam).

From January 1985 to April 2019, a total of 10115 daily discharge samples and 157 measurements of Total Phosphorus were compiled. Firstly, historical data trends were evaluated and compared with monitoring data in field campaigns, presented in Section 5.2.

Secondly, historical discharge data were sorted in gradual values to generate a flow-duration curve, and associated with a corresponding percent of the time that discharges were equaled or exceeded during the flow duration interval for each discharge value. Following the presented by EPA (2007), the cumulative frequency distribution was grouped into five zones of different discharge intervals, representing hydrological conditions such as high flows, moist conditions, mid-range flows, dry conditions, and low flows.

From multiplying the discharge values for the threshold of 0.10 mg/L (according to Brazilian resolution for rivers Class 2) was created a load duration limit curve, being the allowable load at each zone of flow condition.

The historical TP data, along with measurements performed during MuDaK's monitoring period from February 2018 to April 2019, and additional data provided by Sanepar from January 2018 to September 2019 (unpublished data), were associated with the calculated probability of occurrence of the daily mean discharge, creating a dataset of observed loads in kg/day, using a conversion factor of 86.4. The observed loads were plotted as scatter and box plots for comparison of statistical aspects. Points above the load duration limit curve represent daily load exceedances of the threshold.

5.5.3 Daily synthetic series to estimate TP concentrations input

The potential influence of storm events on TP input is usually not considered in mass balance calculations, since most traditional field campaigns were performed during base flow discharges. However, phosphorus load input into reservoirs is closely linked to the hydrological regime of the main tributaries, and increases in discharge are usually associated with increased phosphorus concentration.

In this study, investigations were performed to verify discharge data sensibility on mass balance calculations and loading input values, to obtain better input description and quantify uncertainties involve in mass balance quantification.

The correlation of discharge and TP concentrations were evaluated using all datasets available for TP measurements at Passaúna river, including historical data obtained from Hydrological Information System (SIH), measurements performed during MuDaK's monitoring period (Section 5.2), measurements provided by Sanepar (unpublished data), and survey of two storm events monitored in October 2018 by MuDaK partners in Passaúna River (unpublished data).

Since the interplay between TP concentrations and discharge can not be explained by a simple linear correlation, a strategy of using the ratio between discharge measured and historical mean (Q/Qhist) was evaluated. The calculated discharge ratio (Q/Qhist) was divided into flow ranges every 0.5, and for each group range, the mean ratio and respective TP concentration were obtained.

Plots of correlation between discharge ratio (Q/Qhist) and TP concentration were divided into two groups, below and above discharge of 3.6 m^3/s, and linear equations were adjusted for both groups. The obtained equations were applied in the Passaúna river discharge daily time series, resulting in a synthetic TP series in daily resolution, from February 2018 to January 2019.

The TP synthetic series was further applied as input data in the zero-dimensional model, as steady and unsteady state conditions.

5.5.4 Testing optimal monitoring resolutions of Chlorophyll-a and Total Phosphorus using percentage frequency of occurrence analysis

An investigation of optimal monitoring resolutions was carried out using data series in high temporal resolution of (i) Chl-a from measurements of optical sensors, and (ii) TP from unsteady state application in daily resolution.

Chl-a concentrations in the daily resolution were obtained, and post-processed, from measurements performed by an optical sensor installed at the floating platform system located at the Intake monitoring site, as presented in Section 5.2.2.

While, TP concentrations in the daily resolution were obtained from the application of TP synthetic series as input data in the zero-dimensional model as unsteady state conditions, as presented in Section 6.4.2.

From the daily data series, five datasets of Chl-a and TP concentrations were created to simulate measurements on daily, weekly, monthly, bimonthly, and quarterly resolutions. The created data series of Chl-a and TP started with measurements performed on March 1st, and February 1st, respectively. Additional data positions were created employing vectors, in which the following positions correspond to week, month, bimester, and four-month measurements, depending on the frequency.

The original and created data series were represented through both time series, and box plots for comparison of statistical aspects.

Further, the percentage frequency of occurrence analysis for the WQIR classification was performed for each one of the created series, to determine the interference of monitoring frequency in the reservoir water quality status. This analysis was performed by grouping the data into classes, in which the number of occurrences in each class was counted to represent the frequency distribution.

To assess the WQIR's classification, ranges of concentration values were used from the WQIR classification matrix (Table 2, Section 2.6.2).

6 Optimal spatio-temporal design of reservoir water quality monitoring systems: Case study of Passaúna's Reservoir

6.1 Overview

This chapter is divided in three sections: (i) monitoring Passaúna's reservoir water quality; (ii); modeling Passaúna's Reservoir water quality; and (iii) optimal monitoring strategies.

The first part summarizes the results obtained from water quality monitoring program, considering spatial variability (water sampling, in-situ measurements with sensors, and laboratory analysis) and temporal dynamics (data from optical sensors providing high temporal resolution monitoring).

To establish an ideal monitoring program for water quality in Passaúna reservoir the strategy relies on processing two interconnected sources of data: analysis of several variables spatially distributed in monthly measurement campaigns and high-temporal-resolution measurements. Both monitoring procedures were presented in Section 5.2.1 and 5.2.2.

The second part is composed by evaluation of zero-dimensional Total Phosphorus model of Passaúna's reservoir, with application of Continuously Stirred Tank Reactor (CSTR) as steady and unsteady state solutions.

In the third, and last part are presented strategies to optimize monitoring resolutions considering integration of spatial-temporal water quality dynamics, modeling applications with improvements in temporal TP resolution data, and load duration curves analyses for Passaúna River historical data.

6.2 Monitoring Passaúna's reservoir water quality

As detailed in Chapter 5.2, the spatial variability of water quality variables within the Passaúna reservoir was extensively investigated over a year in several monitoring sites. Passaúna reservoir's monitoring strategy relied on processing two interconnected sources of data: (i) spatially distributed water sampling, in-situ measurements with sensors, and laboratory analysis, and (ii) floating platform system equipped with optical sensors providing high temporal resolution monitoring. The main results of each source of data are presented in the next following sections.

6.2.1 Spatial variability: Water sampling, in-situ measurements with sensors, and laboratory analysis

The spatial variability of water quality in the Passaúna reservoir was evaluated along 11 field campaigns performed in monthly interval, from February 2018 until April 2019, in several points distributed within Passaúna reservoir, inflow, and outflow. More details about field campaigns were presented in Section 5.2.1, and a table of all monitored data is presented in Appendix A.

The TP concentrations were relatively low and indicated overall good ecological status in the investigated watercourses. In general, most of inflow and outflow results did not exceed the threshold for rivers class 2 of 0.10 mg/L according to Brazilian resolution (CONAMA, 2005). In October 2018, a single value at inflow exceeded the threshold (0.0106 mg TP/L).

Table 17 summarize descriptive statistics from water quality assessment of Passaúna reservoir from overall monitoring data of Total Phosphorus (TP, mg TP/L), Total Nitrogen (TN, mg TN/L), Chlorophyll-a (Chl-a, μg Chl-a/L), Dissolved Organic Carbon (DOC, mg DOC/L), and Secchi depth (Secchi, m). 5.2.1

Figure 35 represents the spatial variability of TP, TN, and Chl-a, according to sampling sites. Nutrient concentrations (TN and TP) did not vary strongly between campaigns, but we found a systematic spatial decrease trend along the reservoir. Results showed consistent longitudinal gradients from reservoir's entrance in direction to the deepest region, close to the dam.

Regarding data within the reservoir, during the monitoring period, we recorded a mean TP concentration of 0.027 mg TP/L, from all depths and all campaigns. Spatial variability of TP concentration presented a pronounced decrease towards the dam, suggesting phosphorus sediment deposition, consumption by phytoplankton, and plants retention. An overall mean TP concentration of 0.013 mg TP/L was observed at sites located in the deepest portions of the reservoir (Park, Reservoir Center, Intake, Dam,

Table 17 – Descriptive statistics (mean, standard deviation, minimum, and maximum) of Total Phosphorus (TP, mg TP/L), Total Nitrogen (TN, mg TN/L), Chlorophyll-a (Chl-a, μg Chl-a/L), Dissolved Organic Carbon (DOC, mg DOC/L), and Secchi depth (Secchi, m) during monitored period -February 2018 to April 2019, according to sampling sites.

	TP (mg/L)	**TN (mg/L)**	**Chl-a (μg Chl-a/L)**	**DOC (mg/L)**	**Secchi (m)**
Inflow	0.064 ± 0.018 (0.041 - 0.106)	1.63 ± 0.21 (1.40 - 2.10)	1.04 ± 0.70 (0.27 - 2.41)	2.24 ± 0.66 (1.38 - 3.69)	
Buffer	0.047 ± 0.014 (0.025 - 0.070)	1.40 ± 0.22 (0.80 - 1.57)	4.89 ± 2.88 (2.08 - 10.42)	2.59 ± 0.51 (1.95 - 3.55)	0.68 ± 0.41 (0.20 - 1.25)
Ferraria Bridge	0.054 ± 0.048 (0.012 - 0.233)	1.17 ± 0.21 (0.78 - 1.55)	4.24 ± 1.73 (0.99 - 7.51)	2.63 ± 0.49 (1.85 - 3.65)	1.04 ± 0.96 (0.10 - 2.90)
PPA	0.032 ± 0.018 (0.010 - 0.072)	0.83 ± 0.33 (0.31 - 1.49)	6.35 ± 2.60 (3.21 - 10.28)	2.66 ± 0.34 (2.05 - 3.31)	1.21 ± 0.46 (0.40 - 1.60)
Park	0.013 ± 0.004 (0.005 - 0.019)	0.56 ± 0.13 (0.39 - 0.75)	5.47 ± 2.02 (2.94 - 8.90)	2.78 ± 0.25 (2.28 - 3.08)	2.05 ± 0.75 (1.30 - 2.80)
Res Center	0.011 ± 0.005 (0.006 - 0.018)	0.61 ± 0.19 (0.34 - 0.88)	6.40 ± 2.17 (3.61 - 9.89)	2.59 ± 0.29 (2.29 - 3.06)	2.25 ± 0.55 (1.70 - 2.80)
Intake	0.013 ± 0.004 (0.006 - 0.022)	0.59 ± 0.12 (0.33 - 0.83)	5.04 ± 2.16 (1.34 - 10.40)	2.52 ± 0.28 (2.08 - 3.14)	2.62 ± 0.32 (1.95 - 3.05)
Dam	0.012 ± 0.006 (0.006 - 0.024)	0.73 ± 0.62 (0.30 - 2.72)	5.35 ± 4.83 (2.14 - 20.85)	2.64 ± 0.27 (2.26 - 3.14)	2.70 ± 0.30 (2.40 - 3.20)
Outflow	0.014± 0.005 (0.005 - 0.020)	1.13 ± 0.54 (0.55 - 2.27)	7.69 ± 6.50 (3.34 - 22.41)	2.31 ± 0.19 (1.95 - 2.66)	

and Outflow). The observed data, as well as single outliers, were within the range for WQIR's poorly degraded status (from 0.011 to 0.025 mg TP/L, class 2), and the threshold for lentic watercourses class 2 of 0.30 mg TP/L (CONAMA, 2005).

Lower TP concentrations were recorded in February 2018 at the deepest regions of the reservoir (Park, Reservoir Center, and Dam) ranging between 0.05 mg TP/L and 0.06 mg TP/L. In the same campaign, TP concentrations of all monitoring sites were generally very low, and concentrations of almost all samples were below the analytical method's detection limit employed for the laboratory analyses. Similarly featured was observed at the Intake site (November 2018 and April 2019), and Outflow site (April, May, and November 2018) when the water column was stratified.

A characteristic iron color was revealed in the samples during analytical procedures indicating iron presence. This made it impractical to quantify phosphorus concentration, especially in the non-dissolved forms. Likewise suggested by (ESTEVES, 1998; TUNDISI; TUNDISI, 2011), we believe iron was released from the sediment bounded with phosphate ions.

TP concentrations observed in sites located at the upstream portion of the

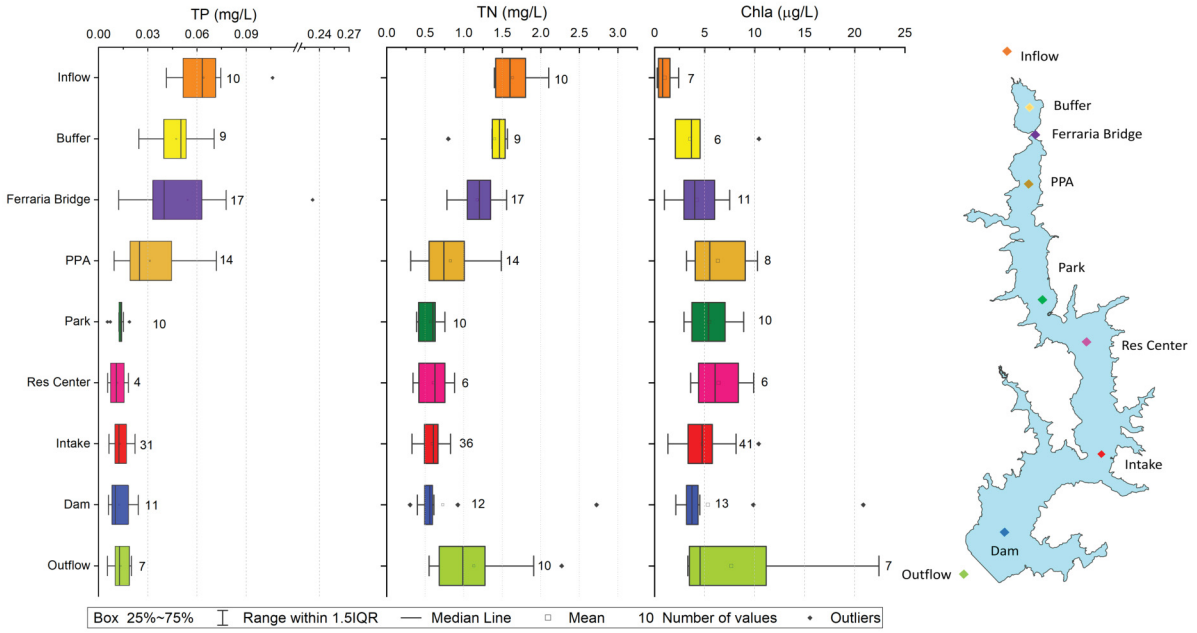

Figure 35 – Spatial variability of Total Phosphorus (TP, mg TP/L), Total Nitrogen (TN, mg TN/L), and Chlorophyll-a (Chl-a, μg Chl-a/L) during monitored period - February 2018 to April 2019, according to sampling sites of all monitored depths.

reservoir exceeded the above-mentioned threshold at Buffer (mean: 0.047 mg TP/L), Ferraria Bridge (mean: 0.054 mg TP/L), and PPA site (mean: 0.032 mg TP/L). The highest concentration value was found at site Ferraria Bridge, with 0.233 mg TP/L (November 2018). However, despite this single outlier, at this station during monitoring period TP levels remained below 0.08 mg TP/L.

The TN concentrations were also decreasing in the dam direction. However, unlike TP concentrations, a strong increase in TN concentrations was observed in the reservoir outflow. At this site we found the larger fluctuations of TN concentrations, ranged between 0.55 mg TN/L (August 2018) and 2.27 mg TN/L (April 2019).

Nutrient concentration decrease with distance from the main inflow is explained with the large organic particles sink to the sediments due to lower water velocity. And the TN increase at the outflow can be explained by the anoxic sediments stimulation denitrification near to the water column bottom (DODDS; WHILES, 2019).

From February 2018 to April 2019, lower TN concentrations were recorded at the deepest regions of the reservoir (Park, Reservoir Center, Intake, Dam) ranging between 0.30 mg TN/L and 0.92 mg TN/L. Generally, at Dam the lowest TN concentrations were found. However, outliers occurred in this site. The largest outliers were 0.92 mg TN/L (February 2019) and 2.72 mg TN/L (February 2018).

The TN observed data were between WQIR's threshold for class 3 (moderately degraded, 0.26 mg TN/L - 0.60 mg TN/L) to class V (heavily polluted, 2 mg TN/L - 5

mg TN/L) according to Brazilian resolution, see Table 2, Chapter 2.

Contrary to nutrient concentrations, Chl-a was lowest in the river inflow (mean: 1.04 μg Chl-a/L). Along the reservoir highest Chl-a concentrations were recorded at the PPA (mean: 6.35 μg/L, ranging between 3.21 μg Chl-a/L and 10.28 μg Chl-a/L), followed by decrease in direction to the dam region. At the dam, Chl-a concentrations outliers were found in samples collected near to the bottom, in February 2019 with 9.87 μg Chl-a/L and 20.85 μg Chl-a/L.

Dodds and Whiles (2019) explanation for maximum productivity downstream from the input, reflected in higher Chl-a concentrations, is trade-off between light and nutrient limitation along the reservoir. The riverine influence with nutrient pulses can be offset by turbidity gradients and light limitation near river inputs.

Likewise observed with TN concentrations, Chl-a concentration also reached highest values in the reservoir outflow (mean: 7.69 μg Chl-a/L). Similar concentrations were found in samples collect at dam bottom and outflow.

During the investigation period, Chl-a concentrations ranged below the threshold for watercourses class 2 of 30 μg Chl-a/L (CONAMA, 2005). On the other hand, values oscillated around WQIR's threshold for class 1 (not impacted to very poorly degraded, <1.5 μg Chl-a/L) to class 5 (heavily polluted, 11 μg Chl-a/L - 32 μg Chl-a/L), see Table 2.

DOC concentrations remained overall constant between campaigns and no significant spatial variability of DOC concentrations was found for the Passaúna reservoir. However, at the inflow site slightly lower DOC concentrations at single measurement dates (1.38 mg DOC/L - May 2018, 1.631 mg DOC/L - June 2018, and 1.764 mg DOC/L - August 2018) was found. Within the reservoir, minimum DOC concentrations were found in August 2018, ranging between 1.909 mg DOC/L at the Buffer site and 2.060 mg DOC/L at the Ferraria Bridge site.

Transparency was measured via Secchi Disk (See Chapter 5.2.1) and, as expected, increased towards the dam. Highest Secchi depth was recorded at the Dam with 3.20 m (August 2018). Secchi depth data were between WQIR's threshold for class I (not impacted to very poorly degraded, > 3.0 m) at deepest reservoir's region, to class V (extremely polluted, < 0.3 m) at Buffer with 0.2 (February 2018).

Figures 36 and 37 presents time series of TP (mg TP/L), TN (mg TN/L), Chl-a (μg Chl-a/L), and DOC (mg DOC/L) throughout the seasons. TN concentrations seems to decrease in the colder seasons, and increase in the summer and spring, even with a small amplitude of concentrations values. TP concentration mean presented strong temporal variability. An interesting behavior was observed during spring season, when TP concentrations measured at the bottom were much higher than the ones measured at

the surface.

Not only Chl-a, but also DOC concentrations did not presented a seasonal or monthly dynamics trend. However, a slight increase in DOC concentrations was observed on February 2019.

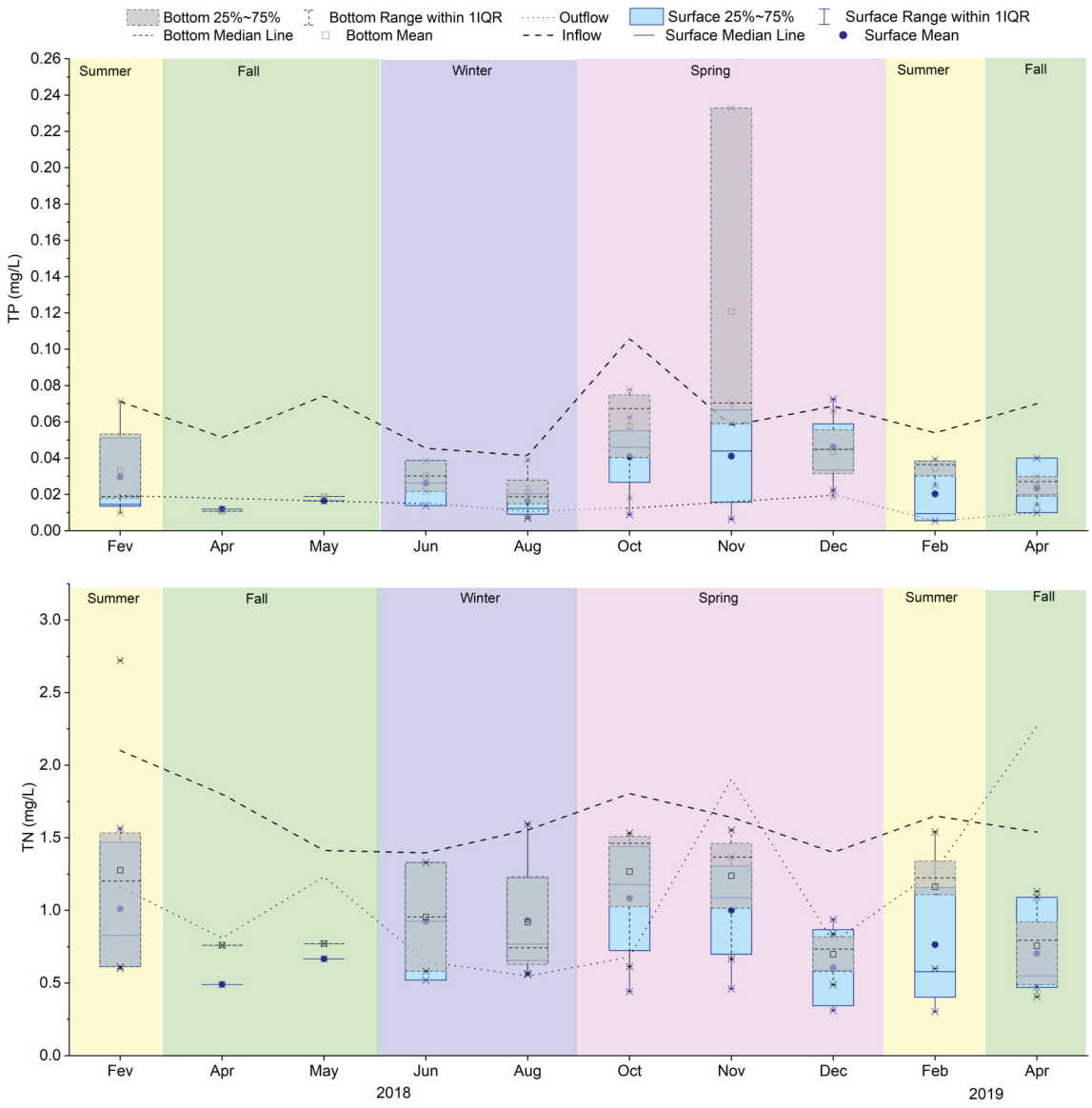

Figure 36 – Time series of TP [mg/L] and TN [mg/L] concentrations in reservoirs measurements at surface (blue boxplot) and at bottom (grey boxplot), inflow (dashed line) and outflow (dotted line) over the monitoring period (from February 2018 to April 2019), background colors indicates seasons.

The spatial distribution of TN, TP and Chl-a, were also explored in three extensive field campaigns (Figure 38) performed in February 2018, August 2018, and February 2019 covering all monitoring sites.

Chl-a concentrations from surface and bottom did not present a clear tendency, and its spatial distribution was diverse. TP and TN variations along reservoir at the extensive campaigns followed the same tendency observed in seven smaller field

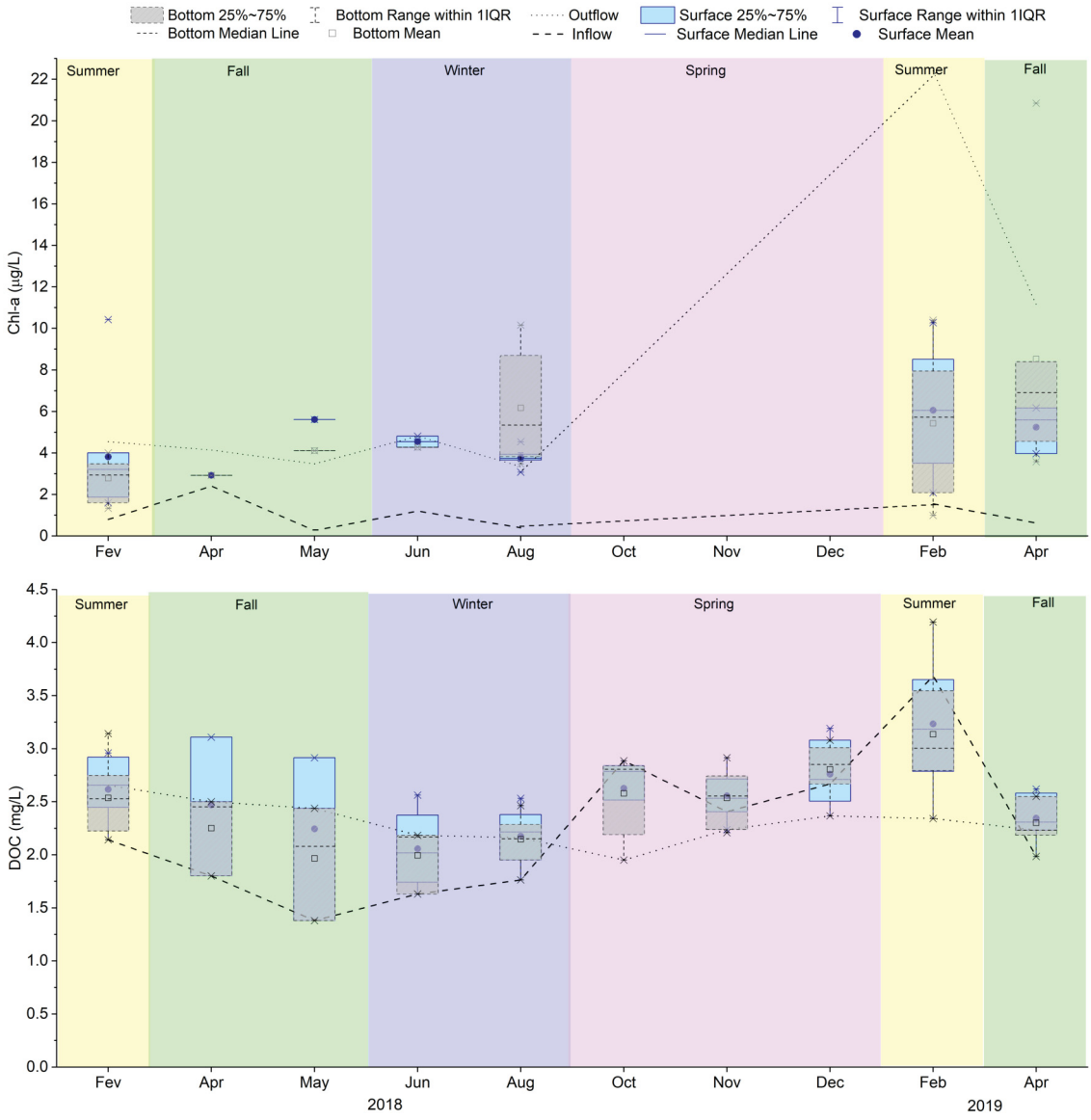

Figure 37 – Time series of Chl-a [μg/L], and DOC concentrations [mg/L] in reservoirs measurements at surface (blue boxplot) and at bottom (gray boxplot), inflow (dashed line) and outflow (doted line) over the monitoring period (from February 2018 to April 2019), background colors indicates seasons

campaigns, decreasing in dam direction. An exception observed in April 2019, when TP concentration measured at the bottom was higher than the surface, possibly due to sediment releasing.

An increase of TN and Chl-a in the outflow monitoring site can be explained by bottom outlet discharge. Chl-a concentrations at both outflow and dam's bottom were specially higher on April 2019, reaching 20.85 μg/L at dam and 22 μg/ at outflow site.

Death algae accumulates next to the dam structure in the water column bottom, producing Total Ammoniacal Nitrogen in its decomposition and presenting an increased Chl-a concentration. During the laboratory analysis it was observed that the samples collected at dam's site bottom and outflow presented brownish color, indicating that at

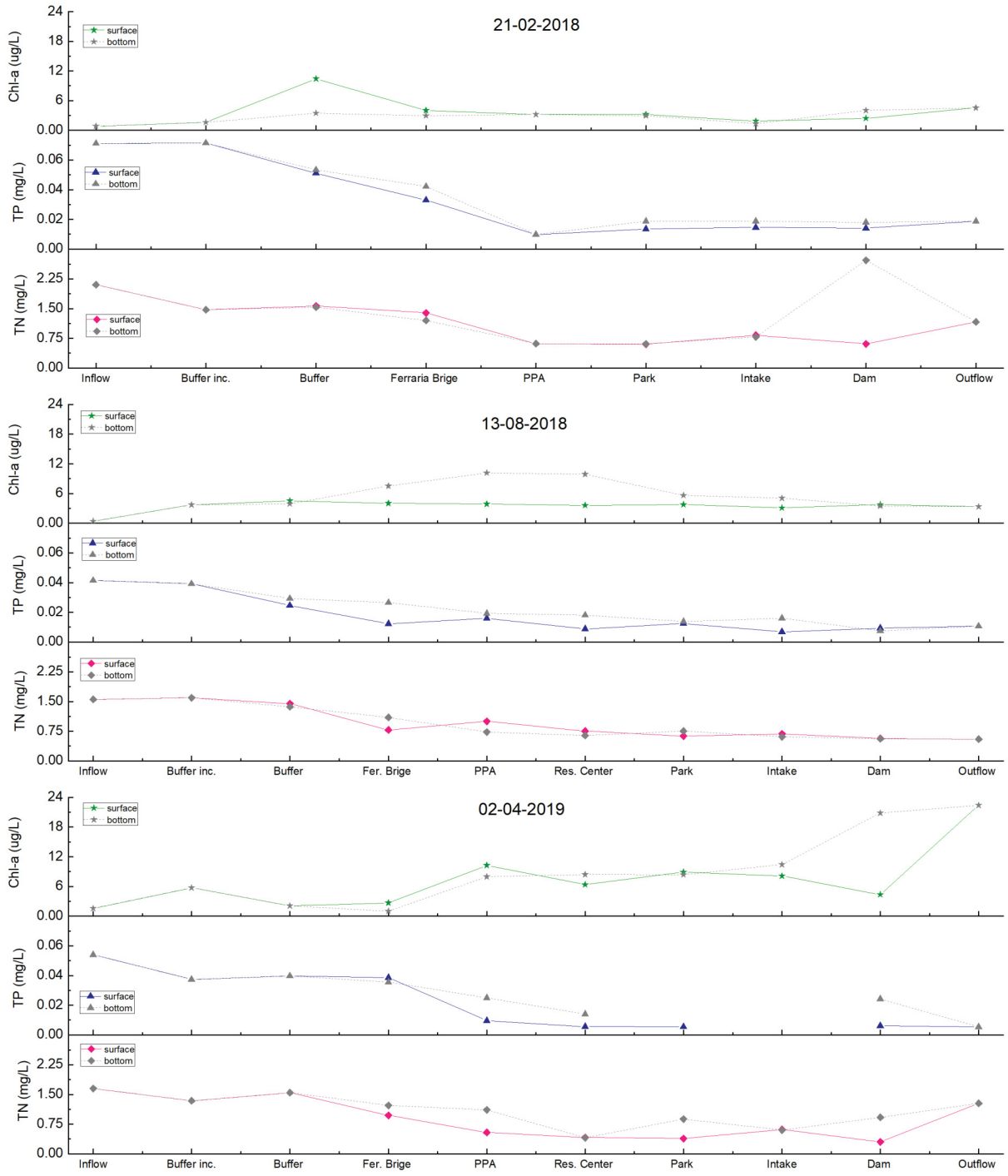

Figure 38 – Spatial variability of Total Nitrogen (TN - mg/L), Total Phosphorus (TP - mg/L) and Chlorophyll-a (Chl-a - μg/L) along Passaúna reservoir from extensive campaigns (February 21, 2018; August 13, 2018, and April 2, 2019). Data series in grey represents results from the water column bottom, and colored ones are from surface.

least part of the phytoplankton was dead.

Total Ammoniacal Nitrogen could also lead to an increase in TN concentrations at the outflow due to stratification of the water column. This was observed in the extensive

campaigns performed in April 2019, when N-NH4 concentration reached its highest value during the monitoring period (0.67 mg N-NH4/L) at the dam's bottom (sample collected at 14 meters of depth). TN for the same sample was 0.92 mg TN/L. In such an extensive campaign, TP concentrations were not able to be quantified in the laboratory due to iron interference in the downstream monitoring sites.

Figure 39 shows the range of phosphorus and nitrogen forms quantified over the monitoring period. As expected, nitrite concentrations represent the small portion of TN, while nitrate presents higher concentrations. Nitrogen forms concentrations presented a significant variability, depending on stratification patterns and DO concentrations measured along the water column. On the other hand, phosphorus forms didn't change significantly, and the particulate form of phosphorus plays the most important role in total phosphorus concentrations.

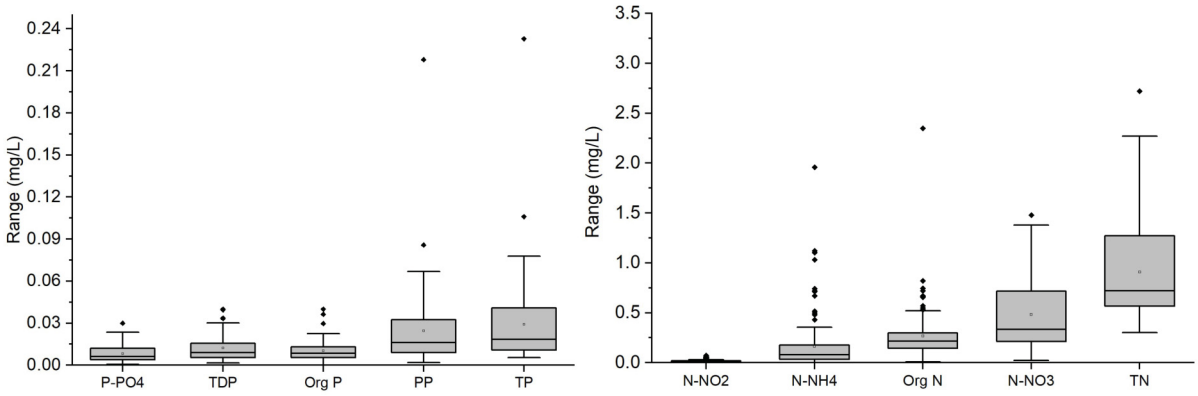

Figure 39 – Variability of Phosphorus and Nitrogen forms over the monitoring period. Phosphorus forms quantified in the laboratory were ortophosphate (mg P-PO4/L), Total Dissolved Phosphorus (mg TDP/L), Organic Phosphorus (mg Org P/L), Particulate Phosphorus (mg PP/L), and Total Phosphorus (mg TP/L). Nitrogen forms quantified in the laboratory were Organic Nitrogen (mg Org N/L), Ammonium (mg N-NH4/L), Nitrate (mg N-NO3/L), Nitrite (mg N-NO2/L), and Total Nitrogen (mg TN/L).

6.2.2 Temporal dynamics: Data from platform equipped with optical sensors providing continuous monitoring

The platform equipped with Opus and Nanoflu sensors placed at Intake monitoring site provided measurements with time resolution of 15 minutes. The measured data was assessed in daily resolution and time series plotted for nitrate, Chlorophyll-a (Chl-a) and Dissolved Organic Carbon (DOC) concentrations, from March 1, 2018 to April 2, 2019, at Figure 40.

There were some periods in with no measurements from the probe, the most significant periods of data failure are from May 4^{th} to May 21^{th}, 2018, from June 12^{th} to August 15^{th}, 2018 and from December 11^{th}, 2018 to February 3^{rd}, 2019. Data gaps were possibly caused by failure in wipers operation or power failure.

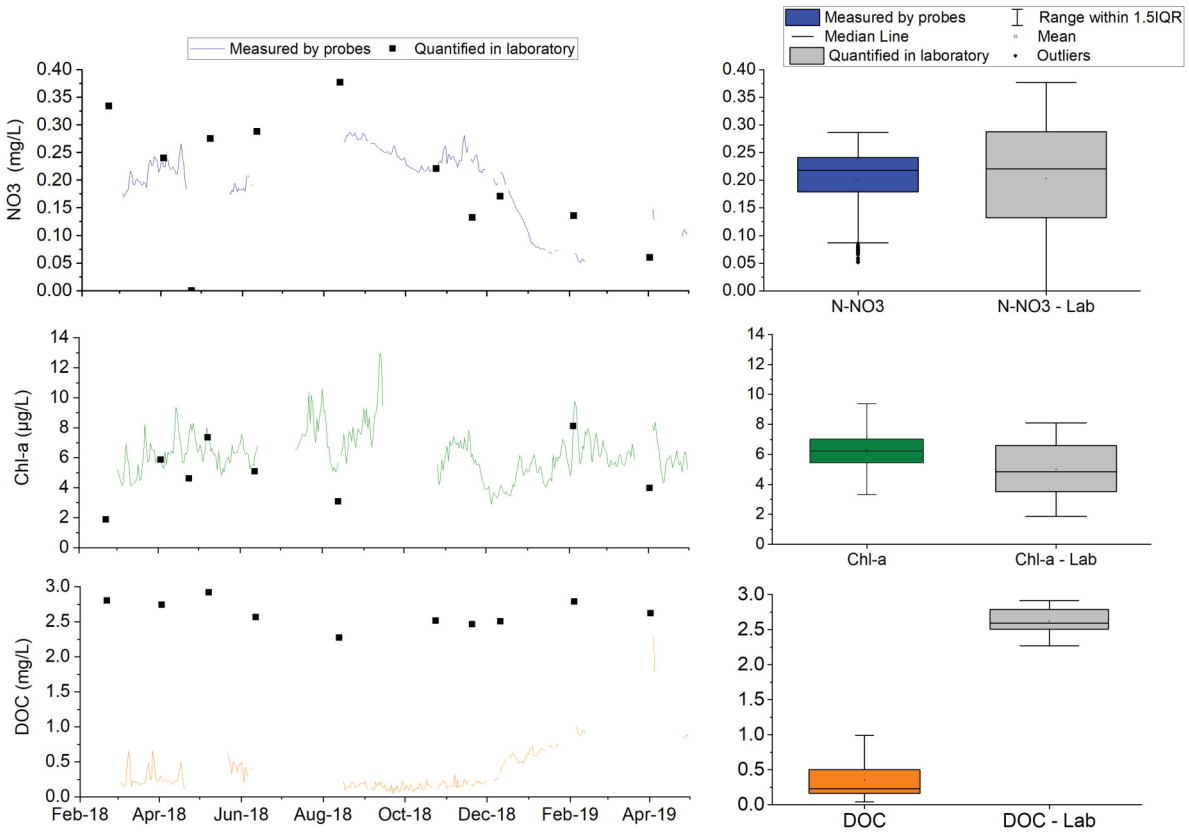

Figure 40 – Time series of nitrate [mg/L], DOC [mg/L], and Chlorophyll-a concentrations [μg/L] measured by sensors during the monitoring period with temporal resolution of 15 min. from platform equipped with Opus and Nanoflu sensors resolution and laboratory results for campaigns performed in 2018 and 2019 at Passaúna reservoir.

The highest nitrate concentration recorded by the sensor was 0.3969 mg/L in May 1st, 2018 the lowest concentration was 0.155 mg N-NO3/L and occurred on August 8th, 2018. The mean concentration was 0.2163 mg N-NO3/L. Although from the total of 11 field campaigns, only five values of nitrate quantified in laboratory could be compared

with sensor's measurements at the same day, correlation of overall values between nitrate concentrations measured by the sensor and at the laboratory resulted in good similarity.

The mean concentrations quantified in laboratory during the monitoring period was 0.24 mg N-NO3/L, varying from 0.13 mg N-NO3/L (November 2018) to 0.38 mg N-NO3/L (August 2018). The largest difference between values occurred at November 2018 (0.11 mg N-NO3/L), while for the remaining measurements difference values did not exceeded 0.05 mg N-NO3/L.

For all measurements, whether in the laboratory or through the sensor, results did not exceed the threshold of 10 mg N-NO3/L for Class 1 according to Brazilian resolution (CONAMA, 2005).

DOC concentrations obtained in laboratory (mean: 2.62 mg DOC/L) were higher than the observed by probes measurements (mean: 0.35 mg DOC/L). DOC values measured by the probe did not exceed 0.75 mg DOC/L, while DOC concentrations quantified in laboratory were all above to 2.27 mg DOC/L.

For DOC parameter was identified no correlation between the data measured by the sensor and analyzed analytically. It may need a more precise calibration or application of a scale factor, considering reservoir characteristics.

This was explored by Bernardini (2019), who build an evolutionary open source algorithm to identify the specific emission, excitation, and absorbance patterns of the organic matter in Passaúna's environment. The algorithm relates DOC's concentration obtained in laboratory with absorption measured by the probe. A scale factor was calculated to minimize the error between both values.

Despite in peak's period (from April to July, 2018), after apply the scale factors to correct the probe's measurements, Bernardini (2019) evaluation showed a good similarity between sensor and laboratory DOC's values.

Finally, from nanoFlu probe measurements of Chl-a, the most significant periods of measurement's failure were from June 14^{th} to August 12^{th}, 2018, from September 30^{th} to October 1, 2018 and from December 9^{th}, 2018 to February 4^{th}, 2019. Also, for this probe, data gaps were possibly caused by failure in wipers operation or power. For such variable, there is also lack of concentration quantified in laboratory analyzes, due to logistical problems in October, November and December, 2018.

Chlorophyll-a measured by the probe (mean: 6.26 μ g Chl-a/L) presented a good similarity with concentrations quantified in laboratory (mean: 5.43 μ g Chl-a/). Chl-a measurements by the sensor reached highest value at September 14th, 2018 (16.67 μ g Chl-a/L), and the lowest at December 9th, 2018 (2.89 μ g Chl-a/L). While laboratory quantification of Chl-a varied from 3.07 μ g Chl-a/L (August 2018) to 8.11 μ g Chl-a/L (February 2019).

Moreover, Ungaratti (2019) examined the measurements of N-N03, Chl-a, and total suspended solids related to local conditions, such as meteorological variables, chloride ions presence, and soil composition. Comparing data from sensor and laboratory, the author used statistical analysis to find a linear regression to obtain a scale factor. After the adjustment process, Ungaratti (2019) conclude that for both nitrate and chlorophyll-a are not necessary to apply a scale factor to fit local conditions.

Even thought, Chl-a measurements and observed values do not exceed the threshold of 30 μ Chl-a/L for Class 3 according to Brazilian resolution (CONAMA, 2005), both concentration values ranged Class 4 (critically degraded or polluted) threshold of 10 μ g Chl-a/L for WQIR. In addition, the highest concentrations measured by the sensors during concentration peaks were between WQIR's threshold for class 5 (heavily polluted, 11 μ Chl-a/L - 32 mg μ Chl-a/L), see Table 2.

Therefore, the identified daily fluctuation measured by the sensor of Chl-a time series indicates that high frequency measurements of this parameter can contribute to a better understanding of the dynamics between phytoplanktonic biomass growth and nutrients availability, providing tools that can be useful in defining sustainable monitoring strategies and focusing on preventive management.

Currently, Chl-a monitoring is carried out in semiannually resolution at Passaúna reservoir (and Paraná state), while most countries have higher sampling frequencies at their waters, varying from 4 to 6 times per year (See Table 7, Section 2.7).

This variable is traditionally tracked in water quality surveys and monitoring programs performed in reservoirs, because Chl-a concentrations are usually considered in water quality indices calculations and represent an indicative of phytoplankton biomass (ESTEVES, 1998). Thus, Chl-a sampling frequency can be decisive in defining ecological status, resulting in misclassification when its frequency resolution is not adequately assessed (MARCÉ et al., 2016). (SØNDERGAARD et al., 2011)

For this reason, further investigations of changes on Chl-a time series using data with high temporal resolution were performed (See Section 6.4.4).

6.2.3 Summary

Although traditional monitoring programs composed by water sampling and further laboratory analyzes represents a well-established method, usually used as a reference for comparison with new monitoring technologies, the limitations of quantification methods, such as difficulties in low concentrations detection and proper procedure, along with delay between sampling and laboratory analyses, strongly influence the spatial resolution and temporal monitoring.

Very often, low-frequency sampling fails in capturing important flood events and

characteristic temporal scale shorter than the sampling frequency (MARCÉ et al., 2016), since frequency and definition of variables monitored by environmental agencies are often restricted by the limitations of sample collection conventional methods and subsequent quantification in the laboratory. Sensors with spectral technology can be combined with monitoring allowing in situ, and sometimes real-time, measurements of several water quality variables.

For water resources management, and especially in water supply reservoirs, measurements on real-time monitoring by field-deployable automated analyzers represent a good strategy for reducing efforts and cost-effective field visits (MARCÉ et al., 2016), providing faster response to events of contamination, especially in the case of contaminants that may need a rapid operation and management decision (STOREY; GAAG; BURNS, 2011).

Automated analyzers for in-situ measurements provide real-time temporal quantification with reliability, practicality, reducing time, and resources that need to be used with field campaigns (U.S. Geological Survey, 2018). In addition, high-temporal resolution quantification with nearly continuous monitoring enables to the characterization of the temporal water quality dynamics in long periods of monitoring data, which makes it possible to evaluate trends in concentrations, from minutes, seasonally, or even annually changes (BLAEN et al., 2016).

However, some drawbacks of those automated analyzers utilization are the presence of noise and possible sunlight interference in measurements (ROUSSO et al., 2021), besides the requirement of highly specialized service to manipulate the data (MARCÉ et al., 2016). Additionally, equipment path length can limit measurements depending on probes settings Silva et al. (2016).

Sensor maintenance requirements are also an important aspect (MARCÉ et al., 2016), especially necessary in tropical environments, to guarantee cleaning for correct quantification with optical technology. Moreover, real-time temporal quantification using field-deployable automated analyzers with reliability is only possible after calibration of probes' measurements through laboratory analyses Silva et al. (2016) and for a limited range of variables.

Furthermore, an important aspect to be considered about the continuous monitoring approach is that mostly because of the costs implied, usually only a single platform system is installed in each site location, which is chosen based on the research examination objective. As consequence, an additional strategy must be implemented to examine spatial variability. This leads to monitoring strategies often complemented with modeling (JIMENEZ et al., 2005; ARAUJO et al., 2008).

Table 18 presents a summary of advantages and drawbacks of water sampling

followed by laboratory analyzes and the use of optical sensors providing continuous monitoring as water quality assessment of reservoirs.

Table 18 – Summary of advantages and drawbacks of monitoring strategies as water quality assessment of Passaúna reservoir.

Strategies	**Water sampling and laboratory analyzes**	**Optical sensors providing continuous monitoring**
Advantages	- Well-established method; - Usually is reference for the comparison with new technologies.	- Taking measurements in situ; - Data in high temporal resolution; - Data can be accessed online; - Characterization of the temporal water quality dynamics in long periods of monitoring data; - Faster response to events of contamination; - Practicality and reduced time for monitoring;
Drawbacks	- Efforts and cost-effective of field visits; - Delay between sampling and laboratory analyzes; Difficulties in low concentrations detection and properly procedure; - Limited number of samples collected and stored; - Fails in capturing important flood events.	- Calibration of probes' measurements through laboratory analyzes; - Path length can limit low measurements; - Quantification method technology cannot be applied to measure all variables - Requirement for highly specialized service to manipulate the data; - Sensor maintenance requirements; - Possible sunlight interference; - Costs associated with acquisition, implementation, and maintenance.

6.3 Modeling Passaúna's reservoir water quality

In addition to monitoring and data analysis, modeling techniques were also applied in this study to achieve improved resolutions for modeling and monitoring the water quality dynamics of Passauna's reservoir.

A zero-dimensional water quality model of Passaúna's reservoir was set up from water quality data described in Section 5.2. Data obtained in the field campaigns were processed and used as the initial condition for the simulation period, to calibrate, and validate the modeling results.

Firstly, a mass balance of phosphorus was set up, and both sources and sinks of phosphorus were connected with discharge coming into and leaving the reservoir. Secondly, a Continuously Stirred Tank Reactor (CSTR) model application was adopted, where the Passaúna reservoir was assumed as a completely mixed system.

Subsequently, annual TP concentrations in the reservoir were calculated through the steady-state solution, where discharge and concentration do not change over time. Further, data were tested for the unsteady state to estimate monthly TP concentrations within the reservoir, with both discharge and TP concentration changing over time.

The unsteady-state model was tested through several scenarios, decreasing the temporal resolution of input data to less frequent measurements, gradually from monthly to bimonthly, seasonally, and lastly as twice per year.

In the following sections are presented results and observations from numerical model performance and simulated scenarios.

6.3.1 Phosphorus mass balance in Passaúna reservoir

A mass balance of phosphorus was set up for Passauna's reservoir, using measurements data from February 2018 to January 2019. Total phosphorus was chosen to be modeled because the data availability of the variable is usually limited since phosphorus quantification requires sampling and further laboratory analysis. Additionally, phosphorus was pointed as a Passaúna reservoir limiting nutrient by Coquemala (2005), and more recently by Barreto (2020).

6.3.1.1 Phosphorus inputs assessment

Figure 41 presents TP loads input (kg TP/day) calculated using TP concentration measured at Inflow site (results presented at Section 6.2.1) and discharge data (m^3/s), as detailed in Chapter 5.3.1. Passaúna river represented the most significant tributary in terms of discharge and TP load input during th monitoring period. Discharges variations dominated TP load changes over time, with the exception

of October 2018 measurement, when load input was influenced by the highest TP concentration measured over the monitoring period, of 0.11 mg TP/L.

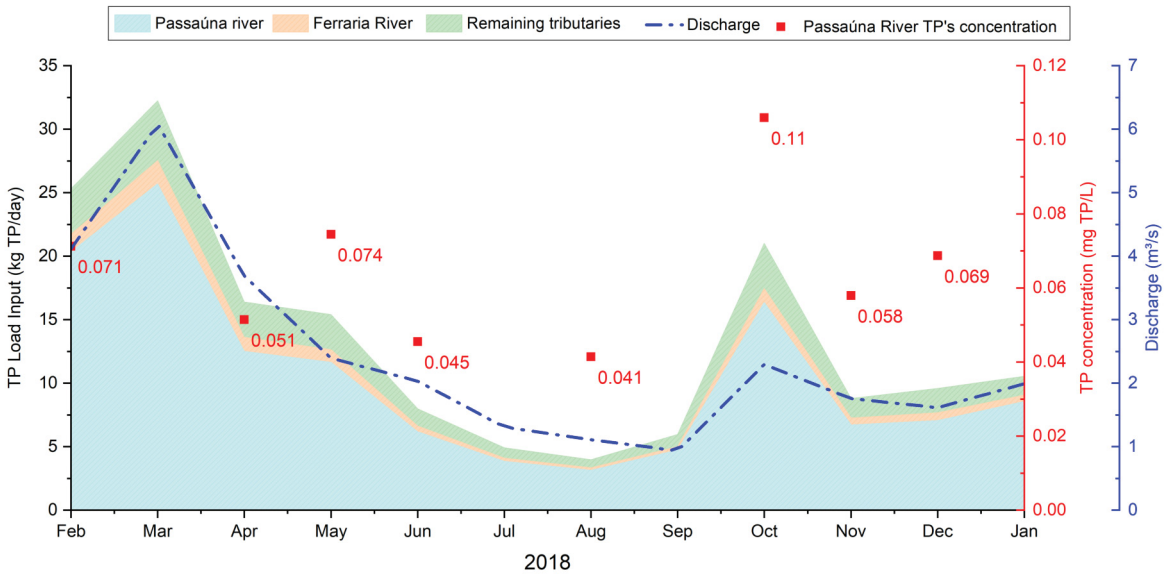

Figure 41 – Monthly mean input discharge in Passaúna reservoir (m^3/s) as blue line, TP concentration (mg TP/L) measured at the Passaúna reservoir's main tributary (Passaúna River) as red squares, and calculated load input (kg TP/year) of the main tributary (Passaúna River), Ferraria River, and remaining tributaries as stacked areas (see the legend)

Daily TP input loads presented a significantly variation over the monitoring period (from 4 kg TP/day to 32 kg TP/day, mean: 10.57 kg/day). Results show a consistent decrease from March to September 2018, when the discharge also increased to 2.3 m^3/s. The highest load input was observed in March 2018, together with the highest discharge measurement over the monitoring period, of 6.08 m^3/s.

Daily input found out in this study are compatible with the ones calculated by Carneiro, Kelderman and Irvine (2016). The authors developed a mass balance budget for Passaúna reservoir in monthly resolution to assess phosphorus sediment water exchange in the 2010 2012 interval. Mean daily TP input load resulted in 22kg/day for 2010, 18kg/day for 2011, and 13kg/day for 2012. Similarly with results found out in this study, Carneiro, Kelderman and Irvine (2016) also observed TP load input peaks during the months of January and February, that presented the highest discharge and precipitation.

Figure 42 illustrate results of cumulative TP load input in Passaúna reservoir. Total TP load input resulted in 4910 kg TP/year, where 78% (3840 kg TP/year) were from Passaúna River, while 6% (281 kg TP/year) were from Ferraria River, and the sum up of the remaining tributaries loading input resulted in 789 kg TP/year, 16% of the total.

The incoming phosphorus loading results of this study is also in agreement with the obtained by Carneiro, Kelderman and Irvine (2016), in which total phosphorus inputs

resulted in 8190 kg/year, 6575 kg/year, and 4800 kg/year, for 2010, 2011, and 2012, respectively.

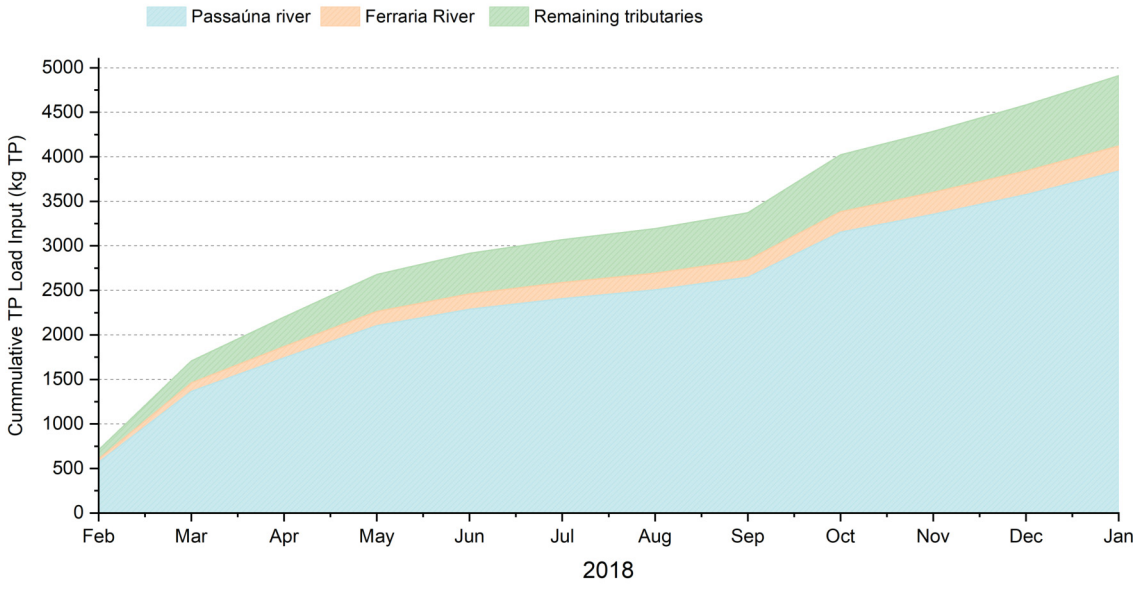

Figure 42 – Cummulative calculated load input (kg TP/year) of the main tributary (Passaúna River), Ferraria River, and remaining tributaries as stacked areas (see the legend)

Loading input results can be also compared with the study developed by Veiga and Dziedzic (2010), in which nutrient loads in the Passaúna reservoir were estimated though the application of FLUX model in simulations from 1990 to 1998. The TP load input estimated by Veiga and Dziedzic (2010) resulted in 10164.2 kg/year, in which Passaúna River represents 57% of the total input with 5789 kg/year, follow by Cachoeira River with a loading of 2038 kg/year, 20% of the total input.

The difference between input loading results can be explained by the fact that in the study developed by Veiga and Dziedzic (2010), concentrations of 13 tributaries were considered and sampled, while in the study developed by Carneiro, Kelderman and Irvine (2016), the three main tributaries in terms of flow (Passaúna River, Eneas River, and Ferraria River) were accounted. The remaining tributaries were considered as a single contribution, as well as adopted in the present study.

Besides, loading calculations were developed based on measurements performed in different monitoring periods, and Veiga and Dziedzic (2010) loading results take into consideration an irregular occupation area, which was responsible for the highest phosphorus export coefficients for each tributary watershed.

More recently, Sotiri et al. (2022) assessed yearly input of TP for Passaúna reservoir based on a regionalized emission-modeling approach combined with monitored data in Passaúna river, which resulted in input load of 3508 kg TP/year during baseflow. The

author's results also revealed high TP concentration (reaching 6700 mg/kg) in irregular occupation areas.

6.3.1.2 Phosphorus outputs assessment

As detailed in Chapter 5.3.1, daily output discharge rates were obtained through the reservoir's operating routine. Figure 43 presents TP loads output (kg TP/day), composed by drinking water abstraction discharge (m^3/s) multiplied by TP concentration (mg TP/L) of samples collected at surface of intake site, and the sum up of discharge via flood spillway and discharge via bottom outlet (m^3/s) multiplied by TP concentration (mg TP/L) of samples collected at outflow site.

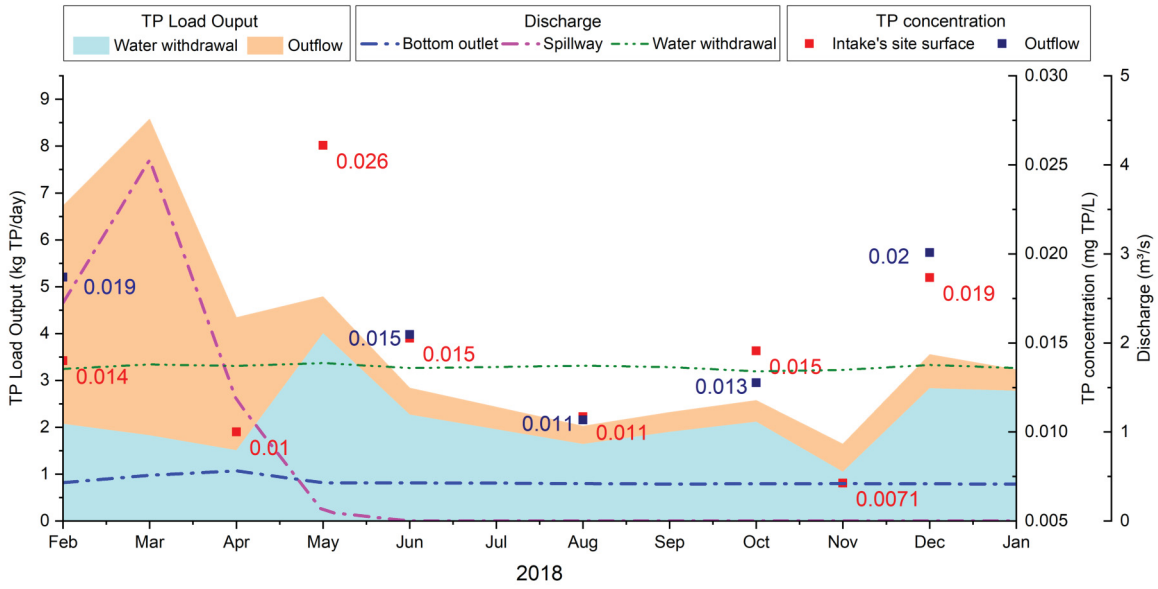

Figure 43 – Monthly mean output discharges of Passaúna reservoir (m^3/s), composed by bottom outlet (blue line), spillway (pink line), and water withdrawal (green line). TP concentration (mg TP/L) measured at surface of intake site (red squares) and outflow site (blue squares). And calculated load output (kg TP/year) of water withdrawal and outflow - spillway sum up with water withdrawal, see the legend

Daily TP output loads presented an significantly variation over the monitoring period (from 1.6 kg TP/day to 8.6 kg TP/day), and mean of 3.69 kg TP/day.

As illustrated in Figure 44, from the total about 1365 kg/year of phosphorus output, water withdrawal represents 58% (790 kg/year), while 42% (574 kg/year) is from so-called outflow, which includes spillway and bottom outlet discharges and phosphorus concentrations.

Output phosphorus loading estimated in this study proved to be below the obtained by Carneiro, Kelderman and Irvine (2016), of 5140 kg/year, 5018 kg/year, and 3663 kg/year, for 2010, 2011, and 2012, respectively. This could be explained by the lack of outflow by spillway in the monitoring period (2018-2019), this sink of phosphorus

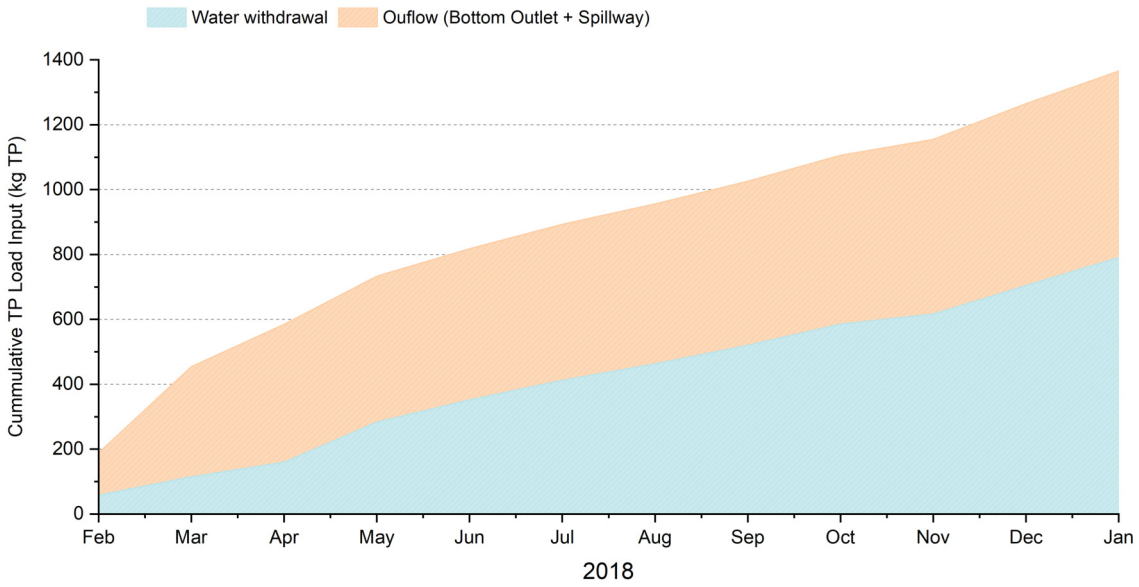

Figure 44 – Cumulative calculated load output (kg TP/year) from water withdrawal and outflow (bottom outlet and spillway) as stacked areas, see the legend.

represented a significantly export in 2010 calculated by Carneiro, Kelderman and Irvine (2016).

6.3.1.3 Phosphorus retained within the reservoir

Based on the mass balance calculations, the amount of phosphorus as loading into the reservoir is about 4910 kg/year, while 1365 kg/year leaves the reservoir, resulting in a load of 3545 kg retained in the reservoir per year.

A premise of applying the continuously Stirred Tank Reactor model is the reservoir acting as a completely mixed system. According to Chapra (1997), in such a system, mass transport is quantified as the product of outflow's concentration and discharge. Therefore, the outflow concentration is equal the in-reservoir concentration.

Although the TP's spatial variability investigation resulted in consistent longitudinal gradients (Section 6.2.1), the unsteady-state solution was evaluated in representing TP dynamics in Passaúna reservoir.

Therefore, in order to compare results of the mentioned application, the reservoir was divided in three regions (Figure 45) to better represent the spatial variability of phosphorus concentration. In the proposed segmentation, the first segment is consisted by Buffer site only, because the region is considered as a pre-dam due to the narrowing created by the Ferraria Bridge. The second zone is composed by Ferraria Bridge and PPA sites, since their locations are more closer and influenced by the main river entrance. The third and last zone is composed by the remaining monitoring sites (Reservoir Center,

Park, Intake, and Dam) situated at the deepest locations of the reservoir, in direction to the dam structure.

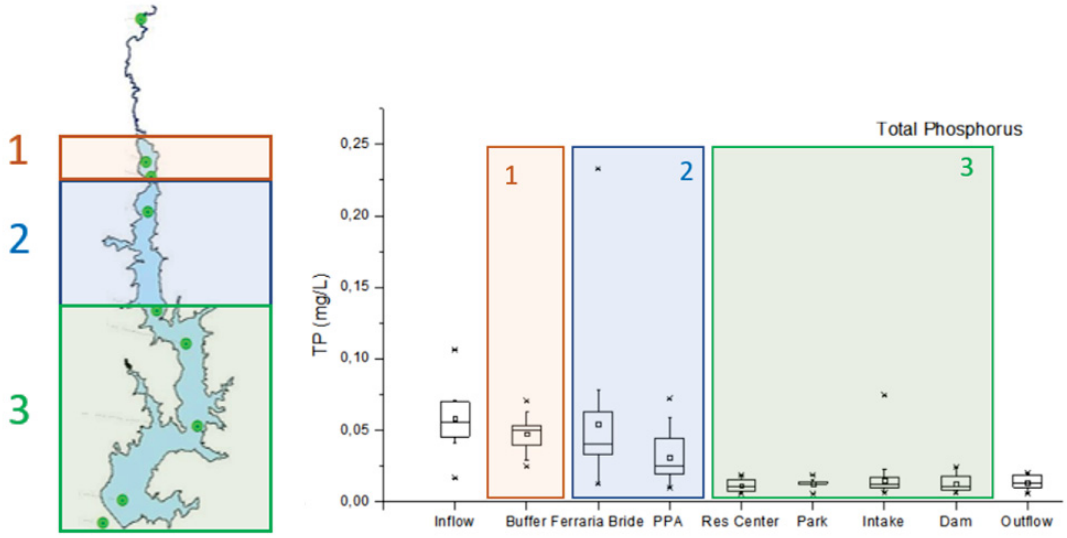

Figure 45 – Segmentation of Passaúna reservoir into three different zones (Zone 1, Zone 2, and Zone 3) based on the spatial variability of monitored Total Phosphorus (TP, mg TP/L) during monitored period - February 2018 to April 2019, according to sampling sites.

Figure 46 provides variations of TP concentrations in each segment. TP concentration measured at the monitoring sites situated in Zone 3 presented a better correlation with the outflow concentration, and for this reason was selected for comparison with results of this application.

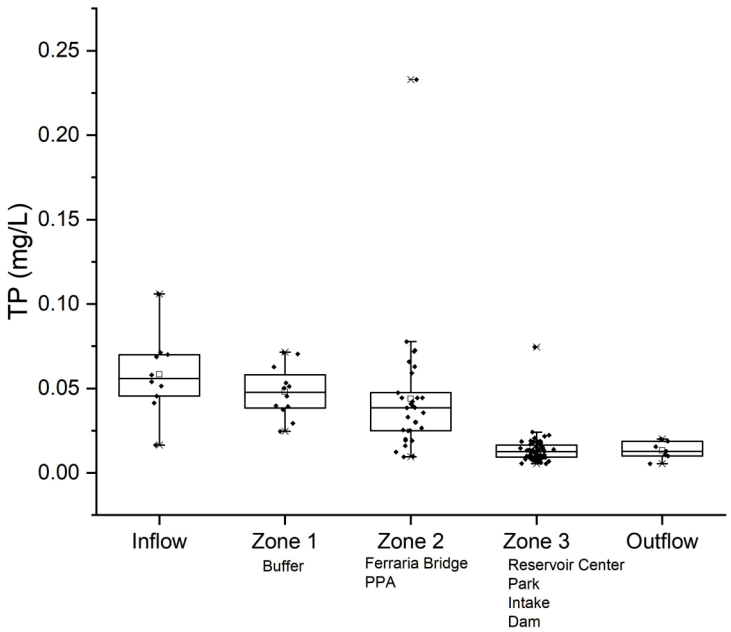

Figure 46 – Variations of measured Total Phosphorus (TP, mg TP/L) concentrations at Inflow, Outflow, and within the Passaúna reservoir divided in three segments: Zone 1, Zone 2, and Zone 3.

To assess concentrations within the reservoir, from mass-balance models for well-mixed systems, phosphorus concentration can be solved with steady-state solution.

6.3.2 Steady-state approach to estimate annual TP concentrations within the reservoir

Annual TP concentrations in the reservoir were calculated through steady-state solution using equation 5.2, presented in Section 5.3.2. The mean volume and discharge over the monitoring period are 6.70E+07m^3 and 2.67 m^3/s, respectively. Applying these data in the Equation 2.1 presented in Chapter 2.2, residence time was calculated as 1.13 years or 466 days.

The annual steady-state TP concentration resulted in 0.01538 mg/L, indicating a good fit with TP concentrations measured at Zone 3 of Passaúna Reservoir (mean: 0.0142 mg/L). However, an additional analyses was performed, testing phosphorus decay coefficient based on proposed by Vollenweider (1976) (k = $1/\sqrt{RT}$) for temperate lakes and by Salas and Martino (1991) (k = $2/\sqrt{RT}$) for tropical reservoirs, and resulted in TP concentrations of 0.34mg/L and 0.024, respectively.

Passaúna Reservoir fitted really well in the approach to estimate overall annual mean of TP concentration within the reservoir using Steady-state approach and monthly measurements as input data at the main inflow. Phosphorus decay coefficient adjusted by Toné (2016) for Brazilian's reservoirs in semi-arid region, resulted in the best agreement with measured TP data.

However, in monitoring the water quality of the Passaúna reservoir, TP concentration presented a significant temporal variation (see Figure 36). Therefore, subsequently, monthly TP concentrations within the reservoir were calculated through the unsteady-state solution to investigate temporal variations on TP concentrations.

6.3.3 Unsteady-state approach to estimate monthly TP concentrations within the reservoir

Monthly phosphorus concentrations were calculated through unsteady-state solution using equation 3.13, as described in section 3.2.3.

The Unsteady-state model was based on the unsteady CSTR model, as presented in Section 3.2.3. The apparent settling velocity (m/year) variable was used as model's calibration coefficient, and a sensibility test was performed for defined its value.

The period assumed for simulation was from February 2018 to January 2019, because of the measured field data availability in this period to verify the simulations results. However, the model was run for a period of two years, starting in February 2017,

as warm up process to define the initial TP concentration. The warm up period was performed with a null initial TP concentration and same variables values adopted for the simulated period. The final TP concentration resulted from the warm up process of 0.0123 mg TP/L was adopted as initial condition for the simulated period.

The applied unsteady-state model was capable of reproducing TP concentrations measured at Zone 3 of Passaúna Reservoir (MAE=0.0051 and RMSE=0.0058), Figure 47.

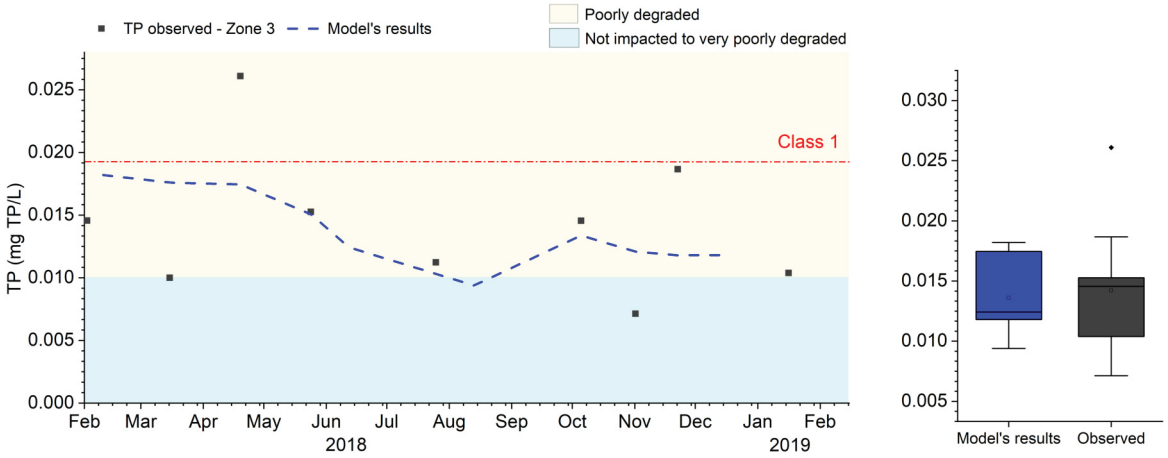

Figure 47 – Time series of TP concentration's simulated with unsteady-state solution in monthly resolution and measured data at Zone 3 in Passaúna reservoir. Red dashed line represents CONAMA'S thresholds for watercourses class I and background colors marks WQIR's threshold for class 1 (not impacted to very poorly degraded and class 2 (poorly degraded). Time series of volume [m³] are indicated in color grey.

The most evident discrepancy between modeling and measurements was observed in May 2018, with the model underestimating highest measured TP concentration (0.0261 mg TP/L) at Zone 3. On the other hand, TP concentrations values measured in February, April, and November 2018 were below model's concentrations results.

During the simulated period, model's concentrations and measured values ranged below the threshold for watercourses class I of 0.02 mg TP/L (CONAMA, 2005), with the exception of above mentioned outlier. Generally, values oscillated around WQIR's threshold for class 2 (poorly degraded, 0.011 - 0.025 mg TP/L).

From April to early October 2018, when inflow discharge into the reservoir are low, the model was able to reproduce well concentrations dynamics, decreasing in June and August followed by a increase peak at October.

Possible limitation on using this approach is the need to calibrate the apparent settling velocity (ν), which resulted during calibration process in a almost null value. This means that, in order to achieve small differences between measured and observed values, sediment process was considered to be equivalent with possible internal loading extend.

However, according to Nowak (2018) studies performed for Passaúna reservoir in 2017, phosphorus release rate from sediments has calculated mean of 6.59 mg/m²/day,

resulting in internal loading rate of 2.4 t/year. These results were obtain through the use of a model for prediction of internal phosphorus loading developed by Nurnberg (2009) for polymictic lakes, applying data of total phosphorus concentrations from samples in water columns and measured in 30 sediment cores, dissolved oxygen measurements at the surface and bottom in the water column, and total phosphorus content spatially obtained by data from echo sounding measurements.

An indication of internal loading process was also observed during laboratory analyzes (Section 6.2.1), due to iron bound with phosphate ions interference influencing laboratory analyzes and making it impractical to quantify phosphorus concentration, when the water column was stratified during sample collection.

In addition, thought analysis of suspended solids collect with sediment traps on campaigns performed in 2019, Ono (2020) estimated nutrients (phosphorus and nitrogen) deposition, and found out that sedimentation process represents an important pathway in phosphorus budget in Passaúna reservoir. According to Ono (2020), total phosphorus and total nitrogen deposition rates were 50.08 mg/m².day and 190.52 mg/m².day, respectively. The author also identified temporal and longitudinal variations, in which sedimentation rates presented higher amounts at end of autumn and winter seasons, and from upstream to downstream in the reservoir.

6.3.3.1 Testing scenarios of unsteady-state approach to estimate monthly TP concentrations within the reservoir

The unsteady-state model was tested through several scenarios, decreasing the temporal resolution of input data to less frequent measurements, gradually from monthly to bimonthly (scenario 1), quartely (scenario 2), and lastly as twice per year (scenario 3), Figure 48.

For all simulated scenarios, temporal resolution reduction of the input data resulted in higher Root Mean Square Error (RMSE). The mean, standard deviation, maximum and minimum values did not change significantly between monthly temporal resolution data (original model's results) and bimonthly resolution (Scenario 1).

Interestingly, quarterly temporal resolutions (Scenario 2) resulted in higher TP concentration simulated values, while semiannually resolutions (Scenario 3) apparently underestimate the calculated phosphorous concentration in the reservoir.

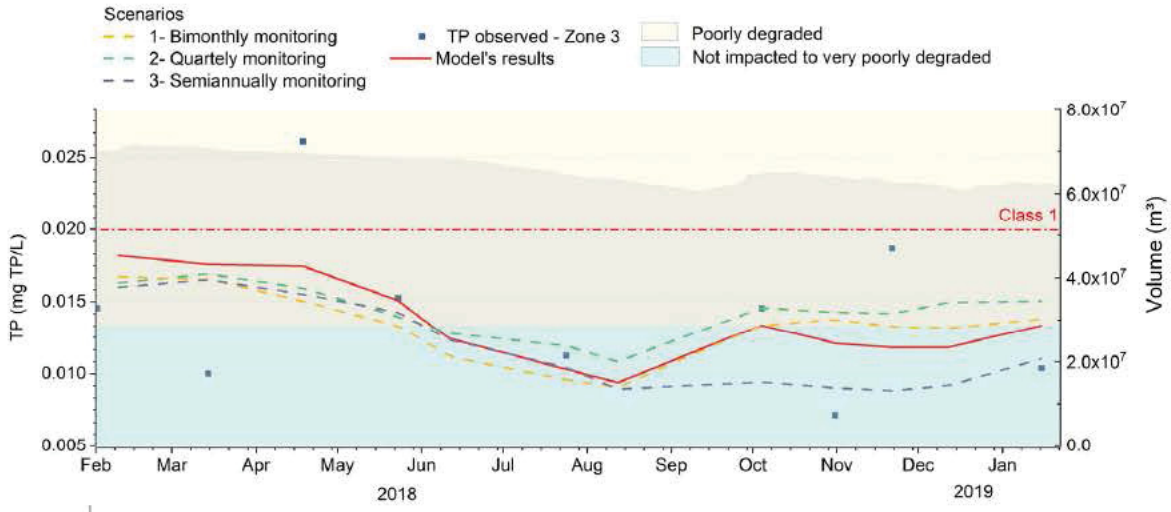

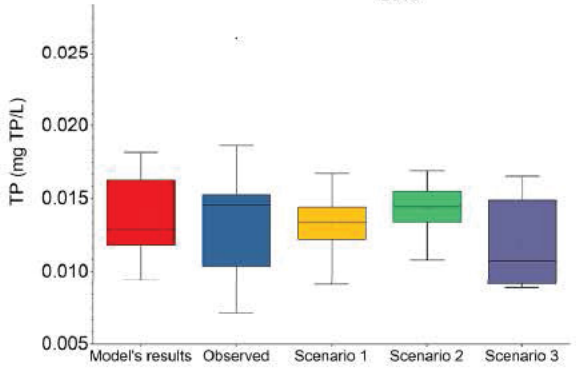

	Monitoring frequency	TP range (mg TP/L)	MAE	RMSE
Observed	Almost monthly	0.0146 ± 0.0058 (0.0071 – 0.0261)		
Model's results	Monthly	0.0138 ± 0.0023 (0.0102 - 0.0167)	0.0037	0.0050
Scenario 1	Bimonthly	0.136 ± 0.0021 (0.0096 - 0.0166)	0.0043	0.0055
Scenario 2	Quarterly	0.0145 ± 0.0016 (0.0119 – 0.0169)	0.0038	0.0053
Scenario 3	Semiannually	0.0120 ± 0.0033 (0.0088 – 0.0165)	0.0044	0.0059

Figure 48 – Time series of TP concentration's simulated scenarios with unsteady-state solution in monthly resolution and measured data at Zone 3 in Passaúna reservoir. Red dashed line represents CONAMA'S thresholds for watercourses class I and background colors marks WQIR's threshold for class I (not impacted to very poorly degraded and class 2 (poorly degraded). Time series of volume [m³] are indicated in color grey.

6.3.4 Summary

Although the application of steady-state solution resulted in annual means compatible with phosphorus measured at Zone 3 of Passaúna Reservoir, through these application was not possible to observe fluctuations and trends in water quality variations.

In this sense, solutions such as unsteady state could be useful to better represent the water quality dynamics. The unsteady-state model was capable of reproducing TP concentrations measured at Zone 3 of Passaúna Reservoir with considerable small error (MAE and RMSE). However, the need to calibrate the apparent settling velocity resulted in a almost null value, which means that sediment process and internal loading exchanges are of minor relevance.

However, according to field and laboratory observation, Nowak (2018), and Ono (2020), both sedimentation and internal loading represent important processes in phosphorus concentration within the reservoir. Indeed, sediments play a key role in the

nutrient dynamics of lakes and reservoirs. The sediment from sink, can become a source of phosphorus and large amounts of phosphorus could be release, worsening the water quality of the watercourse even when external loading is reduced (SØNDERGAARD; JENSEN; JEPPESEN, 2003; NÜRNBERG, 2005; MOURA et al., 2020)

Longitudinal gradients also were found in both studies, indicating that to properly access more reliable results in estimating phosphorus concentrations within Passaúna reservoir, at least models in 2-dimensions are necessary. Such a observation was also obtained in study performed by Ishikawa et al. (2022a), regarding hydrodynamic processes in regulating phytoplankton dynamics.

Additionally, Sotiri et al. (2022) analysis also resulted in important deposition and resuspension events in Passaúna reservoir. The authors observations revealed that the resuspended material make it difficult to distinguish urban and nonurban input.

Finally, testing scenarios of unsteady-state approach to estimate monthly TP concentrations within the reservoir, decreasing the temporal resolution of input data to less frequent measurements, resulted in quarterly temporal resolutions of monitoring data as optimal resolution on monitoring Passaúna's reservoir.

6.4 Optimal monitoring strategies

In this section are evaluated strategies to optimize monitoring resolutions considering not only temporal dynamics and spatial variations, but also modeling application.

The integration of spatial-temporal water quality dynamics in the monitoring period was assessed using a map, followed by load duration curves analyses for Passaúna River historical data.

Additional investigations of temporal resolution improvements of TP concentration data and assessment of storm events influence in mass balance calculations are presented. And optimal monitoring resolutions are evaluated using data in high temporal resolution.

6.4.1 Comparative maps integrating spatial-temporal water quality dynamics through Water Quality Index of Reservoirs (WQIR)

To integrate spatial-temporal water quality dynamics in the monitoring period, the WQIR was compiled integrating data of TP, TIN, and Chl-a for each season in every monitoring sites within the reservoir, Figure 49. The index classification was obtained based on ranges of concentrations from Table 2, Section 2.6.2. For each season and monitoring point, the mean of values collected at all depths were processed, as presented in Appendix B

In spite of ecological status classification assessed by IAP (2017), which only uses Chl-a concentration measured at surface. To obtain WQIR's classification of Chl-a, measurements from all depths measured were considered in mean values. Even thought, WQIR of Chl-a classification did not presented significantly seasonally or spatially variations.

It is important to highlight here, the importance of sampling frequency on evaluating temporal evolution, especially when analyzing reservoirs in terms of a good ecological status for management purposes or compliance. Since Chl-a monitoring frequency could mislead interpretations and ecological status classifications (MARCÉ et al., 2016), further investigations of changes on Chl-a time series using data with high temporal resolution were performed (See Section 6.4.4).

Chl-a WQIR classification presented a marked spatial variability. However, with exception of Ferraria Bridge monitoring site, Chl-a did not present pronounced seasonal dynamics. This same pattern was observed by Ishikawa et al. (2022b), using spatially resolved and high-frequency measurements of Chl-a from satellite remote sensing and in-situ sensors.

On the other hand, TIN concentrations were mostly classified as 'Moderately

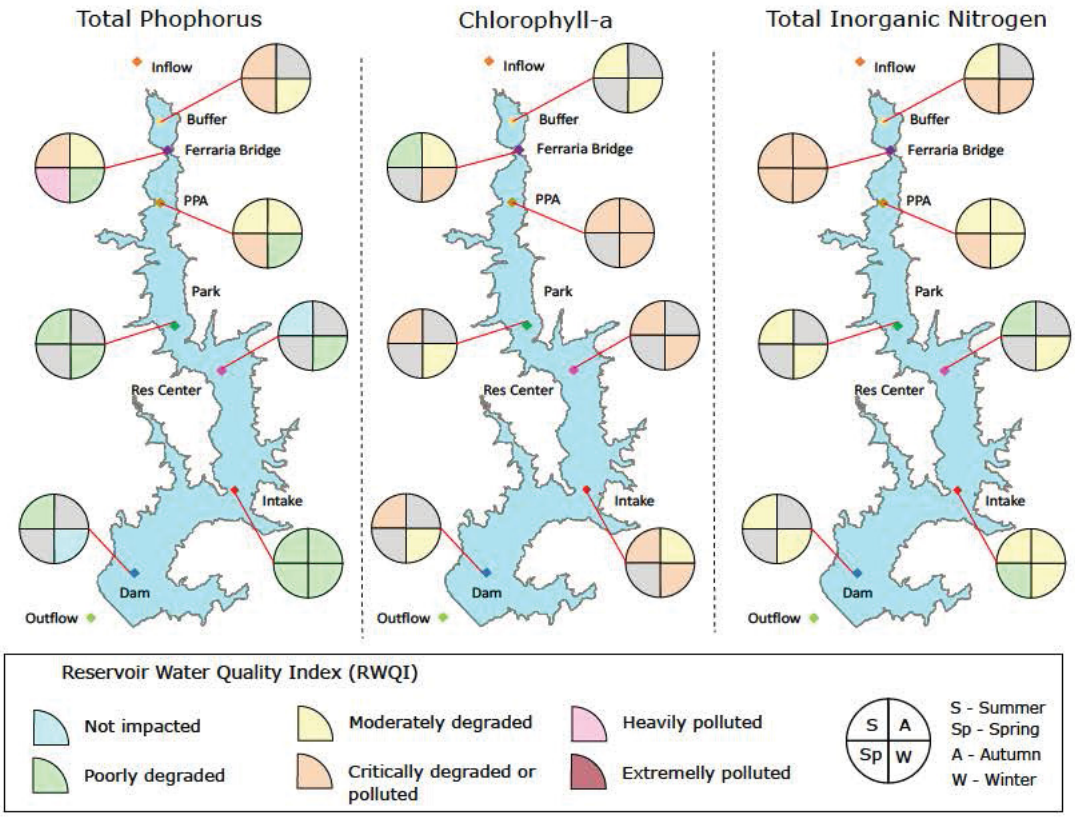

Figure 49 – Comparaive maps integrating spatial-temporal water quality dynamics through Water Quality Index of Reservoirs (WQIR) of measured data of TP, TIN, and Chl-a for each season in every monitoring site, from monitoring program carried out from 2018 to 2019.

degraded'. A decrease tendency in TIN concentrations was observed towards the dam, but strong seasonally variations was not observed. Compared to TP classification, TN presented more marked variation, indicating the importance of internal processing in seasonal pattern.

WQIR overall classification performed by IAP (2017) is moderately degraded, from campaigns carried out twice a year from 1998 to 2013 on Passaúna's reservoir. However, additional variables and weight are applied to obtain the ecological status classification.

The diversity of classification status suggested that depending on the monitoring program purpose, temporal and spatial variations observed in Passaúna reservoir water quality can not be captured with only two campaigns per year in only one monitoring site as performed actually by IAP (2017). For an overall water quality definition it might be enough, however for a preventive water resources management longitudinal trends and seasonal variations are not correctly identified.

Heavily polluted status was only reached at Ferraria Buffer during spring, when TP concentrations ranged 0.23 mg TP/L, indicating possible Passaúna river's inflow influence in phosphorus concentrations at upstream region of the reservoir. Since TP classification presented a decrease and stable tendency towards the dam structure, less sampling is

necessary in such a regions.

According to Ishikawa et al. (2022b) observations, in the upstream region nutrients coming from the main tributary are consumed. Whereas, in the deeper regions phytoplankton dynamics depend on internal loading processes. The authors also claimed that temporal variability at the Passaúna's reservoir occur at the upstream region, in agreement with this study observations of TP and Chl-a classification.

The monitoring site and date of sample collection could be decisive in defining ecological water quality status. However, as indexes represent an overall status of the aquatic body based on the combination of water quality variables, some limitations must be observed.

6.4.2 Daily synthetic series to estimate TP concentrations input

Additional investigations were performed to verify discharge data sensibility on mass balance calculations and loading input values, with the aim of obtaining better input description and quantify uncertainties involves in mass balance quantification.

Potential influence of storm events on TP input are usually not considered in mass balance calculations, since most of traditional field campaigns were performed during base flow discharges. Furthermore, Smaha and Gobbi (2003) stressed the importance of correlation between nutrient loads and storm events. The authors developed an eutrophication model to evaluate degradation degree of Passaúna's reservoir waters. The author results presented Chl-a concentration inertia in returning to equilibrium state, when submitted to high loads of nutrients from discharge events.

Therefore, an evaluating of how storm events influence as input loads to mass balance calculation was performed. Effects of storm events in input loads were assessed based on survey of two storms events performed in October 2018 by MuDaK partners in Passaúna River, Figure 50.

Figure 51 presents measurements of discharge (m^3/s), TP (mg TP/L), TDP (mg TDP/L), TSS (mg TSS/L), and TS (mg TS/L) of the two storm events monitored. The first storm event had a duration of 28 hours, from 13^{th} to 14^{th}, October. Discharge reached the peak of 4.63 m^3/s together with TP concentration peak of 0.41 mg/L. TP concentrations increased and decrease following discharge variation over the storm event duration.

The second monitored storm event had duration of 47 hours, measured discharge reached the peak of 11.9 m^3/s and TP concentration 0.96 mg/L. Differently than the observed on first storm event, as discharge increase TP concentrations decrease in this event. Pattern that could be an indicator of first flush occurrence, since the second storm event took place few days after the first, from 17^{th} to 21^{th}, October.

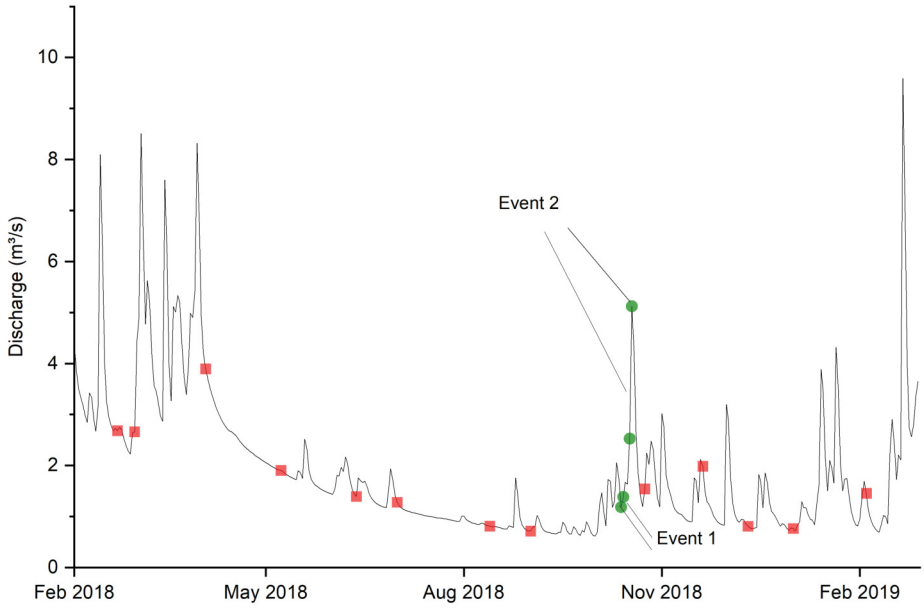

Figure 50 – Time series of daily Passaúna river discharge over the monitored period (from February 2018 to February 2019). Red squares indicate monitoring campaigns performed and green circles the two storm events monitored in a survey by MuDak project partners.

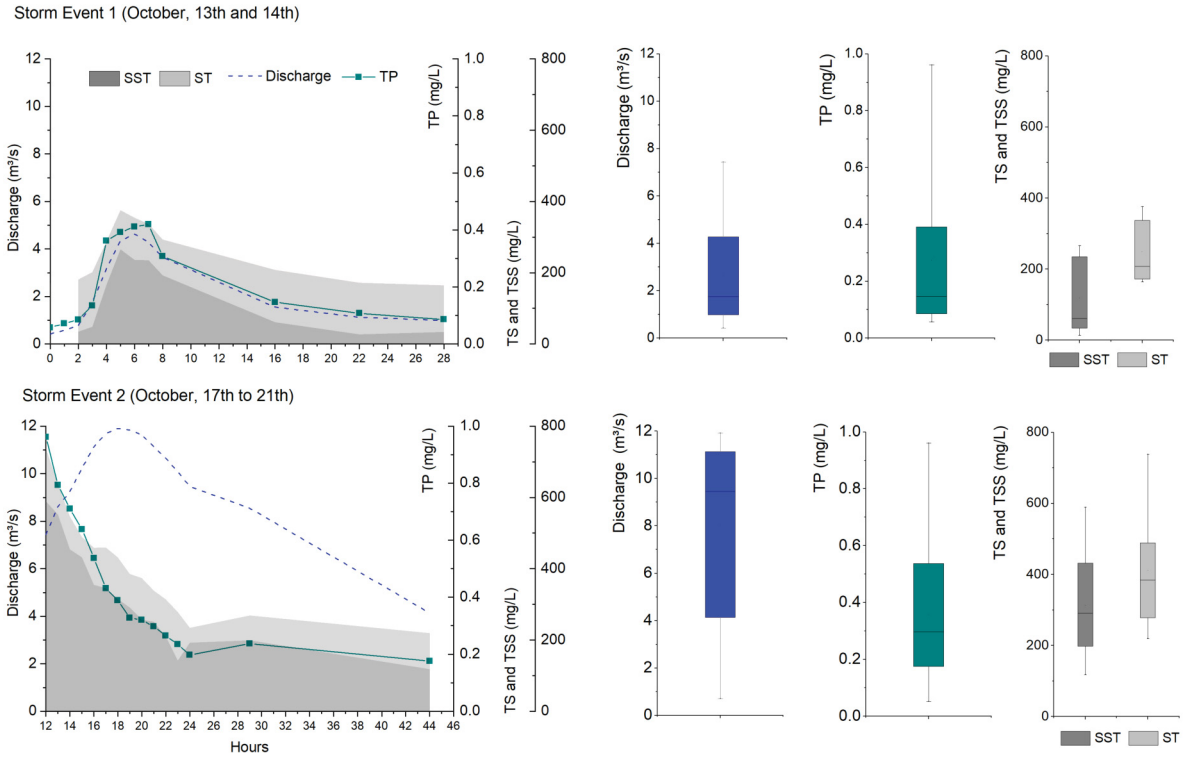

Figure 51 – Time series and box plots of discharge (m^3/s), Total Phosphorus concentration's (TP, mg TP/L), Total Dissolved Phosphorus (TDP, mg TDP/L), Total Suspended Solids (TSS, mg SST/L), and Total Solids (TS, mg ST/L) of the two precipitation events in October 2018, monitored by MuDaK partners.

Clearly, input load from events represents an important source of TP input in Passaúna' reservoir. While mean input load calculated based on monthly monitored campaigns was 10.57 kg/day (see Section 6.3.1.1), TP loading input from the first event was calculated as 37.16 kg/day, and from the second as about 200 kg/day.

Several others storm events were observed along the monitoring period (see Figure 50. Hence, an investigation of daily TP input based on daily discharge measured at Passaúna River was performed, with the purpose of quantified the importance of storm events on the total input TP load.

The TP input load from tributary rivers of Passaúna' reservoir was observed to be related with hydrological regime, not only because of the discharge variability, but also with higher TP concentrations observed in the monitored storm events.

Here is important to mention that discharge-solute relationships present a cyclic form known as hysteresis, in which the shape depends on chemical and hydrological processes (BENDER et al., 2018).

Therefore, correlation of discharge and TP concentrations were evaluated using all dataset available of TP measured at Passaúna river, including historical data obtained from Hydrological Information System, measurements performed during this study monitoring period, and those provided by Sanepar, Appendix C.

The interplay between TP concentrations and discharge can not be explained with a simply linear correlation, Figure 52. Indeed, in study performed by Bender et al. (2018) in southern Brazil, the hysteresis of TP forms were found to be related with crop development period. Therefore, such a correlation involves several more complex watershed processes such as erosion, soil use, among others.

Therefore, a strategy of using ratio between discharge measured and historical mean (Q/Qhist) was evaluated. A similar approach was used by Allion, Kiemle and Fuchs (2022) in study performed in Kraichbach River in Baden-Wuerttemberg (Germany).

The observed discharge mean of Passaúna river since the dam's construction was calculated as 1.8 m^3/s, obtained from historical data (from 1985 to 2020). The calculated discharge ratio (Q/Qhist) were divided into flow ranges every 0.5, and for each group range the mean of ratio and respective TP concentration were obtained, Table 19.

The calculated discharge ratio (Q/Qhist) was divided into flow ranges every 0.5, and for each group range the mean of ratio and respective TP concentration were obtained, Table 19. A better correlation between variables was observed with this approach, with different pattern depending on the ratio range. For discharges below 3.6 m^3/s, mean TP concentration presented a slightly increase tendency together with discharge increase. On the other hand, discharge above 3.6 m^3/s presented non-linear behavior.

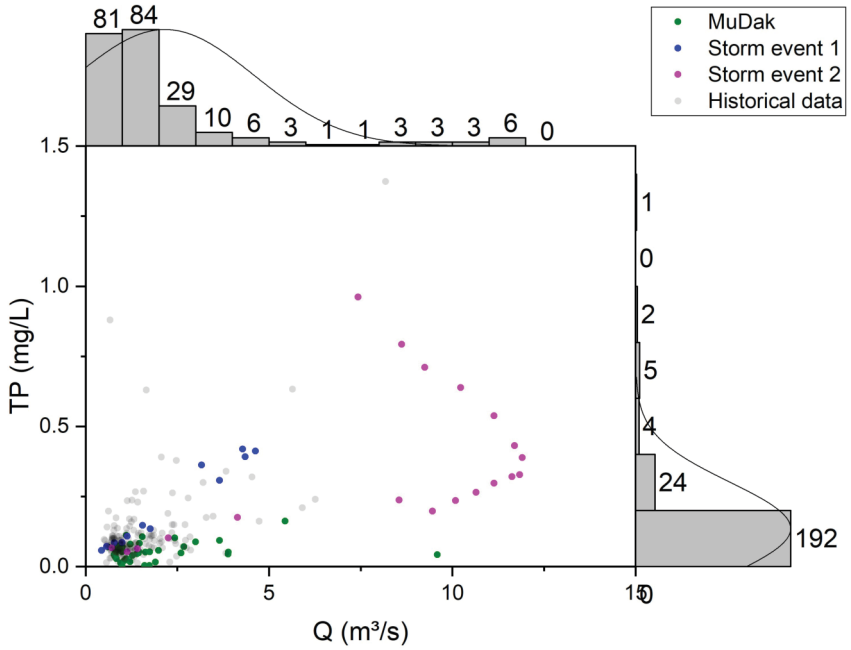

Figure 52 – Plots of correlation between discharge [m^3/s] and Total Phosphorus concentration (mg TP/L) from TP measurements at Passaúna river dataset (historical data obtained from Hydrological Information System - SIH, measurements performed during MuDaK's monitoring period, and data provided by Sanepar).

Table 19 – Discharge ratio (Q/Qhist) and respective mean Total Phosphorus concentration's (TP, mg TP/L) for each discharge ratio distributed in ranges of 0.9 m^3/s.

Discharge range	Q/Qhist	TP (mg TP/L)
< 0.9	0.38	0.078
0.9 - 1.8	0.70	0.091
1.8 - 2.7	1.18	0.111
2.7 - 3.6	1.68	0.113
3.6 - 4.5	2.17	0.074
4.5 - 5.4	2.66	0.178
5.4 - 9	3.31	0.100
> 9	6.11	0.617

Figure 53 show plots of results presented in Table 19 of TP concentration with respective discharge ratio (Q/Qhist). A linear equation was adjusted divided into two groups: below and above discharge of 3.6 m^3/s. Here is important to present that the lack of TP measurements for discharge ratio above 2 Q/Qhist can detour the equation found out for discharge above 3.6 m^3/s.

The obtained equations were applied in the Passaúna river discharge time series, resulting in a synthetic TP series in daily resolution, from February 2018 to January 2019 (Figure 54). Although synthetic TP concentrations were relatively low (mean: 0.1010 mg TP /L), generally values calculated overestimate observed TP concentration (mean: 0.061

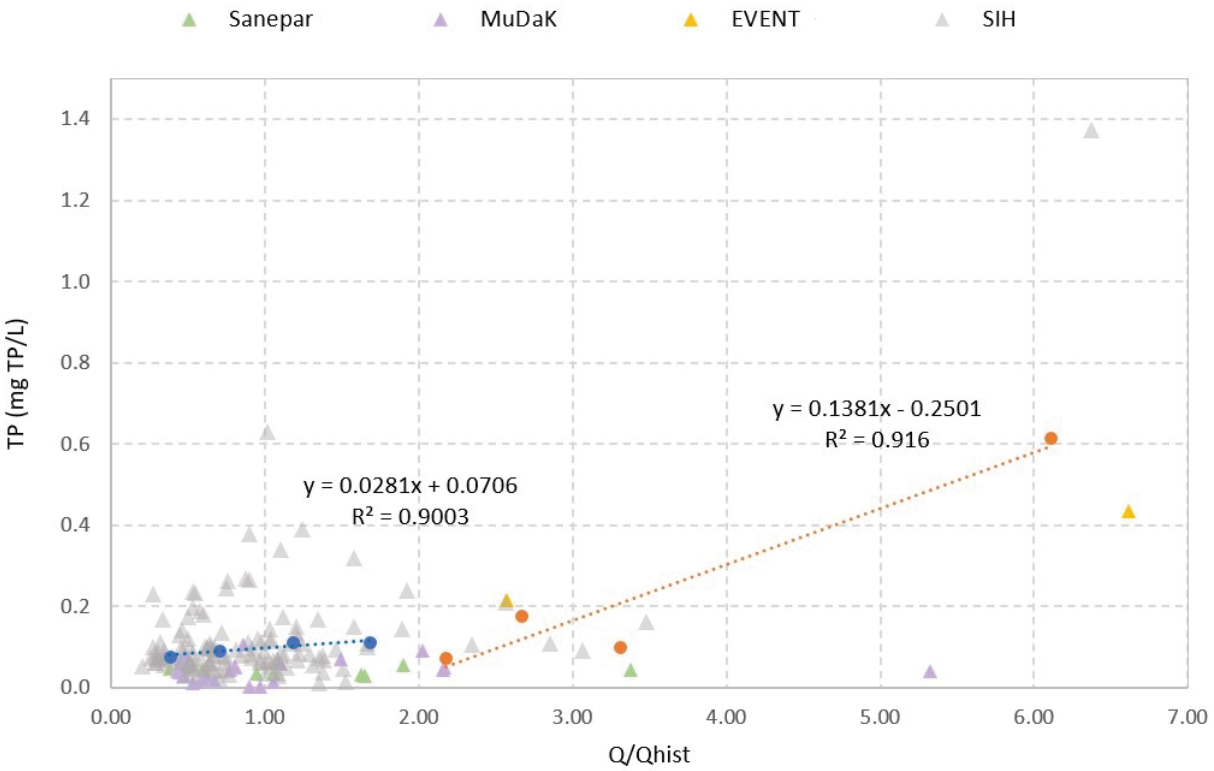

Figure 53 – Plots of correlation between discharge ratio (Q/Qhist) and Total Phosphorus concentration (mg TP/L) from TP measurements at Passaúna river dataset (historical data obtained from Hydrological Information System - SIH, measurements performed during MuDaK's monitoring period, and data provided by Sanepar). Linear equations adjusted for data, and respective R^2, are indicated as blue line (ratio below 2 Q/Qhist) and as orange line (ratio above 2 Q/Qhist).

mg TP /L) measured during base flow. Differences between calculated and observed TP concentrations resulted in a MAE of 0.07014 and RMSE of 0.1011.

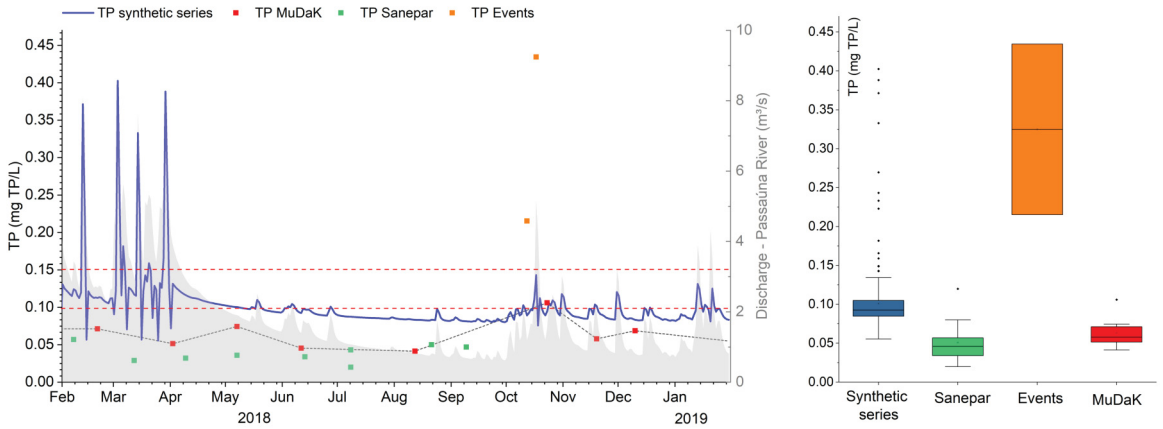

Figure 54 – Time series and box plots of Total Phosphorus concentration's (TP, mg TP/L) calculated with equations correlating discharge ratio (Q/Qhist) and TP concentrations in daily resolution and measurements at Passaúna River. Dashed lines represent thresholds for good ecological status according to CONAMA Resolution nº 357:2005 for rivers class 1 and 2 of 0.10 mg TP/L and class 3 of 0.15 mg TP/L. Time series of discharge [m³/s] in Passaúna river are indicated in color grey.

As a response of input discharge temporal variability, TP calculated concentrations

also presented larger fluctuations from February to April 2018, ranging between 0.055 mg TP/L (March 26, 2018) and 0.4025 mg TP/L (March 4, 2018). However, calculated TP concentrations was not capable of reproducing TP mean concentration data of storm events of 0.215 mg TP/L (storm event 1) and 0.435 mg TP/L (storm event 2).

The threshold for lotic watercourses class 1 and 2 of 0.10 mg TP/L of CONAMA (2005) was exceed in 32.6% of calculated TP concentrations, while class 3 threshold of 0.15 mg TP/L was exceeded in only 3% of calculated TP concentrations.

The calculated TP concentrations in daily resolution resulted on accumulated loading input of 9302.5 kg/year, Figure 55. In contrast with accumulated loading input calcuted using monthly measurements of 4910 kg/year, as presented in Section 6.3.1.1.

From discharge range distribution, 61% of total loading input was from discharge below 3.6 m^3/s, while 23% was from ten days of storm events, in which discharge ranged between 5.4 m^3/s and 9 m^3/s.

This investigation results revealed that, since phosphorus concentrations are usually low during base flow, monitoring efforts could be significantly reduced, and monitoring campaigns should focus more on storm events, in order to achieve more realistic phosphorus input calculations.

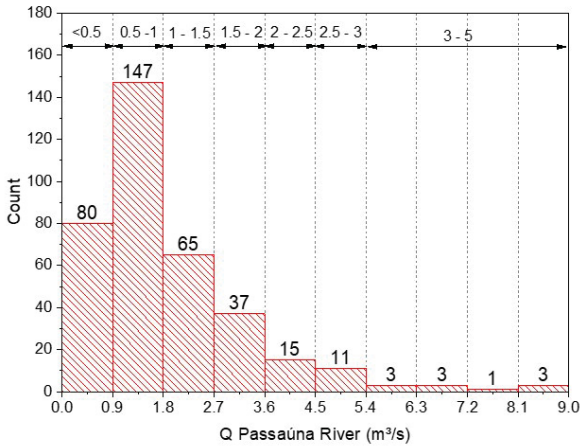

Q/Qmed	Q (m³/s)	Load input (kg)	Percentage	Days
< 0.5	< 0.9	569.76	6%	80
0.5 - 1	0.9 - 1.8	1948.32	21%	147
1 - 1.5	1.8 - 2.7	1679.27	18%	65
1.5 - 2	2.7 - 3.6	1493.25	16%	37
2 - 2.5	3.6 - 4.5	602.29	6%	15
2.5 - 3	4.5 - 5.4	849.14	9%	11
3 - 5	5.4 - 9	2160.43	23%	10
> 5	> 9	0.00	0%	0
TOTAL		**9302.47**	**100%**	**365**

Figure 55 – Count out of measured daily discharge distributed in ranges of 0.9 m^3/s from February 2018 to January 2019 (left hand side). Total load input results from Total Phosphorus concentration's (TP, mg TP/L) calculated with equations correlating discharge ratio (Q/Qhist) and TP concentrations in daily resolution for each discharge ratio distributed in ranges of 0.9 m^3/s (right hand side).

Nadim et al. (2007) application of steady-state nutrient model in two public water supply in eastern Connecticut (EUA) corroborates this findings. Although TN and TP concentrations results presented reasonable accuracy, the author application in Bathtub model results indicated the need of more sampling during high intensity storm events to improve nutrient investigations and model calibration.

Additionally, monitoring TP concentration when discharge is above 3.6 m^3/s could

fulfilled the gap found of TP measurements and improve equations results in correlating discharge ratio with TP concentrations.

Even results of monitoring Passaúna River using an storm event automatic sampler developed by Drummond (2020) present this lack of TP data, since monitoring was performed during the drought period (from July to November, 2019).

Steady-state results presented higher concentrations than those observed and similar to the concentrations found in the reservoir upstream area (zone 1).

The concentration resulting from the application of phosphorus loads considering the precipitation events highlights the importance of evaluating gradients within the reservoir and demonstrates that the concentrations measured in the water column should be higher than those observed on monitoring campaigns.

A possible explanation is sedimentation processes surpass internal loading exits. This stresses the importance of preventive monitoring of water quality variables within the reservoir since the large input of phosphorus can lead to reaching the limit of the phosphorus absorption capacity by the sediments, leading to processes high fluxes of internal loading and consequent water quality impairment.

6.4.3 Load Duration Curves Approach to improve Water Quality Monitoring Program of Passaúna River: a phosphorus load investigation

Data evaluation of historical discharge and TP concentration were performed from the official data water agency, available at Hydrological Information System - SIH, Figure 56. Measurements of phosphorus concentrations, and respective discharge, were available from May 1985 to March 2020.

Regarding the historical data, TP concentrations were relatively low (mean: 0.124mg/L) and discharge measurements ranged between $0.12 m^3$/s and 27.37 m^3/s (mean: $1.75 m^3$/s) between 1985 and 2019. The highest TP concentration was documented in September 1993 with 1.37mg/L, with respectively measured discharge of 14.66 m^3/s. The lowest TP concentration was about 0.013mg/L.

Over the monitoring period (February 2018 to April 2019), TP concentration ranged between 0.041 mg/L (August 2018) and 0.105 mg/L (October 2018), with an overall mean TP concentration of 0.064 mg/L, and discharge ranged from 0.64 m^3/s to 2.86 m^3/s.

For the same monitored period, four data from the SIH repository are available, whose concentration values were compatible with those measured in the project period, with a range from concentrations of 0.063 mg/L (November 2018) to 0.10 mg/L (January

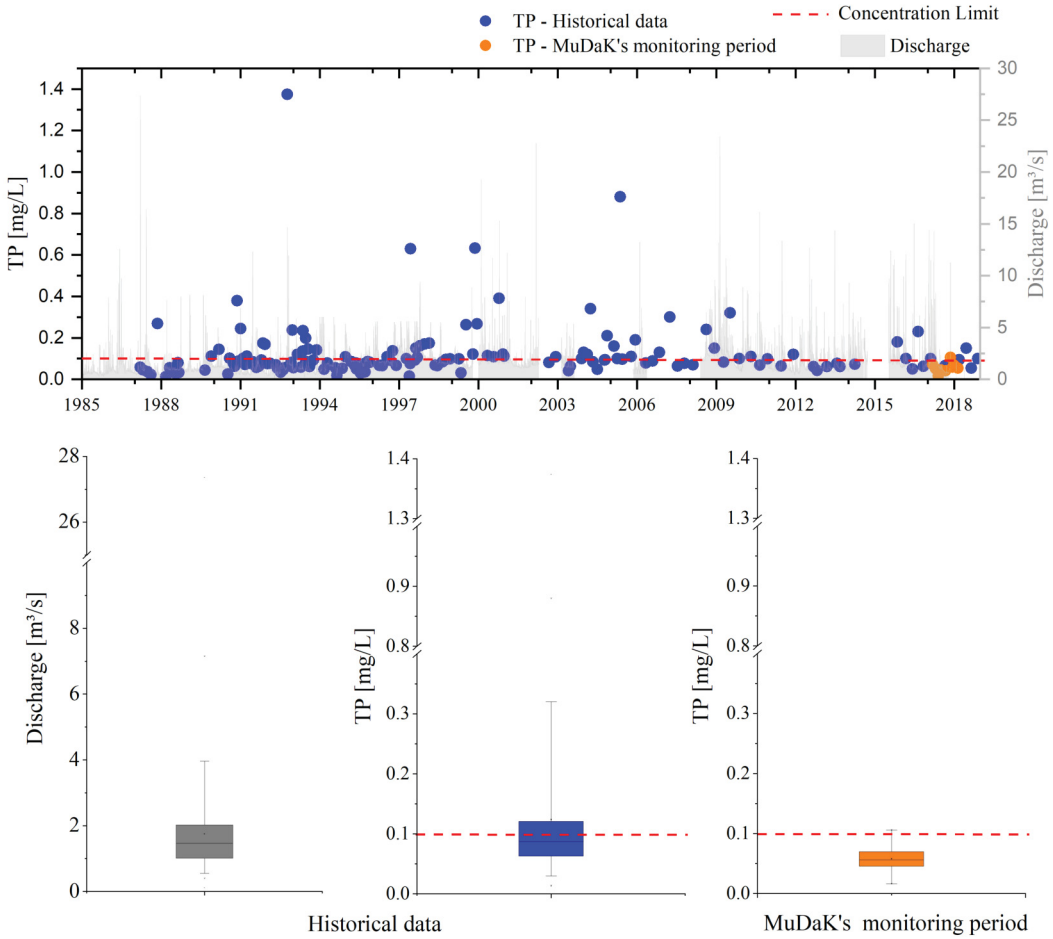

Figure 56 – Time series and box plots of discharge (m^3/s) and total phosphorus concentrations (mg/L) measured at Passaúna River obtained from the Hydrological Information System (SIH) repository from 1985 to 2019, and concentrations of total phosphorus (mg/L) observed in the monitoring carried out in the MuDak project from 2018 to 2019 indicated at the legend. Dashed lines represent thresholds for good ecological status according to CONAMA Resolution nº 357:2005 for rivers class 1 and 2. Data source for discharge: Hydrological Information System (SIH) of the Instituto Água e Terra (INSTITUTO ÁGUA E TERRA, 2021) repository, monitoring station 'BR 277 Campo Largo' - code 65021800 (25.42°S, 49.38°W)

2018), and an average of 0.081 mg/L in total phosphorus concentration.

The historical data along with measurements performed during monitoring period, and additional data provided by Sanepar were applied in a TP load duration curve. Figure 57 illustrates most observed loads in the Passaúna River are above the allowable limit.

Generally, mean observed load remained from low flows to moist conditions were bellow maximum permissible load. With exception of high flow hydrological condition, in which an increasing trend of TP concentrations was observed, and TP load values exceed permissible thresholds. Indicating that an important amount of load could be associated with storm flows.

According to Cleland (2003), loads plot above the curve during high flow conditions are usually associated with surface runoff and pollution from diffuse sources delivering

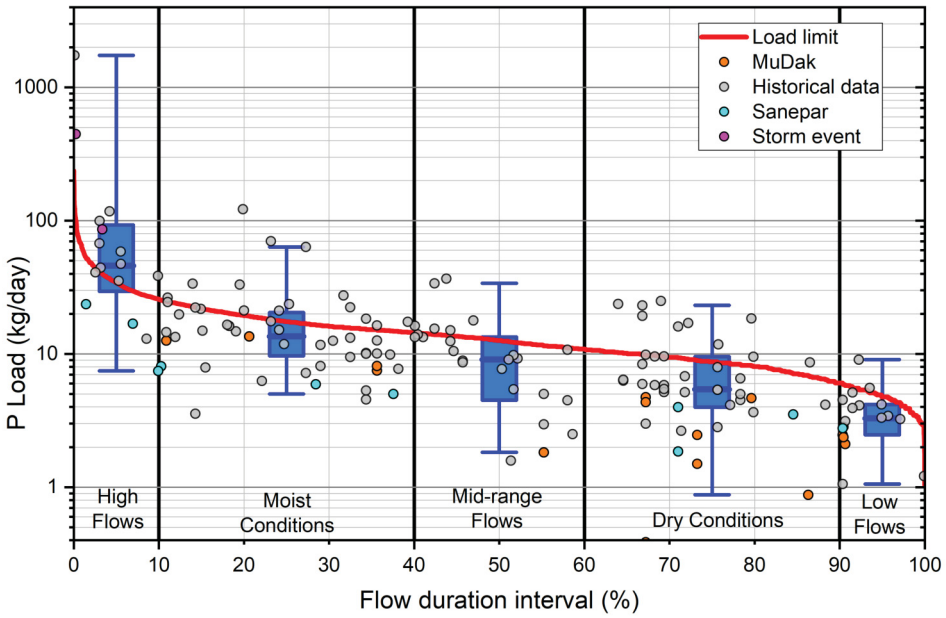

Figure 57 – Phosphorus load (kg/day) observed distributed in ranges of hydrological conditions. Red line indicates maximum permissible load for Total Phosphorus calcuted based on CONAMA Resolution nº 357:2005 for rivers class 1 and 2 threshold (0.10 mg TP/L). Different scatter colors represent sources of data.

sediment and pollutants to stream systems.

Load duration curves approach not only is a useful tool to verify thresholds attendance, but also is helpful in identifying lack of monitoring data for different flow ranges. Since, load duration curves are relatively easy to develop and presents important data in a very simple's way.

The concentration duration curves approach was also performed by Nzama, Kanyerere and Mapoma (2021) in order to evaluate the quality index of groundwater resources in South Africa. Results revealed that the concentration duration curves application succeeded in groundwater quality reserve limits analysis, providing insight on the percentage of time of exceedance of water quality parameters.

For Passaúna River data is possible to observe that data are missing in conditions of mid-range flows. Furthermore, monitoring efforts also should focus on high flow discharges, such as storm events, since thresholds are exceeded in most measurements performed in this hydrological condition. Indeed, storm events, and associated surface runoff, are the driving mechanism responsible for significant transport of sediments and nonpoint source pollutants, such as phosphorus (EPA, 2007).

However, high flow discharges data are usually difficult to assess, whether by automatic probes (and its calibration), or standard water quality sampling programs. This fact leads to underestimation of long-term nutrient inputs from missing pulses of nutrients during short-term events (BLAEN et al., 2016).

6.4.3.1 Synthetic TP daily series input applied to Unsteady-state estimation to estimate TP concentrations

The TP synthetic series in daily resolution obtained from equations correlating discharge ratio (Q/Qhist) and TP concentrations at Passaúna River, presented in Section 6.4.2, was applied in the unsteady state model to assess the impact of using the synthetic series on simulated concentrations within the reservoir (Figure 58).

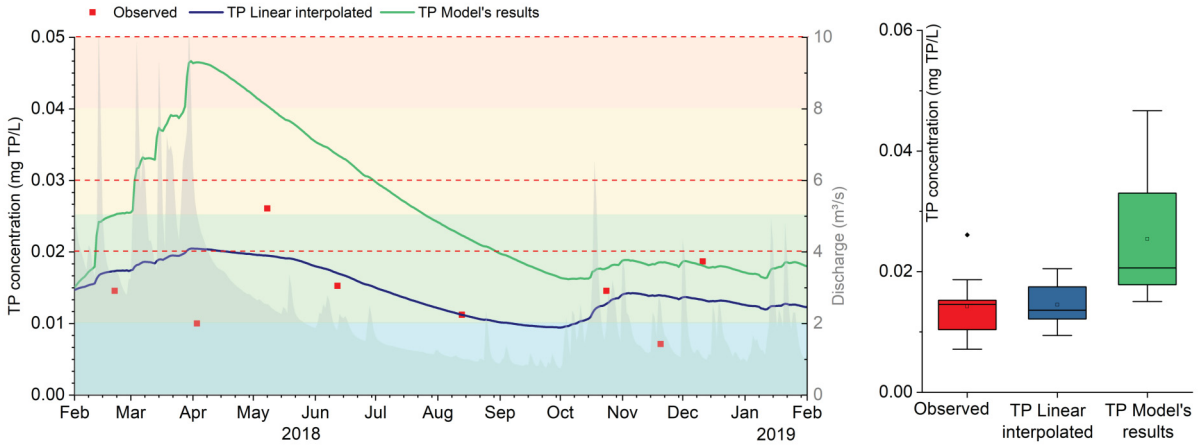

Figure 58 – Time series of TP concentration's simulated with unsteady-state solution using TP synthetic series in daily resolution and measured data at Zone 3 in Passaúna reservoir. Red dashed line represents CONAMA'S thresholds for watercourses class 1 and background colors marks WQIR's threshold for class I (not impacted to very poorly degraded and class 2 (poorly degraded). Time series of discharge [m³/s] in Passaúna river are indicated in grey color.

The same considerations of unsteady state model adopted in simulations in monthly resolution, described in Section 6.3.3 were applied for this daily estimation. For daily simulation, the final TP concentration resulted from the warm up process of 0.018 mg TP/L was adopted as initial condition for the simulated period.

The larger fluctuations from February to April 2018 observed in the TP synthetic series resulted in a response of increasing concentrations tendency from February 1, 2018 to April 1, 2018, when TP concentration reached the peak of 0.0481 mgTP/L. Followed by a decrease trend until mid of October 2018, when TP concentrations stabilize ranging between 0.16 mg TP/L and 0.0189 mg TP/L.

Even though after the warm up period of one year, the application of daily resolution synthetic TP series as input data in the Unsteady-state model did not result in good correspondence with the data measured within the reservoir. This demonstrates that such a solution is more suitable with the application of data with lower temporal resolutions.

6.4.4 Testing optimal monitoring resolutions of Chlorophyll-a and Total Phosphorus using percentage of occurrence analysis

An investigation of optimal monitoring resolutions was carried out with Chl-a and TP data in high temporal resolution.

6.4.4.1 Chlorophyll-a data from platform equipped with optical sensors providing continuous monitoring

In order to assess optimal monitoring resolutions, using data from measurements with time resolution of 15 minutes (presented in Chapter 6.2, Section 6.2.2), five series of chlorophyll-a concentrations were created to simulate measurements on daily, weekly, monthly, bimonthly, and quarterly resolutions (Figure 59). All created data series started with measurement performed on March 1st. Additional data positions followed measurements frequency corresponding to week, month, bimester and four-month period.

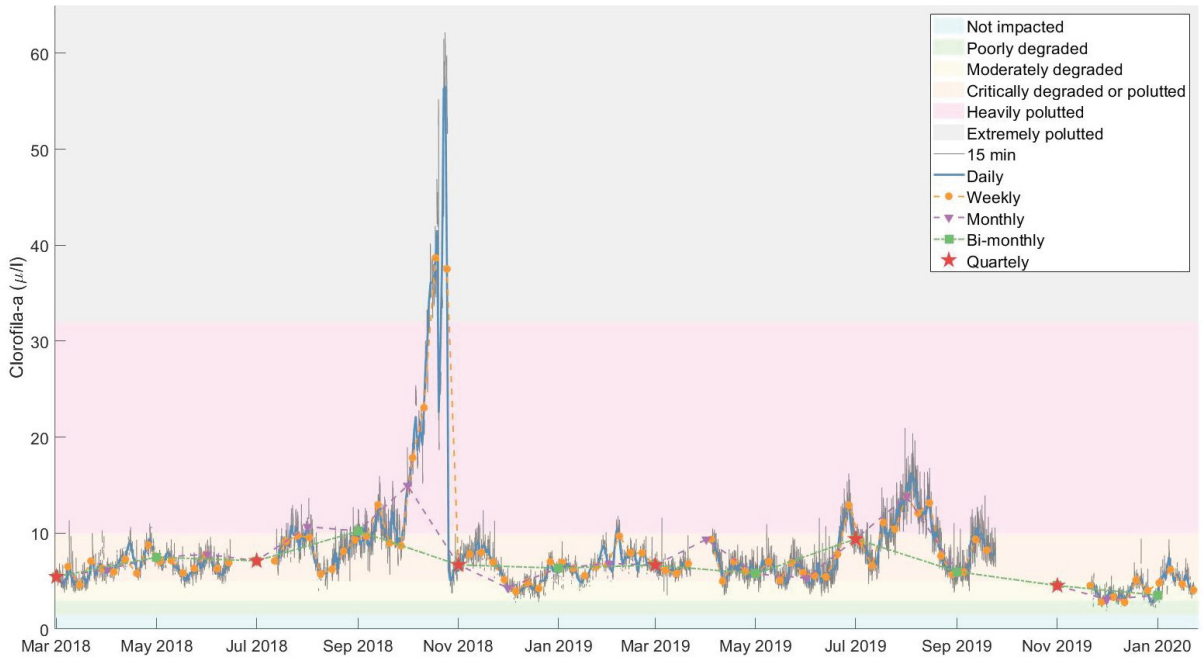

Figure 59 – Time series of chlorophyll-a (Chl-a, μg/L) measurements and synthetic data series in hourly, weekly, monthly, bimonthly and quarterly temporal resolutions. The background colors marks the threshold for WQIR's classifications (see legend).

As expected, data in higher measurement frequencies (15 minutes, daily and weekly) represents better variability and peaks of Chla-a concentrations. The highest concentration recorded reached 62.16 µg/L on October 2018, within the range for WQIR's 'extremely polluted' status. Additionally, a concentration peak of 30.4 µg/L was observed at August 2019, within the range for WQIR's 'very polluted' classification.

For the same period, DOC concentration peaks were also analyzed in the study developed by Bernardini (2019). Likewise, Chl-a concentration peaks were also identified in the monitoring carried out by the IAP (2017) characterized as blooms, in which large algae densities occurred in spring.

Mean values does not present significant variation regardless of the temporal resolution, remaining in the 'critically degraded or polluted' WQIR's classification, Figure 60. However, a slight decreasing trend in mean values was observed in accordance with the measurements frequency reduction, ranging from 6.64 µg/L in quarterly data resolution to 8.40 µg/L in 15 minutes measurements data. This indicates that lower monitoring frequencies may underestimate concentration values.

Similarly, monitoring data carried out by the IAP (2017) with biannual measurements performed from 2005 to 2013 resulted in mean concentration of 5.10 µg/L.

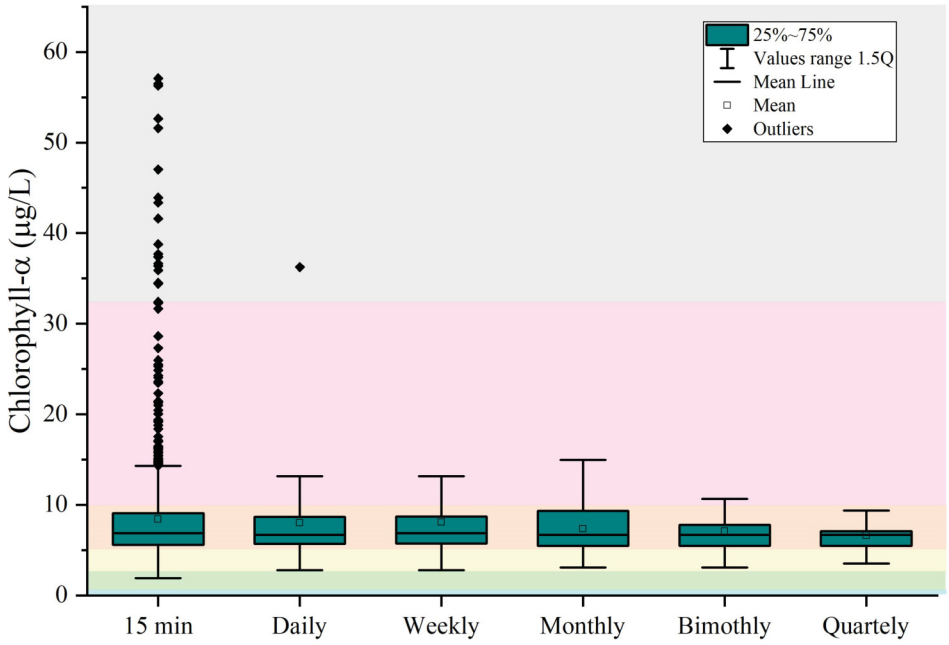

Figure 60 – Variations of chlorophyll-a (Chl-a, μg/L) concentrations of daily, weekly, monthly, bimonthly and quarterly temporal resolutions data series. The background colors marks the threshold for WQIR's classifications.

Additionally, to assess whether the monitoring frequency of chlorophyll-a interferes in the reservoir classification, an analysis of percentage of occurrence for WQIR classification was performed, Figure 61.

Throughout the monitored period, Chl-a concentrations mostly ranged into 'critically degraded or polluted' WQIR's classification. With the exception of monthly resolution data, the above-mentioned classification percentage of occurrence tended to increase as lower the temporal resolution. Furthermore, the quarterly data resolution

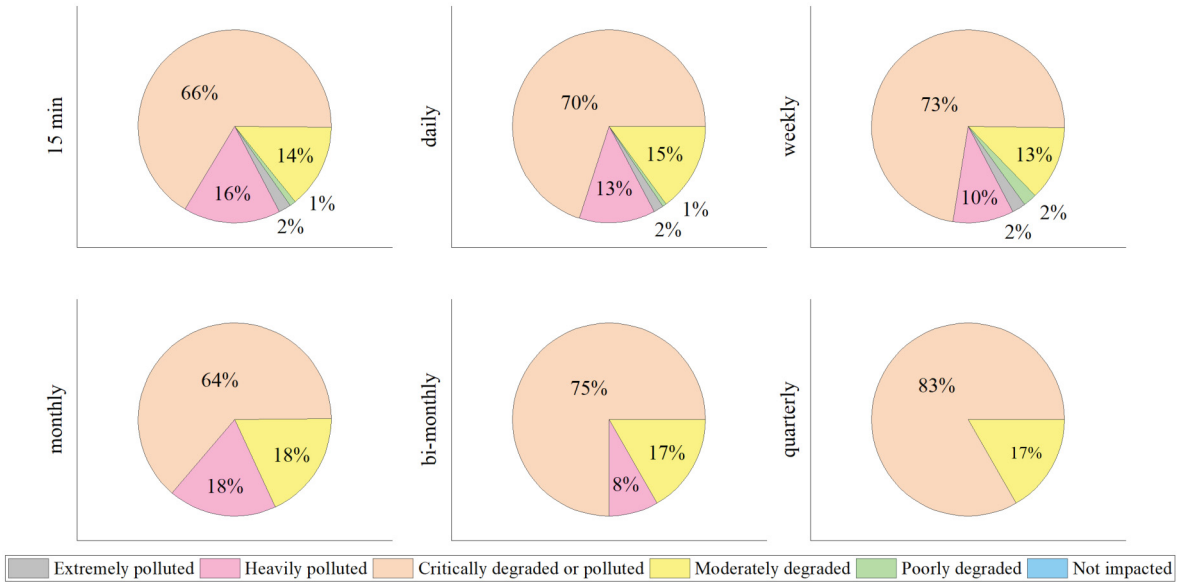

Figure 61 – Percentage of occurrence for Water Quality Index of Reservoirs (WQIR) classification of chlorophyll-a (Chl-a, μg/L) concentrations measurements with 15 minutes of time resolution and data series in daily, weekly, monthly, bimonthly and quarterly temporal resolutions. WQIR ranges are indicated with different colors (see legend).

series had an absence of data classified as 'critically degraded or polluted' (class IV, WQIR's classification).

The algae bloom event measured on October, 2018 which classified the environment as extremely polluted represent only 2% of the classification frequency and were identified in the original measurements data, daily and weekly data resolutions. The same was observed with measurements in 'poorly degraded' classification. Such a result means that frequency resolutions lower than monthly are not sufficient to identify maximum and minimum limits recorded in measurements with high temporal resolution.

Chl-a concentrations from monitoring campaigns performed by IAP (2017) ranged from 0 µg/L to 14.21 µg/L, with most measurements classifying reservoir's water as 'Critically degraded or polluted' in 37.5% of the measurements, followed by 25% in 'moderately polluted', poorly degraded (18.75%), not impacted (12.5%) and heavily polluted (6.25%).

Variability identified in 15 minutes and daily resolution series indicates that measurement date can be decisive in classifying the reservoir's WQIR status.

Even though there is no change in the degradation classification level due to adoption of different temporal resolutions, results show that a bimonthly frequency monitoring chlorophyll-a concentrations is more suitable for control and preventive management of water quality purposes. The use of spectral technology sensors for chlorophyll-a concentrations, once validated and calibrated to the study environment, proved to be a viable, practical and fundamental tool for preventive management

purposes.

Lastly, changes on Chl-a concentrations at the intake monitoring site does not seems to be forced by inflows discharge variability, but internal process. The same was observed by Ishikawa et al. (2022b), using numerical simulations in a three-dimensional hydrodynamic model to assess the influence of density currents on Chl-a dynamics. The authors results revealed little influence on Chl-a concentrations in downstream reservoirs regions due to main inflow dynamics.

6.4.4.2 TP data from Unsteady-state simulations using TP daily synthetic series as input

An investigation of optimal monitoring resolutions of TP was carried out using the same approach applied for Chl-a data, presented in Section 6.4.4. Based on TP synthetic series in daily resolution, four data series were created to simulate measurements on weekly, monthly, bimonthly, and quarterly resolutions, Figure 62. The 'Observed' data series is composed by TP concentrations measured at Zone 3 of Passaúna reservoir, from February 2018 to January 2019 almost monthly.

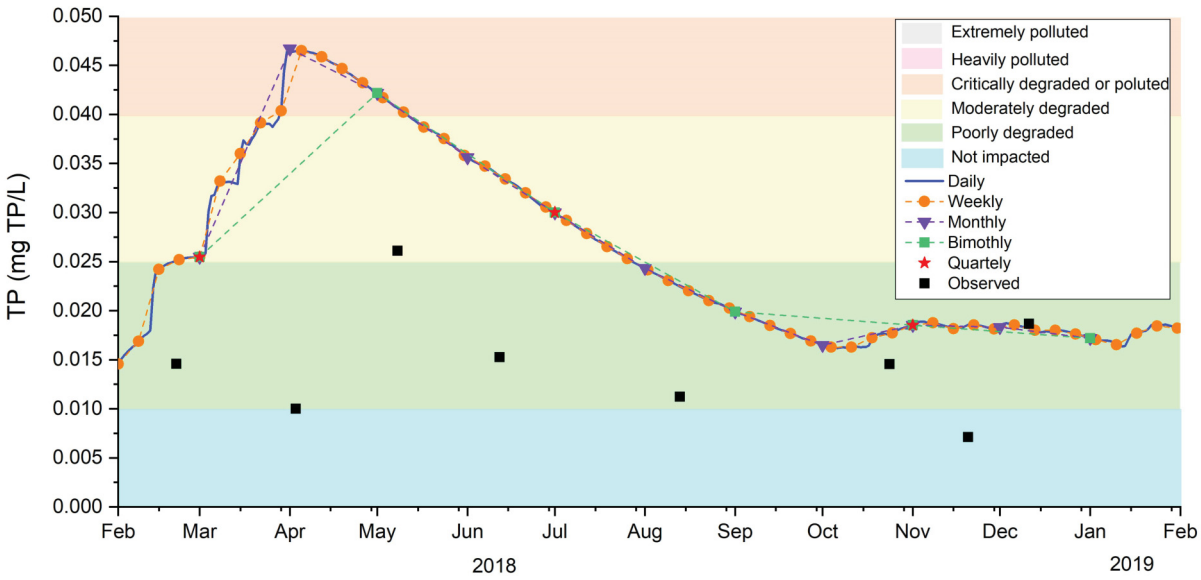

Figure 62 – Time series of TP measurements and synthetic data series in daily, weekly, monthly, bimonthly and quarterly temporal resolutions. Red dashed line represents CONAMA'S thresholds for watercourses class I. The background colors marks the threshold for WQIR's classifications (see legend).

Different than observed of Chl-a data, measured by optical sensors, TP concentrations were obtained from correlation with discharge data, and did not presented strong variability. As a consequence, measurement date is not decisive in classifying the deterioration level of the reservoir for TP concentrations.

Not only in mean values, but also maximum and minimum did not present significant variation from bimonthly to daily data, Figure 63. Mean values of quarterly to daily data remained in WQIR's classification class 2, poorly degraded. Similarly was

observed for measured data mean, although with much smaller value (0.014 mg TP/L). The single noted difference was that in quarterly data series, in which no data ranged WQIR's classification class IV (critically degraded or polluted) as observed for weekly, monthly, and bimonthly series.

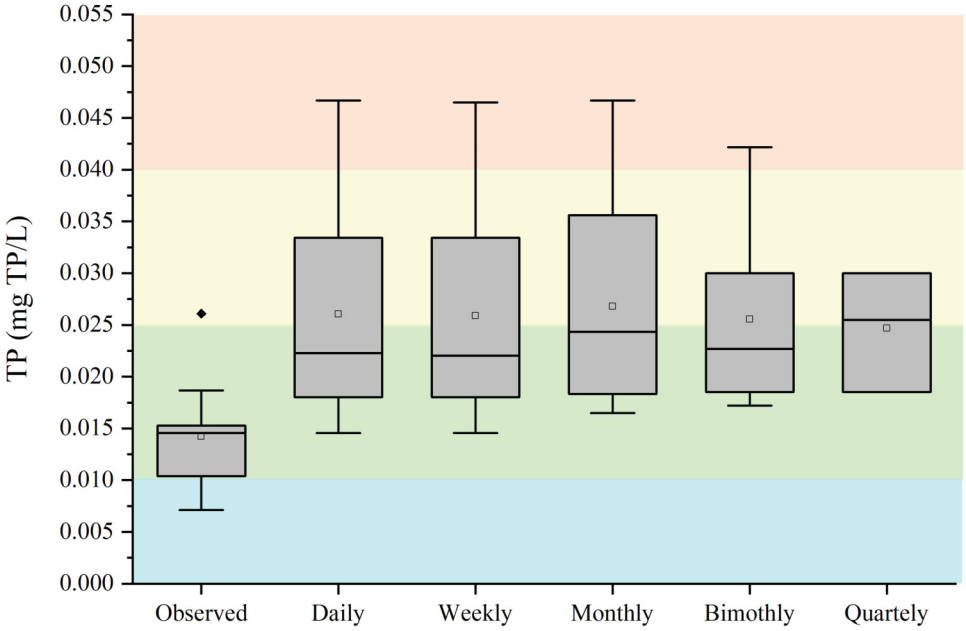

Figure 63 – Variations of Total Phosphorus concentration (TP, mg TP/L) measurements and synthetic data series in daily, weekly, monthly, bimonthly and quarterly temporal resolutions. The background colors marks the threshold for WQIR's classifications.

Throughout the monitored and simulated period, TP concentrations data mostly ranged in 'poorly degraded' WQIR's classification (class 2). WQIR's percentage of occurrence reveled to be similar not only between daily and weekly resolutions, but also between monthly and bi-monthly data, as represent in Figure 64. WQIR's classification class I (not impacted) was observed in measured TP series only, with 11% of occurrence. Nevertheless, for the observed data series, the bigger percentage of occurrence percentage in WQIR's classification class 2 (poorly degraded) was identified, of 77.8%.

The most evident discrepancy noted comparing the weekly, monthly, bimonthly, and quarterly data series was the absence of data classified as 'critically degraded or polluted' (WQIR's classification class IV) in quarterly resolution. As a result, the evaluation performed for TP synthetic series also results in a recommendation of bimonthly frequency monitoring of TP concentrations for control and preventive management of water quality purposes, likewise conclude for Chl-a optimal monitoring resolutions investigation.

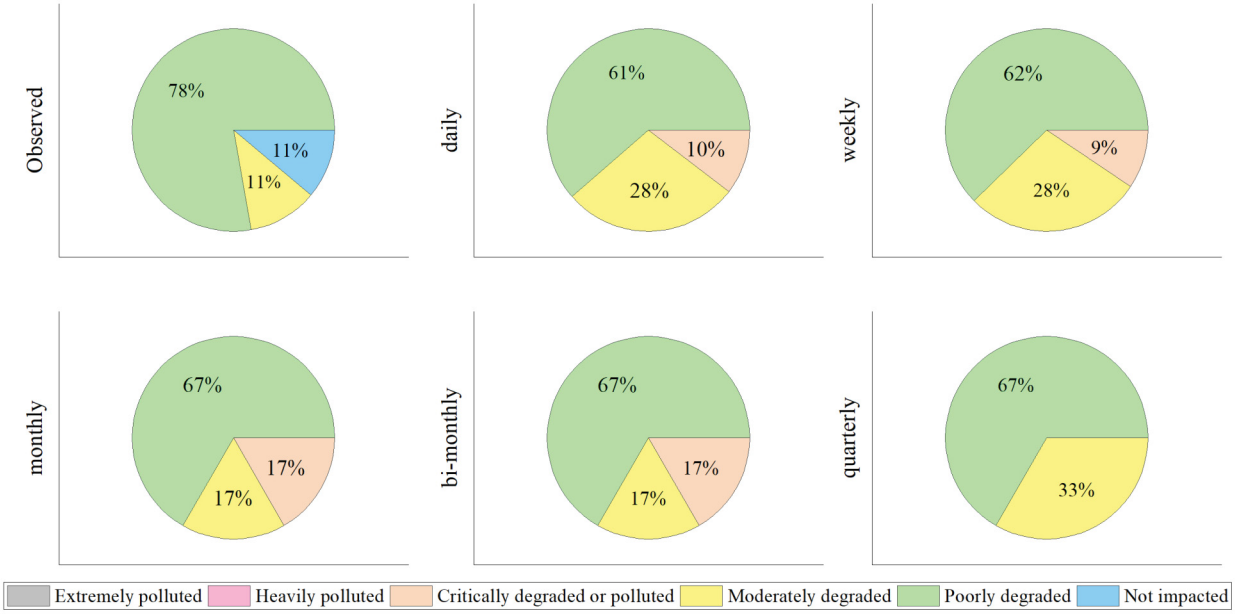

Figure 64 – Percentage of occurrence for Water Quality Index of Reservoirs (WQIR) classification of Total Phosphorus concentration (TP, mg TP/L) measurements and synthetic data series in daily, weekly, monthly, bimonthly and quarterly temporal resolutions. WQIR ranges are indicated with different colors (see legend).

6.4.5 Summary

In this study, some strategies to optimize monitoring resolutions of water quality preventive management are proposed based on temporal and spatial dynamics observed during field monitoring, and further evaluation of results from modeling applications.

Firstly, the integration of spatial-temporal water quality dynamics in the monitoring period was observed using comparative maps, to answer questions related to "What" and "Where", since displays changes in time and space of the variables monitored. Evaluation of this approach showed that the monitoring site and date of sample collection could be decisive in defining ecological water quality status.

Passaúna river's inflow was revealed to play an important role, influencing Total phosphorus concentrations in the upstream region of the reservoir. Therefore, to assess reliable TP concentration in defining ecological status, this variable should be monitored in the upstream region of the reservoir and at the Passaúna's river, especially during high flows, and storm events.

As storm water sampling programs requires substantial planning and resources, an possible alternative is the use of automated equipment, in which a sample strategy can be developed to achieve measurements at high, medium, and low flows. It is not the aim of this study to determinate sampling strategy using automated storm event sampling, since this was already performed in form of flowchart by other authors (HARMEL; KING; SLADE, 2003; HARMEL et al., 2006).

Since Total Inorganic Nitrogen concentrations were mostly classified as 'Critically degraded or polluted', and presented considerably high concentrations, this variable should be monitored at least seasonally.

Secondly, load duration curves analysis, using historical and monitored total phosphorus data measured at Passaúna River, was evaluated in order to identify potential effects of storm events on water quality conditions and answer questions related to "When" monitoring should take place.

Monitoring efforts should focus on high flow discharges, such as storm events, since thresholds are exceeded in most measurements performed in this hydrological condition. Additionally, monitoring should take place at mid-range flows (from 3.6 m^3/s to 5.4 m^3/s), since lack of TP concentration data was observed at Passaúna River for this discharge range.

Thirdly, an evaluation of effects in TP input loading due to storm events was performed, by improving the temporal resolution of the TP data series for Passaúna River associated with discharge data in daily resolution. The created synthetic series was applied as input data in the zero-dimensional model, as steady and unsteady state conditions.

This investigation results revealed that, since phosphorus concentrations are usually low during base flow, monitoring efforts could be substantially reduced, and monitoring campaigns should focus on storm events, in order to achieve more realistic phosphorus input calculations. TP monitoring at the main tributary during mid-range and high flows provides more information regarding TP load input than the higher frequency at a large number of locations during base flow.

Quarterly temporal resolutions of monitoring data TP would be an optimal resolution for monitoring Passaúna's reservoir for modeling purpose, considering 0-dimensional models. However, since longitudinal gradients were strong along Passaúna's reservoir, indicating that to properly access more reliable results in estimating phosphorus concentrations within Passaúna reservoir, at least models in 2-dimensions are necessary.

Monitoring TP concentration when discharge is above 3.6 m^3/s could be fulfilled the gap found in TP measurements and improve equations results in correlating discharge ratio with TP concentrations.

Lastly, investigations of changes in the ecological status of Chl-a (from optical sensor's measurements) and TP (from unsteady state application in daily resolution), in order to answer "How many" data should be monitored through quantification of ecological status variability.

Variability identified in 15 minutes and daily resolution of Chl-a data series

indicates that measurement date can be decisive in classifying the reservoir's WQIR status. Even though there is no change in the degradation classification level due to the adoption of different temporal resolutions, results shows that a bimonthly frequency monitoring chlorophyll-a concentrations is more suitable for control and preventive management of water quality purposes.

Table 20 presents a summary of outcomes, advantages, and drawbacks according to each one of the optimal monitoring strategies.

Table 20 – Summary of outcomes, advantages, and drawbacks from the application of optimal spatio-temporal design of Passaúna's reservoir water quality monitoring system.

Questions	When	What and where	When	How many	How many
Strategies	Unsteady-state approach with daily TP concentration	Graphic in map	Load Duration Curves Approach	Chlorophyll-a testing optimal resolutions	TP testing optimal resolutions
Outcomes	- Quarterly frequency monitoring TP concentrations; - TP concentration should be monitored when discharge is above 3.6 m^3/s.	- TP monitoring at least seasonally upstream and during storm events and at inflow site; - TN monitoring at least seasonally, due to considerable high concentrations.	- Mid-range flows; - High flow discharges (such as storm events), since thresholds are exceeded in most measurements performed in this hydrological condition.	- Bimonthly frequency monitoring chlorophyll-a concentrations	- Monthly frequency monitoring of TP concentrations
Advantages	- Models represents a useful tool to simulate TP concentration when no data is available.	- Overall water quality assessment integrating time and space; - Simple approach that integrate temporal and spatial dynamics.	- Easy to develop and understand; - Integrates qualitative and quantitative aspects of hydrological conditions; - It is useful to evaluate compliance with regulation standards; - Identification of lack of monitoring data for different flow ranges.	- Already Listed in Section 5.1.3	- Daily series considering storm events, and more reliable and not underestimated values of TP in several discharge ranges.
Drawbacks	- The application of daily resolution synthetic TP series as input data in the Unsteady-state model did not result in good correspondence with the data measured within the reservoir. - 0-Dimensional unsteady state input data did not work well for daily input data.	- Lack of measurements data, make it impossible to obtain reliable characterization of seasonally variations; - Chl-a classification did not presented significantly seasonally or spatially variations on WQIR, but it was missclassificated.	- Historical data are necessary; - Concentrations at several hydrological conditions are necessary.		- Data series from created synthetic series, that must be improved with mid-range flow data.

7 Final Remarks: Conclusions, and Recomendations for Further Work and Research

7.1 Conclusions and Outlook

Monitoring reservoirs is essential to identify fluctuations and trends in water quality dynamics, which varies influenced by human activities such as changes in land use, agriculture and urbanization. The employment of field-deployable automated analyzers can contribute in this sense, providing data in high temporal resolution.

In situ installed probes are able to provide real-time measurements with high-quality data and time resolution. This is almost impossible by conventional methods. However, some limitation of this method should be noted as correction equations that need to be applied or built-in within the sensor system.

In addition, it is also important to emphasize that the use of this technology requires specialized labor for maintenance and repair, when it is necessary. Moreover, for different environments, the equipment must be calibrated through comparisons with results obtained by conventional methods.

This thesis results revealed that the use of spectral technology sensors once validated and calibrated to the environment, proved to be a viable, practical and fundamental tool for preventive management purposes.

On the hand, the usage of models is not only limited to sample collection at several locations and depth to provide enough information as input and calibration data, but also is limited by the challenge faced by mathematical models in representing very complex environments dynamics influenced by an interrelation of several processes changing in time and space. Therefore, less complex models can be usuful in quantifying the relevance on considering spatial variation in water quality monitoring programs.

Some remarks about optimal resolutions for modeling are that although the application of steady-state solution resulted in annual means compatible with phosphorus measured along reservoir, through this application it is not possible to observe fluctuations and trends in water quality variations. In this sense, solutions such as unsteady state could be useful to better represent the water quality dynamics in a preventive water resources management.

Concerning unsteady state modeling applications, an important point to be observed is the location of monitoring sites, since data observed in the lacustrine region most closely resembles concentrations at the outflow. Steady-state is recommended for overall annual TP concentration assessment, while unsteady state application is more

suitable for monthly temporal resolution.

The use of different discharge data series influences in a significant way mass balance phosphorus input. Therefore, special attention must be given to the data series that will be used to feed input data into mass balance calculations.

Moreover, the investigations of optimize monitoring resolutions revealed that Passaúna river's inflow play an important role, influencing Total Phosphorus concentrations at upstream region of the reservoir. Therefore, to assess reliable TP concentration in defining ecological status and to achieve more realistic phosphorus input calculations, TP concentrations should be monitored at upstream region of the reservoir and at Passaúna river's, especially during high flows, and storm events. Such an approach can significantly reduced monitoring campaigns along the year.

Longitudinal gradients were strong along Passaúna's reservoir, indicating that to properly access more trustworthy results in estimating phosphorus concentrations within Passaúna reservoir, at least models in 2-dimensions are necessary.

Finally, variability identified Chl-a data series indicates that measurement date can be decisive in classifying the reservoir's WQIR status. Results show that a bimonthly frequency monitoring chlorophyll-a concentrations is more suitable for control and preventive management of water quality purposes.

The results found in this study emphasize the importance of preventive monitoring investigations to guarantee the necessary water quality for water supply, but also demonstrate the importance of managing the basin as a whole.

As noted, the water quality of the reservoir has been deteriorating in recent years, and the results of monitoring, and modeling through scenarios, can serve as tools to guide possible developments in the basin, controls, and necessary actions.

Monitoring, and assessing historical and spatial trends serve as important indicators to identify and determine important developments, which can influence the water quality status of the reservoir.

Further investigations must be performed to better understand and represent Passaúna reservoir water quality dynamics concerning to compartmentalization of the reservoirs and phosphorus mobilization process.

7.2 Recommendations

Based on monitoring Passaúna's reservoir experience and findings from this thesis, a potential flow chart indicating optimal monitoring strategies is proposed (Figure 65). The flow chart is a comprehensive method developed in this study to be applied in dammed reservoirs located in subtropical environments, providing guidelines

for the implementation of water quality monitoring programs for water supply reservoirs.

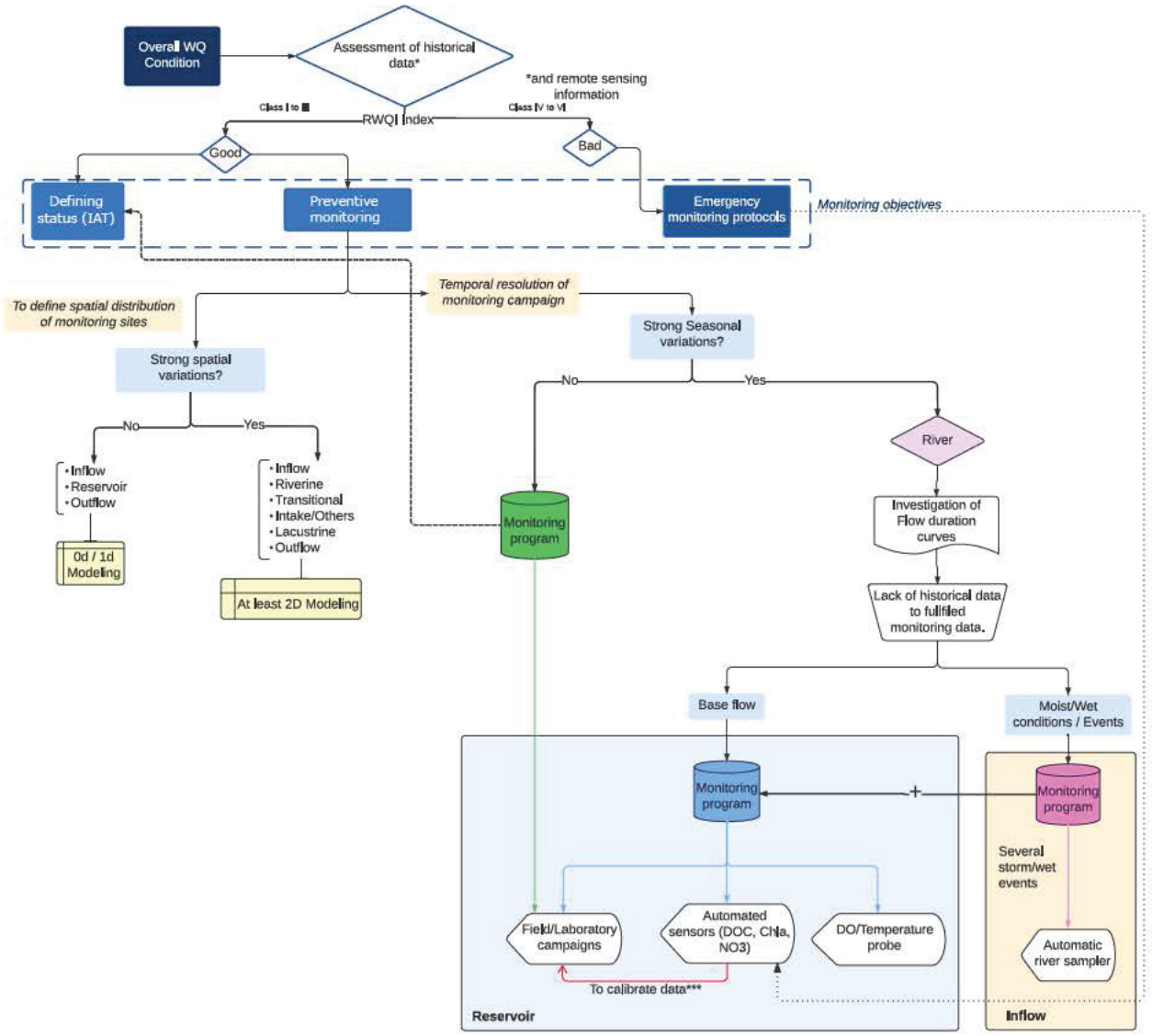

Figure 65 – Potential flow chart indicating optimal monitoring strategies from monitoring Passaúna's reservoir experience and findings from this thesis.

Here is important to highlight a few aspects of Passaúna's reservoir features, which led to thesis findings, and possibly can differ for applications in other environments. Passaúna's reservoir is a man-made water supply reservoir, medium-sized, located in a tropical region and climate region characterized as Cfb, humid subtropical with temperate summer, according to the Koeppen-Geiger classification system.

As expected for a water supply reservoir, Passaúna's water quality presented general good conditions. Reservoirs built for different purposes or even in not-so-good trophic state conditions will probably present higher nutrient concentrations, and consequently algal bloom events can occur.

If located in tropical climates, the reservoir may present latent and more accelerated eutrophication processes. In such a case, nutrients quantification and other variables analyzed in the laboratory do not represent challenges and the need to concentrate samples due to low concentrations, as occurred for the Passaúna reservoir. Therefore, water quality monitoring is recommended at high temporal resolution with automated probes to check trends in an attempt to predict a worsening event in water quality.

Yet about specific characteristics of the study site of this thesis, Passaúna's reservoir is located in a basin with agricultural influence and with urban occupation increase in recent years. Watershed marked by greater urban occupation may present different characteristics related to the organic matter and nutrient input loads in the reservoir, which may be function not only due to discharge flow variations.

There are also specificities regarding the reservoir shape, residence time and tributaries. Passaúna's reservoir entrance is marked by a pre-reservoir, which provides a buffer effect for loads and temperature variations in the reservoir. Reservoirs with narrower formats and without the presence of pre-reservoirs should present more accelerated reactions due to changes in tributary load, or even storm events.

In addition, the Passaúna River is the only main tributary of the reservoir, making the division of regions with concentration gradients more obvious, and making it easier to monitor the entrance, which may not be the reality of many other reservoirs.

The predominant soil type is also a determinant for water quality, as well the influence of groundwater, factors that can result in different water quality variables characteristics than those observed in this study.

Reservoirs with periods of drought and flood, such as those found in the Brazilian semi-arid region, will also possibly present different characteristics of nutrient loads Therefore, the strategies adopted in this study should be adapted for such a situation.

It should also be noted that for purpose of both assessing historical data and checking on strong spatial variations, remote sensing information could be very useful. Therefore, this strategy is reccomend in future studies to improve the aforementioned flow chart tool.

Due to the mentioned conditions, it is recommended the application of this flow chart in different environments with different shapes, sizes, and contributions for further adequation.

Bibliography

ALLION, K.; KIEMLE, L.; FUCHS, S. Four Years of Sediment and Phosphorus Monitoring in the Kraichbach River Using Large-Volume Samplers. *Water (Switzerland)*, v. 14, n. 1, 2022. 152

ALMEIDA, R. G. B. de et al. Spatial optimization of the water quality monitoring network in São Paulo State (Brazil) to improve sampling efficiency and reduce bias in a developing sub-tropical region. *Environmental Science and Pollution Research*, Environmental Science and Pollution Research, v. 29, n. 8, p. 11374 11392, 2022. ISSN 16147499. 66, 67

ALVARES, C. A. et al. Köppen's climate classification map for Brazil. *Meteorologische Zeitschrift*, v. 22, n. 6, p. 711 728, 2013. ISSN 16101227. 85

ANA. *Water Resources Notebook - 1: Overview of Surface Water Quality in Brazil (Panorama da Qualidade das Águas Superficiais no Brasil)*. [S.l.: s.n.], 2005. 179 p. ISBN 8589629066. 67, 69

APHA, A. P. H. A. *Standard Methods for the examination of water and wastewater*. [S.l.: s.n.], 2006. v. 20 Edition. ISBN 0470082127. 40, 43, 44, 45, 46, 47, 49, 100

AQUAREAD. *Instruction Manual for Aquaprobe AP-700, AP-800 & AP-2000*. Kent, 2017. 141 p. 102

ARAUJO, M. et al. Mathematical modelling of hydrodynamics and water quality in a tropical reservoir, northeast Brazil. *Braz. J. Aquat. Sci. Technol*, v. 12, n. (1), p. 19 30, 2008. 27, 74, 135

ASADOLLAHFARDI, G. et al. Optimization of water quality monitoring stations using dynamic programming approach, a case study of the Mond Basin Rivers, Iran. *Environment, Development and Sustainability*, Springer Netherlands, v. 23, n. 2, p. 2867 2881, 2021. ISSN 15732975. 66

AYRES, S. K. *A Simulation of the Mississippi River Salt Wedge Estuary Using a Three-Dimensional Cartesian Z Coordinate Model*. Tese (Doutorado) Texas Tech University, 2015. 78

BALLANCE, J. B.; RICHARD; RICHARD. *Water Quality Monitoring - A Practical Guide to the Design and Implementation of Freshwater Quality Studies and Monitoring Programmes*. [S.l.: s.n.], 1996. pp.348 p. 39, 50, 56, 63

BARRETO, N. P. *Avaliação do grau de trofia e variação de fitoplânctons em reservatório de abastecimento de água: estudo de caso Passaúna/PR*. 142 p. Tese (Doutorado) Federal University of Parana, 2020. 89, 90, 92, 93, 103, 111, 137

BECKER, A. C. C. *Zero-dimensional modelling and total maximum daily loads as tools for reservoir water quality planning and management*. 81 p. Tese (Doutorado) Federal University of Paraná, 2021. 115

BENDER, M. A. et al. Phosphorus dynamics during storm events in a subtropical rural catchment in southern Brazil. *Agriculture, Ecosystems and Environment*, v. 261, n. April, p. 93 102, 2018. 152

BERNARDINI, G. F. *Utilização de sensores óticos in-situ no monitoramento da matéria utilização de sensores óticos in-situ no monitoramento da matéria Curitiba-PR*. 80 p. Tese (Trabalho de Conclusão de Curso) Federal University of Paraná, 2019. 89, 133, 161

BEVERIDGE, D. et al. A geostatistical approach to optimize water quality monitoring networks in large lakes: Application to Lake Winnipeg. *Journal of Great Lakes Research*, Elsevier B.V., v. 38, n. SUPPL. 3, p. 174 182, 2012. ISSN 03801330. 66

BIANEK, J.; MANNICHI, M. Aplicação de curvas de permanência de qualidade da água para a bacia do Rio Passaúna - PR. In: *XXIV Simpósio Brasileiro de Recursos Hídricos*. Belo Horizonte - MG: [s.n.], 2021. p. 1 10. 119

BIGGS, T. W.; DUNNE, T.; MARTINELLI, L. A. Natural controls and human impacts on stream nutrient concentrations in a deforested region of the Brazilian Amazon basin. *Biogeochemistry*, v. 68, n. 2, p. 227 257, 2004. ISSN 01682563. 40

BLAEN, P. J. et al. Real-time monitoring of nutrients and dissolved organic matter in rivers: Capturing event dynamics, technological opportunities and future directions. *Science of The Total Environment*, v. 569-570, p. 647 660, 2016. 74, 135, 158

BOCALON, T. S. *Estudos de sedimentos do rio Passaúna, com ênfase na determinação de metais pesados*. 99 p. Tese (Doutorado) Centro Universitário Positivo (UnicenP), 2007. 88

BOULANGE, J. et al. Role of dams in reducing global flood exposure under climate change. *Nat Commun*, Springer US, v. 12, n. 417, 2021. 32

BROWN, R. et al. Water quality index-do we dare? *Water Sewage Works*, v. 117, n. (10), p. 339 343, 1970. 52

BURT, T. P. et al. Long-term monitoring of river water nitrate: how much data do we need? *J. Environ. Monit.*, Royal Society of Chemistry, v. 12, n. 1, p. 71 79, jan 2010. 44

BURT, T. P. et al. Nitrate in United Kingdom rivers: Policy and its outcomes since 1970. *Environmental Science and Technology*, v. 45, n. 1, p. 175 181, 2011. 44

BUSCH, O. M. S. O. M. S. M. S. *Qualidade da água e saúde humana: riscos potenciais face ao processo de ocupação urbana no entorno da represa do Passaúna - Curitiba PR*. 277 p. Tese (Doutorado) Federal University of Paraná, 2009. 88

CADE-MENUN, B. J.; NAVARATNAM, J. A.; WALBRIDGE, M. R. Characterizing dissolved and particulate phosphorus in water with 31P nuclear magnetic resonance spectroscopy. *Environmental Science and Technology*, v. 40, n. 24, p. 7874 7880, dec 2006. ISSN 0013936X. 49

CAMARA, M. et al. Economic and efficiency based optimisation of water quality monitoring network for land use impact assessment. *Science of the Total Environment*, v. 737, 2020. ISSN 18791026. 66

Canadian Council of Ministers of the Environment. *A Canada-wide Framework for Water Quality Monitoring*. [S.l.], 2006. 29 p. 59, 61

Canadian Council of Ministers of the Environment (CCME). *Guidance manual for optimizing Water Quality Monitoring Program design*. [S.l.], 2015. 58, 59, 63, 65

CANALE, R. P.; SEO, D.-I. Performance, reliability and uncertainty of total phosphorus models for lakes - I. Stochastic Analyses. *Wat. Res*, v. 30, n. 95, p. 95 102, 1996. 78

CARLSON, R. E. A trophic state index for lakes. *Limnological Reserach Center*, p. 361 369, 1977. 52

CARNEIRO, C.; KELDERMAN, P.; IRVINE, K. Assessment of phosphorus sediment water exchange through water and mass budget in Passaúna Reservoir (Paraná State, Brazil). *Environmental Earth Sciences*, Springer Berlin Heidelberg, v. 75, n. 7, p. 1 12, 2016. ISSN 18666299. 88, 138, 139, 140, 141

CARSTEA, E. M. et al. In situ fluorescence measurements of dissolved organic matter: A review. *Science of the Total Environment*, Elsevier B.V., v. 699, p. 134361, 2020. 74

CATHERINE, A. et al. On the use of the FluoroProbe, a phytoplankton quantification method based on fluorescence excitation spectra for large-scale surveys of lakes and reservoirs. *Water Research*, v. 46, p. 1771 1784, 2012. 51

ÇELIK, K. The relationships between chlorophyll - A dynamics, certain physical and chemical variables in the temperate eutrophic Çaygören Reservoir, Turkey. *Iranian Journal of Fisheries Sciences*, v. 12, n. 4, p. 789 801, 2013. ISSN 15622916. 26

CETESB. *Qualidade das águas interiores no estado de São Paulo 2019*. [S.l.: s.n.], 2020. 336 p. ISBN 9786555770117. 69

CETESB, C. A. D. E. D. S. P. *L5.306: Determinação de Clorofila a e Feofitina a: método espectrofotométrico*. 2014. 14 p. 101

CHAPMAN, D. *Water Quality Assessments - A Guide to Use of Biota, Sediments and Water in Environmental Monitoring* -. [S.l.: s.n.], 1996. Second Edi. 609 p. ISSN 00219193. 33, 36, 37, 38, 39, 41, 43, 44, 45, 46, 47, 48, 49, 50, 52, 56, 57, 58, 60, 61, 63, 70

CHAPRA, S. C. *Surface water-quality modeling*. Boston: WCB McGraw-Hill, 1997. 844 p. 33, 38, 39, 43, 45, 47, 57, 77, 79, 80, 111, 114, 115, 141

CHAPRA, S. C.; RECKHOW, K. H. Expressing the Phosphorus Loading Concept in Probabilistic Terms. *Journal of the Fisheries Research Board of Canada*, v. 36, n. 2, p. 225 229, 1979. 79

CHAPRA, S. C.; TARAPCHAK, S. J. A chlorophyll a model and its relationship to phosphorus loading plots for lakes. *Water Resources Research*, v. 12, n. 6, p. 1260 1264, 1976. ISSN 19447973. 79

CHEN, P. et al. Detection of water quality parameters in Hangzhou Bay using a portable laser fluorometer. *Marine Pollution Bulletin*, Elsevier Ltd, v. 93, n. 1-2, p. 163 171, 2015. 51

CHEN, Q. et al. Optimization of water quality monitoring network in a large river by combining measurements, a numerical model and matter-element analyses. *Journal of Environmental Management*, v. 110, p. 116 124, 2012. ISSN 03014797. 56

CHEN, Y.; HAN, D. Water quality monitoring in smart city: A pilot project. *Automation in Construction*, Elsevier, v. 89, n. June 2017, p. 307 316, 2018. ISSN 09265805. 66

CHOI, M. M. F.; XIAO, D. Oxygen-sensitive reverse-phase optode membrane using silica gel-adsorbed ruthenium (II) complex embedded in gelatin film. *Analytica Chimica*, Acta 387, p. 197 2005, 1999. 72

CLELAND, B. R. Tmdl Development From the "Bottom Up" Part Iii: Duration Curves and Wet-Weather Assessments. *Proceedings of the Water Environment Federation*, n. 4, p. 1740 1766, 2003. ISSN 19386478. 157

COALIAR, C. d. B. d. A. I. e. A. d. A. R. *Resolução nº 04, de 11 de julho de 2013*. 2013. 86

CONAMA. *CONAMA 357 Classificação corpos d'água*. 2005. 43, 45, 46, 116, 117, 124, 125, 127, 133, 134, 144, 155

CONCEIÇÃO, J. R. da. *Metodologia para identificação de áreas prioritárias para redução da erosão hídrica em bacias de mananciais de abastecimento público do Paraná: Estudo de Caso Bacia do Passaúna*. 94 p. Tese (Doutorado) Universidade Federal do Paraná, 2014. 87

COQUEMALA, V. *Variação anual do fitoplâncton no reservatório Passaúna, Paraná*. 92 p. Tese (Doutorado) Universidade Federal do Paraná, 2005. 26, 32, 87, 88, 111, 137

CORAGGIO, E. et al. Water Quality Sampling Frequency Analysis of Surface Freshwater: A Case Study on Bristol Floating Harbour. *Frontiers in Sustainable Cities*, v. 3, n. January, p. 1 14, 2022. 61

CUNHA, D. G. F.; CALIJURI, M. d. C.; MENDIONDO, E. M. Integração entre curvas de permanência de quantidade e qualidade da água como uma ferramenta para a gestão eficiente dos recursos hídricos. *Engenharia Sanitaria e Ambiental*, v. 17, n. 4, p. 369 376, 2012. ISSN 14134152. 119

DALU, T.; WASSERMAN, R. J. Cyanobacteria dynamics in a small tropical reservoir: Understanding spatio-temporal variability and influence of environmental variables. *Science of the Total Environment*, Elsevier B.V., v. 643, p. 835 841, dec 2018. ISSN 18791026. 26

DIAS, L. N. *Estudo Integrado da bacia hidrográfica do reservatório Passauna (Araucária - Paraná - Brasil), considerando a interrelação da ocupação dos solos com a qualidade das águas*. 153 p. Tese (Doutorado) Universidade de São Paulo, 1997. 88

DILLON, P. J.; RIGLER, F. H. The phosphorus-chlorophyll relationship in lakes. *Limnol. Oceanog*, v. 19, n. 5, p. 767 773, 1974. 79

DODDS, W. K.; WHILES, M. R. *Freshwater ecology*. [S.l.: s.n.], 2019. 1 981 p. ISBN 9780128132555. 79, 111, 126, 127

DRUMMOND, S. B. M. *Análise Temporal de Poluentes Difusos no Rio Passaúna por Meio da Utilização de Amostrador Automático*. Tese (Doutorado) Federal University of Paraná, 2020. 89, 156

DRUMMOND, S. B. M. et al. Evolução do uso e ocupação do solo na bacia hidrográfica do Rio Passaúna (1990 2017). *XXIII Simpósio Brasileiro de Recursos Hídricos*, p. 1 10, 2019. 87

EPA. An Approach for Using Load Duration Curves in the Development of TMDLs. *U.S. Environmental Protection Agency*, p. 68, 2007. 120, 158

ESTEVES, F. d. A. *Fundamentos de Limnologia*. Rio de Janeiro: [s.n.], 1998. 602 p. 26, 34, 38, 42, 43, 46, 47, 48, 49, 50, 125, 134

ETHERIDGE, A. B. Evaluation of Total Phosphorus Mass Balance in the Lower Boise River, Southwestern Idaho. p. 82, 2013. Disponível em: . 80

European Communities. *Common Implementation Strategy for the water framework directive (2000/60/EC), Guidance Document No 7. Monitoring under the Water Framework Directive. Policy Summary to Guidance No. 7. With assistance of Produced by Working Group 2.7 - Monitoring*. [S.l.], 2003. 58

FEPAM. *Relatório Da Qualidade Da Água Superficial Do Estado Do Rio Grande Do Sul*. [S.l.], 2020. 69

FERRARESI, A. C. d. S. *Macroinvertebrados como indicadores de qualidade de água no reservatório do Rio Passaúna, PR, Brasil*. 101 p. Tese (Doutorado) Universidade Positivo, 2015. 50, 51, 88

FILHO, L. V. d. S. *Qualidade e percepção ambiental: estudo de caso da bacia hidrográfica do Rio Passaúna*. 210 p. Tese (Doutorado) Universidade Federal do Paraná, 2010. 87, 88

FORMIGONI, Y. et al. Análise Crítica da Curva de Permanência de Qualidade da Água Com Base em Dados Históricos. *XIX Simpósio Brasileiro de Recursos Hídricos*, p. 1 14, 2011. 119

FRANZEN, M. *Dinâmica do fósforo na interface água-sedimento em reservatórios*. 244 p. Tese (Doutorado) Federal University of Rio Grande do Sul, 2009. 26

GILLIOM, R. J.; ALLEY, W. M.; GURTZ, M. E. Design of the National Water-Quality Assessment Program: occurrence and distribution of water-quality conditions. *US Geological Survey Circular*, v. 1112, 1995. ISSN 03646017. 61

GODOY, R. B. Dinâmica da qualidade da água em reservatório de abastecimento público: estudo de caso do Passaúna - PR. 2017. 89

GOLYJESWSKI, O. W. *Simulation of thermal stratification using the a 2DV (CE-QUAL-W2) and a 3D (Delft3D) model. The case study: Passaúna reservoir*. 72 p. Tese (Doutorado) Federal University of Paraná, 2020. 110

GRUDZIEN, J. P. *Utilização de amostrador automático experimental para a identificação do aporte de poluentes no Rio Passaúna*. 139 p. Tese (Doutorado) Universidade Federal do Paraná, 2019. 89

HARMANCIOGLU, N.; OZKUL, S.; ALPASLAN, M. *Water Quality Monitoring Network Design*. [S.l.: s.n.], 1999. 290 p. 56, 61, 63

HARMEL, R. D. et al. Practical guidance for discharge and water quality data collection on small watersheds. *American Society of Agricultural and Biological Engineers*, v. 49, n. 4, p. 937 948, 2006. 165

HARMEL, R. D.; KING, K. W.; SLADE, R. M. Automated storm water sampling on small watersheds. *Applied Engineering in Agriculture 2003*, v. 19, n. 6, p. 667 674, 2003. 165

HAVENS, K. E.; JAMES, R. T. The phosphorus mass balance of lake okeechobee, Florida: Implications for eutrophication management. *Lake and Reservoir Management*, v. 21, n. 2, p. 139 148, 2005. ISSN 10402381. 79

HAYES, N. M. et al. Key differences between lakes and reservoirs modify climate signals: A case for a new conceptual model. *Limnology And Oceanography Letters*, v. 2, n. 2, p. 47 62, 2017. ISSN 23782242. 34

HEM, J. D. *Study and interpretation of the chemical characteristics of natural water*. Department. [S.l.: s.n.], 1985. ISSN 01479563. 58

HENNEMANN, M. C.; PETRUCIO, M. M. Seasonal phytoplankton response to increased temperature and phosphorus inputs in a freshwater coastal lagoon, Southern Brazil: a microcosm bioassa. *Acta Limnologica Brasiliensia*, v. 22, n. 3, p. 295 305, 2010. 51

HORIBA. *Multi water quality checker U-50 series*. [S.l.], 2009. 35 p. 102

HORNE, A. J.; GOLDMAN, C. R. *Limnology*. United States of America: Mc Graw Hill, 1994. 576 p. 34, 35, 36, 37, 38, 39, 40, 41, 47, 48, 49, 50

HORTON, R. An index number system for rating water quality. *J. Water Pollu. Cont. Fed.*, v. 37, n. (3), p. 300 306, 1965. 52

IAP. *Qualidade das Águas Rios da Bacia do Alto Iguaçu, na Região Metropolitana de Curitiba, 2005 a 2009*. [S.l.], 2009. 114 p. 54, 55, 87, 117

IAP. *Monitoramento da qualidade das águas dos reservatórios do Estado do Paraná no período de 1999 a 2013*. [S.l.], 2017. 119 p. 41, 54, 69, 85, 89, 90, 91, 92, 148, 149, 161, 162

ISHIKAWA, M.; BLENINGER, T.; LORKE, A. Hydrodynamics and mixing mechanisms in a subtropical reservoir. *Inland Waters*, Taylor & Francis, v. 11, n. 3, p. 286 301, 2021. 110

ISHIKAWA, M. et al. Effects of dimensionality on the performance of hydrodynamic models for stratified lakes and reservoirs. *Geoscientific Model Development*, v. 15, n. 5, p. 2197 2220, 2022. ISSN 19919603. 110, 147

ISHIKAWA, M. et al. Hydrodynamic Drivers of Nutrient and Phytoplankton Dynamics in a Subtropical Reservoir. *Water (Switzerland)*, v. 14, n. 1544, 2022. 89, 148, 150, 163

JIANG, D. et al. Evaluating the spatiotemporal variations of nutrients and their effects on Chl-a using deviation rate method in a stratified reservoir. *Water Science and Technology: Water Supply*, v. 18, n. 4, p. 1173 1182, 2017. 26, 40, 46

JIANG, J. et al. A comprehensive review on the design and optimization of surface water quality monitoring networks. *Environmental Modelling and Software*, Elsevier Ltd, v. 132, n. June, p. 104792, 2020. ISSN 13648152. 56, 58, 65, 66, 70

JIMENEZ, N. et al. A methodology for the design of quasi-optimal monitoring networks for lakes and reservoirs. *Journal of Hydroinformatics*, v. 7, n. 2, p. 105 116, 2005. ISSN 1464-7141. 27, 65, 66, 74, 135

KALFF, J. *Limnology: inland water ecosystems*. [S.l.: s.n.], 2001. ISBN 0-13-033775-7. 32, 33, 34, 41, 48

KHALIL, B.; OUARDA, T. B. Statistical approaches used to assess and redesign surface water-quality-monitoring networks. *Journal of Environmental Monitoring*, v. 11, n. 11, p. 1915 1929, 2009. 63, 66

KLEEMOLA, S. *Manual for integrated monitoring*. [S.l.: s.n.], 1998. v. 2000. 46 p. ISBN 9514775783. 56, 64

KNAPIK, H. G. *Organic matter characterization and modeling in polluted rivers for water quality planning and management*. Tese (Doutorado) Federal University of Paraná, Curitiba, 2014. 42, 43

KNAPIK, H. G.; FERNANDES, C. V. S.; AZEVEDO, J. C. R. D. Caracterização E Monitoramento De Matéria Orgânica Em Rios : Aplicabilidade Na Gestão De Recursos Hídricos Orgânic Matter Characterization and Monitoring in Surface Waters : Applicabitlity on Water Resources. p. 1 8, 2013. 43

KNOWLTON, M. F.; JONES, J. R. Temporal variation and assessment of trophic state indicators in missouri reservoirs: Implication for lake monitoring and management. *Lake and Reservoir Management*, v. 22, n. 3, p. 261 271, 2006. 27, 74

KRISTENSEN, P.; BOGESTRAND, J. *Surface Water Quality Monitoring*. [S.l.: s.n.], 1996. 82 p. ISBN 9291670014. 67

KRÖCKEL, L. et al. Spectral optical monitoring of nitrate in inland and seawater with miniaturized optical components. *Water Research*, v. 45, n. 3, p. 1423 1431, 2011. 40

LAMPARELLI, M. C. *Graus de trofia em corpos d'água do estado de São Paulo: avaliação dos métodos de monitoramento*. Tese (Doutorado) University of São Paulo, 2004. 53, 90, 91, 92

LEE, C.; PAIK, K.; LEE, Y. Optimal sampling network for monitoring the representative water quality of an entire reservoir on the basis of information theory. *Journal of Water and Climate Change*, v. 5, n. 2, p. 151 162, 2014. ISSN 20402244. 65

LEHNER, B. et al. High-resolution mapping of the world's reservoirs and dams for sustainable river-flow management. *Frontiers in Ecology and the Environment*, v. 9, n. 9, p. 494 502, nov 2011. ISSN 15409295. 26, 32

LEITHOLD, J. et al. Quali-quantitative characterization of organic matter in urbanized drainage basins as a basis for the application of Water Resources Management Instruments. *RBRH*, FapUNIFESP (SciELO), v. 22, n. 0, oct 2017. 42, 43

LOPES, S. M.; ARRUDA, N. M. B.; PAGIORO, T. A. Study of the stratification process at the reservoir of the hydroelectric power plant Gov. Pedro Viriato Parigot de Souza (Capivari-Cachoeira), Paraná, Brazil. *Eclética Química Journal*, v. 43, p. 23 31, 2018. 38

LOUCKS, D. P.; BEEK, E. van. *Water resources systems planning and management*. Unesco pub. [S.l.: s.n.], 2005. ISBN 9231039989. 34

LOVETT, G. M. et al. Who needs environmental monitoring? *Frontiers in Ecology and the Environment*, v. 5, n. 5, p. 253 260, 2007. 59

MARCÉ, R. et al. Automatic High Frequency Monitoring for Improved Lake and Reservoir Management. *Environmental Science and Technology*, v. 50, n. 20, p. 10780 10794, 2016. ISSN 15205851. 56, 57, 134, 135, 148

MARCON, L. High temporal resolution measurement of ebullition in a subtropical reservoir. p. 99, 2018. 89

MAYMANDI, N.; KERACHIAN, R.; NIKOO, M. R. Optimal spatio-temporal design of water quality monitoring networks for reservoirs: Application of the concept of value of information. *Journal of Hydrology*, Elsevier B.V., v. 558, p. 328 340, 2018. 65, 66

MEGER, D. G. *Material particulado suspenso e macroconstituintes iônicos em um reservatório de abastecimento: o caso do rio Passaúna, Curitiba, Paraná, Brasil*. 145 p. Tese (Doutorado) Centro Universitário Positivo (UnicenP), 2007. 88

MERCANTE, C. T. J.; TUCCI-MOURA, A. A Comparação Entre os Indices de Carlson e de Carlson Modificado Aplicados a Dois Ambientes Aquáticos Subtropicais.". *Acta Limnológica Brasiliensia*, A, n. 11 (1), p. 1 14, 1999. 53

MHLANGA, L.; MHLANGA, W.; MWERA, P. The application of a phosphorus mass balance model for estimating the carrying capacity of Lake Kariba. *Turkish Journal of Veterinary and Animal Sciences*, v. 37, n. 3, p. 316 319, 2013. 79

MOREIRA, A. C. P. et al. Aplicação de índices de qualidade de água IQA para o monitoramento dos mananciais de abastecimento público da região metropolitana de Curitiba, Paraná, Brasil. In: *Congresso ABES - FENASAN 2017*. [S.l.: s.n.], 2017. p. 1 14. 90, 91, 92, 117

MOURA, D. S. et al. Internal loading potential of phosphorus in reservoirs along a semiarid watershed. *RBRH*, FapUNIFESP (SciELO), v. 25, 2020. ISSN 1414-381X. 147

MULLIGAN, M.; SOESBERGEN, A. V.; SÁENZ, L. GOODD , a global dataset of more than 38 , 000 georeferenced dams. *Sci. Data*, v. 7, n. 31, 2020. 32

NADIM, F. et al. Application of a steady-state nutrient model and inferences for load reduction strategy in two public water supply reservoirs in eastern connecticut. *Lake and Reservoir Management*, v. 23, n. 3, p. 264 278, 2007. ISSN 10402381. 155

NIKOO, M. R. et al. Stakeholder engagement in multi-objective optimization of water quality monitoring network, case study: Karkheh Dam reservoir. *Water Science and Technology: Water Supply*, v. 17, n. 4, p. 966 974, 2016. ISSN 16069749. 66

NOWAK, J. *Investigation of internal phosphorus loading in the Passauna reservoir*. Tese (Doutorado) Karlsruher Institute of Technology, 2018. 144, 146

NÜRNBERG, G. K. Quantification of internal phosphorus loading in polymictic lakes. *Verh. Internat. Verein. Limnol.*, Informa UK Limited, v. 29, p. 623 626, 2005. ISSN 0368-0770. 147

NURNBERG, G. K. Assessing internal phosphorus load - Problems to be solved. *Lake and Reservoir Management*, v. 25, n. 4, p. 419 432, 2009. ISSN 07438141. 145

NZAMA, S. M.; KANYERERE, T. O.; MAPOMA, H. W. Using groundwater quality index and concentration duration curves for classification and protection of groundwater resources: relevance of groundwater quality of reserve determination, South Africa. *Sustainable Water Resources Management*, Springer International Publishing, v. 7, n. 3, p. 1 11, 2021. ISSN 23635045. 158

OLC. *Course 3 - Water Quality Monitoring and Assessment*. [S.l.]: Water Quality Assessment. UNESCO-IHE Institute for Water Education, 2014. 56 p. 66

OLIVEIRA, D. M. et al. Estudo da estratificação e oxiredução de carbono na coluna de água do reservatório do Passaúna Curitiba , Brasil. *Xxi Congreso Chileno Ingenieria Sanitaria Y Ambiental - Viii Congreso Iv Región Aidis*, IX, p. 1 5, 2015. 26

ONO, G. M. *Monitoramento e análise da sedimentação no Reservatório Passaúna-PR*. 90 p. Tese (Doutorado) Federal University of Paraná, 2020. 89, 145, 146

PEREIRA, R. d. S. *Processos que regem a qualidade da água da lagoa dos patos, segundo o modelo Delft3D*. Tese (Doutorado) Fundation Federal University of Rio Grande, 2003. 77, 78

PITRAT, D. M. J. J. *Avaliação da contaminação por metais em rios: estudo de caso da bacia do Rio Passaúna*. Tese (Doutorado) Federal University of Paraná, Curitiba, 2010. 88

POLONSCHII, C.; GHEORGHIU, E. A Multitiered Approach for Monitoring Water Quality. In: *Energy Procedia*. [S.l.]: Elsevier Ltd, 2017. v. 112, p. 510 518. ISSN 18766102. 70

POONAM, T.; TANUSHREE, B.; SUKALYAN, C. water Quality Indices - Important tools for water quality assessment: A review. *International Journal of Advances in Chemistry*, v. 1, n. 1, p. 15 29, 2013. 51, 52

POURSHAHABI, S. et al. Spatio-Temporal Multi-Criteria Optimization of Reservoir Water Quality Monitoring Network Using Value of Information and Transinformation Entropy. *Water Resources Management*, Water Resources Management, v. 32, n. 10, p. 3489 3504, 2018. ISSN 15731650. 66

PRADO, L. L. *Procedimentos analíticos aplicados na análise de fósforo. Amostras de reservatórios, rios e águas com pH > = 8,3*. Curitiba - PR, 2018. 11 p. 101

RAUEN, W. B.; CASTRO, C. O. D.; SILVA, M. G. D. Caracterização hidrossedimentológica do Rio Passaúna, PR, Brasil, a partir de dados históricos. In: *XX Simpósio Brasileiro de Recursos Hídricos*. Florianópolis: [s.n.], 2017. p. 8. 88

RAUEN, W. B. et al. Index-based and compliance assessment of water quality for a brazilian subtropical reservoir. *Engenharia Sanitaria e Ambiental*, v. 23, n. 5, p. 841 848, 2018. 90, 92, 117

REID, A. J. et al. Emerging threats and persistent conservation challenges for freshwater biodiversity. *Biol. Rev.*, v. 94, p. 849 873, 2019. 32

RICKWOOD, C. J.; CARR, G. M. Development and sensitivity analysis of a global drinking water quality index. *Environmental Monitoring and Assessment*, v. 156, n. 1-4, p. 73 90, 2009. 52

RIPL, W. Water : the bloodstream of the biosphere. *Phil. Trans. R. Soc. Lond. B*, v. 358, n. November, p. 1921 1934, 2003. 32

ROUSSO, B. Z. et al. Light-induced fluorescence quenching leads to errors in sensor measurements of phytoplankton chlorophyll and phycocyanin. *Water Research*, v. 198, p. 117133, 2021. 108, 135

SADEGHIAN, A. et al. Improving in-lake water quality modeling using variable chlorophyll a/algal biomass ratios. *Environmental Modelling and Software*, v. 101, p. 73 85, 2018. 26, 51

SALAS, H. J.; MARTINO, P. A simplified phosphorus trophic state model for warm-water tropical lakes. *Wat. Res.*, v. 25, n. 3, p. 341 350, 1991. ISSN 00951137. 53, 143

SALES, G. G. N. *Water quality modeling in a subtropical water supply reservoir*. 89 p. Tese (Doutorado) Federal University of Paraná, 2020. 89, 110

SAUNITTI, R. M.; FERNANDES, L. A.; BITTENCOURT, A. V. L. Estudo do assoreamento do reseravatorio da barragem do Rio Passauna, Curitiba, PR. *Boletim Paranaense de Geociencias*, v. 54, p. 65 82, 2004. 26, 87, 88

SCHNOOR, J. L. *Environmental modeling. Fate, and transport of pollutants in water, air, and soil.* [S.l.]: Wiley Interscience, 1996. 81

SEMA. *Boletim Qualiágua SC - Monitoramento da qualidade das águas vertente litorânea de Santa Catarina*. [S.l.], 2020. 69

SENER, S.; SENER, E.; DAVRAZ, A. Evaluation of water quality using water quality index (WQI) method and GIS in Aksu River (SW-Turkey). *Science of The Total Environment*, Elsevier, v. 584-585, p. 131 144, 2017. 52

SENGUPTA, M.; DALWANI, R. Determination of Water Quality Index and Suitability of an Urban Waterbody in Shimoga Town, Karnataka. In: *The 12th World Lake Conference*. [S.l.: s.n.], 2008. p. 342 346. 51

SERRANO, L. d. O. et al. A new approach to use load duration curves to evaluatewater quality: A study in the Doce River Basin, brazil. *Water (Switzerland)*, v. 12, n. 3, p. 1 21, 2020. ISSN 20734441. 119

SHIN, Y.-H.; Teresa Gutierrez-Wing, M.; CHOI, J.-W. Review Recent Progress in Portable Fluorescence Sensors. *Journal of The Electrochemical Society*, IOP Publishing, v. 168, n. 1, p. 017502, 2021. ISSN 0013-4651. 71, 72

SILVA, T. et al. Comparison of cyanobacteria monitoring methods in a tropical reservoir by in vivo and in situ spectrofluorometry. *Ecological Engineering*, v. 97, p. 79 87, 2016. ISSN 09258574. 26, 51, 135

SINGH, J. et al. Water Pollutants : Origin and Status. *Sens Water Pollut Monit Role Mater*, Springer Singapore, 2020. 32

SMAHA, N.; GOBBI, M. F. Implementação de Um Modelo para Simular a Eutrofização do Reservatório do Passaúna - Curitiba PR. *Revista Brasileira de Recursos Hídricos*, v. 8, n. iii, p. 59 69, 2003. 88, 111, 150

SOKOLOV, D. I. et al. Choosing the optimal frequency of water quality monitoring on tributaries of a lowland reservoir. *Limnology and Freshwater Biology*, v. 2020, n. 4, p. 697 698, 2020. 64

SØNDERGAARD, M.; JENSEN, J. P.; JEPPESEN, E. *Role of sediment and internal loading of phosphorus in shallow lakes*. [S.l.], 2003. v. 506, 135 145 p. 147

SØNDERGAARD, M. et al. Using chlorophyll a and cyanobacteria in the ecological classification of lakes. *Ecological Indicators*, v. 11, n. 5, p. 1403 1412, 2011. ISSN 1470160X. 134

SONTEK. *CastAway CTD User's Manual 1.5*. San Diego, 2012. 34 p. 102

SORENSEN, J. P. R. et al. Online fluorescence spectroscopy for the real-time evaluation of the microbial quality of drinking water. *Water Research*, v. 137, p. 301 309, 2018. 51

SOTIRI, K. *A multi-frequency echo-sounding method for sediment analysis in Lake Passauna , Brazil*. Tese (Doutorado) Karlsruher Institute of Technology, 2016. 89

SOTIRI, K. et al. *Assessment of Phosphorus Input from Urban Areas in the Passaúna River and Reservoir*. 2022. 89, 139, 147

SOUZA, C. F. de. *Fotodegradação da matéria orgânica em um reservatório de abastecimento público em clima temperado úmido (cfb): estudo de caso do reservatório do Passaúna/PR, Brasil*. Tese (Doutorado) Federal University of Paraná, 2020. 89

SPERLING, M. V. *Estudos e modelagem da qualidade da água de rios*. Belo Horizonte - MG: [s.n.], 2007. 588 p. ISBN 85-88556-07-2. Disponível em: <www.desa.ufmg.br>. 34, 47, 48, 52, 53

SREBOTNJAK, T. et al. A global Water Quality Index and hot-deck imputation of missing data. *Ecological Indicators*, v. 17, p. 108 119, jun 2012. 52

STEDMON, C. A. et al. A potential approach for monitoring drinking water quality from groundwater systems using organic matter fluorescence as an early warning for contamination events. *Water Research*, Elsevier Ltd, v. 45, n. 18, p. 6030 6038, 2011. 72

STEINHART;, C. E.; SCHIEROW;, L.; SONZOGNI, W. C. Environmental Quality Index for the Great Lakes. *Water Resour. Bull.*, Vol.18, n. No. 6, p. 1025 1031, 1982. 52

STOREY, M. V.; GAAG, B. van der; BURNS, B. P. Advances in on-line drinking water quality monitoring and early warning systems. *Water Research*, Elsevier Ltd, v. 45, n. 2, p. 741 747, 2011. 26, 70, 135

STRASKRABA, M.; TUNDISI, G. *Guidelines of Lake Management: Reservoir Water Quality Management*. [S.l.: s.n.], 1999. v. 9. 229 p. ISBN 4906356265. 61, 63

STRASKRABA, M.; TUNDISI, J. G.; DUNCAN, A. *Comparative Reservoir Limnology and Water Quality Management*. [S.l.: s.n.], 1993. 213 288 p. 35, 39, 51

STROBL, R. O.; ROBILLARD, P. D. Network design for water quality monitoring of surface freshwaters: A review. *Journal of Environmental Management*, v. 87, n. 4, p. 639 648, 2008. ISSN 03014797. 59, 61, 62, 63, 66

SUHETT, A. L. et al. O Papel da Foto-Degradação do Carbono Orgânico Dissolvido (COD) nos Ecossistemas Aquáticos. *Oecologia Brasiliensis*, v. 10, n. 02, p. 186 204, 2006. ISSN 19806442. 43, 44

TALEBBEYDOKHTI, N. et al. Review of Reservoir Water Quality Monitoring and Modelling. In: *Long-Term Behaviour and Environmentally Friendly Rehabilitation Technologies of Dams*. [S.l.: s.n.], 2017. ISBN 9783851255645. 57

TEMINO-BOES, R. et al. Anthropogenic impact on nitrification dynamics in coastal waters of the Mediterranean Sea. *Marine Pollution Bulletin*, Elsevier Ltd, v. 145, p. 14 22, 2019. 46

THOMANN, R. V.; MUELLER, J. A. *Principles of Surface Water Quality Modeling and Control*. Harper & r. [S.l.: s.n.], 1987. 61, 79

THOMAS, O.; BAURÈS, E.; POUET, M. F. UV spectrophotometry as a non-parametric measurement of water and wastewater quality variability. *Water Quality Research Journal of Canada*, v. 40, n. 1, p. 51 58, 2005. ISSN 12013080. 43

TONÉ, A. J. d. A. *Análise e modelagem de fósforo em reservatórios localizados em regiões semiáridas*. Tese (Doutorado) Federal University of Ceará, 2016. 35, 115, 143

TORRES, C. et al. Evaluation of sampling frequency impact on the accuracy of water quality status as determined considering different water quality monitoring objectives. *Environmental Monitoring and Assessment*, Springer International Publishing, v. 194, n. 7, 2022. ISSN 15732959. 58, 63

TRAUTMANN, N. M.; MCCULLOCH, C. E.; OGLESBY, R. T. Statistical Determination of Data Requirements for Assessment of Lake Restoration Programs. *Can. J. Fish. Aquat. Sci.*, v. 39, p. 607 610, 1982. 65

TRIOS, M. *nanoFlu - Operating Instructions*. [S.l.], 2017. 43 p. 73, 106

TRIOS, M. *OPUS - Operating Instructions*. [S.l.], 2017. 57 p. 105, 106, 107, 108, 109

TUNDISI, J. *Impactos ecológicos da construção de represas: aspectos específicos e problemas de manejo*. p.1 76 p. Tese (Doutorado) USP/EESC/CRHEA, 1988. 37, 38

TUNDISI, J. G. Typology of reservoirs in Southern Brazil. *SIL Proceedings, 1922-2010*, Taylor & Francis, v. 21, n. 2, p. 1031 1039, 1981. 39

TUNDISI, J. G.; TUNDISI, T. M. *Limnology*. [S.l.: s.n.], 2011. 870 p. ISBN 9780203803950. 34, 35, 36, 37, 44, 125

TYAGI, S. et al. Water Quality Assessment in Terms of Water Quality Index. *American Journal of Water Resources*, v. 1, n. 3, p. 34 38, 2013. 51, 52

UNEP, U. N. E. P. G. E. M. S. G. P. *Global Drinking Water Quality Index Development and Sensitivity Analysis Report*. Ontario, Canada, 2007. 60 p. 51

UNGARATTI, N. N. *Comparação entre sensores óticos e parâmetros análiticos para a avaliação da qualidade de água no reservatório do Passaúna Curitiba - Paraná*. 70 p. Tese (Trabalho de Conclusão de Curso) Federal University of Paraná, 2019. 89, 134

U.S. Geological Survey. *The Strategy for Improving Water-Quality Monitoring in the United States. Book Final Report of the Intergovernmental Task Force on Monitoring Water Quality*. [S.l.], 1995. 161 p. 58

U.S. Geological Survey. *Guidelines and Standard Procedures for Continuous Water-Quality Monitors - Station Operation , Record Computation , and Data Reporting*. U.s. geolo. [S.l.], 2006. 51 p. 74

U.S. Geological Survey. *Lakes and Reservoirs - Guidelines for Study Design and Sampling Techniques and Methods 9 A10 Supersedes USGS Techniques of Water-Resources Investigations*. U.s. geolo. [S.l.: s.n.], 2018. 48p p. 26, 34, 35, 59, 61, 62, 63, 70, 71, 74, 135

VEIGA, B. V. *Modelagem Computacional do processo de eutrofização e aplicação de um modelo de balanço de nutrientes a reservatórios da região metropolitana de Curitiba*. 248 p. Tese (Doutorado) Federal University of Paraná, 2001. 88

VEIGA, B. V.; DZIEDZIC, M. Estimating nutrient loads in the Passaúna reservoir with FLUX. *Water International*, v. 35, n. 2, p. 210 222, 2010. ISSN 02508060. 77, 78, 87, 139

VIDAL, T. F.; NETO, J. C. Dinâmica de nitrogênio e fósforo em reservatório do semiárido utilizando balanço de massa. *Revista Brasileira de Engenharia Agricola e Ambiental*, v. 18, n. 4, p. 402 407, 2014. 79, 80, 111

VIRTANEN, M. et al. *Three-dimensional water-quality-transport model compared with field observations*. [S.l.], 1986. v. 31, 185 199 p. 77, 78

VOLLENWEIDER, R. A. The scientific basis of lake and stream eu- trophication, with particular reference to phosphorus and nitrogen as eutrophication factors. *Organ. Econ. Coop. Develop.*, Tech. Rep., 1968. 79

VOLLENWEIDER, R. A. Input-output models - With special reference to the phosphorus loading concept in limnology. *Schweizerische Zeitschrift für Hydrologie*, v. 37, n. 1, p. 53 84, 1975. 79

VOLLENWEIDER, R. A. Advances in defining critical loading levels for phosphorus in lake eutrophication. *Memorie dell' Istituto Italiano di Idrobiologia*, v. 33, p. 53 83, 1976. 79, 143

WAGNER, A. *Event-Based Measurement and Mean Annual Flux Assessment of Suspended Sediment in Meso Scale Catchments*. Tese (Doutorado) Karlsruher Institute of Technology, 2019. 89

WALKER, W. W.; HAVENS, K. E. Development and application of a phosphorus balance model for Lake Istokpoga, Florida. *Lake and Reservoir Management*, v. 19, n. 1, p. 79 91, 2003. 79

WATERS, S.; WEBSTER-BROWN, J. G. The use of a mass balance phosphorus budget for informing nutrient management in shallow coastal lakes. *Journal of Hydro-Environment Research*, Elsevier B.V., v. 10, p. 32 49, 2016. 80

WENDT, T. *Aplicação de Modelo Computacional Hidrodinâmico a Jusante de uma Estrutura Hidráulica*. Tese (Doutorado) Federal University of Paraná, Curitiba, 2009. 77

WETZEL, R. G. *Limnology*. Second edi. [S.l.]: Saunders College Publishing, 1983. ISBN 0-03-057913-9. 36, 37, 41, 43, 44, 45, 46, 47, 49, 50

WETZEL, R. G.; LINKENS, G. E. *Limnological analyses*. [S.l.: s.n.], 2000. 429 p. ISBN 0-387-98928-5. 39, 40, 45, 46, 47, 50

WMO. *Planning of Water Quality Monitoring Systems*. [S.l.: s.n.], 2013. 128 p. ISBN 9789263111135. 32, 64, 67, 70, 72, 73

WORSFOLD, P.; MCKELVIE, I.; MONBET, P. Determination of phosphorus in natural waters: A historical review. *Analytica Chimica Acta*, v. 918, p. 8 20, 2016. 47, 48, 74, 75

WOSIACKI, L. F. K. *Surrogate technologies for suspended solid dynamics assessment in surface waters*. Tese (Doutorado) Federal University of Paraná, 2020. 89

WU, Z. et al. Imbalance of global nutrient cycles exacerbated by the greater retention of phosphorus over nitrogen in lakes. *Nature Geoscience*, Springer US, v. 15, n. 6, p. 464 468, 2022. ISSN 17520908. 79, 111

XAVIER, C. d. F. *Avaliação da influência do uso e ocupação do solo e de características geomorfológicas sobre a qualidade das águas de dois reservatórios da região metropolitana de Curitiba Paraná*. 167 p. Tese (Doutorado) Federal University of Paraná, 2005. 85

XU, H. et al. Nitrogen and phosphorus inputs control phytoplankton growth in eutrophic Lake Taihu, China. *American Society of Limnology and Oceanography*, v. 55, p. 420 432, 2010. ISSN 00243590. 48, 51

YANG, K. et al. Spatial and temporal variations in the relationship between lake water surface temperatures and water quality - A case study of Dianchi Lake. *Science of the Total Environment*, Elsevier B.V., v. 624, p. 859 871, 2018. ISSN 18791026. 26, 77

YAO, X. et al. A bibliometric review of nitrogen research in eutrophic lakes and reservoirs. *Journal of Environmental Sciences (China)*, Elsevier B.V., v. 66, p. 274 285, 2018. ISSN 18787320. 26, 44

YENILMEZ, F.; DÜZGÜN, S.; AKSOY, A. An evaluation of potential sampling locations in a reservoir with emphasis on conserved spatial correlation structure. *Environmental Monitoring and Assessment*, v. 187, n. 1, 2015. ISSN 15732959. 65

ZAMYADI, A. et al. *A review of monitoring technologies for real-time management of cyanobacteria: Recent advances and future direction*. [S.l.]: Elsevier B.V., 2016. 83 96 p. 72

ZAREBSKA, Z. *Small scale sediment analysis in a Brazilian reservoir*. 57 p. Tese (Doutorado) Karlsruher Institute of Technology, 2016. 89

ZARFL, C. et al. A global boom in hydropower dam construction. *Aquatic Sciences*, v. 77, n. 1, p. 161 170, 2014. 32

Appendix

APPENDIX A – Monitored Data

Monitored data of Passaúna reservoir assessed along 11 field campaigns performed in monthly interval, from February 2018 until April 2019, in several points distributed within Passaúna reservoir, inflow, and outflow.

Date	Site	Depth	Secchi	pH	DO	Temp	DOC	Chl-a	NH3	NO2	NO3	NT	TON	PO4	PTD	PT	PTP	P Org	Turb.	TS	TSS	TDS
		m	m		mg/L	ºc	mg/L	mg/L	mg/L	mg/L	mg/L	mg/L	mg/L	mg/L	mg/L	mg/L	mg/L	mg/L	(NTU)	mg/L	mg/L	mg/L
21/02/2018	Buffer	0.2				22.43	2.14	10.4	0.04	0.02	1 21	1 57	0.30	0.007	0.020	0.051	0.031	0.014	20.9	139	8	
21/02/2018	Buffer	1.0				21.23	2.09	-2.9	0.04	0.02	1 23	1.46	0.17	0.006	0.005	0.050	0.045	<LLD	23.1	133	9.3	
21/02/2018	Buffer	2.0				20.80	2.45	3.5	0.11	0.02	1 24	1 53	0.17	0.003	0.008	0.053	0.045	0.005	29.5	132.3	14.7	
21/02/2018	Buffer in.	0.2				22.34	2.16	1.6	0.11	0.01	1 26	1.47	0.09	0.009	0.024	0.071	0.048	0.015	33.3	135.1	19.1	
21/02/2018	Dam	0.2				23.19	2.96	2.4	0.03	0.01	0 32	0.61	0.26	<LLD	0.003	0.014	0.010	<LLD	2.0	88.5	1.5	
21/02/2018	Dam	2.0				23.19	3.14	3.2	0.11	0.01	0 28	0.49	0.09	<LLD	0.005	0.011	0.006	<LLD	1.8	82.5	0.6	
21/02/2018	Dam	5.0				23.20	2.94	3.2	0.10	0.01	0 28	0.49	0.10	<LLD	0.013	0.021	0.008	0.013	1.7	85.0	1.4	
21/02/2018	Dam	10.0				22.36	2.72	2.1	0.12	0.01	0 28	0 56	0.15	<LLD	0.015	0.009	<LLD	0.015	1.9	86.0	1.2	
21/02/2018	Dam	14.0				19.66	2.61	4.0	0.18	0.00	0.19	2.72	2.35	<LLD	0.017	0.018	<LLD	0.017	8.5	92.5	4.8	
21/02/2018	Ferraria Brige	1.0				21.90	2.54	4.0	0.05	0.02	1.05	1 39	0.28	0.004	0.033	0.033	<LLD	0.030	1.9	80	1.9	
21/02/2018	Ferraria Brige	2.0				21.65	2.64	3.5	0.05	0.02	1.15	1 35	0.14	0.003	0.039	0.041	<LLD	0.036	2.7	63.5	16.3	
21/02/2018	Ferraria Brige	3.0				21.52	2.30	2.9	0.05	0.02	1.05	1 20	0.09	0.008	0.030	0.042	0.012	0.022	2.2	64.5	2.2	
21/02/2018	Inflow	0.2				-	2.14	0.8	0.01	0.01	1 33	2.10	0.74	0.008	0.028	0.071	0.044	0.019	33.0	157.5	171.5	
21/02/2018	Intake	0.2				23.14	2.80	1.9	0.74	0.01	0 33	0 83	-0.25	<LLD	0.003	0.015	0.011	<LLD	2.5	74 5	1.9	
21/02/2018	Intake	6.0				23.10	2.77	2.9	0.15	0.01	0 33	0.61	0.13	<LLD	0.005	0.013	0.009	<LLD	2.8	77 5	1.6	
21/02/2018	Intake	9.0				22.34	2.76	2.9	0.13	0.01	0 33	0 50	0.02	<LLD	0.006	0.009	0.003	0.006	2.9	79.5	1.6	
21/02/2018	Intake	11.0				21.70	3.14	1.3	0.31	0.01	0 37	0.79	0.09	<LLD	0.006	0.019	0.013	0.006	2.3	78	2	
21/02/2018	Outflow	0.5				22.14	2.66	4.5	0.71	0.00	0 24	1.16	0.21	0.004	0.021	0.019	<LLD	0.018	4.2	99	2.9	
21/02/2018	Park	0.2				23.04	2.94	3.2	0.09	0.01	0 35	0.60	0.15	<LLD	0.011	0.013	0.002	0.011	2.5	67	1.8	
21/02/2018	Park	3.0				22.83	3.08	5.9	0.10	0.01	0 37	0.71	0.23	<LLD	0.012	0.014	<LLD	0.012	2.8	106	2.1	
21/02/2018	Park	5.0				22.61	2.88	3.7	0.07	0.01	0 37	0 56	0.11	<LLD	0.003	0.015	0.012	<LLD	2.4	97	1.4	
21/02/2018	Park	6.0				21.91	2.84	2.9	0.09	0.01	0 37	0.61	0.15	<LLD	0.020	0.019	<LLD	0.020	2.7	99	1.6	
21/02/2018	PPA	0.2				22.96	2.92	3.2	0.05	0.01	0 29	0.61	0.26	0.005	0.014	0.010	<LLD	0.009	3.7	99.5	1.1	
21/02/2018	PPB	0.2				22.80	2.89	2.4	0.05	0.01	0.46	0.64	0.12	0.003	0.021	0.016	<LLD	0.018	2.9	107	1	
03/04/2018	Inflow	0.2					1.80	2.4	0.09	0.05	1 34	1 80	0.28	0.001	0.013	0.012		0.012	1.69	73.20	3.10	
03/04/2018	Intake	0.2	2.7			24.10	3.11	2.9	0.04	0.01	0.03	0.49	0.18	0.001	0.009	0.007		0.008	1.96	74.00	3.20	
03/04/2018	Intake	1.5	2.7			23.85	2.74	5.8	0.04	0.01	0 24	0 57	0.27	0.003	0.008	0.010	0.002	0.005	2.14	76.30	2.80	
03/04/2018	Intake	4.0	2.7			23.76	2.49	7.1	0.03	0.01	0 24	0.48	0.18	0.01	0.009	0.011	0.002		5.74	81.50	4.40	
03/04/2018	Intake	10.0	2.7			22.40	2.45	2.9	0.25	0.01	0 29	0.76	0.20	0.02	0.020	0.051	0.032	0.001	26.9	143.00	35.00	
03/04/2018	Outflow	0.2				23.05	2.50	4.1	0.51	0.01	0 20	0 81	0.08	0.004				0.000	8.47	83.20	5.70	
08/05/2018	Inflow	0.2					1.380	0.3	0.05	0.02	1 36	1.41	< LLD		0.003	0.009	0.007		2.00	93.50	1.50	
08/05/2018	Intake	0.2	2.4	7.18	7.51	22.45	2.916	5.6	0.11	0.01	0 27	0.67	0.28		0.007	0.017	0.010		1.00	83.75	1.12	
08/05/2018	Intake	1.5	2.4		6.31	22.43	2.422	7.4	0.09	0.01	0 28	0.62	0.24		0.002	0.010	0.009		1.00	82.75	1.04	
08/05/2018	Intake	6.0	2.4	7.06	6.07	22.28	2.286	5.7	0.09	0.01	0 30	0.62	0.23		0.003	0.019	0.016		2.00	85.25	1.10	
08/05/2018	Intake	10.0	2.4	6.51	0.56	22.15	2.183	4.4	0.17	0.01	0 32	0.68	0.18		0.014	0.074	0.061		6.00	89.00	1.76	
08/05/2018	Intake	12.0	2.4	6.04	0.13		2.079	4.1	0.36	0.01	0 25	0.77	0.16		0.006	0.016	0.010		11.00	148.50	11.75	
08/05/2018	Outflow	0.2		7 3	5.67	21.02	2.438	3.5	1.10	0.01	0.14	1 23	< LLD		0.010				25.00	111.50	14.50	
12/06/2018	Ferraria Brige	0.2		7.38	4.72		1.853	4.3	0.10	0.04	1 31	1,33*	< LLD	<LLD	0.005	0.014	0.009	0.004	3	88.30	3.20	
12/06/2018	Inflow	0.2					1.631	1.2	0.25	0.06	1.06	1.40	0.02	<LLD	0.005	0.013	0.008	0.004	2.7	88.50	2.90	
12/06/2018	Intake	0.2	2.0		7.13	18.19	2.563	4.8	0.25	0.01	0 29	0,52*	< LLD	<LLD	0.004	0.012	0.008	0.004	2	86.00	3.50	
12/06/2018	Intake	1.5	2.0		5.75	18.19	2.248	5.1	0.22	0.01	0 30	0 58	0.06	<LLD	0.004	0.022	0.017	0.004	2.1	72.80	5.50	
12/06/2018	Intake	6.0	2.0		4.86	18.16	2.221	4.7	0.23	0.01	0 28	0 56	0.04	<LQ	0.009	0.039	0.030	0.006	6.9	89.80	8.30	
12/06/2018	Intake	12.0	2.0		4.35	17.93	2.168	4.3	0.26	0.01	0 27	0 58	0.04	0.013	0.019	0.045	0.027	0.006	12.1	151.80	13.00	
12/06/2018	Outflow	0.2				18.17	2.184	4.8	0.28	0.01	0 30	0.65	0.06	<LLD	<LQ	0.015	0.012	<LQ	2	72.50	8.10	

Date	Site	Depth	Secchi	pH	DO	Temp	DOC	Chl-a	NH3	NO2	NO3	NT	TON	PO4	PTD	PT	PTP	P Org	Turb.	TS	TSS	TDS
		m	m		mg/L	ºc	mg/L	mg/L	mg/L	mg/L	mg/L	mg/L	mg/L	mg/L	mg/L	mg/L	mg/L	mg/L	(NTU)	mg/L	mg/L	mg/L
13/08/2018	Buffer	0.2	1.3	7.87	7.86	17.24	1.951	4.5	0.01	0.02	1.19	1.45	0.22	<LLD	<LQ	0.009	0.008	0.001	1.98	80.0	1.0	79.0
13/08/2018	Buffer	1.0	1.3	8.11	8..54	17.77	2.259	3.9	0.02	0.02	1.17	1.37	0.15	<LLD	0.008	0.010	<LQ	0.010	1.93	81.7	0.8	80.9
13/08/2018	Buffer in.	0.2	1.3	7.85	8.19	17.50	1.909	3.7	0.04	0.02	1.26	1.60	0.27	<LLD	0.006	0.008	<LQ	0.008	1.92	105.3	1.0	104.3
13/08/2018	Dam	0.2	3.2	7.91	6.6	17.34	2.379	3.7	0.06	0.01	0.31	0.57	0.19	<LQ	0.004	0.007	<LQ	<LQ	2.13	86.8	1.3	85.5
13/08/2018	Dam	4.0	3.2	7.34	6.53	17.10	2.338	3.7	0.07	0.01	0.31	0.56	0.17	<LLD	0.004	0.007	<LQ	0.006	2.83	82.0	1.4	80.6
13/08/2018	Dam	8.0	3.2	7.23	6.3	16.70	2.259	4.0	0.07	0.01	0.31	0.57	0.18	<LLD	<LQ	0.011	0.008	0.007	3.12	83.0	1.1	81.9
13/08/2018	Dam	13.0	3.2	7.41	6.14	16.49	2.413	3.5	0.09	0.01	0.31	0.56	0.15	<LLD	<LQ	0.010	0.007	0.007	3.37	84.3	2.7	81.6
13/08/2018	Ferraria Brige	0.2	2.9	8.09	7.99	18.73	2.406	4.0	<LLD	0.01	0.50	0.78	0.27	<LLD	0.004	0.016	0.012	0.007	4.36	82.2	2.9	79.3
13/08/2018	Ferraria Brige	1.0	2.9	7.75	7.93	17.48	2.060	6.0	0.02	0.01	0.87	1.05	0.14	<LQ	<LQ	0.012	0.009	<LQ	4.34	100.3	2.9	97.4
13/08/2018	Ferraria Brige	2.0	2.9	7.73	8.23	15.92	2.099	7.5	0.01	0.02	0.91	1.10	0.16	0.006	0.006	0.025	0.020	<LLD	7.26	126.0	5.4	120.6
13/08/2018	Inflow	0.2		6.79	8.85	-	1.764	0.4	0.18	0.04	1.48	1.55	<LLD	<LQ	0.008	0.027	0.019	0.005	7.81	132.5	5.2	127.3
13/08/2018	Intake	0.2	3.1	8.19	7.57	17.65	2.269	3.1	0.07	0.01	0.38	0.68	0.22	0.004	0.007	0.012	0.005	<LQ	2.70	91.0	2.6	88.4
13/08/2018	Intake	4.0	3.1	7.89	6.89	16.70	2.349	8.2	0.08	0.01	0.33	0.65	0.24	0.005	0.005	0.013	0.008	<LLD	3.63	92.5	3.7	88.8
13/08/2018	Intake	8.0	3.1	7.14	6.19	16.58	2.328	6.8	0.08	0.01	0.32	0.63	0.22	0.004	0.004	0.014	0.010	<LLD	3.82	89.3	4.9	84.4
13/08/2018	Intake	10.0	3.1	7.14	5.41	16.56	2.281	5.1	0.06	0.01	0.32	0.61	0.22	0.007	0.007	0.009	<LQ	<LLD	2.73	91.3	2.1	89.2
13/08/2018	Outflow	0.2		7.69	7.6	16.44	2.162	3.3	0.10	0.01	0.33	0.55	0.11	0.004	0.005	0.013	0.007	<LQ	3.41	94.5	2.8	91.7
13/08/2018	Park	0.2	2.8	8.36	7.99	18.76	2.532	3.7	0.04	0.01	0.36	0.63	0.22	0.004	0.004	0.018	0.014	<LLD	8.42	103.7	5.8	97.9
13/08/2018	Park	3.0	2.8	7.75	7.86	16.99	2.275	5.2	0.04	0.01	0.36			<LQ	<LQ	0.016	0.014	<LQ	3.93	112.5	3.5	109.0
13/08/2018	Park	6.0	2.8	7.66	6.89	16.56	2.463	5.6	0.05	0.01	0.36	0.75	0.34	<LQ	<LQ	0.019	0.016	<LQ	6.25	110.3	5.9	104.4
13/08/2018	PPA	0.2	1.6	8.22	7.99	18.37	2.046	3.9	<LLD	0.01	0.58	1.00	0.41	<LLD	<LQ	0.019	0.016	<LQ	5.65	108.7	6.8	101.9
13/08/2018	PPA	1.0	1.6	8.16	8.44	17.50	2.222	4.3	<LLD	0.01	0.48	0.75	0.26	<LQ	0.004	0.025	0.020	<LQ	5.73	135.2	3.3	131.9
13/08/2018	PPA	2.0	1.6	8.31	8.19	17.14	2.141	10.2	0.01	0.01	0.47	0.73	<LLD	<LQ	0.005	0.029	0.024	<LQ	4.48	124.3	4.0	120.3
13/08/2018	Res.Center	0.2	2.8	8.23	7.58	17.78	2.329	3.6	0.08	0.01	0.34	0.76	0.33	0.004	0.010	0.039	0.030	0.006	10.88	114.5	7.8	106.7
13/08/2018	Res.Center	4.0	2.8	7.52	7.39	16.83	2.329	4.4	0.07	0.01	0.34	0.60	0.19	0.01	0.02	0.041	0.020	0.012	4.24	140.7	2.0	138.7
13/08/2018	Res.Center	8.0	2.8	7.25	5.27	16.46	2.286	9.9	0.06	0.01	0.36	0.64	0.21	<LQ	<LQ	0.011	0.008	<LQ	3.54	96.7	2.4	94.3
24/10/2018	Buffer	0.2			7.79		2.84		0.19	0.06	0.81	1.53	0.47	<LQ	<LQ	0.009	0.008	<LLD		90.4		
24/10/2018	Ferraria Brige	0.2			5.21		2.77		0.21	0.05	0.60	1.35	0.49	<LQ	<LQ	0.018	0.016	<LQ		94.8		
24/10/2018	Ferraria Brige	2.0			4.14		2.80		0.22	0.06	0.66	1.44	0.50	<LQ	<LQ	0.017	0.014	<LQ		84.8		
24/10/2018	Inflow	0.2			5.26		2.89		0.18	0.07	0.90	1.81	0.66	0.004	0.008	0.063	0.055	0.004	15.3	125.5		
24/10/2018	Intake	0.2	2.7		6.66		2.52		0.04	0.01	0.22	0.44	0.18	0.007	0.009	0.048	0.038	<LQ	12.6	123.8		
24/10/2018	Intake	10.0	2.7		5.7		2.19		0.43	0.01	<LLD	0.61	0.18	0.013	0.014	0.078	0.064	<LQ	24.7	130.4		
24/10/2018	Intake	1,5	2.7		7.9		2.27		0.03	0.01	0.16	0.45	0.26	0.013	0.020	0.106	0.086	0.007	26.8	164.5		
24/10/2018	Outflow	0.2		7.65	6.45		1.95		0.48	<LLD	<LLD	0.68	0.20	<LQ	<LQ	0.013	0.012	<LQ	7	89.4		
24/10/2018	PPA	0.2			4.93		2.80		0.20	0.03	0.43	1.01	0.34	0.004	0.008	0.044	0.036	0.004	12.5	114		
24/10/2018	PPA	2.5			4.19		2.81		0.24	0.06	0.67	1.49	0.52	0.008	0.01	0.072	0.058	0.006	21.7	132.4		
20/11/2018	Buffer	0.2	0.4	8.42	6.93	21.66	2.92		0.08	0.03	0.72	1.37	0.55	<LLD	0.025	0.006	<LLD	0.040	1.5		2.8	
20/11/2018	Ferraria Brige	0.2	0.6	7.54	7.04	20.89	2.71		0.08	0.02	0.57	1.24	0.57	<LLD	<LLD	0.008	0.012	0.010	1.8		2.4	
20/11/2018	Ferraria Brige	2.5	0.6	7.95	6.04	20.39	2.74		0.10	0.03	0.71	1.55	0.72	<LLD					1.5		84.9	
20/11/2018	Inflow	0.2		7.42	6.4		2.41		0.07	0.03	1.07	1.64	0.48	<LLD	<LLD	0.025	0.026	0.011	4.7		5.0	
20/11/2018	Intake	0.2	2.4	8.39	7.04	22.73	2.46		0.01	0.01	0.13	0.46	0.31	0.003	0.01	0.059	0.048	0.008	13.3		11.3	
20/11/2018	Intake	1.5	2.4		7.42	22.73	2.43		0.01	0.01	0.13	0.81	0.67	0.003	0.016	0.063	0.047	0.014	11.5		9.3	
20/11/2018	Intake	10.0	2.4		0.33	19.62	2.21		0.14	0.01	0.11	0.67	0.41	0.006	0.015	0.233	0.218	0.009	20.8		55.0	
20/11/2018	Outflow	0.2		8.24	7.57	18.94	2.24		1.03	0.01	0.05	1.91	0.82	0.018	0.016	0.070	0.055	<LLD	24.0		18.67	
20/11/2018	PPA	0.2	1.0	7.97	6.25	23.22	2.60		0.07	0.02	0.39	0.94	0.46	0.013	0.013	0.058	0.045	0.000	23.2		30.00	

Date	Site	Depth	Secchi	pH	DO	Temp	DOC	Chl-a	NH3	NO2	NO3	NT	TON	PO4	PTD	PT	PTP	P Org	Turb.	TS	TSS	TDS
		m	m		mg/L	ºc	mg/L	mg/L	mg/L	mg/L	mg/L	mg/L	mg/L	mg/L	mg/L	mg/L	mg/L	mg/L	(NTU)	mg/L	mg/L	mg/L
20/11/2018	PPA	2.0	1.0	8.35	5.85	22.18	2.70		0.08	0.02	0.54	1.37	0.72	<LLD					11.9		62.8	
11/12/2018	Buffer	0.2	0.9	9.01	7.21	25.11	3.08		0.03	0.02	0.74	0.80	0.01	<LQ	0.02	0.022	0.006	0.015	1.5			
11/12/2018	Ferraria Brige	0.2	0.8	9.05	7.2	25.46	3.19		0.02	0.02	0.74	0.94	0.15	<LQ	0.01	0.015	0.007	0.007	1.8			
11/12/2018	Ferraria Brige	2.5	0.8		7.45	23.82	2.97		0.04	0.02	0.69	0.84	0.09	<LQ	0.004	0.019	0.015	<LQ	7.6			
11/12/2018	Inflow	0.2		7.01	4.66		2.67		0.11	0.05	1.30	1.40		<LLD	0.005	0.044	0.039	0.005	4.2			
11/12/2018	Intake	0.2	3.0	8.68	6.2	24.92	2.51		0.03	0.01	0.17	0.37	0.17	<LLD	0.011	0.044	0.033	0.011	8.3			
11/12/2018	Intake	1.5	3.0	8.72	6.11	24.77	2.39		0.03	0.01	0.17	0.33	0.12	0.01	0.013	0.045	0.033	<LLD	13.2			
11/12/2018	Intake	10.0	3.0	8	0.08	20.56	3.01		0.48	0.00	0.08	0.67	0.11	<LQ	0.006	0.073	0.067	<LQ	11.3			
11/12/2018	Outflow	0.2		8.19	5.96	20.11	2.37		0.72	0.00	0.02	0.78	0.03	<LLD	0.012	0.066	0.053	0.012	15.4			
11/12/2018	PPA	0.2	1.5	8.92	6.78	24.64	2.75		0.02	0.01	0.25	0.31	0.03	0.02	0.034	0.069	0.035	0.010	22.9	145.33	35.1	110.23
11/12/2018	PPA	2.0	1.5	8.94	7.65	23.76	2.74		0.03	0.01	0.34	0.49	0.11	<LQ	0.009	0.020	0.011	0.005	24.8	89.06	10.73	78.33
04/02/2019	Buffer	0.2	0.2	7.35	4.48	20.96	3.55	2.1	0.22	0.05	0.96	1.54	0.31	<LLD					2.4	85.8	3.9	81.9
04/02/2019	Buffer in.	0.2	0.2				4.19	5.7	0.17	0.04	0.73	1.34	0.40	<LLD					2.2	79.8	3.4	76.4
04/02/2019	Dam	0.2	2.4	8 5	2.56	26.58	2.78	4.3	0.02	0.01	0.04	0.30	0.23	<LLD					2.4	82.0	8.0	74.0
04/02/2019	Dam	6.0	2.4	8.54	1.84	26.58	2.88	4.5	0.02	0.01	0.12	0.40	0.25		<LQ	<LQ	<LQ	<LQ	2.5	80.8	3.1	77.7
04/02/2019	Dam	10.0	2.4	7.58	0.46	22.18	2.53	9.9	0.07	0.01	0.12			<LLD	<LQ	0.006	<LQ	<LQ	1.7	94.2	4.4	89.7
04/02/2019	Dam	14.0	2.4	9.35	0	19.29	2.40	20.8	0.67	0.01	0.07	0.92	0.18	<LLD	<LQ	<LQ	<LLD	<LQ	1.2	97.7	1.9	95.7
04/02/2019	Ferraria Brige	0.2	0.1	7.57	4.37	20.50	3.65	2.7	0.10	0.03	0.58	0.97	0.26	<LLD	<LQ	<LQ	<LQ	<LLD	1.4	94.0	2.1	91.9
04/02/2019	Ferraria Brige	2.0	0.1	7.19	3.35	20.08	3.53	1.0	0.18	0.04	0.74	1.22	0.27	<LLD	<LQ	0.024	0.021	<LQ	10.1	119.0	10.8	108.2
04/02/2019	Inflow	0.2		7.79	6.1	20.58	3.69	1.6	0.50	0.05	1.05	1.65	0.05	<LLD	<LQ	0.006	<LQ	<LLD	2.9	87.0	3.2	83.8
04/02/2019	Intake	0.2	2.7	8.24	4.76	26.36	2.79	8.1	0.01	0.01	0.14	0.62	0.46	<LQ					2.5	89.8	7.3	82.5
04/02/2019	Intake	2.5	2.7	8.28	2.93	26.32	2.81	7.6	0.02	0.01	0.15	0.60	0.42	<LLD	<LLD	<LQ	<LLD	<LLD	3.4	93.0	4.7	88.3
04/02/2019	Intake	7.0	2.7	8.27	1.63	26.28	2.75	7.4	0.02	0.01	0.15	0.50	0.32	<LQ	<LQ	0.005	<LQ	<LLD	5.3	87.3	4.6	82.8
04/02/2019	Intake	10.0	2.7	7.96	0	22.33	2.86	10.4	0.01	0.01	0.05	0.60	0.53	<LQ	<LQ	0.007	0.005	<LLD	5.1	91.3	4.6	86.7
04/02/2019	Outflow	0.2		7.11	5.79	20.24	2.34	22.4	1.12	0.01	0.07	1.27	0.07	<LLD	<LQ	0.014	0.011	<LQ	6.4	95.0	6.7	88.3
04/02/2019	Park	0.2	1.3	8.49	6.47	26.62	2.97	8.9	0.03	0.01	0.14	0.39	0.21	<LLD	0.006	0.010	<LQ	0.006	13.1	117.5	9.5	108.0
04/02/2019	Park	3.0	1.3	8.57	5.36	26.58	2.91	7.1	0.02	0.01	0.09	0.41	0.29	<LQ	<LQ	0.025	0.022	<LLD	20.5	118.5	15.6	102.9
04/02/2019	Park	7.0	1.3	8.33	2.51	26.16	2.88	8.4	0.02	0.01	0.14	0.41	0.23	0.01	0.008	0.040	0.032	<LLD	48.0	142.0	42.6	99.4
04/02/2019	PPA	0.2	0.4	8.49	6.71	24.75	3.31	10.3	0.00	0.01	0.28	0.54	0.25	0.006	0.021	0.037	0.016	0.015	88.4	165.0	52.0	113.0
04/02/2019	PPA	1.5	0.4	7.96	4.27	22.23	3.13	7.9	0.04	0.02	0.39	1.11	0.66	0.005	0.007	0.039	0.032	<LQ	83.1	143.5	51.0	92.5
04/02/2019	Res.Center	0.2	1.7	8.41	5.92	26.48	3.06	6.4	0.02	0.01	0.11	0.42	0.27	0.01	0.013	0.036	0.022	<LLD	90.3	161.5	56.7	104.8
04/02/2019	Res.Center	3.0	1.7	8.45	5.41	26.48	2.75	5.7	0.01	0.01	0.12	0.34	0.20	0.01	0.014	0.054	0.039	<LLD	70.7	158.0	65.0	93.0
04/02/2019	Res.Center	9.0	1.7	8.39	1.89	24.14	2.80	8.4	0.09	0.01	0.12	0.88	0.66	<LLD	<LQ	0.005	<LQ	<LQ	33.7	87.5	12.8	74.7
02/04/2019	Ferraria Brige	0.2	0.8			25.16	2.31	6.2	0.02	0.02	0.98	1.09	0.07	<LLD	<LLD	0.010	0.010	<LLD	2.10	98.2	1.8	96.40
02/04/2019	Ferraria Brige	3.5	0.8			20.99	2.19	4.6	0.04	0.01	0.88	1.13	0.20	0.004	0.010	0.010	<LLD	0.010	2.20	98.3	2.8	95.50
02/04/2019	Inflow	0.2				19.09	1.99	0.6	0.07	0.02	1.38	1.54	0.07	<LLD	<LLD	<LLD	<LLD	<LLD	2.10	98.5	2.5	96.00
02/04/2019	Intake	0.2	2.7			25.11	2.62	4.0	0.16	0.01	0.06	0.47	0.23	<LLD	<LLD	0.020	0.020	<LLD	4.00	106.0	4.0	102.00
02/04/2019	Intake	1.5	2.7			24.19	2.81	3.7	0.16	0.01	0.15	0.46	0.15	0.01	0.020	0.030	0.010	0.010	7.70	121.3	6.8	114.50
02/04/2019	Intake	11.0	2.7			22.74	2.55	3.6	0.16	0.01	0.19	0.49	0.14	0.03	0.040	0.040	<LLD	0.010	10.70	147.0	8.5	138.50
02/04/2019	Outflow	0.2				-	2.23	11.1	1.96	0.002	0.08	2.27	0.23	0.03	0.030	0.030	<LLD	<LLD	17.90	151.3	11.5	139.80
02/04/2019	PPA	0.2	1.6			25.71	2.58	5.6	0.02	0.01	0.37	0.55	0.15	<0.04	0.040	0.070	0.030	<LLD	22.10	184.0	17.5	166.50
02/04/2019	PPA	2.5	1.6			21.97	2.55	5.4	0.02	0.01	0.42	0.71	0.26	<LLD	<LLD	0.010	0.010	<LLD	43.60	134.5	17.5	117.00

APPENDIX B – Dataset of Comparatives Maps

Dataset of comparatives maps integrating spatial-temporal water quality dynamics through Water Quality Index of Reservoirs (WQIR).

Spring											
Date	Site	Depth	Chrophyll-a			TIN			TP		
		(m)	(mg/L)	Mean	RWQI	(mg/L)	Mean	RWQI	(mg/L)	Mean	RWQI
24/10/2018	Buffer	0.2				1.06	0.94	Class 4	0.06	0.067	Class 4
20/11/2018	Buffer	0.2				0.83			0.07		
24/10/2018	Ferraria Brige	2.0				0.84	0.83	Class 4	0.08	0.105	Class 5
24/10/2018	Ferraria Brige	0.2				0.94			0.05		
20/11/2018	Ferraria Brige	2.5				0.86			0.23		
20/11/2018	Ferraria Brige	0.2				0.67			0.06		
24/10/2018	Intake	10.0				0.15	0.20	Class 2	0.02	0.012	Class 2
24/10/2018	Intake	0.2				0.26			0.01		
24/10/2018	Intake	1,5							0.02		
20/11/2018	Intake	10.0				0.15					
20/11/2018	Intake	0.2				0.20			0.006		
20/11/2018	Intake	1.5				0.26			0.008		
24/10/2018	PPA - Bridge Park A	2.5				0.97	0.69	Class 4	0.07	0.050	Class 4
24/10/2018	PPA - Bridge Park A	0.2				0.64			0.04		
20/11/2018	PPA - Bridge Park A	0.2				0.67			0.02		
20/11/2018	PPA - Bridge Park A	2.0				0.48			0.06		
Summer											
Date	Site	Depth	Chrophyll-a			TIN			TP		
		(m)	(mg/L)	Mean	RWQI	(mg/L)	Mean	RWQI	(mg/L)	Mean	RWQI
21/02/2018	Buffer	1.0		4.7	Class 3	1.23	1.18	Class 3	0.05	0.050	Class 4
21/02/2018	Buffer	2.0	3.4749			0.79			0.05		
21/02/2018	Buffer	0.2	10.4247			1.26			0.05		
11/12/2018	Buffer	0.2				1.29			0.05		
04/02/2019	Buffer	0.2	2.08			1.36			0.04		
21/02/2018	Buffer incoming	0.2	1.6038			0.94			0.07		
04/02/2019	Buffer incoming	0.2	5.72			1.38			0.04		
21/02/2018	Dam	10.0	2.1384	6.1	Class 4	0.07	0.34	Class 3	0.01	0.015	Class 2
21/02/2018	Dam	0.2	2.4057			0.36			0.01		
21/02/2018	Dam	5.0	3.2076			0.40			0.02		
21/02/2018	Dam	2.0	3.2076			0.39			0.01		
21/02/2018	Dam	14.0	4.0095			0.15			0.02		
04/02/2019	Dam	14.0	20.85			0.20			0.02		
04/02/2019	Dam	10.0	9.87			0.41					
04/02/2019	Dam	6.0	4.52			0.74					
04/02/2019	Dam	0.2	4.34			0.37			0.006		
21/02/2018	Ferraria Brige	1.0	4.0095	2.8	Class 2	0.72	0.95	Class 4	0.03	0.047	Class 4
21/02/2018	Ferraria Brige	3.0	2.9403			0.78			0.04		
21/02/2018	Ferraria Brige	2.0	3.4749			1.11			0.04		
11/12/2018	Ferraria Brige	0.2				0.96			0.07		
11/12/2018	Ferraria Brige	2.5				1.21			0.07		
04/02/2019	Ferraria Brige	2.0	0.99			0.75			0.04		
04/02/2019	Ferraria Brige	0.2	2.67			1.11			0.04		

21/02/2018	Intake	9.0	2.9403			1.08			0.01		
21/02/2018	Intake	11.0	1.3365			0.48			0.02		
21/02/2018	Intake	6.0	2.9403			0.47			0.01		
21/02/2018	Intake	0.2	1.8711			0.69			0.015		
11/12/2018	Intake	10.0				0.16			0.02		
11/12/2018	Intake	1.5		5.3	Class 4	0.21	0.39	Class 3	0.02	0.016	Class 2
11/12/2018	Intake	0.2				0.20			0.02		
04/02/2019	Intake	10.0	10.40			0.18					
04/02/2019	Intake	7.0	7.36			0.18					
04/02/2019	Intake	2.5	7.64			0.07					
04/02/2019	Intake	0.2	8.11			0.56					
21/02/2018	Park	0.2	3.2076			0.18			0.01		
21/02/2018	Park	3.0	5.8806			0.45			0.01		
04/02/2019	Park	7.0	8.41			0.12			0.014		
04/02/2019	Park	3.0	7.05	5.7	Class 4	0.48	0.33	Class 3	0.007	0.013	Class 2
04/02/2019	Park	0.2	8.90			0.18			0.005		
21/02/2018	Park	6.0	2.9403			0.45			0.02		
21/02/2018	Park	5.0	3.7422			0.46			0.02		
21/02/2018	PPA - Bridge Park A	0.2	3.2076			0.29			0.01		
11/12/2018	PPA - Bridge Park A	0.2				0.28			0.04		
11/12/2018	PPA - Bridge Park A	2.0		7.1	Class 4	0.35	0.35	Class 3	0.04	0.027	Class 3
04/02/2019	PPA - Bridge Park A	1.5	7.95			0.45			0.025		
04/02/2019	PPA - Bridge Park A	0.2	10.28			0.38			0.01		
04/02/2019	Reservoir Center	9.0	8.38			0.14					
04/02/2019	Reservoir Center	3.0	5.74	6.8	Class 4	0.14	0.17	Class 2		0.006	Class 1
04/02/2019	Reservoir Center	0.2	6.38			0.22			0.006		

Autumn

Date	Site	Depth	Chrophyll-a			TIN			TP		
		(m)	(mg/L)	Mean	RWQI	(mg/L)	Mean	RWQI	(mg/L)	Mean	RWQI
12/06/2018	Ferraria Brige	0.2	4.2768			1.45			0.04		
02/04/2019	Ferraria Brige	3.5	4.555	5.0	Class 3	0.93	1.13	Class 4	0.028	0.036	Class 3
02/04/2019	Ferraria Brige	0.2	6.170			1.02			0.041		
03/04/2018	Intake	10.0	2.9240			0.55			0.01		
03/04/2018	Intake	1.5	5.8479			0.29			0.01		
03/04/2018	Intake	0.2	2.9240			0.08			0.01		
03/04/2018	Intake	4.0	7.0663			0.29			0.01		
08/05/2018	Intake	12.0	4.1123			0.61			0.074		
08/05/2018	Intake	10.0	4.4105			0.50			0.019		
08/05/2018	Intake	0.2	5.6133			0.39			0.009		
08/05/2018	Intake	6.0	5.7470	4.8	Class 3	0.40	0.41	Class 3	0.010	0.017	Class 2
08/05/2018	Intake	1.5	7.3508			0.38			0.017		
12/06/2018	Intake	0.2	4.8114			0.54			0.01		
12/06/2018	Intake	12.0	4.2768			0.54			0.02		
12/06/2018	Intake	1.5	5.0787			0.52			0.01		
12/06/2018	Intake	6.0	4.6778			0.52			0.01		

02/04/2019	Intake	11.0	3.575			0.36					
02/04/2019	Intake	0.2	3.968			0.23			0.01		
02/04/2019	Intake	1.5	3.655			0.32			0.01		
02/04/2019	PPA - Bridge Park A	0.2	5.593	5.5	Class 4	0.45	0.43	Class 3	0.025	0.028	Class 3
02/04/2019	PPA - Bridge Park A	2.5	5.440			0.40			0.030		
Winter											
Date	Site	Depth	Chrophyll-a			NT			PT		
		(m)	(mg/L)	Mean	RWQI	(mg/L)	Mean	RWQI	(mg/L)	Mean	RWQI
13/08/2018	Buffer	0.2	4.5441	4.1	Class 3	1.22	1.25	Class 4	0.02	0.031	Class 3
13/08/2018	Buffer	1.0	3.9204			1.21			0.03		
13/08/2018	Buffer incoming	0.2	3.7260			1.32			0.04		
13/08/2018	Dam	13.0	3.4749	3.7	Class 3	0.39	0.39	Class 3	0.01	0.009	Class 1
13/08/2018	Dam	8.0	4.0095			0.38			0.01		
13/08/2018	Dam	4.0	3.7422			0.41			0.01		
13/08/2018	Dam	0.2	3.7422			0.39			0.01		
13/08/2018	Ferraria Brige	1.0	6.0143	5.8	Class 4	0.94	0.92	Class 4	0.03	0.021	Class 2
13/08/2018	Ferraria Brige	0.2	4.0095			0.91			0.01		
13/08/2018	Ferraria Brige	2.0	7.5133						0.03		
13/08/2018	Intake	10.0	5.0787	5.8	Class 4	0.46	0.42	Class 3	0.02	0.011	Class 2
13/08/2018	Intake	8.0	6.8162			0.42			0.01		
13/08/2018	Intake	4.0	8.1527			0.41			0.01		
13/08/2018	Intake	0.2	3.0740			0.39			0.01		
13/08/2018	Park	3.0	5.1678	4.8	Class 3	0.40	0.41	Class 3	0.01	0.013	Class 2
13/08/2018	Park	0.2	3.7422			0.41			0.01		
13/08/2018	Park	6.0	5.6133			0.41			0.01		
13/08/2018	PPA - Bridge Park A	0.2	3.8759	6.1	Class 4		0.49	Class 3	0.02	0.018	Class 2
13/08/2018	PPA - Bridge Park A	2.0	10.1574						0.02		
13/08/2018	PPA - Bridge Park A	1.0	4.2768			0.49			0.02		
13/08/2018	Reservoir Center	8.0	9.8901	6.0	Class 4	0.42	0.42	Class 3	0.02	0.013	Class 2
13/08/2018	Reservoir Center	4.0	4.4105			0.43			0.01		
13/08/2018	Reservoir Center	0.2	3.6086			0.41			0.01		

APPENDIX C – Dataset of Total Phosphorus Concentrations

Dataset available of Total Phosphorus measured at Passaúna river, including historical data obtained from Hydrological Information System, measurements performed during this study monitoring period, and those provided by Sanepar correlated with discharge.

Date	TP (mg TP/L)	Data source2	Q (m^3/s)	Data source	Q/Qhist
07/05/1985	0.130	SIH	0.80	SIH	0.44
29/02/1988	0.059	SIH	1.16	SIH	0.64
07/04/1988	0.046	SIH	0.92	SIH	0.51
06/06/1988	0.037	SIH	2.48	SIH	1.38
26/07/1988	0.023	SIH	1.26	SIH	0.70
26/10/1988	0.269	SIH	1.57	SIH	0.87
16/02/1989	0.013	SIH	2.44	SIH	1.36
11/04/1989	0.055	SIH	0.95	SIH	0.53
29/06/1989	0.029	SIH	0.86	SIH	0.48
03/08/1989	0.080	SIH	1.52	SIH	0.84
17/08/1989	0.033	SIH	0.92	SIH	0.51
14/08/1990	0.044	SIH	1.35	SIH	0.75
08/11/1990	0.112	SIH	1.61	SIH	0.89
20/02/1991	0.144	SIH	1.85	SIH	1.03
25/06/1991	0.026	SIH	1.13	SIH	0.63
19/07/1991	0.102	SIH	0.92	SIH	0.51
05/09/1991	0.080	SIH	0.50	SIH	0.28
26/09/1991	0.062	SIH	0.92	SIH	0.51
30/10/1991	0.379	SIH	1.62	SIH	0.90
25/11/1991	0.088	SIH	0.55	SIH	0.31
18/12/1991	0.245	SIH	1.35	SIH	0.75
22/01/1992	0.102	SIH	0.49	SIH	0.27
19/02/1992	0.071	SIH	0.61	SIH	0.34
11/03/1992	0.111	SIH	0.57	SIH	0.32
12/05/1992	0.075	SIH	0.54	SIH	0.30
03/06/1992	0.084	SIH	2.32	SIH	1.29
21/07/1992	0.057	SIH	0.88	SIH	0.49
25/08/1992	0.062	SIH	1.34	SIH	0.74
29/09/1992	0.093	SIH	0.84	SIH	0.47
20/10/1992	0.174	SIH	0.90	SIH	0.50
17/11/1992	0.169	SIH	0.60	SIH	0.33
21/12/1992	0.075	SIH	0.46	SIH	0.26
27/01/1993	0.077	SIH	0.64	SIH	0.35
19/04/1993	0.070	SIH	0.55	SIH	0.31
11/05/1993	0.052	SIH	0.36	SIH	0.20
22/06/1993	0.034	SIH	1.80	SIH	1.00
27/07/1993	0.045	SIH	1.20	SIH	0.67
17/08/1993	0.055	SIH	0.92	SIH	0.51
21/09/1993	1.374	SIH	11.48	SIH	6.38
16/11/1993	0.081	SIH	1.20	SIH	0.67
30/11/1993	0.237	SIH	0.95	SIH	0.53
16/12/1993	0.055	SIH	0.62	SIH	0.35
07/02/1994	0.120	SIH	1.71	SIH	0.95
28/03/1994	0.058	SIH	0.92	SIH	0.51
25/04/1994	0.136	SIH	1.29	SIH	0.72
28/04/1994	0.235	SIH	0.99	SIH	0.55
03/06/1994	0.198	SIH	0.95	SIH	0.53
06/06/1994	0.086	SIH	0.95	SIH	0.53
05/07/1994	0.146	SIH	3.40	SIH	1.89

25/07/1994	0.061	SIH	0.81	SIH	0.45
20/09/1994	0.093	SIH	0.61	SIH	0.34
01/11/1994	0.141	SIH	0.82	SIH	0.46
14/02/1995	0.048	SIH	2.72	SIH	1.51
29/03/1995	0.078	SIH	1.32	SIH	0.73
17/07/1995	0.056	SIH	2.36	SIH	1.31
09/08/1995	0.018	SIH	0.99	SIH	0.55
23/10/1995	0.053	SIH	1.89	SIH	1.05
05/12/1995	0.109	SIH	5.13	SIH	2.85
21/02/1996	0.085	SIH	1.99	SIH	1.11
11/04/1996	0.067	SIH	1.96	SIH	1.09
26/04/1996	0.079	SIH	2.03	SIH	1.13
06/05/1996	0.050	SIH	2.06	SIH	1.14
02/07/1996	0.030	SIH	1.96	SIH	1.09
07/08/1996	0.074	SIH	1.64	SIH	0.91
02/09/1996	0.035	SIH	1.96	SIH	1.09
08/10/1996	0.086	SIH	2.20	SIH	1.22
06/11/1996	0.081	SIH	2.48	SIH	1.38
18/03/1997	0.067	SIH	1.90	SIH	1.06
09/04/1997	0.067	SIH	1.94	SIH	1.08
28/04/1997	0.066	SIH	1.96	SIH	1.09
03/07/1997	0.108	SIH	3.00	SIH	1.67
31/07/1997	0.094	SIH	1.20	SIH	0.66
14/08/1997	0.092	SIH	1.78	SIH	0.99
17/09/1997	0.137	SIH	2.17	SIH	1.20
04/11/1997	0.067	SIH	1.75	SIH	0.97
26/03/1998	0.100	SIH	3.00	SIH	1.67
06/05/1998	0.016	SIH	2.74	SIH	1.52
19/05/1998	0.075	SIH	2.44	SIH	1.36
21/05/1998	0.630	SIH	1.82	SIH	1.01
21/07/1998	0.093	SIH	5.52	SIH	3.07
03/08/1998	0.150	SIH	2.17	SIH	1.21
25/08/1998	0.106	SIH	4.23	SIH	2.35
02/10/1998	0.162	SIH	6.27	SIH	3.48
01/12/1998	0.170	SIH	2.42	SIH	1.34
03/02/1999	0.175	SIH	2.01	SIH	1.12
27/04/1999	0.068	SIH	2.18	SIH	1.21
25/05/1999	0.065	SIH	1.85	SIH	1.03
09/08/1999	0.084	SIH	1.63	SIH	0.91
22/09/1999	0.095	SIH	1.46	SIH	0.81
17/11/1999	0.098	SIH	1.12	SIH	0.62
22/03/2000	0.098	SIH	1.16	SIH	0.65
19/04/2000	0.031	SIH	1.38	SIH	0.77
27/06/2000	0.263	SIH	1.37	SIH	0.76
28/09/2000	0.121	SIH	1.87	SIH	1.04
27/11/2000	0.267	SIH	1.62	SIH	0.90
17/04/2001	0.114	SIH	1.85	SIH	1.03
13/07/2001	0.109	SIH	2.09	SIH	1.16
25/09/2001	0.391	SIH	2.24	SIH	1.24
16/11/2001	0.121	SIH	2.18	SIH	1.21

05/12/2001	0.111	SIH	1.76	SIH	0.98
14/08/2003	0.081	SIH	1.33	SIH	0.74
20/11/2003	0.109	SIH	1.15	SIH	0.64
11/05/2004	0.041	SIH	1.27	SIH	0.71
08/06/2004	0.063	SIH	1.75	SIH	0.97
14/03/2005	0.340	SIH	1.99	SIH	1.10
13/06/2005	0.049	SIH	1.13	SIH	0.63
28/09/2005	0.094	SIH	2.64	SIH	1.46
27/10/2005	0.210	SIH	4.62	SIH	2.56
16/03/2006	0.100	SIH	1.21	SIH	0.67
26/05/2006	0.097	SIH	0.81	SIH	0.45
21/11/2006	0.190	SIH	1.04	SIH	0.58
16/04/2007	0.078	SIH	0.61	SIH	0.34
29/07/2009	0.240	SIH	3.46	SIH	1.92
17/11/2009	0.150	SIH	2.84	SIH	1.58
24/03/2010	0.082	SIH	1.19	SIH	0.66
22/06/2010	0.320	SIH	2.84	SIH	1.58
26/10/2010	0.100	SIH	1.10	SIH	0.61
04/04/2011	0.110	SIH	2.23	SIH	1.24
08/08/2011	0.069	SIH	2.49	SIH	1.38
22/11/2011	0.099	SIH	1.64	SIH	0.91
28/05/2012	0.064	SIH	1.16	SIH	0.65
13/11/2012	0.120	SIH	0.91	SIH	0.50
20/08/2013	0.061	SIH	1.80	SIH	1.00
08/10/2013	0.043	SIH	1.09	SIH	0.61
18/02/2014	0.061	SIH	0.52	SIH	0.29
09/07/2014	0.077	SIH	0.70	SIH	0.39
20/08/2014	0.061	SIH	0.52	SIH	0.29
11/03/2015	0.072	SIH	1.06	SIH	0.59
18/10/2016	0.180	SIH	1.08	SIH	0.60
16/02/2017	0.100	SIH	1.16	SIH	0.65
15/05/2017	0.050	SIH	0.95	SIH	0.53
03/08/2017	0.230	SIH	0.49	SIH	0.27
16/10/2017	0.063	SIH	1.15	SIH	0.64
22/01/2018	0.045	SANEPAR	6.09	Larsim	3.38
23/01/2018	0.100	SIH	1.13	SIH	0.63
08/02/2018	0.057	SANEPAR	3.43	Larsim	1.90
21/02/2018	0.071	MuDaK	2.68	Larsim	1.49
13/03/2018	0.029	SANEPAR	2.97	Larsim	1.65
03/04/2018	0.051	MuDaK	3.90	Larsim	2.16
10/04/2018	0.032	SANEPAR	2.93	Larsim	1.63
08/05/2018	0.016	MuDaK	1.91	Larsim	1.06
08/05/2018	0.036	SANEPAR	1.91	Larsim	1.06
14/05/2018	0.003	MuDaK-LVS	1.74	Larsim	0.97
24/05/2018	0.004	MuDaK-LVS	1.61	Larsim	0.89
11/06/2018	0.049	MuDaK-LVS	1.44	Larsim	0.80
12/06/2018	0.045	MuDaK	1.39	Larsim	0.77
14/06/2018	0.034	SANEPAR	1.71	Larsim	0.95
02/07/2018	0.017	MuDaK-LVS	1.21	Larsim	0.67
09/07/2018	0.043	SANEPAR	1.07	Larsim	0.60

09/07/2018	0.020	SANEPAR	1.07	Larsim	0.60
23/07/2018	0.013	MuDaK-LVS	0.95	Larsim	0.53
09/08/2018	0.066	SIH	0.79	SIH	0.44
13/08/2018	0.041	MuDaK	0.81	Larsim	0.45
13/08/2018	0.049	MuDaK-LVS	0.81	Larsim	0.45
22/08/2018	0.050	SANEPAR	0.82	Larsim	0.45
29/08/2018	0.042	MuDaK-LVS	0.77	Larsim	0.43
10/09/2018	0.047	SANEPAR	0.68	Larsim	0.38
21/09/2018	0.037	MuDaK-LVS	0.80	Larsim	0.44
13/10/2018	0.215	EVENT	4.63	Event	2.57
18/10/2018	0.435	EVENT	11.91	Event	6.62
24/10/2018	0.106	MuDaK	1.54	Larsim	0.86
08/11/2018	0.063	SIH	0.99	SIH	0.55
09/11/2018	0.021	MuDaK-LVS	1.06	Larsim	0.59
20/11/2018	0.058	MuDaK	1.99	Larsim	1.10
27/11/2018	0.073	MuDaK-LVS	0.89	Larsim	0.50
11/12/2018	0.069	MuDaK	0.81	Larsim	0.45
28/12/2018	0.028	MuDaK-LVS	0.84	Larsim	0.47
14/01/2019	0.044	MuDaK-LVS	3.89	Larsim	2.16
28/01/2019	0.028	MuDaK-LVS	1.11	Larsim	0.62
04/02/2019	0.054	MuDaK	1.45	Larsim	0.81
14/02/2019	0.073	MuDaK-LVS	0.86	Larsim	0.48
21/02/2019	0.042	MuDaK-LVS	9.59	Larsim	5.33
28/02/2019	0.093	MuDaK-LVS	3.65	Larsim	2.03